EFFECT OF FIBER IN ENHANCEMENT OF MECHANICAL PROPERTIES AND STRUCTURAL BEHAVIORS OF OIL PALM SHELL CONCRETE

YAP SOON POH

THESIS SUBMITTED IN FULFILMENT OF THE
REQUIREMENT FOR THE DEGREE OF
DOCTOR OF PHILOSOPHY

FACULTY OF ENGINEERING
UNIVERSITY OF MALAYA
KUALA LUMPUR

2015

UNIVERSITI MALAYA

ORIGINAL LITERARY WORK DECLARATION

Name of Candidate: YAP SOON POH (I.C/Passport No: 870210-14-6155)

Registration/Matric No: KHA 110011

Name of Degree: DOCTOR OF PHILOSOPHY

Title of Project Paper/Research Report/Dissertation/Thesis ("this Work"):

EFFECT OF FIBER IN ENHANCEMENT OF MECHANICAL PROPERTIES AND STRUCTURAL BEHAVIORS OF OIL PALM SHELL CONCRETE

Field of Study: STRUCTURAL ENGINEERING

I do solemnly and sincerely declare that:

(1) I am the sole author/writer of this Work;
(2) This Work is original;
(3) Any use of any work in which copyright exists was done by way of fair dealing and for permitted purposes and any excerpt or extract from, or reference to or reproduction of any copyright work has been disclosed expressly and sufficiently and the title of the Work and its authorship have been acknowledged in this Work;
(4) I do not have any actual knowledge nor do I ought reasonably to know that the making of this work constitutes an infringement of any copyright work;
(5) I hereby assign all and every rights in the copyright to this Work to the University of Malaya ("UM"), who henceforth shall be owner of the copyright in this Work and that any reproduction or use in any form or by any means whatsoever is prohibited without the written consent of UM having been first had and obtained;
(6) I am fully aware that if in the course of making this Work I have infringed any copyright whether intentionally or otherwise, I may be subject to legal action or any other action as may be determined by UM.

Candidate's Signature Date

Subscribed and solemnly declared before,

Witness's Signature Date

Name:

Designation:

ABSTRACT

The significance contribution of utilizing locally available waste materials to replace conventional concrete materials gained considerable attention during the past two decades in the realization of sustainable building materials. One such industrial waste material available abound in South East Asia is lightweight oil palm shell (OPS). Earlier researches on OPS showed that OPS could be considered as an ideal replacement of granite aggregates to produce a sustainable lightweight concrete called oil palm shell concrete (OPSC). The development of OPSC has the advantage as a lightweight concrete in addition to environmental benefits. However, the application of OPSC in structural members is less convincing due to its low tensile strength and the addition of fibers has been effective to solve this weakness. The initial challenge in the development of oil palm shell fiber reinforced concrete (OPSFRC) lies in selection of appropriate fibers. In this study, fibrillated and monofilament fibers, nylon fibers and steel fibers of aspect ratio 55, 65 and 80 were added in the OPSC to investigate the effects of different fibers on the mechanical properties of OPSFRC and thereby to select the suitable type of fiber. This would enable to study the effect of volume fraction of fibers on the mechanical properties and structural behaviors under flexural and torsion. In addition, by using a high volume fraction of 3% of steel fibers was added in OPSC to further enhance the tensile strength of OPSFRC to be applied as structural members for special usage which requires high tensile strength. The high tensile strength OPSFRC was tested for mechanical properties, toughness and flexure beam testing. The results show that the synthetic fibers including polypropylene and nylon fibers produced slight increments on the mechanical properties of OPSFRC without significant changes in density. On contrary, steel fibers of aspect ratio 65 outperformed other fibers to produce the highest compressive and flexural strength of 47 MPa and 7 MPa, respectively. Therefore steel fiber of aspect ratio 65 with amount up to 1% was added in the OPSC

beams to investigate the flexural and torsional behaviors of OPSFRC beams. The experimental results reported that the increase in the fiber volume resulted in a higher enhancement of the flexural, torsional and cracking resistance of the OPSFRC beams. The OPSFRC beams reinforced with 1% steel fiber show significant increment in flexural and torsional toughness compared to the plain OPSC specimens. OPSFRC beam with 3% steel fibers produced high tensile strength with flexural strength of 18 MPa. The flexural behaviors of high tensile strength OPSFRC showed drastic improvement in moment capacity and cracking resistance compared to OPSFRC beam with 1% steel fiber. It can be concluded that the addition of steel fiber up to 3% enabled the production of high tensile strength OPSFRC which is suitable for structural application.

ABSTRAK

Sumbangan penting pengggunakan bahan-bahan buangan tempatan yang sedia ada untuk menggantikan bahan konkrit konvensional mendapat perhatian yang besar dalam tempoh dua dekad yang lalu dalam merealisasikan bahan binaan lestari. Satu seperti bahan sisa industri melimpah ruah yang ada di Asia Tenggara adalah tempurung kelapa sawit (OPS) yang ringan. Penyelidikan awal atas OPS menunjukkan bahawa OPS boleh dipertimbangkan untuk mengganti agregat granit untuk menghasilkan konkrit ringan yang mampan dipanggil konkrit tempurung kelapa sawit (OPSC). Pemprosesan OPSC mendapat kelebihan sebagai konkrit ringan sebagai tambahan kepada faedah alam sekitar. Walau bagaimanapun, penggunaan OPSC sebagai ahli struktur adalah kurang meyakinkan kerana kekuatan tegangan yang rendah dan penambahan gentian adalah berkesan untuk menyelesaikan kelemahan ini. Cabaran awal kepada pembangunan konkrit kelapa sawit shell bertetulang gentian (OPSFRC) terletak pada pemilihan serat. Dalam kajian ini, fibrillated dan serat monofilament, gentian nilon dan gentian keluli nisbah aspek 55, 65 dan 80 telah ditambah ke dalam OPSFRC untuk menyiasat kesan gentian yang berbeza ke atas sifat mekanikal OPSFRC untuk memilih jenis gentian yang optimum. Apabila gentian optimum dipilih, kerja diikuti dengan kajian tentang kesan pecahan isipadu gentian terhadap sifat mekanikal dan tingkah laku struktur di bawah bebanan lenturan dan kilasan. Ini bertujuan untuk membuktikan kemungkinan OPSFRC dalam aplikasi struktur. Sebagai tambahan, pecahan isipadu gentian yang lebih tinggi telah ditambah ke dalam OPSFRC untuk meningkatkan kekuatan tegangan OPSFRC supaya digunakan sebagai anggota struktur untuk kegunaan khas yang memerlukan kekuatan tegangan yang tinggi. OPSFRC berkekuatan tegangan tinggi OPSFRC telah diuji di bawah sifat mekanikal and ujian kekuatan lenturan rasuk. Keputusan menunjukkan bahawa gentian sintetik termasuk gentian-gentian polipropilena dan nilon menghasilkan sedikit kenaikan ke atas sifat mekanik OPSFRC

tanpa perubahan ketara dalam kepadatan. Sebaliknya, gentian keluli nisbah aspek 65 mengatasi gentian lain untuk menghasilkan mampatan yang paling tinggi dan kekuatan lenturan 47 MPa dan 7 MPa, masing-masing. Oleh itu gentian keluli nisbah aspek 65 dengan jumlah sehingga 1% ditambah ke dalam rasuk OPSC untuk menyiasat tingkah laku lenturan dan kilasan rasuk OPSFRC. Keputusan eksperimen melaporkan bahawa peningkatan jumlah gentian mengakibatkan peningkatan yang lebih tinggi lenturan, rintangan kilasan dan retak rasuk OPSFRC. Rasuk OPSFRC yang diperkuatkan dengan 1% gentian keluli menunjukkan kenaikan yang jelas dalam keliatan lenturan dan kilasan berbanding spesimen OPSC biasa. OPSFRC dengan 3% jumlah gentian keluli menghasilkan kekuatan tegangan tinggi OPSFRC dengan kekuatan lenturan 18 MPa. Kelakuan lenturan tegangan tinggi kekuatan OPSFRC menunjukkan peningkatan drastik dalam kemuluran, kapasiti masa dan rintangan retak berbanding dengan OPSFRC dengan 1% gentian keluli. Dengan itu boleh disimpulkan bahawa penambahan gentian keluli sehingga 3% membolehkan pengeluaran kekuatan tegangan yang tinggi OPSFRC yang sesuai untuk aplikasi struktur.

ACKNOWLEDGEMENTS

First and foremost, I would like to express my utmost gratitude to my supervisors, Prof. Ir. Dr. Mohd Zamin Jumaat and Dr. U. Johnson Alengaram for their guidance and support throughout my graduate studies. It has been a great pleasure working under their research group.

Furthermore, I express my appreciations to my fellow research group members for helping in miscellaneous research works. They constantly assisted and gave advises to my research. Special thanks are given to Mr. Mo Kim Hung and Mr. Syamsul Bahri for their guides and helps in the experiment instrumentations. In addition, I wish to thank the science officers and lab technicians who helped to perform tests and analyses, particularly Mr. Sreedharan A/L V. K. Raman and Mr. Mansor Hitam.

I would also like to thank the Malaysian Ministry of Higher Education and University of Malaya for providing funding for this project and my scholarship. Finally, I wish to thank my family members and friends for their unconditional supports throughout my study.

TABLE OF CONTENTS

CHAPTER 2 LITERATURE REVIEW

LIST OF FIGURES

CHAPTER 4

CHAPTER 5

CHAPTER 6

CHAPTER 8

APPENDIX

LIST OF TABLES

CHAPTER 5

CHAPTER 6

CHAPTER 7

CHAPTER 8

APPENDIX

LIST OF SYMBOLS AND ABBREVIATIONS

1/r	Curvature
a/c	OPS to cement ratio
$A_{M0.75f}$	Area of load-displacement curve up to 75% of post-peak load
A_{Mu}	Area of load-displacement curve up to moment capacity
A_{Myld}	Area of load-displacement curve up to tensile steel yield
ACI	American Concrete Institute
AIV	Aggregate impact value
ASTM	American Society for Testing and Materials
BS	British stardard
BS EN	British Standard European Norm
CaOH	Calcium hydroxide
C_d	Deflection factor
CMOD	Crack Mouth Opening Displacement
CH	Calcium hydroxide
C_s	Strength factor
CSH	Calcium silicate hydrate
D_c	Density of steel fiber-reinforced lightweight concrete
δ_f	Deflection at failure
δ_{ult}	Deflection at ultimate load
δ_{yld}	Deflection at yield load
D_m	Density of lightweight concrete
D_s	Density of steel fiber
^oC	Degree Celsius

EC	Eurocode
E_{flex}	First crack flexural toughness
E_s	Modulus of elasticity
f_{cu}	Compressive strength
FRC	Fiber-reinforced concrete
FRLWC	Fiber-reinforced lightweight concrete
f_r	Flexural strength
f_{st}	Splitting tensile strength of steel fiber-reinforced lightweight concrete
f_{sw}	Flexural strength of steel fiber-reinforced lightweight concrete
f_t	Splitting tensile strength of lightweight concrete
f_w	Flexural of lightweight concrete
GGBFS	Ground granulated blast furnace slag
GPa	Gigapascal
I_5	Toughness index (ratio of flexural toughness up to 3 times the first crack deflection)
I_{10}	Toughness index (ratio of flexural toughness up to 5.5 times the first crack deflection)
I_{30}	Toughness index (ratio of flexural toughness up to 15.5 times the first crack deflection)
I_g	Second moment of inertia of gross area ignoring reinforcement
kg/m^3	Kilogram per cubic meter
K	A constant depends on the distribution of bending moments of a member
K_{ic}	Fracture toughness index
km/s	Kilometer per second
kN	Kilonewton
kNm	Kilonewton meter (unit for moment)
l	Effect span of beam
l/d	Aspect ratio of fiber
LVDT	Linear variable displacement transducer

LWC	Lightweight concrete
M_{cr}	Cracking moment
μ_D	Deformation-based ductility ratio
μ_{D2}	Deformation-based ductility ratio from Jaeger et al.
μ_{E1}	Energy-based ductility ratio up to ultimate load
μ_{E2}	Energy-based ductility ratio up to 75% of post-peak load
μm	Micrometer
μm/m	Micrometer per meter length
mm	Milimeter
mm/m	Milimeter per meter length
MOE	Modulus of elasticity
MPa	Megapascal
MPa $m^{0.5}$	Megapascal to the square root of meter
$M_{u,ACI}$	Theoretical ultimate moment predicted by using ACI code
$M_{u,BS}$	Theoretical ultimate moment predicted by using BS code
$M_{u,EC}$	Theoretical ultimate moment predicted by using Eurocode
$M_{u,exp}$	Experimental ultimate moment
x	Multiply
NaCl	Sodium chloride
NAOH	Sodium Hydroxide
NDT	Non-destructive test
N/mm^2	Newton per millimeter square
NWC	Normal weight concrete
ODD	Oven-dry density
OPS	Oil palm shell
OPSC	Oil palm shell concrete
OPSFRC	Oil palm shell fiber-reinforced concrete
P_{cr}	Cracking load

%	Percent
PFCS	Post-failure compressive strength
ρ	Density
ρ_{ODD}	Oven-dry density
ρ_{SSD}	Saturated surface-dry density
Ø	Twist
$Ø_{cr}$	Twist at cracking torque
$Ø_{f}$	Twist at failure torque
$Ø_{u}$	Twist at ultimate torque
+	Plus
POFA	Palm oil fuel ash
PP	Polypropylene
PR	Poisson's ratio
P_{ult}	Ultimate load
P_{yld}	Yield load
RCPT	Rapid chloride penetration test
$R_{5,10}$	Residual strength factor between I_5 and I_{10}
$R_{10,20}$	Residual strength factor between I_{10} and I_{20}
s/c	Sand to cement ratio
Σ	Total
SF	Silica fume
Sm	Theoretical crack spacing
SP	Superplasticizer
SSD	Saturated surface dry
T	Torque
T_{cr}	Cracking torque
T_{f}	Torque at failure
T_{u}	Ultimate torque

PVA	polyvinyl alcohol
UPV	Ultrasonic pulse velocity
V	Volt
V_f	Volume fraction of fiber
w/b	Water to binder ratio
y_t	Distance from the extreme tension face to the neutral axis

CHAPTER 1

INTRODUCTION

1.1 Research background

This research work reports on the effects of fibers in lightweight concrete (LWC) developed using a local waste material, oil palm shell (OPS) as lightweight coarse aggregate. The concrete that replaces conventional coarse aggregate by OPS is christened as oil palm shell concrete (OPSC). In Malaysia, OPS has emerged as a potential substitute for conventional crushed granite aggregate in recent years due to its lightweight characteristic and good impact and abrasion resistance. However, most of the past investigations on OPSC were focused on the mechanical properties of OPSC. Hence, this work aims to enhance the mechanical properties and structural behaviors of oil palm shell fiber-reinforced concrete (OPSFRC) using fibers.

1.1.1 Oil palm shell concrete as lightweight concrete

In the oil palm producing countries such as Indonesia, Malaysia and Thailand, the waste derived from the palm oil extraction poses negative environmental impacts. Being the second largest oil palm production country in the world, Malaysia produces about 4 million tons of OPS every year as waste material after the palm oil extraction (Alengaram et al., 2013) In the early practice, palm oil wastes include OPS, empty fruit bunches, fibers, palm trunks and related wastes were disposed by uncontrolled dumping, and this eventually lead to air and soil pollution. In addition, disposal of these wastes requires vast storage space and proper waste management. On the other hand, the OPS and fibers are also used as fuel in the production of steam in the palm oil mills, which provides a means of waste disposal and energy recovery. However the by-product from the fuel incineration known as palm oil fuel ash (POFA) is light and very fine-sized

particles, which carries a high risk for reducing traffic visibility and bronchi & lung diseases (Holgate et al., 1999; Tay & Show, 1995). Though OPS is used as an incinerating material for energy production, still large quantity of OPS is dumped in the vicinity of palm oil mills.

The introduction of bio-diesel in recent years has further boosted the demand of oil palm production and hence the production of OPS is expected to increase significantly in the future. Therefore the replacement of conventional granite aggregates by OPS has been envisaged as a solution to reduce the waste materials which could lead to a more sustainable environment. OPS is light and naturally-sized which enable it to be suitable as aggregate in lightweight concrete (LWC) (Mannan & Ganapathy, 2001a). OPS has a good potential to be used as coarse aggregate to produce lightweight OPSC which met the requirement of structural LWC stated in ASTM C330 (2002). The history of research on OPSC as a LWC could be traced back to 1984 (Abdullah, 1984). Abdullah (1984) replaced 100% granite aggregate with OPS and produced OPS with compressive strength up to 20 MPa. The latter researchers showed that LWC could be produced by using OPS as coarse aggregate with a density and compressive strength in the range of 1700-1850 kg/m^3 and 5-25 MPa, respectively (Basri et al., 1999; Mannan & Ganapathy, 2001a, 2001b, 2002, 2004; Okafor, 1988; Okpala, 1990). The density reduction of OPSC were 550-700 kg/m^3 or about 20-30% compared to normal weight concrete (NWC) of density 2400 kg/m^3. Despite the notable density reduction in OPSC relative to NWC, the low strength of OPSC has limited the potential application of OPSC in low-cost lightweight structural or non-load bearing structures in which the compressive strength is not important such as low cost houses, pavement and drains (Mannan & Ganapathy, 2004).

Further researches were carried out in the past decade to enhance the compressive strength of OPSC (Alengaram et al., 2010a; Alengaram et al., 2010b; Mannan et al., 2006; Shafigh, Jumaat, & Mahmud, 2011; Shafigh, Jumaat, Mahmud, & Alengaram, 2011). These researches revealed that the enhancement of the mechanical properties of OPSC was dependent on density, water to cement ratio, incorporation of cementitious materials, aggregate content, and particle size of OPS. Shafigh *et al*. (2011a & 2011b) reported further improvement in the compressive strength of OPSC of up to 53 MPa with density of about 2000 kg/m^3. However, in general, the density of LWC is limited to 2000 kg/m^3 (Newman & Owens, 2003) and LWC is weak in mechanical properties such as compressive and tensile strengths (Short & Kinniburgh, 1978). As OPSC faced the density bottleneck of 2000 kg/m^3, other options have to be considered to further enhance the properties of OPSC.

In this study, the addition of fibers serves as a new method to improve the properties of OPSC as the fiber-reinforced concrete (FRC) exhibits improved concrete properties compared to the plain concrete. Thus, this research work compares the effects of steel and synthetic fibers to enhance the mechanical properties and structural behaviors of OPSC.

1.1.2 Fiber-reinforced concrete

Fiber-reinforced concrete (FRC) is now gaining the attention of both construction industry and researchers. The use of fibers in the enhancement of concrete properties is well established. Many researchers reported the effect of fibers on the enhancement of the concrete characteristics including mechanical properties, shrinkage, freeze-thaw resistance, ductility, energy absorption, fatigue strength, post-cracking toughness, shear

strength, torsion strength, impact resistance, fire resistance and even, blast resistant property (Balendran et al., 2002; Hassanpour et al., 2012; Mo, et al., 2014a).

There are many types of fibers available commercially, where steel and synthetic fibers are widely used in both construction industry and researches. The examples of synthetic fibers include polypropylene (PP), nylon, acrylic, polyvinyl alcohol (PVA) and more (Bentur & Mindess, 2007). Among all these fibers, steel, PP and nylon fibers are more popular and applied in the production of FRC. In addition, geometries of fibers have significant effect on the characteristics of FRC (Gao et al., 1997). Hence steel and synthetic (PP and nylon) fibers of different aspect ratio (length to diameter ratio, l/d) are added in OPSC to investigate the effect of types and geometries of steel and PP fibers in the mechanical properties of OPSFRC.

1.1.3 Oil palm shell fiber-reinforced concrete

In the case of LWC, the addition of fibers in LWC made from expanded clay aggregate, sintered fly ash aggregate, pumice and other lightweight aggregates changed the design philosophy of LWC. The higher brittleness and lower mechanical properties especially tensile and shear strengths of LWC compared to NWC limits the LWC from being widely used in the construction industry (Hassanpour et al., 2012). Yet, the beneficial effect of fibers in LWC had been proven to be significant. The inclusion of fibers, particularly steel fibers, increases the density, compressive, tensile strengths and post-cracking toughness of LWC; while other fibers such as PP fibers further enhances the strength of LWC in the hybrid system along with steel fibers.

The previous studies on OPSC were mainly focused on the enhancement of mechanical properties by using crushed OPS and cementitious materials except one investigation on the use of steel fiber in OPSC. The recent work on the use of steel fibers in the OPSC (Shafigh et al., 2011c) reported that the use of steel fibers significantly improved the mechanical properties of OPSC. However, their work was conducted on the steel fiber of aspect ratio 65 only. Gao et al. (1997) had shown that both aspect ratio and volume fraction of fibers significantly affected the mechanical properties of LWC made from expanded clay. In this research, hooked-end steel fibers of three aspect ratios (55, 65 and 80) are used in OPSC aiming to produce OPSFRC with enhanced mechanical properties and structural behaviors and compared with the control OPSC. This could lead to a deeper understanding on the selection of the steel fibers in the production of structural members made from OPSFRC.

Apart from steel fibers, comparison among the three types of synthetic fibers (i) fibrillated PP; (ii) multi-filament PP and (iii) nylon fibers to improve the mechanical properties of OPSC was investigated. The more flexible and ductile synthetic fibers could lead to improved toughness and strain capacity in the post-cracking zone (Qian & Stroeven, 2000). The other advantage of synthetic fibers is that the lightweight synthetic fibers do not impart drastic increase in the density of FRC compared to the steel fibers. Following the recent works on OPSC (Shafigh, Jumaat, Mahmud, et al., 2011; Shafigh, Mahmud, et al., 2011), the OPSC produced are facing the density bottleneck of 2000 kg/m^3, as the enhancement of concrete strength is always incorporated along with the increase in density. Hence the use of synthetic fibers with low specific gravity serves as a solution to improve the strength of the OPSC while maintaining the density of LWC within its limit.

1.1.4 Structural behaviors of OPSC and OPSFRC

Structural behaviors of concrete are mainly referred to the performance of reinforced concrete under flexure (bending), shear, bond and torsion. The use of LWC in structural applications gained increasing demands within the recent years attributed to its lower self-weight which eventually could lead to reduced cross section of the beams, columns and foundation. In this work, after the study on the effect of different type, geometry and volume fraction of fiber on the mechanical properties as mentioned in the Section 1.1.3, the optimum fiber is selected for the study of structural behaviors (flexure and torsion) of OPSC and OPSFRC. The addition of fibers in OPSC beams was targeted to improve both flexural and torsional resistances of OPSC. Published literature reported that the fiber reinforcement improved the load carrying capacity, post-cracking behaviors, toughness and crack resistance of concrete. In addition, design codes such as ACI, Eurocode and BS, do not provide the design provisions for the design of LWC such as OPSC, which deviates from NWC with higher ductility but lower mechanical properties. Hence, a detailed study on the structural performance is necessary to improve the knowledge and feasibility of OPSC and OPSFRC as structural members. Other than that, the beam testing could pave way for the accurate and efficient design of reinforced OPSC and OPSFRC beams.

1.2 Problem statements

After the introduction of the OPSC since 1980s, the development of the OPSC remained hindered until last decade. This might attributed to the following reasons:

1. LWC including OPSC is generally weak in mechanical properties such as compressive and tensile strengths, compared to the NWC. Despite the advantage of density reduction to use LWC instead of NWC, the weak mechanical properties of

LWC narrowed the design flexibility of the LWC as structural members subjected to high loading. For example, OPSC was suggested to be applied in low cost house, pavement and footbridge which subjected to low applied loading. Therefore, the mechanical property of the LWC, especially OPSC in this research, requires improvement before it is introduced to the application in construction industry.

2. There was an investigation on the use of fibers in OPSC by Shafigh, Mahmud, et al. (2011). However the study investigated the effect of steel fibers on the mechanical properties of OPSC only. Though their results revealed that the use of steel fibers resulted in significant improvement on the mechanical properties of OPSC, the challenge of OPSFRC remains on the selection of the appropriate type, geometry and volume of fibers to optimize the strength, density and workability of OPSFRC.

3. Previous studies are available on the structural behaviors including flexural and shear strength of OPSC reinforced concrete beams but the number of studies are limited. In addition, there is no study on the structural behaviors of OPSFFRC. The literature review on fiber-reinforced concrete revealed that the use of fibers in concrete improved the structural load capacity and crack resistance of reinforced concrete beams. Hence the comparison between the structural behaviors of OPSC and OPSFRC is necessary to ascertain the applicability of OPSFRC as structural members.

4. High tensile strength is a key property for structural members with special application such as earthquake, impact and blast resistant members. However, low tensile strength is one of the weaknesses of LWC including OPSC. In order to widen the applications of OPSFRC, the development of high tensile strength OPSFRC by using high volume of fibers should be endeavored.

1.3 Research objectives

The research objectives of this thesis are as follows:

1. To study the material properties of oil palm shell (OPS) used for the development of oil palm shell fiber reinforced concrete (OPSFRC).
2. To investigate the effect of synthetic fibers on mechanical properties and density of OPSFRC.
3. To compare the effect of aspect ratio and volume fraction of steel fibers in OPSFRC and to select appropriate fiber for OPSFRC.
4. To evaluate the flexural performance of OPSFRC by using steel fiber.
5. To compare the torsional strength of OPSFRC unreinforced concrete prisms to the OPSFRC reinforced concrete beams.
6. To develop high tensile strength OPSFRC with high volume steel fibers.

1.4 Significance of study

The main advantages of this study could be summarized into the following 2 categories:

1. OPSFRC as LWC with enhanced properties

The core benefit of the OPSC as LWC is the density reduction. The previous studies on OPSC showed that OPSC has a density reduction of about 20-30% compared to NWC. This benefit can further be derived into the cost saving and more flexible design in structural application.

Meanwhile, the addition of fibers in the concrete leads to improved concrete properties. The properties cover from the basic mechanical properties such as

compressive and tensile strengths, modulus of elasticity, Poisson's ratio,. Therefore, the addition of fibers in OPSC in this study aims to develop OPSFRC with combined advantages of LWC and FRC. With the enhanced properties attributed to the addition of fibers, the applications of the OPSC and OPSFRC could be widened.

Some research findings have been published in the past two decades on the enhancement of the mechanical properties of OPSC using different methods including pre-treatment method of OPS (Mannan et al., 2006) and using crushed OPS (Shafigh, Jumaat, Mahmud, et al., 2011). However there is limited study on the utilization of fibers in OPSC and hence more detailed investigation using different types and volume fractions of fibers have been investigated.

2. Enhanced knowledge on the static performance of the OPSC and OPSFRC reinforced beams

After the investigation on the effect of fibers on the mechanical properties of the OPSFRC, the optimum fiber type and amount was determined. The next stage of this research is to study the structural performance of OPSC and OPSFRC beams under flexure and torsion. The flexure and torsion testing increases the understanding of the static performance of OPSC and OPSFRC beams and it serves as a preparation step for the future design of OPSC and OPSFRC. The design codes including BS, ACI and Eurocode do not include provisions on brittleness, low mechanical properties and high ductility of LWC relative to the normal aggregate concrete.

1.5 Scope of work and chapter outline

Chapters 1 and 2 in this research are Introduction and Literature Review, respectively. Chapters 3 to 8 present the main findings of this work. The experimental works are subdivided into four main stages as follows:

(a) Stage 1, which consists of the development of OPSC mix as the control mix design as the fibers are added into the control OPSC mix in latter stage. The scopes of this part are (i) to determine the material properties of OPS and (ii) to carry out trial mixes to optimize the mix design of OPSC. Before the trial mixes are carried out, it is essential to determine the material properties of OPS as the physical properties affect the mix design carried out using specific gravity method. After the material properties of OPS were determined, a series of trial mixes have been conducted to optimize the strength of OPSC before the addition of fiber. The original mix design is modified from the OPSC investigated by Alengaram et al. (2010a) in order to provide a comparison of the structural behavior between OPSC and OPSFRC. Chapter 3 reported both the physical properties and results of trial mixes.

(b) Stage 2, which consist of the development of OPSFRC by the addition of steel and synthetic fibers. In the first part, synthetic fibers of polypropylene, PP fibers (fibrillated and monofilament) and nylon fibers are added into OPSFRC mixes. The volume fractions of each fiber are 0.25%, 0.50% and 0.75%. Effects of hooked end steel fibers were compared in the second part in this stage. The parameters studied for the steel fibers are the aspect ratio (55, 65 and 80) and volume fraction of steel fibers The reason is that the OPS are finer than the grading of the coarse aggregate used in the conventional mix design. Hence the fiber geometry of the steel fibers in OPSFRC has to be studied to provide the optimum anchorage and fiber-matrix bonding which eventually provides the highest improvement on the mechanical properties of OPSFRC.

Similar to the synthetic fibers, the volume fractions studied were 0.25%, 0.50% and 0.75%. Chapters 4 and 5 reported the mechanical properties of synthetic and steel fiber-reinforced OPSC, respectively.

(c) Stage 3 consists of the investigation of the structural behaviors of OPSFRC. After the optimum type of fibers is determined in the Stage 2, the fiber is then applied in the OPSFRC mix to study the flexural and torsional strengths of the OPSFRC reinforced beams. The volume fractions studied were 0.25%, 0.50%, 0.75% and 1.00%. This stage aims to study the applicability of the OPSFRC as structural members. Chapters 6 and 7 investigated the effect of volume fractions of steel fibers on the flexural and torsional behaviors of OPSFRC reinforced concrete beams, respectively.

(d) Stage 4 consists of the development of high tensile strength OPSFRC, by incorporating a higher volume of fibers. After the Stage 3 has proven that the OPSFRC is suitable for structural members, a higher volume of fibers is added into the mix design to further enhance the mechanical properties and flexural behavior of OPSFRC. The volume fraction used is up to 3% which is approaching to the volume limit of fiber-reinforced concrete. This stage is targeted to understand the feasibility of OPSFRC to be further applied as structural members subjected to special loading such as high tensile, torsion or even impact and blast loadings. The experimental results of mechanical properties and flexural behaviors of high tensile strength OPSFRC were reported in Chapter 8.

The flow of the above-mentioned stages is summarized in Figure 1.1. Finally, Chapter 9 concludes the results of this thesis and recommends future works that can be carried out to bring the research on oil palm shell concrete to the fore.

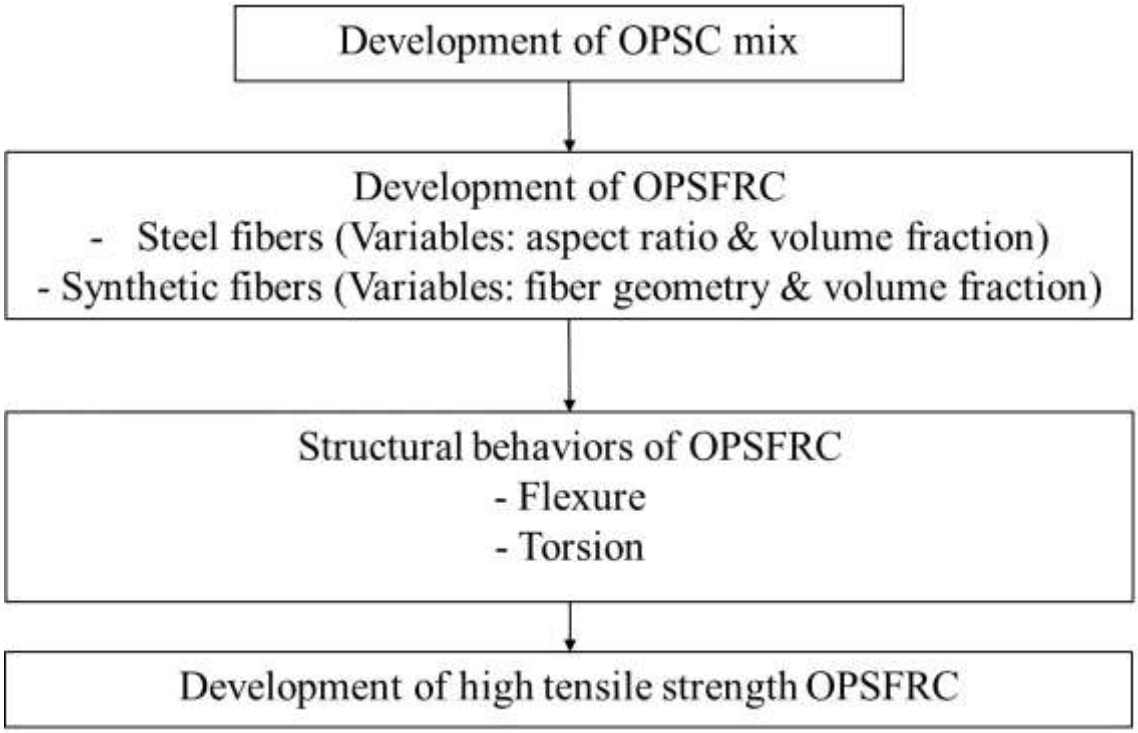

Figure 1.1 Research flow chart

CHAPTER 2

LITERATURE REVIEW

2.1 Lightweight concrete

The recent trend of the building architecture focuses on the concept of economical and space efficient structural members. Lightweight concrete (LWC) had been in use for a long period of time in developed countries and it served the purpose of both structural stability and economic viability (Alengaram et al., 2013). The use of LWC as structural member decreases the dead load of the structure, substantially permits greater design flexibility and cost savings (Alengaram et al., 2010a; Shafigh et al., 2010). Moreover, the green rating for infrastructure and buildings has been increasingly widespread since last decade to accomplish the concept of sustainable buildings. The selection of the green concrete materials from waste materials contributes positively on the sustainable construction, directly (like using asbestos-material) or indirectly (like using recycled materials and diverting them from landfill) (Shafigh et al., 2014). This situation prompted extensive researches on the utilization of waste materials to produce sustainable lightweight concrete. The LWC from waste materials is a relatively new field of concrete and has yet to be explored.

First of all, the key property which distinguish LWC from normal weight concrete (NWC) would be its reduced density. Different classifications are available to define LWC:

1. BS EN 206: 2013 defines lightweight concrete (LWC) as concrete having an oven-dry density (ODD) of not less than 800 kg/m^3 and not more than 2000 kg/m^3 produced using lightweight aggregate for all or part of the total aggregate.

2. ASTM C330/ C330M-02 defines the LWC as the concrete with air-dry density not exceeding 1840 kg/m^3.

3. Mehta and Menteiro (2006) defines structural LWC as a concrete with an oven dry density of no greater than 2000 kg/m^3.

4. Neville (2012) states that the density of LWC is to be between 350 and 1850 kg/m^3.

5. Clarke (1993) and Short & Kinniburgh (1978) defines structural LWC as concrete having density within the range of 1200 to 2000 kg/m^3.

Taking the density of NWC to be 2400 kg/m^3, LWC possess an advantage of at least 17% density reduction compared to NWC. However, the density of LWC for the mentioned classifications covers a wide range of 350 to 2000 kg/m^3. The reason is that the density and concrete properties of LWC is highly dependent on aggregates and cement paste of the LWC (Santhakumar, 2006). The type and content of aggregates used has significant effect on the properties of LWC, as the aggregates have different physical properties including shape, surface, bulk density, stiffness and etc. It is extremely challenging to provide a specific design method for concrete mixes with different lightweight aggregates. For example, the increase in the cement content of LWC produced a denser cement matrix, but substantially increases the density and strength of LWC. In addition, some variations in casting methodology may arise where the LWC are not fully compacted and the partial compaction is difficult to be reproduced (Santhakumar, 2006; Short & Kinniburgh, 1978). Judging from the complexity to classify the LWC, it is essential to understand the type of LWC in order to select the appropriate classification.

There are three main types of LWC, which can be differentiated by the methods to produce voids within the LWC (Santhakumar, 2006; Short & Kinniburgh, 1978):

1. *No-fines concrete*, at which the finer sized aggregates are omitted from the aggregate grading to induce voids within the concrete, with partial compaction.
2. *Aerated concrete*, which is produced by creating air bubbles in the cement matrix to produce large air voids in the cement matrix by partial compaction.
3. *Lightweight aggregate concrete*, which is a concrete with the partial or full replacement of gravel aggregates by porous lightweight aggregates.

Among the three types of LWC, both no-fines concrete and aerated concrete are mainly used only for non-load bearing structural members such as walls and partitions. This is due to the fact that the voids increases the sound and thermal insulation abilities of the LWC walls, but decreases the strength of the LWC. In addition, both the no-fines concrete and aerated concrete are made using partial compaction but the partial compaction is difficult to be reproduced. On the other hand, the lightweight aggregate concrete which is produced by complete compaction like NWC is more widely used in load bearing structural and non-structural members. The lightweight aggregate concrete outperforms another two LWC by producing higher strength and consistency. Hence the lightweight aggregate concrete is generally denoted for LWC directly, as such stated in BS EN 206.

2.1.1 Lightweight aggregate concrete

The utilization of lightweight aggregates with high porosity enables the production of LWC. The examples of such lightweight aggregates are oil palm shell (OPS), coconut shell, furnace clinker, pumice, volcanic tuff, volcanic slag, diatomite, vermiculite, expanded clay, expanded slag, pulverized fuel ash, corn cob, tobacco waste, furnace bottom ash and wood particles (Arisoy & Wu, 2008; Chandra, 1996; Santhakumar, 2006; Shafigh et al., 2014; Short & Kinniburgh, 1978). The reason of the increasing research interests on LWC lies within the numerous benefits of LWC. It has been previously mentioned that the use of LWC allows for cost savings and greater design flexibility. The reduced density of LWC relative to the NWC permits smaller cross sections and longer span of a structural member, substantially reduces the reinforcing steel requirement and the costs on scaffolding, framework and foundation, as well as the cost of transport and erection. Furthermore, LWC also achieve improvement in properties compared to NWC such as fire and frost resistance, heat and sound insulation, earthquake damping ability (Alengaram et al., 2013; Gao et al., 1997; Libre et al., 2011; Shafigh et al., 2010). Furthermore, the use of LWC surpassed NWC in the case of insufficient soil bearing capacity (Mehta & Menteiro, 2006). Mehta and Menteiro (2006) showed that a 52-storey structure was made with LWC mixture of 1840 kg/m^3 density and 41.2 MPa compressive strength could be built on a land with limited soil bearing capacity instead of a 35-storey NWC structure using NWC.

The vast and expanding construction industry in developing countries is facing the rapid depletion of conventional concrete materials such as granite aggregate and mining sand. It is predicted that the world's demand on concrete will be increased to 18 billion tons per year by 2050 (Mehta & Menteiro, 2006). Under such circumstances, the huge concrete demand will result in a considerable increase in the demand for energy

and natural resources including water, energy, food, river sources, common goods and services (Rosković & Bjegović, 2005). Furthermore, the blasting of granite boulders and sand mining caused severe environmental problems including air, water, and soil contaminations. The material scarcities and pollution issues from extraction processes created an ecological imbalance and prompted the necessity to produce a greener and sustainable concrete. Therefore, the recent trend of the research also focuses on the utilization of waste materials originated from both agricultural and industrial activities. Among the mentioned lightweight aggregates, the OPS, pumice and clinkers are gaining increasing attentions as potential candidates to replace coarse aggregates to produce LWC. The utilization of waste materials in the concrete production paves way for the production of sustainable LWC as it could solve the issues on both the materials scarcity and pollution problems associated with the extraction process of virgin materials, while cost saving is also an add-on advantage of LWC (Yildiz et al., 2012). Agricultural wastes are normally destroyed or disposed in the environment. Salvaging them in the form of aggregates for concrete production is one of the environmental benefits that will be recognized by most of the sustainability rating system. It serves to be a breakthrough to make the construction industry to be more environmentally friendly and sustainable (Shafigh et al., 2014).

2.2 Oil palm shell concrete

The recent researches for converting palm oil into biodiesel and the need for vegetable oil globally have increased the production of palm oil, especially in the palm oil producing countries, such as Indonesia and Malaysia. The production of palm oil also increases the wastes generated from the palm oil extraction processes and these wastes include oil palm shell (OPS), empty fruit bunches, palm oil fuel ash (POFA), fibers,

palm trunks and more. Being the second largest palm oil production country, Malaysia produces 4 million tons OPS as waste annually (Alengaram et al., 2013). The common way of handling the OPS waste is by uncontrolled dumping in open air spaces. Figure 2.1 shows an example of open disposal of OPS in empty compound of a palm oil factory in Selangor, Malaysia. The open disposal eventually causes storage problems such as insufficient storage space in addition to environmental pollutions. The residual palm oil in the OPS might leach into the ground and substantially polluted the surrounding land and underground water.

Figure 2.1 Open dumping of oil palm shell in open space of palm oil factory

Different approaches have been applied to solve the vast generation of the palm oil wastes. One of the solutions is the combusting the palm oil wastes including OPS, palm trunk, palm leaves and fruit bunches in boiler to generate power (Foo & Hameed, 2009). Other uses of OPS are as granular filter material for water treatment, floor roofing and road based material (Alengaram et al., 2013; Basri et al., 1999). However, the research interest has been focused on utilizing OPS as one of the potential lightweight aggregates in the development of LWC, attributed to its lightweight

characteristics, good aggregate impact value (AIV) and good Los Angeles abrasion resistance (Jumaat et al., 2009; Mannan & Ganapathy, 2004). The early researches on the utilization of OPS as replacement of coarse aggregate was pioneered by Abdullah (1984). Abdullah (1984) replaced the normal weight aggregates with lightweight OPS to produce a LWC called Oil Palm Shell Concrete (OPSC) with density and compressive strength within the range of 1750–2050 kg/m^3 and 5–20 N/mm^2, respectively. In the other hand, Okafor (1988) and Okpala (1990) also reported that OPS is applicable to structural-grade OPSC with the maximum compressive strength of approximately 25–30 MPa. Hence the latter researches had been presented on the OPSC.

2.2.1 Compressive strength and density

During the last decade, there have been many research works on OPSC pertaining to strength enhancement, durability and structural behavior. These researches from Malaysia showed that LWC with a density and compressive strength in the range of 1700-1850 kg/m^3 and 5-30 MPa, respectively could be produced by using OPS as coarse aggregate (Basri et al., 1999; Mannan et al., 2002, 2006; Mannan & Ganapathy, 2001a, 2001b, 2002, 2004; Teo, Mannan, & Kurian, 2006; Teo , Mannan & Kurian, 2006, 2009; Teo et al., 2007). Considering the density of NWC is 2400 kg/m^3, the reported density of OPSC produced a density reduction of about 20-30% compared to NWC. Hence it prompted the application of OPSC is structural members such as footbridge and single storey house as shown in Figure 2.2. Both structures were built in the year of 2003 and they are still being used up to now.

Figure 2.2 (a) Footbridge and (b) single-storey building made from oil palm shell concrete (Teo et al., 2006)

However, Haque et al., (2007) suggested that it would not be wise to use LWC with a compressive strength of less than 50 MPa. Hence, the latter research interest on OPSC has been concentrated on the strength development of OPSC by different methods. The reason for the study is that the failure of the OPSC is mainly caused by the weak adhesion between OPS and cement paste (Alengaram et al., 2010b; Mannan & Ganapathy, 2004; Okpala, 1990; Shafigh et al., 2011a). The convex and smooth surfaces of bigger OPS shells produced weaker aggregate-paste bonding (Alengaram et al., 2010b). Mannan et al. (2006) investigated different pre-treatment methods to improve the quality of OPS aggregates. They reported that among different solutions, the PVA solution coating formed a thin layer on the OPS surface and this prevented water from infiltrating, eventually increased the compressive strength of OPSC.

The second method proposed to enhance the strength of OPSC is by the incorporation of supplementary cementitious materials. Alengaram et al. (2010a) incorporated 10% silica fume to produce OPSC of compressive strength of 37 MPa with density of 1850 kg/m^3. The silica fume was added into OPSC mixes to improve the

OPS-cement paste bond and the strength of OPSC by the reaction between the silica fume with the liberated calcium hydroxide produced calcium silicate and aluminate hydrates. The compressive strength of OPSC was further improved to 45 MPa with the use of lower water to binder ratio and cement content of 0.30-0.33 and 550 kg/m^3, respectively (Mo et al., 2014b; Shafigh et al., 2013). The use of lower water to binder ratio and higher cement content resulted in a denser OPSC with air-dry density of about 1900-2000 kg/m^3. In another study from Shafigh et al., (2013), the OPSC with density and compressive strength of about 1950 kg/m^3 and 42.5 MPa was achieved by the use of cement content of 500 kg/m^3. Moreover, they have reported by replacing cement content by ground granulated blast furnace slag (GGBFS) up to 70%, grades 30 and 35 OPSC can be produced. In this case, a green structural LWC was produced with about 50% of its concrete volume consists of waste materials.

The third method to improve the strength of OPSC is by varying the aggregate size of OPS. The study from Alengaram et al. (2010b) on the effect of aggregate size on the compressive strength of OPSC showed that both fracture of OPS and aggregate-cement paste bonding governed the failure of specimens. Smaller-sized produced better aggregate-cement paste bond compared to the larger-sized OPS. Hence the following published papers were focused on the use of crushed OPS with smaller-sized OPS (Shafigh et al., 2011a, 2011b, 2012a, 2012b). Shafigh et al. (2011a) used crushed OPS between the 2.36-9.5 mm to produce high strength LWC with compressive strength up to 53 MPa. By crushing the larger size OPS aggregates, the total broken edges of OPS increases. These rough and spiky edges produce stronger physical bond between the OPS and the hydrated cement paste compared to uncrushed OPS, hence results in a higher compressive strength (Shafigh et al., 2011a; Shafigh et al., 2014). However the

density of the OPSC produced by using crushed OPS were found within the range of 1850-2000 kg/m^3 and the densities were approaching the density limit of LWC.

The final approach to improve the strength of OPSC is by the addition of fibers. Shafigh et al. (2011c) studied the effect of hooked end steel fibers up to 1% by volume on the mechanical properties of the OPSC. The 28 day compressive strength of steel fiber-reinforced OPSC was found in the range of 41–45 MPa, compared to the 39 MPa in the non-fibrous OPSC mix. However the increase in the compressive strength was associated with the significant reduction in the slump and density increase in the OPSC. However, the air dry density of the OPSC reinforced with 1% steel fiber was found within the range for structural lightweight concrete.

2.2.2 Fresh properties

The fresh properties of the LWC are different from that of NWC. A high slump value of LWC will result in the floating of the lightweight coarse aggregates away from the heavier cement mortar, which then leads to poor finishing and compaction. Moreover, LWC does not require high slump to perform like the normal aggregate concrete, because the work done by the gravity on the lightweight aggregate is lower (Hossain, 2004). Both reasons prompted the ACI 213R-87 to limit the maximum slump of LWC to 100 mm in order to achieve good surface (Mehta & Menteiro, 2006). Mehta and Menteiro (2006) stated that a slump value within the range of 50-75 mm is sufficient for the LWC to achieve good compaction which is compatible for the workability of 100–125 mm in NWC. The slump value out of this range is not favored as it affects flow ability, compaction and finishing. In addition, the workability of fresh concrete and bonds between aggregates and mortar phase are influenced significantly by physical properties such as roughness, shape and texture of aggregates. The bond is the

development of anchorage and it depends on the roughness and porosity of the surface of aggregate (Mannan & Ganapathy, 2004). Moreover, the high porosity and water absorption of the lightweight aggregates further increase the difficulty to control the workability of LWC. The lightweight aggregates will absorb and reduce the effective water content designated for the hydration and substantially reduces the workability of the LWC.

The published literature on OPSC reported that OPSC produced poor workability with slump value below 10 mm (Mannan & Ganapathy, 2001a; Okafor, 1988; Okpala, 1990), without the use of superplasticizer. Moreover, the air content in the fresh OPSC is higher than the normal concrete (Mannan & Ganapathy 2001a, 2004). The rough, flaky and irregular shapes of OPS obstructed the full compaction of fresh OPSC. In addition, the OPS are porous and have high water absorption, these may cause a higher air entrapment in fresh concrete (Mannan & Ganapathy, 2004). However, the low slump and high air content in OPSC were shown to be able to be compensated by the addition of fly ash and superplasticizer (Alengaram et al., 2010a, 2010b; Mannan & Ganapathy, 2004). Hereafter the use of superplasticizer is vital in the mix design of OPSC in order to achieve uniform compaction in the fresh OPSC. Shafigh et al. (2011b) also reported that to achieve the better workability for OPSC, it needs more time for mixing of about 15-30 minutes.

By improving the workability and compatibility of the mixture, the strength of the interfacial transition zone tends to improve and, thus, improves the strength of the concrete (Shafigh et al., 2011b). Shafigh et al. (2011b) reported that the slump increased slightly when the maximum size of OPS aggregate was changed from 9.5 mm to 12.5 mm. In addition, other studies on the use of supplementary cementitious materials revealed that the application of supplementary cementitious materials including rice

husk ash and palm oil fuel ash produced lower workability of concrete attributed to their high specific surface area and high carbon content (Hwang et al., 2011; Tay & Show, 1995). Meanwhile the addition of fibers into the cement matrix also reduced the workability of fresh concrete. Therefore, it is important to take account for the workability of OPSC when applying the enhancement approaches mentioned in Section 2.2.1.

2.2.3 Tensile strength

Most of the LWC have inferior mechanical properties especially tensile strength. LWC is also more brittle than the NWC of the same compressive strength (Arisoy & Wu, 2008; Gao et al., 1997; Hassanpour et al., 2012; Mo et al., 2014c). The LWC with higher brittleness is more prone towards catastrophic failure that occurs without much warning and this could be hazardous to the surroundings (Mo et al., 2014c). Hence, the tensile strength is an important property that affects the safety and serviceability of concrete. ASTM: C330/C330M-09 specified that the structural LWC requires a minimum splitting tensile strength of 2.0 MPa. The published works on OPSC showed that splitting tensile and flexural strengths were found in the range of 2.0-2.6 MPa and 3-6 MPa, respectively (Alengaram et al., 2011; Alengaram et al., 2010a; Mannan & Ganapathy, 2002; Okafor, 1988; Shafigh et al., 2012b; Teo et al., 2006; Teo et al., 2007). The reported splitting tensile strength of OPSC slightly exceeded the minimum requirement of splitting tensile strength of LWC and fell within the range of the splitting tensile strength of LWC at 1.8–2.7, 2.2–3.3 and 2.5–3.8 MPa corresponding to cube compressive strengths of 30, 40 and 50 MPa, respectively (Shafigh et al., 2012b). However, the splitting tensile and flexural strengths of OPSC were found 60% lower than NWC. The low tensile strength of OPSC might lead to significant tensile cracking to occur at a much lower loading capacity compared to the NWC and hence LWC with

high tensile strength is desirable for the structural design to arrest tensile cracking. Hence, the enhancement of the mechanical properties, especially the tensile strength of OPSC, becomes the priority issue for the development of OPSC

2.2.4. Durability

Though LWC is advantageous in both economic and environmental aspects, the uses of LWC particularly OPSC in structural applications are not well established compared to NWC or high strength concrete. This is mainly attributed to the questionable reliability and durability properties of OPSC as OPS are originated from agricultural wastes which contain organic compounds. The OPS are subjected to the risk of decomposition over time and hence the study on the long term durability of OPSC is essential to convince the construction application of OPSC as structural members. Hence, in order to apply LWC for structural purpose, the LWC has to be durable and exhibit adequate strength, ductility or a combination of three (Arisoy & Wu, 2008).

Pre-treatment is necessary for OPS aggregate before using in concrete because it contains dust and oil coating after the palm oil extraction process (Mannan & Ganapathy, 2004). Okafor (1988) presented a method to remove the fibers and oil on the OPS by air drying the OPS for a period of more than 6 months. Then the OPS was washed with detergent to remove the oil coating and other impurities. The pre-treatment was being applied in all the researches on OPSC (Alengaram et al., 2008; Alengaram et al., 2010a; Mannan et al., 2006; Mannan & Ganapathy, 2001a, 2004; Shafigh et al., 2011a, 2011b). In addition, it was shown that the water absorption and water permeability of OPSC concrete were also comparable to other lightweight concretes with pumice and the water absorption and water permeability are dependent on the curing conditions (Teo et al., 2007). The permeability of concrete has a high bearing on

the concrete durability as it controls the penetration rate of moisture that may contain harmful or aggressive chemicals, which causes steel reinforcement corrosion embedded in the concrete. In another study, OPSC showed 14% and 12-40% higher drying shrinkage and initial surface absorption, respectively, compared to control NWC (Mannan & Ganapathy, 2002). The reason for the higher water absorption and shrinkage in OPSC is attributed to the high porosity of OPS. This statement was supplemented from the microscopic analysis using scanning electron microscope by Alengaram et al. (2011) as shown in Figure 2.3. The tiny pores of size in the range of 16–24 lm on the convex surface of OPS that are responsible for high water absorption. Hence Mannan et al. (2006) used polyvinyl alcohol (PVA) solution to treat the OPS; the coating of PVA solution around OPS reduced the water absorption to 4% compared to uncoated OPS that has absorption as high as 25%. Mannan and Ganapathy (2001a) also investigated compressive strength up to 365 days of OPSC prepared using OPS in saturated surface dry (SSD) condition and they reported that OPSC had no retrogression in strength due to different curing conditions.

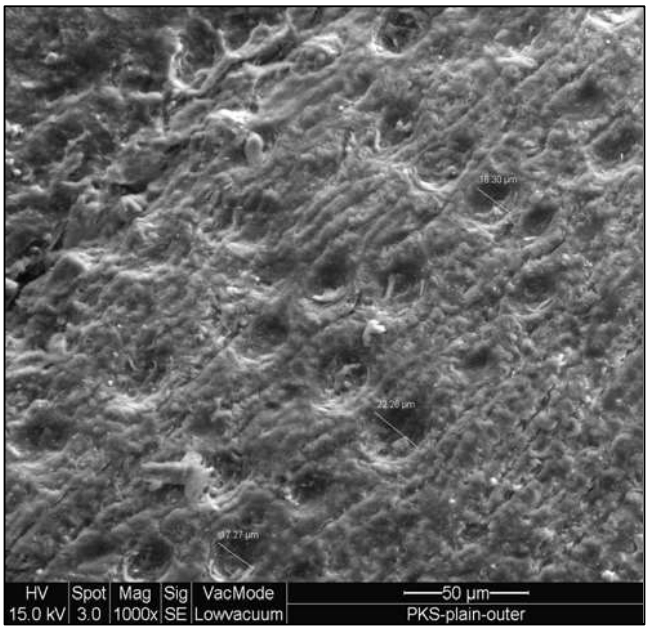

Figure 2.3 Microscopic of surface pores of OPS (U. Johnson Alengaram et al., 2011)

2.2.5. Bond property and structural behaviors

The bond strength is imperative in reinforced concrete, as it enables the concrete and reinforcement to act as a unit to bear the tensile force. The published papers on OPSC also showed that the bond strength of the OPSC is comparable to the bond strength of other lightweight aggregate concretes including lightweight sawdust and Lytag (pulverized fuel ash) concretes. The bond strengths of plain and deformed bars in OPSC were 10–24% and 24–42% of the compressive strength, respectively. The plain bar failed by bar pullout while the deformed bar failed by cracking from the concrete cover. The failure was very sudden with the formation of longitudinal cracks. When the cracks materialized, the bond forces were directed outward from the bar surface and these forces caused anchorage failure by splitting off the confining concrete (Teo et al., 2007). In addition, the experimental results from Alengaram et al. (2010a) reported that the ultimate bond stresses of OPSC were nearly 2½ times higher than the theoretical values calculated based on BS-8110.

In terms of structural behavior, OPSC showed enhanced performance in flexure and shear compared to NWC (Alengaram et al., 2008, 2011). Flexural beam tests carried out by Alengaram et al. (2008) and Teo et al. (2006) showed ductile failure in OPSC beams with more but smaller cracks and higher deflection, compared to NWC. The ductility ratio of OPSC was twice that of NWC (Alengaram et al., 2008). The ultimate moments and deflections at service load predicted using BS 8110 provides a conservative estimate for OPS concrete beams up to a reinforcement ratio of 3.14%, with experimental ultimate moments of approximately 4% to 35% higher compared to the predicted moments (Teo et al., 2006). Moreover, both studies also presented that the crack width at service load of OPSC beams did not exceed the limiting value of 0.3 mm as stipulated by BS 8110 for durability requirements and OPSC beams also showed shorter and narrower cracks with rough surfaces. In another study on shear strength of OPSC beams, the OPSC beams produced 24% higher shear strength than the corresponding NWC. The shorter narrower cracks with rough surfaces in the OPSC beams showed good aggregate interlock that enhanced the shear strength of the OPSC (Alengaram et al., 2011).

However, the published papers on OPSC beams only limited to OPSC with relatively lower compressive strength of 25-35 MPa. Teo et al. (2006) suggested that the OPSC can be used to produce low-cost structures such as single storey house and footbridge as shown in Figure 2.2. There is no study on the structural behaviors of OPSC of higher strength to further expand the structural applications of OPSC such as in high rise building.

2.2.6. Other application of OPS

Other than utilizing the OPS to produce LWC called OPSC, the OPS was also studied in other applications, including foamed concrete and geopolymer. Non-structural grade oil palm shell foamed concrete of oven-dry density ranging from 1100 to 1600 kg/m^3 was produced by inducing foam inside the OPSC. Non-structural grade oil palm shell foamed concrete with a density of 1100 kg/m^3 showed the lowest thermal conductivity of 0.40 W/m K, which is 33% and 56% lower than the conventional materials – block and brick – respectively (Alengaram et al., 2013). Moreover, the experimental results on shear beams also indicated that the shear capacities of oil palm shell foamed concrete beams without shear links are higher than those of the NWC beams and they exhibited more flexural and shear cracks (Jumaat et al., 2009). Other than that, the OPS was used as lightweight aggregate to produce lightweight geopolymer which used fly ash, palm oil fuel ash and ground granulate blast furnace slag as binders (Islam et al., 2014; Kupaei et al., 2013; Liu et al., 2014; Ranjbar et al., 2014). The OPS lightweight geopolymer gains significant environmental benefit by reducing carbon dioxide emission due to the cement hydration as there is no cement used in the geopolymer, in addition to the benefits of LWC. However, the compressive strength of both OPS foamed concrete and OPS geopolymer are non-structural grade with compressive strength lower than 35 MPa.

2.3 Fiber-reinforced concrete

Section 2.2.1 discussed the enhancement methods to improve the compressive strength of OPSC throught (i) pre-treatment of OPS; (ii) incorporation of cementitious materials; (iii) crushing of OPS and (iv) addition of fibers. In the case of NWC and LWC, fiber reinforcement is the best method to enhance the concrete properties, particularly in LWC which is weaker in mechanical properties relative to NWC (Hassanpour et al.,

2012). However, the concrete properties of fiber-reinforced lightweight concrete (FRLWC) depends on the types and amount of fibers and lightweight aggregates used. Hereafter the effects of different fibers in LWC are being discussed, aiming to provide a better understanding on the fiber-lightweight concrete composites. Firstly, the types of fibers are compared for the optimization of fiber selection.

2.3.1. Types of fibers

Table 2.1 shows the examples of fiber from a number of studies, including steel, polypropylene, polyester, polyvinyl alcohol, nylon, glass, carbon, palm and coconut fibers.

(a) Steel fiber

Among the fibers available, steel fiber is preferred by the researchers and construction industry due to its significant contribution on the enhancement of the concrete properties. The reason for the good performance of steel fiber-reinforced concrete is the high tensile strength of steel fiber. The tensile strength of commercially-used steel fiber (Table 2.1) is about 1100 MPa and can be increased up to 2000 MPa in high carbon steel fiber. The range of fiber length for the steel fiber is 20-60 mm. Studies have showed that the steel fiber with higher length or aspect ratio contributed in further improvement in bonding and tensile strength compared to shorter fibers (Gesoğlu et al., 2013). Other than that, the high specific gravity of steel fiber of about 8 relative to other fibers such as polymer and carbon fibers could lead to a drastic increase in the concrete density (Libre et al., 2011). Finally, the high melting point of steel fiber at about 800^{o}C was proven to improve the fire resistance. However, one of the drawbacks of steel fiber

is its risk of corrosion. When exposed to moisture, the steel fiber is subjected to high risk of oxidation, at which the water is essential for the hydration process.

(b) Polymer fiber

Polypropylene fiber is another well-established material to be utilized in cement-fiber composite system. The tensile strength of polypropylene covers a wide range of 35-750 MPa (Table 2.1) and the reason is that the polypropylene fibers are fabricated into different geometries such as monofilament, fibrillated, straight stick (like steel fiber) and more. One of the noteworthy properties of polypropylene fiber is its low melting point (160-180^{o}C). Though the polypropylene fibers melts at low temperature when subjected to fire, the melted polypropylene serves to reduce the explosive spalling. Therefore, this fiber reinforcement is popular among researchers studying the fire resistance properties of polypropylene fiber-reinforced concrete.

Compared to the steel fiber, the polymer fibers like polyester and polypropylene fibers are effective to prevent the negative effects of corrosion, alkaline reactions, acidic water, salts, chlorine, chemicals and microorganisms. They also have water repellent properties which contributes to maximum adhesion (Bolat et al., 2014). Other polymer fibers including polyester, polyvinyl alcohol, polyolefin and nylon (Table 2.1) produced similar physical properties compared to polypropylene fibers and they are gaining considerable research interests within the past decade. The shortcomings of polymer fibers are higher manufacturing cost and less effective improvement compared to addition of steel fibers.

(c) Glass/ Carbon fiber

Glass fiber is a newly developed material which gains considerable attention in concrete research as it shows comparable properties compared to steel fiber (Table 2.1). Carbon fiber exhibits higher tensile strength (~4000 MPa) than steel fiber (Table 2.1). Other than offering superior properties, the glass and carbon fibers also do not corrode like steel fiber. However, manufacturing cost of these two fibers are particularly high and hence the development of glass/carbon fiber-concrete composite is limited.

(d) Natural fiber

The applicability of natural fibers like palm and coconut fibers are also studied (Table 2.1). The natural fiber-reinforced concrete gains the benefits from its significant impact on the sustainable concrete as the natural fibers are wastes generated from agricultural processes. However, the research on natural fiber reinforcement remains modest due to the organic nature of these fibers. The utilization of natural fibers in concrete raises the concern on the decomposition of these organic matters with time. In addition, the properties of natural fibers exhibit big variations as the fibers are generated from different plant species and origins.

Table 2.1 Examples of fibers and their respective physical properties

No.	Fibers	Length (mm)	Diameter (mm)	Specific gravity	Tensile strength (MPa)	Modulus of elasticity (GPa)	Melting temperature (ºC)	Reference
1	Steel 	20-60	0.45-0.90	7.8-8.0	1100- 2000	170-200	800	(Bolat et al., 2014; Dawood & Ramli, 2012; Giner, et al. 2012; Libre et al., 2011; Olivito & Zuccarello, 2010; Topçu & Canbaz, 2007)
2	Polypropylene 	6.35-35	0.016-0.1	0.90-0.95	35-750	3.8-4.2	160-180	(Banthia & Gupta, 2006; Bilodeau, et al. 2004; Bolat et al., 2014; Çavdar, 2012; Corinaldesi & Moriconi, 2011; Kakooei et al., 2012; Libre et al., 2011; Shihada, 2011; Song, et al., 2005; Topçu & Canbaz, 2007)
3	Polyester 	12-30	0.03-0.035	1.34-1.40	400-800	8.417.2	253-260	(Bolat et al., 2014; Kakooei et al., 2012; Siddique, Kapoor, Kadri, & Bennacer, 2012)

Table 2.1 Examples of fibers and their respective physical properties (Cont'd)								
4	Polyvinyl alcohol 	12-15	0.037-0.2	1.30	900-1400	23-40	>200	(Arisoy & Wu, 2008; Çavdar, 2012; Corinaldesi & Moriconi, 2011; Hamoush et al., 2010)
5	Polyolefin 	50	-	0.91	470	46.3	-	(Won et al., 2008)
6	Nylon 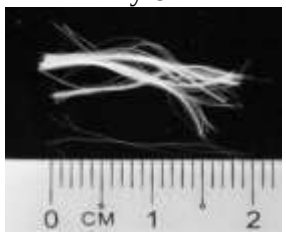	19	0.03	1.13	300-900	5.17	225	(Song et al., 2005)

Table 2.1 Examples of fibers and their respective physical properties (Cont'd)								
7	Glass 	12	0.135	2.7	1200-1700	72-73	860	(Çavdar, 2012; Kakooei et al., 2012; Mirza & Soroushian, 2002)
8	Carbon 	3.5-12	0.007	1.76	3800-4200	240	3500	(Çavdar, 2012; Giner et al., 2012)
9	Palm	30	-	1.24	21.2	-	-	(Dawood & Ramli, 2012)
10	Coconut	18-36	-	-	12-24	-	-	(Ali & Chouw, 2013)

2.3.2. Benefits of fibers in lightweight concrete

The incorporation of fibers into the concrete matrix is widely accepted for its significant effect to enhance the concrete properties. The most distinct effect is to improve the strength and toughness of concrete and transform the brittle LWC to a ductile material (Hassanpour et al., 2012). Hence, fiber-reinforced LWC has been applied in tunnels, wall claddings, bridge decks, pavements, precast tunneling materials and repair materials for rehabilitation and strengthening of existing concrete structures (Balendran et al., 2002; Meda et al., 2012). These advantages of fiber addition have prompted the increasing researches on FRLWC. After the introduction of the types of fibers in previous section, the following sections will focus on the effects of these fibers on the different concrete properties.

2.3.2.1 Workability

The fresh properties of the LWC are different from that of NWC. A high slump value of LWC will result in the floating of the lightweight coarse aggregates away from the heavier cement mortar, which then leads to poor finishing and compaction. Moreover, LWC does not require high slump to perform like the normal aggregate concrete, because the work done by the gravity on the lightweight aggregate is lower (Anwar Hossain, 2004). Both reasons prompted the ACI 213R-87 to limit the maximum slump of LWC to 100 mm in order to achieve good surface (Mehta & Menteiro, 2006). Mehta & Menteiro (2006) stated that a slump value within the range of 50-75 mm is sufficient for the LWC to achieve good compaction. The slump value out of this range is not favored as it affects satisfactory flowability, compaction and finishing. In addition, the high porosity and water absorption of the lightweight aggregates further increase the difficulty to control the workability of LWC. The lightweight aggregates will absorb

and reduce the effective water content designated for the hydration and substantially reduces the workability of the LWC.

The addition of fibers into the LWC changes the design philosophy on the workability of LWC. Fiber-reinforced normal aggregate concrete generally exhibit lower workability than non-fibrous normal aggregate concrete. The presence of the fibers in normal concrete changed the concrete matrix by forming a fiber network. The network then restricts the flowability of the concrete and hence reduced workability is obtained (Atiş & Karahan, 2009; Dawood & Ramli, 2012; Topçu & Canbaz, 2007). Therefore the conventional slump value cannot indicate the workability of fiber-reinforced concrete and alternative workability test methods has to be applied. Such methods include inverted slump cone, vebe test and compaction factor (Hassanpour et al., 2012; Libre et al., 2011; Topçu & Canbaz, 2007).

The addition of fibers induces negative effect on the workability of the normal aggregate concrete; however, in the case of LWC, the fiber reinforcement is advantageous. The fibers form a network structure in concrete, at which can effectively restrain the segregation of lightweight concrete from the mortar and improve the concrete uniformity and stability (Chen & Liu, 2005; Libre et al., 2011). In addition, due to larger surface area than aggregates, fibers need to adsorb a lot of cement paste to wrap around, eventually increases the viscosity of the mixture (Chen & Liu, 2005). Therefore, this explains why the compaction of the concrete remains satisfactory even though many FRLWC mixes achieved very low or even zero slump.

Despite the benefits of fibers on the workability of FRLWC, the main challenge retains on the design of FRLWC with desired workability. It has been previously mentioned that 50-75 mm slump is sufficient for the LWC, but the degree of decreased workability of FRLWC depends on the type and amount of fiber and superplasticizer used. Chen & Liu (2005) reported that for fixed volume content of fibers, different types of fibers produced different effects on the workability of high strength lightweight aggregate concrete from expanded clay. The slump of the concrete without fibers is 180 mm but reduced significantly by 20.8% and 54.2% to 140 mm and 30 mm upon addition of polypropylene and steel fibers, respectively. The slump loss in the steel fiber-reinforced concrete is much higher than the polypropylene and carbon fibers. Furthermore, Libre et al. (2011) conducted the inverted slump cone test on LWC from natural pumice and showed that the fluidity of concrete was reduced significantly after addition of fibers. Their experimental results showed that the discharging time of plain concrete is 22 s while the addition of 0.4% polypropylene fibers increased the discharging time up to 67 s. In the case of steel fibers, addition of 0.5% and 1% fibers increased the discharging time to more than 120 s. Moreover, study from Mazaheripour, et al. (2011) also pointed out that the addition of polypropylene fibers reduced the slump flow and filling height in U-box test, as well as increased the V-funnel time of expanded clay self-compacting concrete remarkably. In another study by Dawood & Ramli (2012), it is observed that the use of 2% steel fibers reduced the slump flow from 650 mm to 550 mm in spite of raising the superplasticizer content from 1.8% to 2.2%; while palm fiber and Barchip fiber produced less reduction than steel fiber. The common finding from the above discussions is that the steel fiber reinforcement reduced the workability at the most extent, compared to other type of fibers including polypropylene, palm and Barchip fibers.

However, one of the drawbacks of the fiber reinforcement is the "balling effect" at which the fibers tend to agglomerate within the fresh mixes under the conditions of low water content or poor fiber dispersion. To overcome the balling effect, a certain amount of superplasticizer could be added to improve the workability of FRLWC and fiber dispersion and to reduce the balling effect (Hassanpour et al., 2012). Campione, Miraglia, and Papia (2001) showed that good workability of the steel fiber-reinforced LWC from pumice and expanded clay was obtained by adding 1.5% of superplasticizer by cement weight. Nili & Afroughsabet (2012) also mentioned that a minimum of 1% superplacticizer was needed to adjust for the presence of the steel fiber specimens.

2.3.2.2 Density

Density is the most important requirement for the classification of LWC. However, the addition of steel fiber yields negative effect on the density of LWC due to the high specific gravity of steel fiber (~ 8.0) (Bolat et al., 2014; Düzgün et al., 2005; Gao et al., 1997; Libre et al., 2011; Shafigh et al., 2011c). Studies from Libre et al. (2011) and Gao et al. (1997) reported that the incorporation of 1% and 2% steel fiber, respectively raised the density of both pumice concrete and expanded clay concrete by about 120 kg/m^3; while Düzgün *et al*. (2005) showed that a volume of 1.5% steel fiber increased the density of pumice concrete by 6.5%. There is a case where the addition of 0.75% steel fiber which results in the density of OPSC increased beyond the density limit of 2000 kg/m^3. Therefore the steel fiber-reinforced LWC has to be designed properly in order to meet the density requirement of LWC. Gao et al. (1997) proposed a numerical equation (Eq. 2.1) to predict the density of steel fiber-reinforced LWC with respect to volume fraction and aspect ratio of steel fiber:

$$D_c = D_m (1+V_f) + D_s V_f \quad (2.1)$$

where D_c is the density of steel fiber reinforced high-strength, lightweight concrete; D_m is the density of high-strength, lightweight concrete, D_s is the density of steel fiber and V_f is the volume fraction of steel fiber. From the equation, it can be seen that the density of FRLWC depends on the volume fraction of steel fiber, where the increased density of FRLWC is mainly attributed to the high specific gravity of steel fiber. However, it is also showed that increasing the aspect ratio of steel fiber would create mixing problems and may result in concrete of a lower density (Gao et al., 1997). The long steel fibers has high tendency to clog together and eventually entrap air within the concrete.

In order to prevent the density of FRLWC to exceed the density limit, Hassanpour et al. (2012) and Gao et al. (1997) recommended the maximum steel fiber content to be 1% and 2.5%, respectively, or the use of synthetic fiber and steel-synthetic hybrid fibers. A higher quantity of steel fiber usually yields heavier concrete, and contrariwise, synthetic fiber produces lighter concrete (Bolat et al., 2014). The observation follows the explanation from previous discussion at which the fibrillation produced the polypropylene with larger thickness and the fibrillated polypropylene fibers are easier to clog and entrap air bubbles within the concrete matrix. In the case of synthetic polymer fibers, the shape and geometry of fiber affect the density of LWC. The effect of polypropylene fiber in the hybrid fiber system is evident to reduce the density of FRLWC based on the study of Mo et al. (2014a). The oven-dry density of 1% steel fiber-reinforced oil palm shell concrete was found about 1900 kg/m^3, the partial replacement of the fibers by 0.1-0.4% polypropylene in the fiber hybridization system resulted in a decreased density. Moreover, the 0.6% steel-0.4% polypropylene hybrid fibers produced similar density with the non-fibrous oil palm shell concrete.

2.3.2.3 Compressive and tensile strengths

The effects of different fibers in the compressive and tensile strengths of different LWC are summarized in Table 2.2. The effectiveness of fibers depends strongly on the type of lightweight aggregate, then secondly on the fiber (Domagała, 2011). Based on Table 2.2, the steel fiber reinforcement imparted significant improvement of compressive strength (95%), splitting tensile strength (105%) and flexural strength (54%) of NWC (Topçu & Canbaz, 2007). However, the effect of fiber on the compressive and tensile strengths of LWC shows diverse trends. Firstly, the fiber reinforcement produced negative or negligible changes on the compressive strength, but significantly enhanced the tensile strength of LWC. The results from Kayali et al. (1999) showed that the addition of both steel and polypropylene fibers produced slight reduction in the compressive strength but about 100% higher splitting tensile and flexural strength in the sintered fly ash aggregate concrete. Similar observation was also presented by other studies (Altun et al., 2007; Balendran et al., 2002; Domagała, 2011; Gao et al., 1997; Gesoğlu et al., 2013; Mazaheripour et al., 2011; Ramezanianpour et al., 2013). Domagała (2011) explained such ineffectiveness of steel fiber to enhance the compressive strength is caused by inappropriate rheological properties of the mixture which prevented it from being homogeneous and well compacted. Despite the insignificant effect on the compressive strength, these studies showed that low volume of steel fiber increased cylinder splitting tensile strength and flexural strength. Moreover, the increments in tensile strengths were much more for FRLWC than for NWC attributed to the higher brittleness of LWC (Domagała, 2011). If the rheological defects of the FRLWC is controlled by appropriate mix design or by the addition of superplasticizer, both the compressive and tensile strengths of FRLWC increased considerably with an increase of fiber content (Corinaldesi & Moriconi, 2011; Düzgün et al., 2005; Gao et al., 1997). For example, the steel and high toughness polypropylene fibers reinforcement increased the compressive

strength of concrete from 53 to 60 MPa; while Arisoy and Wu (2008) reported that the ultimate flexural strength of FRLWC is improved by 50-250% compared to plain LWC. Although the summarized compressive and tensile strengths of FRLWC in Table 2.2 showed different values, but the addition of steel fiber showed consistent fractions of improvement correspond to the non-fibrous LWC. Based on Table 2.2, the addition of steel fiber of up to 2% enhanced the compressive, splitting tensile and flexural strengths by about 30-50%, 70-150%, 60-130%, respectively. However, the increment of steel fiber due to increasing volume fraction has its limit. In the studies of Libre et al. (2011), Mirza & Soroushian (2002) and Gao et al. (1997), it was found that the dispersion of fiber became very difficult when the volume fraction was further increased to 0.5%, 1.5% and 2.5%, respectively and therefore the increase in volume fraction beyond these values will result in insignificant effect on the strength of FRLWC.

The ultimate strength of LWC is mainly controlled by the strength of the lightweight coarse aggregate itself. Under increasing compressive/tensile loading, vertical compressive strain and transverse tensile strain occurred in concrete compressive strength test specimens, and the concrete deformation continuously increased. When transverse tensile strain exceeded the ultimate tensile strain of coarse aggregates, cracks occurred in coarse aggregates in concrete. These cracks were prone to expand with further increase of load, and eventually propagate into cement paste. When the tensile strain reached the ultimate tensile strain of concrete, failure occurred. The incorporation of steel fiber into matrix serves to increase the ultimate compressive strength by the resultant arresting growth of cracks based on the bond between steel fiber and cement paste (Gao et al., 1997). The steel fibers act as a means of stress transfer whereby the tensile stress was transferred across fibers, which subsequently delayed the propagation of macro-cracks and improved the splitting tensile strength of

concrete. This process is termed as the crack bridging effect (Mo et al., 2014c). The crack bridging effect will be elaborated in latter section.

In order to correlate the effect of aspect ratio and volume fraction of steel fiber on the tensile strengths of FRLWC, Gao et al. (1997) proposed Eqs. 2.2 and 2.3 to predict the splitting tensile and flexural strengths of high strength expanded clay LWC, respectively.

$$f_{st} = 0.94f_t (1-V_f) + 3.02 V_f (l/d) \quad (2.2)$$

where f_{st} is splitting tensile of FRLWC; f_t is the splitting tensile strength of plain LWC; V_f is the volume fraction of steel fiber and l/d is the aspect ratio of fiber (length/diameter ratio).

$$f_{sw} = 0.92f_w (1-V_f) + 4.19 V_f (l/d) \quad (2.3)$$

where f_{sw} is flexural strength of FRLWC; f_w is the flexural strength of plain LWC.

The effects of polymeric fibers such as polypropylene, nylon and polyvinyl alcohol fibers are not significant as the steel fiber. For example, the splitting tensile strengths of the nylon-fiber-reinforced and polypropylene-fiber-reinforced concretes were 17.1% and 9.7% higher, respectively, than that of the unreinforced normal concrete (Song et al., 2005). In the case of LWC which is weak under tension loadings, the addition of polypropylene and nylon fibers produced increments up to 60% and 80% in the splitting tensile and flexural strengths, respectively as seen in Table 2.2. On the

other hand, the addition of polypropylene shows no impact on the compressive and tensile strengths of concrete (Libre et al., 2011; Mazaheripour et al., 2011; Ramezanianpour et al., 2013).

Table 2.2 Comparison between the compressive and tensile strengths of LWC and FRLWC

Type of Concrete	Type of fiber	Compressive strength (MPa)			Splitting tensile strength (MPa)			Flexural strength (MPa)			Reference
		LWC	FRLWC	Increment	LWC	FRLWC	Increment	LWC	FRLWC	Increment	
Normal weight concrete	Steel (0.6%)	-	-	95%	-	-	105%	-	-	54%	(Topçu & Canbaz, 2007)
	Polypropylene (0.05-0.075%)	-	-	18%	-	-	5%	-	-	22%	
Cold bonded fly ash aggregate concrete	Steel (0.25-0.75%)	43	45-47	5-9%	-	-	-	3.70	4.92-8.10	32-120%	(Gesoğlu et al., 2013)
Sintered fly ash aggregate concrete	Steel (0.4-0.8%)	53	53-59	0-11%	3.65	4.25-6.30	16-73%	6.00	6.50-9.60	12-60%	(Domagała , 2011)
Sintered fly ash aggregate concrete	Steel (0.6-1.7%)	65	58-65	-10-0%	3.4	5.4-6.6	60-94%	-	-	-	(Kayali et al., 1999)
	Polypropylene (0.28-1%)	65	61	-6%	3.4	4.1-7.4	20-118%	-	-	-	
Expanded clay concrete	Steel (0.6-2.0%)	70	71-85	1-21%	4.95	5.67-8.80	9-78%	6.20	6.80-11.80	9.6-90%	(Gao et al., 1997)
Expanded clay concrete	Steel (0.5-2.0%)	23	30	30%	2.12	4.10	13-93%	3.69	8.04	27-117%	(Campione et al., 2001)
Pumice LWC	Steel (0.5-2.0%)	20	20	0	1.93	2.27	3-18%	4.07	5.82	7-42%	(Campione et al., 2001)
Pumice LWC	Steel (0.5-1.0%)	19	29-30	53-58%	1.9	2.8-4.1	47-215%	2.1	3.5-6.3	67-198%	(Libre et al., 2011)
	Popypropylene (0.2-0.4%)	19	17-21	-9-11%	1.9	1.9-2.4	0-26%	2.1	2.6-3.3	28-57%	
Perlite aggregate concrete	Glass (0.125-0.75%)	-	-	-	-	-	-	1.85	3-4.25	62-130%	(Mirza & Soroushian , 2002)
Oil palm shell concrete	Steel (0.5-1.0%)	33.5	37-46	10-40%	2.5	4.8-6.9	93-178%	4.7	5.9-8.9	26-89%	(Mo et al., 2014a)

2.3.2.4 Toughness

Toughness is a measurement of energy absorption capacity of concrete. It is usually characterized by the area under the load-displacement curve obtained during compressive or flexure test (Taylor et al., 1997). The most beneficial characteristics of fiber-reinforced concrete are increased tensile capacity, toughness, post-failure ductility and crack control (Erdem et al., 2011; Hassanpour et al., 2012; Kim et al., 2010; Nataraja et al., 2005; Sun & Xu, 2009). The presence of fibers in the fiber-concrete composite system changed the concrete from a brittle to ductile materials, eventually increased the post-cracking ductility and energy capacity of concrete. Hence it is essential to study the effect of fibers in the enhanced toughness of LWFRC.

ASTM C1018-97 explained the measurement procedures to obtain the first cracking strength, toughness indices and residual strength factor, as shown in Figure 2.4(a). The toughness indices, I_5, I_{10} amd I_{30} are taken as the ratio of flexural toughness up to 3, 5.5 and 15.5 times the first crack deflection, respectively to its first crack flexural toughness, while residual strength factors $R_{5,10}$ and $R_{10,20}$ are taken as $20(I_{10} - I_5)$ and $10(I_{20} - I_{10})$, respectively. The toughness indices and residual strength factors reflect the post-crack behavior of fiber-reinforced concrete under static flexural loading. Toughness and first-crack strength are influenced in different ways by the amount and type of fiber in the concrete matrix.

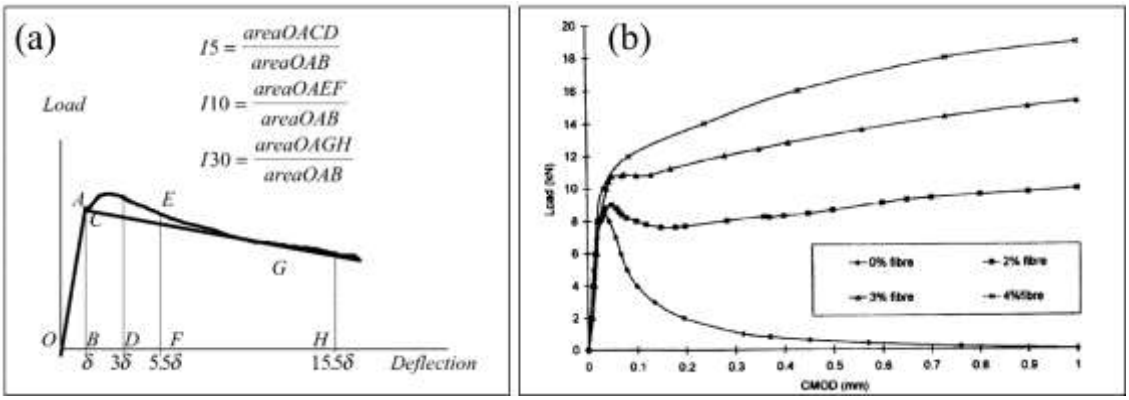

Figure 2.4 (a) Definition of toughness indices according to ASTM C1018 (Balendran et al., 2002); (b) Flexural load versus CMOD curves (Taylor et al., 1997)

Figure 2.4(b) shows the load-displacement curves of steel fiber-reinforced concrete under compression and flexural loading, respectively. Higher peak stress and pre-cracking flexural toughness were observed when the volume fraction of steel fiber increases (Figure 2.4(b)). Under increasing loading, the compressive strains and transverse tensile strains occur in the concrete until the ultimate strength in LWC is achieved. Then a further increase in the load produces an extension and propagation of cracks into the cement paste, until the maximum load is reached. After this stage, further deformation produces a brittle softening response due to the absence of interlock forces in LWC (Campione et al., 2001; Gao et al., 1997). In such cases without the fiber reinforcement, the failure is brittle at which both cracking and ultimate strength of LWC achieve almost at the same time. If fibers are present in the concrete, further deformations without significant loss of bearing capacity is achievable in the softening branch, due to the resulting growth of cracks arrested by fiber-matrix interfacial bonding. This explained the increased compressive and tensile strengths in FRLWC. Following the post-cracking behaviors after the peak stress in Figure 2.4(b), plain LWC failed by a drastic drop in the load and produced a steep falling branch in the load-deflection curve, which eventually results in a low toughness of the plain LWC. In the

case of FRLWC, the crack bridging effect improved the post-cracking toughness. The increase in the flexural fracture toughness is because of fiber pullout and fiber debonding (Gao et al., 1997). Additional energy is consumed for both pullout and debonding processes which leads to narrower crack width and the formation of multiple fine cracks. Even after the failure, fibers ensure high levels of deformation (Campione et al., 2001). This is evident from the results of Taylor et al. (1997) which reported that the flexural displacement measured in closed-mouth opening displacement (CMOD) of plain concrete at first crack is less than 0.5mm and the post-cracking curve follows a steep falling slope. The addition of steel fibers up to 4% increased the post-cracking flexural ductility with flat slope.

Balendran et al. (2002) and Libre et al. (2011) showed that toughness indices of LWC are lower than that of normal weight concrete. Libre et al. (2011) explained that this situation might be attributed to the high brittleness of LWC than the NWC. While the enhanced toughness of steel fiber-reinforced LWC was evident in the study from Mo et al., (2014c). The addition of steel fiber was found to dramatically increase the toughness of the oil palm shell concrete by with about 6, 9 and 17 times higher than that of the control concrete with the addition of 0.5%, 0.75% and 1.0% of steel fibers, respectively. In addition, the increase of steel fiber content from 0.5% to 0.75% and 0.5% to 1.0% enhanced the fracture energy by approximately 1.5 and 2.9 times, respectively. Similar observation was presented by Şahin & Köksal (2011) at which the fracture energy increased by about 2.2 and 3.6 times for the addition of steel fibers from 0.33% to 0.67% and 0.33% to 1.0%, respectively. Moreover, Mo et al. (2014c) also showed that the fracture toughness, K_{ic} which is a measure of the crack propagation for the control OPSC is 0.563 MPa $m^{0.5}$, which is comparable to self-compacting concrete with higher compressive strength and the addition of 1% steel fibers improved the fracture

toughness improved to 1.877 MPa $m^{0.5}$. On the other hand, study from Deng (2005) also showed that the total energy dissipated values for carbon fiber-reinforced concrete specimens are 9.6–13.7 times larger than that of plain concrete during the flexure fatigue/fracture tests.

Compared to steel and carbon fiber, other fibers produced less beneficial effects on the toughness of FRLWC. Compression toughness of steel and high toughness polypropylene fiber-reinforced concrete was found higher than that of polypropylene fibers (Corinaldesi & Moriconi, 2011; Libre et al., 2011).

2.3.2.5 Modulus of elasticity and Poisson's ratio

The modulus of elasticity is a function of the compressive strength (Düzgün et al., 2005). The modulus of elasticity of concrete is generally affected by the stiffness and volume of the components, particularly coarse aggregates (Campione et al., 2001; Gao et al., 1997). In the case of LWC, the coarse aggregate consists of porous lightweight aggregate and the stiffness of lightweight aggregate is much lower than normal aggregate. Hence the LWC is characterized by significantly lower modulus of elasticity (on average by 45%) in relation to normal weight concrete of the same strength class (Domagała, 2011). In the case of expanded clay, when the volume fraction of fibers increases from 0% to 2% the average secant elastic modulus increases from 14.5 GPa to 17.0 GPa, while in the case of pumice stone it decreases from 15.2 GPa to 13.4 GPa (Campione et al., 2001).

The addition of steel fiber into FRLWC composites was found to increase the modulus of elasticity of FRLWC (Domagała, 2011; Düzgün et al., 2005; Gao et al., 1997; Kayali et al., 1999; Mo et al., 2014a). The modulus of elasticity of concrete was improved with increasing volume fraction of steel fiber. This can be explained by the higher modulus of elasticity of steel fiber and the decrease in the number original shrinkage cracks owing to the crack arresting capability of fibers (Gao et al., 1997; Kayali et al., 1999). The fibers enhanced the stress redistribution and reduced the localized strain, thus giving a steeper slope in the stress-strain curve (Gencel et al., 2011). In the study on oil palm shell concrete, the effect of steel fibers on the modulus of elasticity is evident as the highest modulus of elasticity of 16.2 GPa was obtained for the mix with 1% steel fiber, 70% more than the non-fibrous control mix (Mo et al., 2014a). On the other hand, the Poisson's ratio of FRLWC decreased with the increase in steel fiber content (Gao et al., 1997). The addition of fibers to the mixtures increased the strain of the sample corresponds to the peak stress. The strain capacity and deformation capability of the concrete matrix are increased considerably with the inclusion of steel fiber to the mixtures (Düzgün et al., 2005). This has proved that the fiber-matrix interfacial bond holds the cement matrix together and allows the concrete to further deform under increasing load. However, similar to the observations in compressive and tensile strengths, the enhancement effect of steel fiber is limited up to a certain volume fraction. The results from Mo et al. (2014a) showed negligible effect in the enhancement of modulus of elasticity of steel fiber-reinforced oil palm shell concrete when the amount of steel fiber is increased from 0.75 to 1.00%.

However, there are some studies which reported that polypropylene and polyvinyl alcohol did not affect the values of modulus of elasticity (Corinaldesi & Moriconi, 2011; Mazaheripour et al., 2011). CEP-FIP manual presented Equation 2.4

for the prediction of modulus of elasticity based on the compressive strength of LWC. This is because there is a direct relationship between compressive strength and modulus of elasticity.

$$E_s = (\rho/2400)^2 \times f_{cu}^{1/3} \times A \quad (2.4)$$

where E_s is the modulus of elasticity (in GPa); ρ is the air-dry density (in kg/m^3); f_{cu} is the compressive strength (in MPa) and A is coefficient with value 9.1 for natural and manufactured lightweight aggregate. It is noteworthy that Equation 2.4 is applicable for the prediction of modulus of elasticity for different LWC and FRLWC by modifying the coefficient A. Alengaram et al. (2011) used A = 5 for the plain oil palm shell concrete.

2.3.2.6 Ductility

The flexural ductility, or in other words, flexural deflection under flexural and compression testing is always ignored. Deflection is one of the most important serviceability limit states requirement to be considered in the design of reinforced concrete. Under the flexural load, a high deflection will greatly affect both the appearance and efficiency of during the initiation of crack. Eurocode 2 states that the final deflection of a beam should not exceed span/250 (Mosley et al., 2012). However, the deflection limit may not be applicable to LWC and FRLWC. Plain LWC was shown to be capable of offering higher deformability during compression and flexural loading compared to normal weight concrete because of the lower modulus of elasticity in plain LWC (Alengaram et al., 2011; Domagała, 2011). Thus, high research interest lies on the ductility behaviors of FRLWC.

In addition to the increase in ultimate compressive and flexural strengths, the ductility of the FRLWC is much improved compared to plain LWC, as seen in Figure 3. Based on Figure 2.4(a), ASTM C1018 (1997) stated that the toughness index I_{30} of fiber-reinforced concrete up to 15.5 times of the first crack deflection could be achieved. This indicates that the fiber reinforcement might be capable to produce notably enhancement on the ductility. The 50–150 times (5000–15000%) increase in flexural displacement (ductility) at ultimate load in FRLWC compared to plain LWC were reported by Arisoy & Wu (2008). Moreover, from the compression load-displacement in Figure 2.4(c), the ultimate failure displacement of plain OPSC was found at only 1.5mm. The inclusion of steel fiber in the oil palm shell concrete composites enhanced the compressive ductility to about 3-5mm with the increment range of 100-235%. Besides, the load-CMOD curves by Taylor et al. (1997) (Figure 2.4(b)) also showed that the post-cracking flexural ductility of fiber-reinforced concrete is higher than the plain concrete, as the slope of the descending curve after the cracking is getting flat. This indicates that the concrete specimen could further deform and sustain more energy after the cracking, and eventually results in improved toughness in fiber-reinforced concrete. Therefore, we can conclude that the fiber addition in FRLWC significantly improved the compressive and flexural ductility at failure.

The enhancement effect on the ductility of FRLWC is not limited to the post-cracking ductility alone, but also improved the first cracking ductility. Studies from Düzgün et al. (2005) and Domagała (2011) reported that the increase in the peak strain corresponding to the ultimate strength is maximum for high volume fraction of steel fiber compared to the non-fibrous concrete.

2.3.2.7 Cracking resistance

Another property related to the toughness enhancement of fibers is cracking resistance. Plain concrete is a brittle composite material. When the plain concrete reaches its ultimate strength, the concrete loses its load bearing capacity thus fail in a sudden way without giving any sign of cracking. Such brittle failure is not desirable in the structural design. Referring to the discussions on the toughness of FRLWC, the crack bridging effect improved the energy absorption capacity in FRLWC by the crack bridging mechanism. In addition to that, the failure characteristics of fiber-reinforced concrete are completely changed to a more ductile failure as a result of the addition of fibers. After the occurrence of initial cracking, the sample did not fail suddenly (Düzgün et al., 2005). Domagała (2011) reported that the use of small content of steel fibers (V_f = 0.4%) was capable to eliminate the explosive nature of damage of concrete. The randomly oriented fibers act as "bridge" across the crack and the fiber-matrix interfacial bond blunts the crack propagation and holds the cracked matrix together, eventually reduces the crack opening, as shown in Figure 2.5(a). Other studies such as Sun & Xu (2009) and Mirza & Soroushian (2002) also showed that polypropylene and glass fibers are capable to retard the appearance of the first cracking and resist crack development. In addition, the fiber-matrix interfacial bond contributes to a higher toughness in fiber-concrete composites as more energy is consumed to overcome the fiber-matrix interfacial bond by means of fiber-debonding or fiber pullout (Figure 2.5(b)). Moreover, the presence of high stiffness fibers across the crack blunts and diverts the direction of the primary crack to form multiple finer secondary cracks, as seen in Figure 2.5(c). The discussions of crack bridging effect of fibers will be further elaborated in latter section.

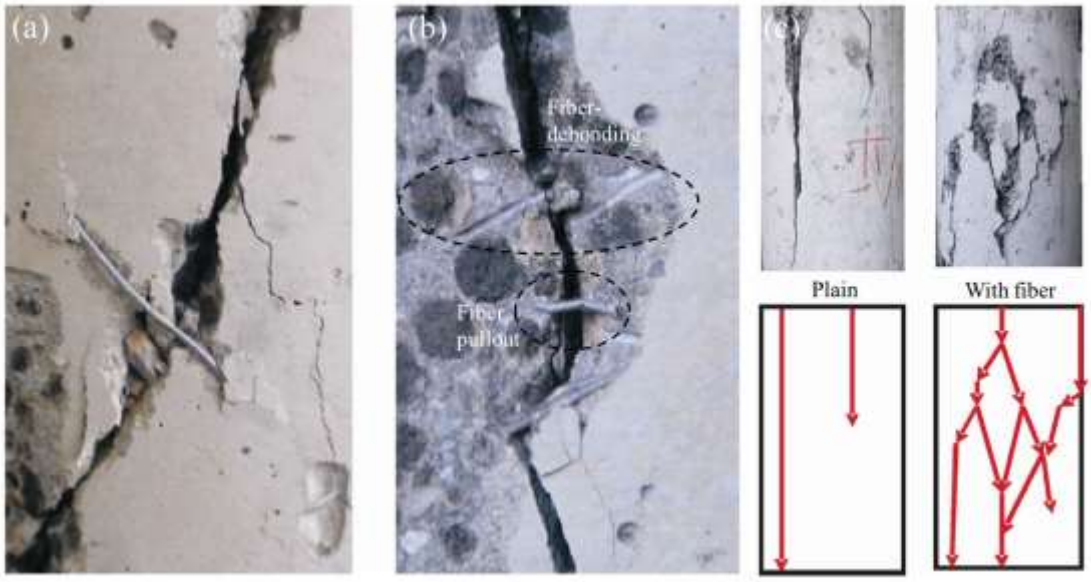

Figure 2.5 (a) Crack bridging effect of fiber; (b) fiber-debonding and fiber pullout from concrete and (c) Comparison of crack pattern of plain and fiber-reinforced concrete (Domagała, 2011)

2.3.2.8 Structural behaviors

The low mechanical properties and durability issue of LWC and FRLWC had limited the studies and development of both concrete in structural applications. Moreover, the control of the uniformity of the fiber dispersion in the FRLWC is difficult and this hindered to be applied in construction industry. However, some studies were presented on the effects of fiber to improve the structural behaviors like flexural and torsion capacity. Hamoush et al. (2010) studied the PVA microfiber-reinforced concrete beams aiming to prevent or control the tensile cracking and to increase the ductility and toughness in the strain softening region. Their results showed noticeable increase in the post-crack energy absorption capacity or toughness under flexural loading. The increase in the post-cracking flexural behaviors of fiber-modified reinforced concrete beams is attributed to the strong bond of the PVA microfiber with the cement paste. This strong bonding effect causes the fiber to rupture instead of being pulled out. Meanwhile, addition of fibers was found to produce marginal increase on the ultimate flexural strength of steel fiber-reinforced concrete slabs but it improved the energy absorption

capacity of slabs. The energy absorption of slabs with fiber volume up to 1.5% was improved by 36 times compared to that of plain concrete slabs (Khaloo & Afshari, 2005). In another study by Ghavami (1995), it was shown that for the bamboo-reinforced lightweight concrete beam, the ultimate applied load was increased up to 400% as compared with the concrete beams without bamboo reinforcement. It was also found that the addition of 3% of bamboo, in relation to the concrete section, is the recommended value. It is desirable to have concrete that exhibits strain-hardening behavior achieved through multiple cracking of the reinforced matrix, and fiber-reinforcement concrete is proven to possess this characteristic. Furthermore, the torsion behaviors of normal aggregate concrete and LWC were enhanced by the inclusion of steel fibers (Khaloo & Sharifian, 2005; Okay & Engin, 2012; Rao & Seshu, 2003). It was shown that the addition of steel fibers improves the ultimate torsional strength, torsional toughness and torsional stiffness of the beams. Sufficient addition of steel fibers to concrete causes a decrease in the widths of cracks, whereas an increase in the number of cracks (Okay & Engin, 2012).

Structural behavior of OPSC is one of the important objectives in this work. Hence, more information of structural behaviors will be elaborated in latter section.

2.3.2.9 Crack bridging mechanism of fibers

The previous sections discussed on enhanced concrete properties and structural performances of fiber-reinforced concrete and FRLWC. Most of the studies attributed the enhancement to the crack bridging effects (Abu-Lebdeh et al., 2011; Bischoff, 2007; Campione et al., 2001; Erdem et al., 2011; Gao et al., 1997; Hamoush et al., 2010; Singh et al., 2004; Song et al., 2005; Sun & Xu, 2009; Yang et al., 2013; Zīle & Zīle, 2013). For the pre-cracking behaviors of fiber-reinforced concrete, the fiber-matrix

interfacial bond serves to improve the ultimate strength of concrete. The fibers are randomly distributed in the concrete matrix and the fibers bridge across the potential cracks. Once the cement matrix fractures, multiple microcracks will form and propagate until the microcracks join up to form primary cracking. When a primary crack approaches the fibers, the crack tip stress is significantly reduced by the fiber-matrix interfacial bond. The fibers eventually blunt, stop or change the crack propagation. The blunting effect reduces the crack tip stress and hence permits the concrete to sustain further loading and to undergo higher deformation before the ultimate strength is achieved. The primary crack width is significantly reduced and multiple finer secondary cracks are form in this stage, as shown in Figure 2.5(c). This explains for the enhancement of the ultimate strength capacity and its corresponding strain in fiber-reinforced concrete. It is generally known that the steel fibers produced the highest improvement effect on the ultimate strength than other fibers. This might be attributed to the high tensile strength and modulus of elasticity of the fibers. When the crack is approaching the stiff steel fibers, the blunting effect and crack tip stress reduction are higher compared to other fibers.

For the enhancement effect on the post-cracking behaviors, after the cement matrix fractures upon reaching the ultimate strength, the bridging of fibers across the crack aids to hold the cracked cement matrix together (Mode 3 in Figure 2.6). Additional energy is required for the fiber pullout/debonding/fracture from the matrix for the cracks to further open up and propagate. This allows the concrete to sustain a higher energy capacity after the cracking and hence the residual strength/post-cracking toughness of fiber-reinforced is greatly improved by the incorporation of fibers. Similar to the pre-cracking behaviors, the steel fibers always outperform other fibers such as polymeric fibers. It can be explained by the high stiffness of steel fibers. The steel fibers

do not fracture as of Mode 1 in Figure 2.7, but most of the steel fibers failed by fiber-debonding and fiber pullout which is evident from Figure 2.5(b). Both fiber-debonding and fiber pullout consumes higher energy to overcome the fiber-matrix interfacial bond, and eventually results in more significant crack closure and reduction in stress intensity factor at the crack tip. While in the case of fibers of lower stiffness such as polypropylene and nylon fibers, the fibers might fracture before the fibers are either pullout or debond from the matrix. Hence it explains the reason for the higher increment of concrete properties is observed in the fibrillated polymeric fibers than the monofilament fibers.

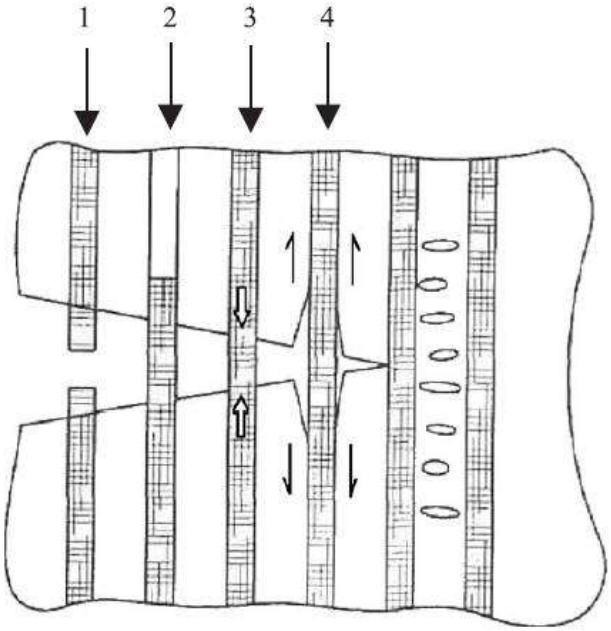

Figure 2.6 Toughening mechanisms of fiber in crack bridging effect (Singh et al., 2004)

The crack bridging effect of fibers can be further explained in microstructural scale. Figure 2.7 showed the crack bridging effect of polypropylene fibers in the microstructural scale presented by Sun and Xu (2009). Figure 2.7(c) shows the plain concrete mixture contains many crystalline with the leaf-like, needle or fiber shape which interweave together among CSH, along with many other villiform gels. However, microscopic image with the magnifying ratio of 5000 shows that the CH crystalline exists in a layered structure with high orientation (Figure 2.7(a)). Meanwhile, many voids are noticeable among these crystalline structures (Figure 2.7(c)). In contrast, polypropylene fiber-reinforced concrete mixture contains many gel components and has much less voids than the plain concrete (Figure 2.7(d)). Its crystalline size is obviously smaller than that of plain concrete, at which the size of the needle-shaped crystalline decreases from 8–10μm (plain concrete) to 2–4μm (mixture with fiber). The polypropylene fiber-reinforced concrete mixture contains very few voids among crystalline, and its gels look very integral and continuous as seen from Figure 2.7(b).

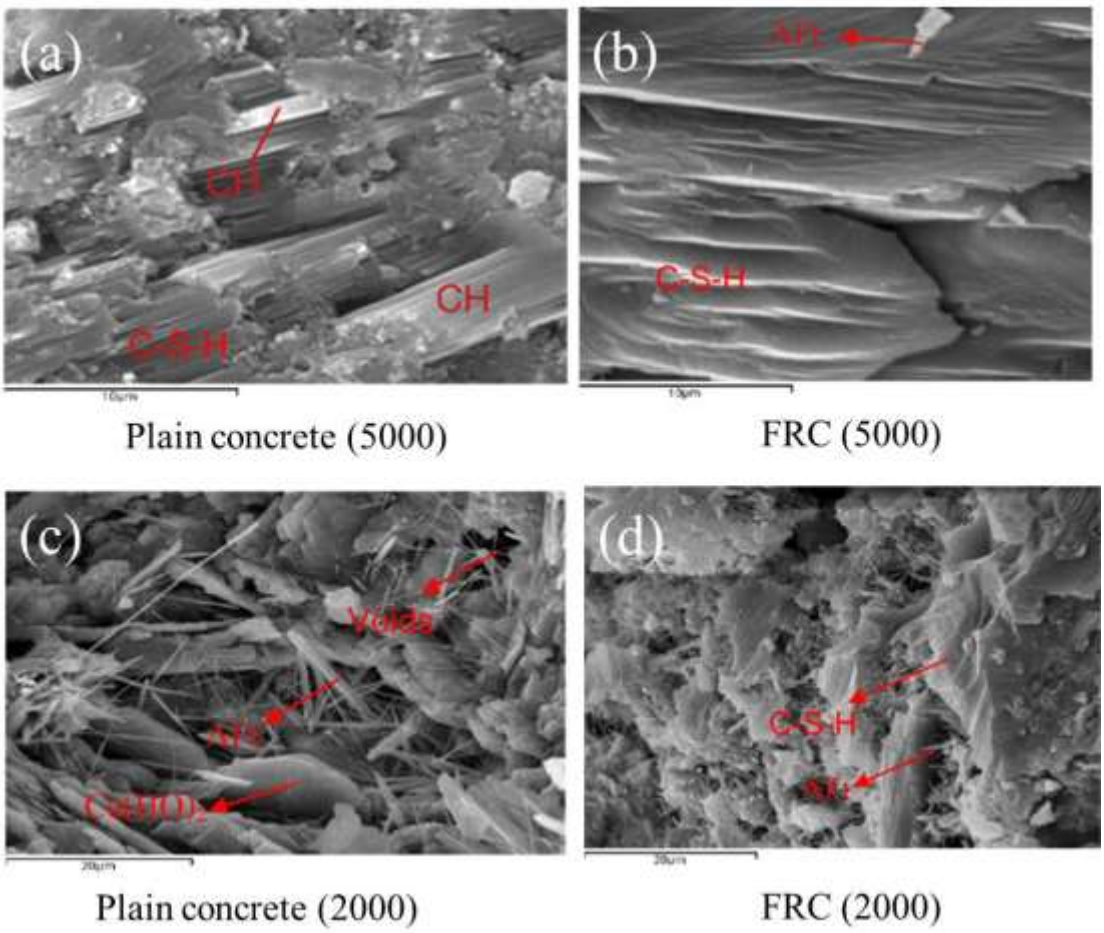

Figure 2.7 Microscopic images of plain and polypropylene fiber-reinforced concrete (Sun & Xu, 2009)

Furthermore, Figure 2.8 shows the microstructures of the aggregate-cement interfacial transition zone for the plain and polypropylene fiber-reinforced concretes with a magnifying ratio of 3000. The microscopic image from Figure 2.8(a) shows that plain concrete contains many morifolium-shaped CSH gel and hexagonal sill CH crystalline with relatively large particle sizes, and it has noticeable voids and microcracking at the interfacial transition zone. However, the microstructures at the interfacial transition zone of the polypropylene fiber-reinforced concrete mixture looks much denser with more uniform particle sizes than that of C1, the voids at its interfacial transition zone are very minimal (Figure 2.8(b)). The observations from Figure 2.7 and 2.8 showed that the addition of fibers into concrete matrix does not only toughened the

concrete by fiber-matrix interfacial bond, but the fiber reinforcement also densifies the interfacial transition zone and the CSH gel and reduces the formation of CH crystallines.

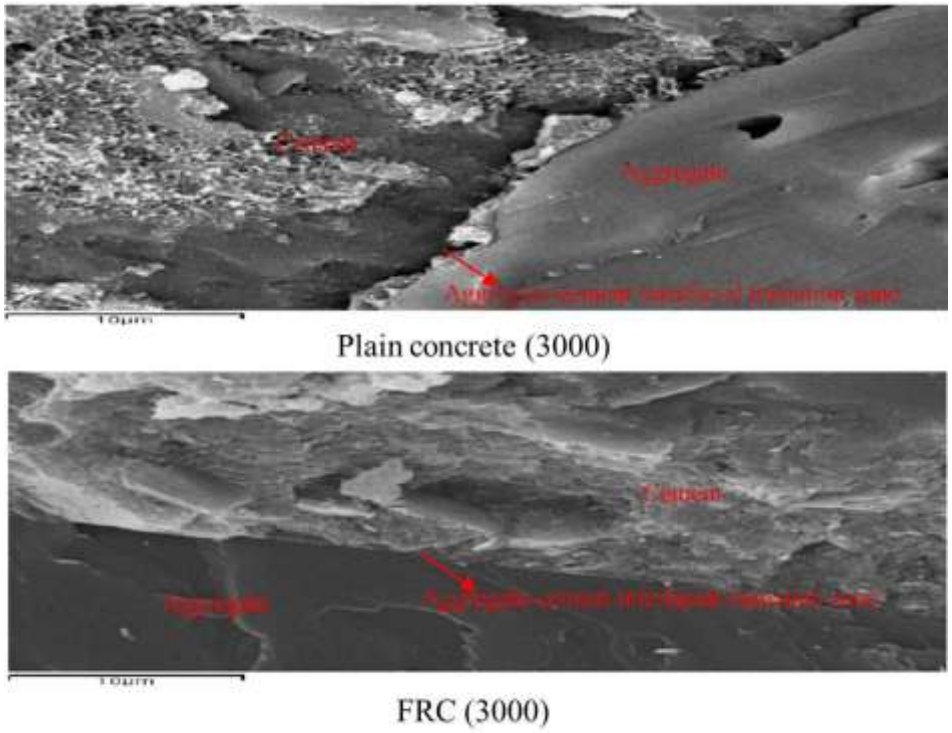

Figure 2.8 Microscopic images of interfacial transition zones of (a) plain and (b) polypropylene fiber-reinforced concrete (Sun & Xu, 2009)

2.3.2.10 Design considerations for fiber-reinforced lightweight concrete

This section provides the design considerations and limitations according to the recommendations provided by different researchers. The maximum fiber amount for concrete given by Santhakumar (2006) is 3% by volume. Fiber volume beyond 3% is suggested for mortar only as there is insufficient mortar to bind with the fibers and aggregates at the same time. The summary of the recommendations based on the studies on fiber-reinforced concrete are given in Table 2.3. Firstly, the use of >1% superplasticizer is necessary to ensure satisfactory workability and compaction in the FRLWC. In addition, addition of a maximum amount of 2.5% of steel fibers was suggested by Gao et al. (1997), as further increase in fiber volume possesses

insignificant effect on the concrete strength. Meanwhile, a minimum fiber volume of 1% is required in order to achieve desirable enhancements in the concrete properties such as tensile strength, ductility, shrinkage, and structural performance.

Table 2.3 Design considerations for fiber-reinforced concrete

Properties	Type of fiber/ superplasticizer	Amount recommended	Reference
Workability	Superplasticizer	>1%	Nili & Afroughsabet (2010)
		>1.5%	Campione et al. (2001)
Density	Steel fiber	<2.5%	Gao et al. (1997)
		<1%, or use of hybrid fiber	Hassanpour et al. (2012)
Tensile strength	Steel fiber	>1%	Gao et al. (1997)
Ductility	Steel fiber	>0.9%	Rao and Seshu (2003)
Shrinkage	Glass fiber	>1%	Mirza & Soroushian (2002)
Structural behaviors (torsion)	Steel fiber	>0.6%	Okay & Engin (2012)

2.4 Structural behaviors of reinforced concrete beams

The strength of an entire structure depends on the quality of concrete, and therefore, it is necessary to ensure that quality concrete of required strength is made use of (Santhakumar, 2006). Section 2.3 discussed on the effects of fibers in enhancing the concrete properties including mechanical properties, durability, structural behaviors and more, particularly in LWC with lower strength compared to NWC. Hence this research work focuses on the addition of fibers into OPSC to produce Oil Palm Shell Fiber-reinforced Concrete (OPSFRC) and the fiber reinforcement is expected to improve the mechanical properties and structural behaviors of OPSFRC. The commonly studied structural behaviors of concrete are flexure, shear and torsion. Meanwhile the effects of fibers in the flexural and torsional behaviors of OPSFRC are being investigated in this study.

2.4.1 Flexural behaviors of reinforced concrete beams

There are two journal papers available on the flexural performance of OPSC reinforced concrete (Alengaram et al., 2008; Teo et al., 2006). The investigation from Teo et al. (2006) revealed that the flexural behavior of reinforced OPSC beams was comparable to that of other LWC and their experimental results compare reasonably well with the current Codes of Practice such as ACI and BS codes. In addition, they also reported that OPSC beams showed good ductility behavior by exhibiting considerable amount of deflection within the allowable deflection limit in both the ACI and BS codes. Similar observation was reported by Alengaram et al. (2008). The deflection of the OPSC beams at service loads were close to the deflection of the NWC beams of similar compressive strength. However, the larger deflections at near maximum load of the OPSC beams exhibited higher ductile behavior that gave ample warning before total collapse. The reported ductility ratio of OPSC beams fell within the range of 4.2-5.4 (Alengaram et al., 2008). Ashour (2000) mentioned that members with a displacement ductility in the range of 3 to 5 has adequate ductility and can be considered for structural members subjected to large displacements, such as sudden forces caused by earthquake. Both researches on OPSC had proven that the OPSC beam exhibited improved ductility compared to the NWC. However, due to a great diversity in the type and geometry of fibers and, consequently, varying bond characteristics and hence limits application of fiber-reinforced concrete in structural members (Gribniak et al., 2012). Furthermore, the flexural behaviors of FRLWC was further complicated attributed to the type of lightweight aggregate used. Different LWC exhibits different flexural performance. Therefore, the novelty of this research is that there is no literature available on the use of fibers in the flexural behaviors of OPSC.

From the past literature, the effect of fibers on the flexural performances of reinforced concrete beams showed a few common benefits by the incorporation of fibers. The first advantage is to avoid a sudden and brittle concrete crushing owing to ability of fibers to enhance concrete toughness in compression (Meda et al., 2012). Researchers reported that the reduced brittleness of fiber-reinforced concrete beam was attributed to the enhanced crack resistance in the reinforced concrete beams (Altun & Aktaş, 2013; Altun et al., 2007; Chunxiang & Patnaikuni, 1999; Wang & Belarbi, 2011; J.-M. Yang, Min, Shin, & Yoon, 2012). Steel fiber reinforcement could reduce the number of cracks and the size at comparable load levels (Chunxiang & Patnaikuni, 1999). Moreover, the additional significant role of fibers is to resist the formation and growth of cracks (Altun & Aktaş, 2013). This is supplemented by the delayed initiation of flexural cracks, decreased the crack widths and the doubled first crack load in the flexural beam test conducted by Yang et al. (2012).

Other than that, the addition of steel fiber into the reinforced concrete system improved flexural rigidity before yield, yield load, ultimate load (moment capacity) and toughness of reinforced concrete beam, independent of the longitudinal steel reinforcement ratio (Altun et al., 2007; Chunxiang & Patnaikuni, 1999; Kamal et al., 2014; Mahmud et al., 2013; Wang & Belarbi, 2011; You et al., 2011). Fibers significantly enhance the behavior at service conditions by increasing the stiffness in the cracked-stage and, therefore, by limiting the crack openings and deformations (Meda et al., 2012). Most of these researches utilized low reinforcement ratio. In another study from Meda et al. (2012), for high reinforcement ratio, the beam without fibers collapsed with an explosive concrete crushing and a relatively low ductility, whereas the FRC beam showed a more ductile softening behavior with a flat post-ultimate load curve). The confinement and the enhanced ductility in compression allowed the element to

develop a progressive plasticity associated with a decrease in the internal lever arm, with a gradual softening of the structural response.

However, the complication in the study on the effect of fibers in the flexural behavior of reinforced concrete beam lies on the diverged observations on the flexural ductility. In the plain concrete without reinforcement, steel fibers improved the flexural ductility (Yap et al., 2014). Meda et al. (2012) has demonstrated that the fiber reinforcement can lead to a reduction in the rotation capacity of reinforced concrete members and, as a consequence, to a reduction of the sectional ductility. A high fiber contents can determine a lower ductility as they lead to an early strain concentration in the rebars as shown by an early rebar collapse. Similar conclusion was also drawn by You et al. (2011). On the other hand, Altun & Aktaş (2013) showed that the addition of steel fiber increased the flexural ductility by 9-18%. Chunxiang & Patnaikuni (1999) and Wang & Belarbi (2011) also reported that steel fibers can increase displacement of beams at failure. Another measurement of the ductility of reinforced concrete beam is the ductility index. The ductility index of beam containing 1% steel fibers was found increased as much as 100% (Alsayed & Alhozaimy, 1999). The study from Yang et al. (2012) showed that FRC beams exhibited inelastic and ductile behaviors near failure, and a higher ultimate flexural strength than the beam with no fibers because of increased ultimate compressive strain and improved and more softened post-peak behavior of FRC. The deflection at failure in the FRC beams contains 2% steel fibers were found higher than FRC with 1% steel fibers.

The effects of fibers enhanced the load capacity and crack resistance of FRC beams. The contribution of fibers can be introduced in two different ways: (1) by addition of a term (dependent on the fiber geometry and orientation) to represent the

fiber stress and fiber-reinforcement ratio in a crack and (2) by considering FRC as a homogeneous material with higher toughness characterized by the ability of a cracked section to resist a substantial fraction of tensile strength. Most of the researchers used the latter approach due to its simplicity and effectiveness (Gribniak et al., 2012; Mahmud et al., 2013).

2.4.2 Torsional behaviors of reinforced concrete beams

The recent trend of building structures has focused on the concepts of being more economical and space efficient, as well as the aesthetic design in which the structural members are designed to be irregular or curved in shape. In such circumstances, the curved members will be eccentrically loaded, which will induce torsion in the members. Examples of torsion-loaded structures include utility poles, eccentrically loaded box bridge girders, spiral staircases, spandrel beams in building frames and curved beams (Rahal, 2013). The torsion force normally occurs by combining with the flexure and shear forces. In structures with the combined forces, the design procedures are normally based on the force interactions, and, hence, the behaviors of the members under pure torsion need to be known and quantified (Bernardo & Lopes, 2013). There have been numerous studies concerning the torsional resistance of concrete in recent years (Bernardo & Lopes, 2013; Chiu et al., 2007; Okay & Engin, 2012; Pawlak & Kamiński, 2012; Rahal, 2013; Rao & Seshu, 2005; Rao & Seshu, 2003, 2006; Yang et al., 2013). The studies showed the significance of the torsion design. An under-reinforced torsion-loaded member will result in torsional cracking commencing before the flexural or shear failures, as the torsional strength is highly dependent on the tensile strength, which is the weakest component in brittle concrete (Hsu, 1968), and, ultimately, causes an early loss of serviceability. Furthermore, the cracking of reinforced concrete elements under torsion belongs to one of the least explored phenomena which occur in reinforced

concrete structures (Pawlak & Kamiński, 2012). The above-mentioned studies focused on the torsional characteristics of normal weight concrete (NWC), high strength concrete and high performance concrete; however, the investigation of the torsional strength of lightweight concrete (LWC) is limited. This is because the conventional torsional design from the ACI code is based on the skew bending theory (Chiu et al., 2007), and then further theories including the Thin Tube theory, Variable Angle Truss Model and Softened Membrane Model were developed for the prediction of the torsional behavior of concrete (Luis et al., 2013; Bernardo & Lopes, 2011, 2013; Chiu et al., 2007). However, there are no studies available on the torsional behavior of LWC.

Previous literature on effects of fiber on the torsional behaviors reported positive impact of fibers to improve the torsional strength of concrete. Firstly, the published studies have reported that the pre-cracking torsional behavior of concrete is independent of the reinforcement (Hsu, 1968; Okay & Engin, 2012). Hsu (1968) stated that the cracking torque, T_{cr} of a reinforced concrete beam is 1-1.3 times of that the torque at failure, T_f of its corresponding plain concrete. It has observed that the torsional behavior of concrete beams is linear until the first cracking torque. It has also been observed that the uncracked torsional stiffness of the beam, that is the slope of linear part of the torque-twist (T-Ø) diagram, is independent of the presence and amount of the reinforcement (Hsu, 1968; Okay & Engin, 2012). Chiu et al. (2007) stated that the pre-cracking torsional behaviors of concrete depends on the compressive strength of the concrete. However, Khaloo & Sharifian (2005) reported that the ultimate strength of plain specimens is almost equal to their cracking strength and for the specimens reinforced with steel fibers, the torsional behavior up to first cracking was almost similar to that of the plain specimens and this indicated that the fiber reinforcement produced marginal effect on the pre-cracking torsional behaviors of concrete. On the

other hand, other researchers reported that the addition of fibers enhanced the cracking and ultimate torque of concrete (Okay & Engin, 2012; Rao & Seshu, 2003, 2006; Yang et al., 2013). There are two diverse observations of the effect of fibers on the torsional strength of concrete and hence, a further investigation on the torsional behaviors of FRLWC is necessary.

According to the theory of elasticity, when the specimens are subjected to pure torsion, the first inclined crack normally initiates in the middle of the wider face of the cross section. The crack initiates as the maximum applied tensile stress arrives at the tensile strength of concrete (Chiu et al., 2007). Under greater load the cracks would interconnect, forming a cracking pattern typical for elements loaded with torsional moment (the cracking spiral being consistent with the direction of torsion) (Pawlak & Kamiński, 2012). Once the cracking torque of the concrete is reached, plain concrete and reinforced beams cracked by a primary torsional crack included at 45 degree to the longitudinal axis of longer side of the specimens (Hsu, 1968; Khaloo & Sharifian, 2005; Okay & Engin, 2012; Pawlak & Kamiński, 2012; Rao & Seshu, 2003; Yang et al., 2013). Upon cracking, the angle of twist increased significantly under a constant torque, and suddenly. This behavior indicates that the equilibrium condition that existed in uncracked reinforced beam was upset by the cracking so that the beam sought a new equilibrium condition by transferring to the reinforcement (Hsu, 1968). When cracking occurs, the torsional beam behaves like beam under flexure: the slope of the moment-rotation curve suddenly decreases and the curve begins to follow a new slope called cracked torsional stiffness. The cracked torsional stiffness was found lower than the initial torsional stiffness (slope of torque-twist curves before cracking). In addition, it was also found that the increase in reinforcement ratio and the addition of fibers improved the cracked torsional stiffness (Hsu, 1968; Okay & Engin, 2012). Upon

achieving the crack torque, the cracked concrete could not sustain further torsion and the increasing torque is taken by the reinforcement (Hsu, 1968). This explained that the plain concrete without any reinforcement and fibers failed suddenly when the cracking torque was reached (Khaloo & Sharifian, 2005). In the comparison, the LWC failed predominantly under bond failure at the aggregate-matrix interfaces, whereas in NWC specimens, the torsional shear cracks passed through 20-35% of the aggregates along its path (Khaloo & Sharifian, 2005). The benefit of fibers was found evident to reduce the brittleness and changed the failure mode of the concrete to ductile with increased cracked torsional stiffness, ultimate torque and twist (Khaloo & Sharifian, 2005; Rao & Seshu, 2003, 2006). Moreover, the post-cracking torsional behaviors and crack resistance of fiber-reinforced concrete were also improved (Rao & Seshu, 2006; Yang et al., 2013). For the torsional design of fiber-reinforced concrete, (Rao & Seshu, 2003) proposed that a minimum volume fraction of fiber content of 0.9% is required to impart noticeable ductility to the steel fiber-reinforced concrete beams under torsion.

From the numerous numbers of papers on torsional behaviors of concrete, the papers mentioned only covered the NWC, high strength concrete and high performance concrete except study from Khaloo and Sharifian (2005) which investigated the torsional resistance of LWC. In addition, different analytical and numerical models were proposed to predict the torsional responses of concrete. However, there are limited studies on the torsional strength of LWC, and there is no paper available on OPSC.

2.4.3 Structural behaviors of reinforced concrete beams with high tensile strength

The previous section mentioned that the LWC generally weak in tensile strength, which limits its application to a wider area (Mo, Yap, Alengaram, & Jumaat, 2014; Xiao, Li, & Poon, 2012). Concrete with high tensile strength is desirable for the design of larger and longer structural members to arrest tensile cracking and to improve the tensile loading capacity. In the design of special structures, such as impact and blast resistant structural members, high tensile strength (minimum tensile strength 10MPa) is mandatory (Habel & Gauvreau, 2008; Roy et al., 2014; Wu et al., 2009). In addition, high strength is one of the vital requirements for the large and complex structures such as high-rise structures, marine structures, long-span bridge and other special constructions (Zhou et al., 2014).

Generally, the flexural strength of OPSC in the range of about 3-5 MPa (Alengaram et al., 2011, 2013) is about 60% lower than NWC. Thus, the enhancement of the tensile strength of OPSC is vital to broaden its applications. Furthermore, in order to achieve the above-mentioned high tensile strength in the concrete, the researchers generally utilized only high strength concrete and high performance concrete and there is no literature on the development of the high strength LWC by the addition of fibers. Therefore, OPSFRC plays the role as a newly-developed method to produce high strength LWC. The latter stage of this research presents the investigation on the flexural behaviors of high tensile strength OPSFRC containing high volume of fibers.

2.5 Research gap

The research gaps based on the literature discussed in previous sections are summarized in Table 2.4.

Table 2.4 Summary of research gap in OPSC

Paper	Finding(s)	Research gap
Alengaram et al. (2013)	Flexural strengths of OPSC from the past literature until 2010 were within the range of 2.1-6.2 MPa.	The improvement of mechanical properties of OPSC, especially tensile strength is required to widen the feasibility of OPSC in structural application.
Alengaram et al. (2010a)	- The addition of silica fume enhanced the mechanical and bond properties of OPSC. - The bond strength of OPSC was comparable to NWC.	In comparison between the three approaches to enhance the strength of OPSC, the addition of fibers produced higher improvement on the tensile strength compared to the other two methods. There is only one research on the effect of steel fiber on the mechanical properties of OPSC. The challenges of the OPSFRC lie on the selection of the fibers, including the type of fibers. For examples, there are different types of fibers such as steel, and synthetic fibers. In addition, fiber geometry affects the concrete properties as well. Furthermore, the literature showed that the addition of fibers increased the concrete density and reduced the workability; hence the fiber selection in the design of OPSFRC has to be investigated thoroughly.
Shafigh et al. (2011a)	- The use of crushed OPS aggregate significantly enhanced the compressive strength of OPSC	
Shafigh et al. (2011c)	- The addition of hooked-end steel fibers up to 1% produced significant improvement in the mechanical properties of OPSC, especially in tensile strength. The flexural strength of steel fiber-reinforced OPSC with 1% steel fibers was 31% higher than the plain concrete.	

Table 2.4 Summary of research gap in OPSC (cont'd)		
Alengaram et al. (2008)	- OPSC reinforced concrete beam produced larger flexural deflections at near maximum load compared to NWC and this indicated that OPSC has high ductile behavior that gave ample warning before total collapse. - Larger number of cracks with smaller crack widths was observed in OPSC beam than the NWC beams.	- Most of published papers on OPSC discussed on the mechanical properties but there are limited papers discussed on the structural behaviors of OPSC. However, the low compressive and tensile strengths of OPSC limits its application in low cost house only. Therefore, the addition of fibers in OPSC beams aims to enhance both the mechanical properties and structural behaviors of OPSFRC. - Currently there is no literature available on the structural behaviors of OPSFRC. The reason for the limited studies on the beam testing of both the LWC and FRLWC is mainly caused by the design codes such as ACI, Eurocode and BS, do not provide the specific design provisions for the reinforced concrete design of LWC.
Okay & Engin (2012)	It is observed that torsional behavior of normal strength concrete beams is changed positively with the addition of steel fibers.	- There is no study on the torsional strength of OPSC and OPSFRC yet. - The addition of fibers into OPSC aims to produce OPSFRC reinforced concrete beams with enhanced torsional behaviors.
Habel & Gauvreau (2008)	High strength concrete with >130 MPa in compression and >8 MPa in tension is essential to structural members subjected to severe loading and environmental action.	- There is no study to produce high strength LWC using high volume of fibers. - The production of high strength OPSFRC could paves way for the widened applications as special members subjected to severe loading such as impact and blast resistant structures.

CHAPTER 3

MIX DESIGN FOR OIL PALM SHELL CONCRETE

3.1 Chapter introduction

The main objective of this chapter is to investigate an optimum mix design for the control OPSC concrete for the development of OPSFRC in latter stage. This chapter presents the experimental results on the materials properties of oil palm shell (OPS) and the trial mixes to optimize the strength of Oil Palm Shell Concrete (OPSC). It is important to determine the physical properties of OPS before proceed to the mix design of OPSC because the concrete properties of LWC is highly dependent on aggregates other than the cement content used (Santhakumar, 2006). Once the physical properties of OPS are determined, the next step is to carry a series of trial mixes to produce OPSC with the highest strength. The parameters changed in the trial mixes include sand content, OPS content, amount of superplasticizer and water to binder ratio. A total number of 23 trial mixes had been conducted and reported in this chapter.

3.2 Materials and methods

3.2.1 Materials

3.2.1.1 OPS as coarse aggregate

The main material in OPSC is the lightweight OPS. Figure 3.1 shows the OPS with diverse shapes and sizes. The OPS have both concave and convex surfaces with broken and spiky edges. The size of OPS covers from a maximum size of about 15 mm to very fine powder sized below 1 mm.

Figure 3.1 Oil Palm Shell with diverse shapes and sizes

For the preparation of OPS for the mixing process, the method given by Okafor (1988) was followed in all the mixing in this research. Old OPS were collected from the local crude palm oil mill as displayed in Figure 2.1. Old OPS was meant by disposing and leaving the OPS for more than 6 months in the palm oil mill area to remove the oil coating and fibers on the surface of fresh OPS. The reason of using the old OPS is that the fibers on the surface of OPS increase the demand for water and the oil coating causes a weak bond between OPS and cement paste (Shafigh et al., 2011b). In addition, the OPS below 2.36 mm was removed and only OPS between 2.36 and 15 mm was used in the mixes because the small-sized OPS requires higher amount of cement paste and eventually reduces the workability of OPSC. The OPS used in the preparation of OPSC and OPSFRC was soaked in water for 24 hours before the mixing to keep the OPS in the saturated surface-dry (SSD) condition attributed to the high water absorption of OPS. By keeping OPS is SSD condition could prevent the mixing water to be absorbed by the OPS during the mixing process.

3.2.1.2 Mining sand as fine aggregate

Mining sand was used as fine aggregate. The fineness modulus, specific gravity and water absorption of mining sand are 2.68, 2.7 and 1.0%, respectively.

3.2.1.3. Cement and cementitious materials

For all mixes, Ordinary Portland Cement (OPC) with a Blaine specific surface area and specific gravity of 335 m^2/kg and 3.10, respectively, was used. Condensed silica fume was added as cementitious material.

3.2.1.4. Water and Superplastcizer

Potable water with a pH value of 6.20 was used for all mixes. A polycarboxylate-based superplasticizer named Glenium ACE 388 supplied by BASF Malaysia was used in all mixes.

3.2.2 Mixing, specimen preparation and testing

The physical properties of OPS measured are fineness modulus, bulk density, specific gravity/ 1 hour and 24 hours water absorption, aggregate impact value (AIV), Los Angeles abrasion value, flakiness index and elongation index, in accordance to ASTM C136-01, ASTM C29/C29M, ASTM C127-12, BS 812-112 (1990), ASTM C131-03, BS 812-105.1 (1989) and BS 812-105.2 (1990), respectively

Meanwhile, the trial mixes were carried out by using small vertical shaft mixer and only cube specimens were prepared for the testing of compressive strength. The mix design method for OPSC was Specific Gravity Method, which has been applied by the previous researchers. The mixing procedures were shown in Figure 3.2. Each material was added one by one to ensure uniform and consistent mixing of all the materials. It should be noted that the mixing time after the water and superplasticizer is slightly longer at 8 minutes attributed to the type of polycarboxylate-based superplasticizer used in this study. The superplasticizer possesses strong water reducing effect but it requires a longer time for an uniform dispersion among the fresh concrete. After the placement of the concrete in moulds for 24 hours, the specimens were removed from the moulds and then cured in water until the age of testing. The compressive strength of the cube specimens were tested at the age of 1- and 7-day according to BS EN 12390-Part 3 ("BS EN 12390: Part 3 Testing hardened concrete- Compressive strength of test specimens," 2000).

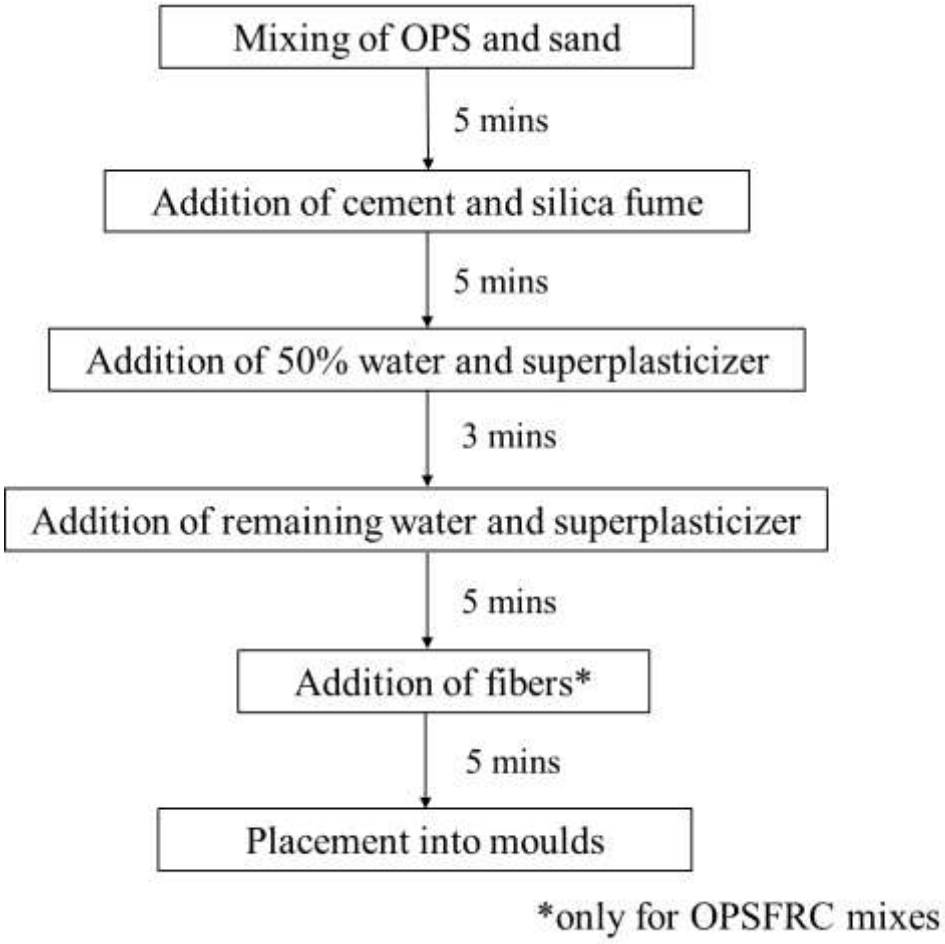

Figure 3.2 Flow chart for the mixing processes

3.3 Results and discussion

3.3.1 Physical properties of oil palm shell

The physical properties of the oil palm shell (OPS) are determined before the mixing of oil palm shell concrete (OPSC) in order to ensure an accurate and consistent mix design for the experimental works in following chapters. The physical properties include maximum size, fineness modulus, bulk density, water absorption, specific gravity, aggregate impact value, Los Angeles (LA) abrasion value, flakiness and elongation indexes. The calculations for the physical properties are reported in Appendix A and the physical properties are summarized in Table 3.1.

Table 3.1 Summary of physical properties of OPS

Properties	Unit	Value
Maximum size	mm	15
Fineness modulus	-	6.41
Bulk Density (loose condition)	kg/m^3	538
Bulk Density (compacted condition)	kg/m^3	635
Water absorption (1 hr)	%	16.4
Water absoption (24 hrs)	%	24.3
Specific gravity (oven-dry)	-	1.08
Specific gravity (SSD)	-	1.37
Apparent specific gravity	-	1.46
Aggregate impact value, AIV	%	2.11
LA abrasion value	%	5
Flakiness index, FI	%	41
Elongation index, EI	%	59

3.3.2 Trial mixes on oil palm shell concrete

After the physical properties of OPS are determined in Section 3.3.1, a total of 23 trial mixes on OPSC had been conducted before proceed to the study on the OPSFRC. The basic mix design of the trial mixes was taken from the work conducted by Alengaram et al. (2008) in order to provide a clear comparison of the OPSC and OPSFRC. The mix design method used is Specific Gravity Method. The parameter studied in the trial mixes were type and amount of superplasticizer, sand to cement ratio, OPS to cement

ratio, water to binder ratio and grading of OPS and sand. In this research, the crushing effect of OPS is not investigated. The reason is that both the crushing of OPS and addition of fibers will results in significant reduction in the workability of OPSC. The changes in the mix designs and compressive strengths of the trial OPSC are shown in Table 3.2.

Table 3.2 Trial mix results

Trial No.	**Changes in mix design (w/b = water to binder ratio; s/c= sand to cement ratio; a/c= OPS to cement ratio; SF= silica fume; SP= superplasticizer)**	**Parameter studied**	**1-day compressive strength (MPa)**	**7-day compressive strength**
1	w/b: 0.35 s/c: 1.2 a/c: 0.8 SF: 10% SP: 0%	Sand to cement ratio	10.1 (with segregation)	18.5
2	s/c increased to 1.5		11.9 (with slight segregation)	19.1
3	s/c increased to 1.7		12.8	21.1
4	s/c increased to 1.8		13.7	24.6
5	s/c increased to 1.9		Insufficient cement paste	
6	Use mix No. 4, a/c reduced to 0.7	OPS to cement ratio	14.4	25.9
7	a/c reduced to 0.65		14.9	25.8
8	a/c reduced to 0.6		16.1	27.5
9	a/c reduced to 0.55		18.5	32.0
10	Use mix No. 8 (as mix No. 9 use cement content above 600 kg/m^3) w/b reduced to 0.34	w/b ratio	16.5	28.1
11	w/b ratio reduced to 0.33		16.6	28.9
12	w/b ratio reduced to 0.32		Insufficient compaction	
13	w/b 0.32, SP 1.0%	SP content	Segregation	
14	w/b 0.32, SP 0.8%		Segregation	
15	w/b 0.32, SP 0.5%		18.0	32.1
16	w/b reduced to 0.31	w/b ratio & SP content	18.3	32.5
17	w/b reduced to 0.30		Insufficient compaction	
18	w/b 0.30, SP 0.6%		Insufficient compaction	
19	w/b 0.30, SP 0.65%		18.9	33.5
20	Use mix No. 19, OPS below 2.36 mm removed	OPS grading	19.4	34.6
21	Use mix No. 19, OPS below 1.2 mm removed		17.9	32.5
22	Use mix No. 20, sand below 0.15 mm removed	Sand grading	19.2	35.0
23	Use mix No. 20, sand below 0.30 mm removed		18.9	34.5

Therefore, based on the trial mix results, the mix design of OPSC can be summarized in Table 3.3.

Table 3.3 Final mix design for oil palm shell concrete

Properties	Unit	Value
Cement	kg/m^3	539
Silica fume (10% of cement weight)	kg/m^3	53
OPS (remove size below 2.36 mm)	kg/m^3	323
Sand	kg/m^3	971
Superplasticizer	% (cement weight)	0.65
Water to binder ratio	-	0.30

3.4 Chapter conclusions

1. The testing on the OPS aggregates showed that the OPS are lightweight and possess good impact and abrasion resistance. In addition, in order to prevent the effect of the high water absorption of OPS, the OPS has to be kept in SSD condition before the mixing.

2. A total of 23 trial mixes were conducted to optimize the compressive strength of OPSC.

CHAPTER 4

EFFECTS OF SYNTHETIC FIBERS ON THE MECHANICAL PROPERTIES OF OIL PALM SHELL CONCRETE

4.1 Chapter introduction

The main objective of this chapter is to investigate the effects of polypropylene (PP) and nylon fibers in OPSC at different volume fractions of 0.25%, 0.50% and 0.75%, by utilizing the optimum trial mix design from Chapter 3. The experimental results and discussions within this chapter has been published in the journal paper titled "Enhancement of mechanical properties in polypropylene– and nylon–fiber reinforced oil palm shell concrete".

The addition of fibers into LWAC is a new area of research, which is gaining considerable attention. Although a number of research works are ongoing in Southeast Asia and Africa on the use of OPS, very limited literature is available concerning the use of fibers in the OPSC. The ductility and high impact resistance characteristics of OPS combined with the tensile strength provided by fibers is an added advantage of OPSC in the development of ductile material. Most of the researchers used steel fibers; however, there is limited literature available on the use of PP and nylon fibers in LWC. PP fibers are mainly used to improve the ductility, toughness and impact resistance of concrete, and they are not expected to increase the concrete strength (Alhozaimy, Soroushian, & Mirza, 1996; Banthia & Gupta, 2006; Comiloli et al., 2007; Song et al., 2005). Other advantages of PP fibers are the enhancement of electric resistivity and spalling resistance (Han et al., 2005; Kakooei et al., 2012). However, the addition of PP fibers greatly decreases the workability of concrete (Mazaheripour et al., 2011), which restricts the quantity of PP fibers (Alhozaimy et al., 1996; Comiloli et al., 2007; Han et

al., 2005; Kakooei et al., 2012; Mazaheripour et al., 2011). However, Tanyildizi (2009) utilized up to 2% of PP fibers in LWC made from pumice. He reported that the use of 1% and 0.5% of PP fibers produced the highest compressive strength and flexural strength, respectively. Thus, the utilization of high PP fiber content is applicable in LWC. There are contrast observations on the use of PP fibers in the concrete, hence it arises the necessity to study the effect of synthetic fibers in LWC including OPSC. Meanwhile, a study from Song et al. (2005) reported that nylon fiber-reinforced concrete (FRC) outperformed its PP companion in the upgrading of compressive and splitting tensile strength, modulus of rupture and impact resistance. Nevertheless, nylon fibers remain unpopular compared to PP fibers. Therefore, a study on nylon fibers in OPSC is significant due to its superior performance in LWC.

In this study, the comparison between the effects of fibrillated and multi-filament PP fibers and muilti-filament nylon fibers on the mechanical properties of OPSC were investigated. In addition, the effects of volume fractions of each of these fibers were also studied. The advantage of using PP and nylon fibers in OPSC is that the density could be brought to 2000kg/m^3, the limit set for LWC, without significantly reducing the mechanical properties of OPSC. There is limited literature available concerning the comparison of the different geometry and type of fibers. The present works serve to expand the knowledge on the influence of fibers with different geometries (shapes and lengths) on the mechanical properties of OPS fiber-reinforced concrete (OPSFRC).

4.2 Experimental program

4.2.1 Materials

The mix proportion from Chapter 3 was used as the control mix and also in the preparation of OPSFRC. All the constituent materials were kept constant the variables investigated include three different fibers and three fiber volumes, V_f of 0.25%, 0.50% and 0.75% in OPSC. The three different fibers used in this study are: (i) fibrillated PP; (ii) multi-filament PP and (iii) nylon fibers. The properties of the fibers are shown in Table 4.1.

Table 4.1 Properties of polypropylene (PP) and nylon fibers

Fiber		Fiber type	Length (mm)	Diameter (μm)	Specific gravity	Tensile strength (MPa)
PP1	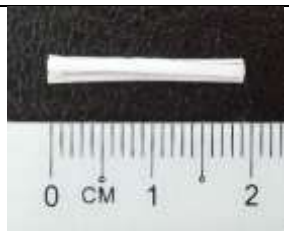	Fibrillated	19	400	0.90	400
PP2	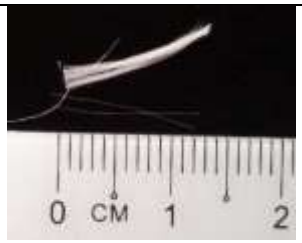	Multi-filament	12	50	0.90	400
N1	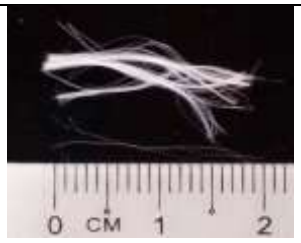	Multi-filament	19	30	1.13	300

4.2.2 Mixing proportion

The mix proportioning for all the mixes are summarized in Table 4.2. A control mix without any fibers was also prepared for comparison by using the mix design from Chapter 3. A number of nine mixes for OPSFRC were prepared. The different between

the OPSC and OPSFRC are three types of synthetic fibers and three fiber volume fractions, V_f of 0.25%, 0.50% and 0.75% for each fibers.

Table 4.2 Mix proportioning for OPSFRC containing polypropylene and nylon fibers

No.	Mix	Cement (kg/m^3)	Silica fume (kg/m^3)	OPS (kg/m^3)	Mining sand (kg/m^3)	Water (kg/m^3)	Fiber (% vol.)		
							PP1	PP2	N1
1	Control	539	53	323	971	178	0	0	0
2	PP1/25	539	53	323	971	178	0.25	0	0
3	PP1/50	539	53	323	971	178	0.50	0	0
4	PP1/75	539	53	323	971	178	0.75	0	0
5	PP2/25	539	53	323	971	178	0	0.25	0
6	PP2/50	539	53	323	971	178	0	0.50	0
7	PP2/75	539	53	323	971	178	0	0.75	0
8	N1/25	539	53	323	971	178	0	0	0.25
9	N1/50	539	53	323	971	178	0	0	0.50
10	N1/75	539	53	323	971	178	0	0	0.75

4.2.3 Specimen preparation and testing

The mixing processes for both OPSC and OPSFRC mixes followed the flow as shown in Figure 3.2. After the placement into the moulds for 24 hours, the specimens were removed from the moulds and cured in water until the age of testing. The fresh properties of all mixes were measured by using the slump test in accordance with ASTM C143/C143M-12. Cubes measuring 100 mm were prepared for testing the compressive strength (BS EN 12390: Part 3, 2000) and ultrasonic pulse velocity (UPV) (ASTM C597, 2009) at the age of 1-, 3-, 7-, 28- and 56-days. The cube specimens that were tested and failed in the compression test were reloaded to measure their post-failure compressive strength (PFCS). At the age of 28-day, the splitting tensile strength, flexural strength and modulus of elasticity (MOE) were measured in accordance to ASTM C496/C496M-11 2011), ASTM C78-10 (2010) and ASTM C469-10 (2010), respectively.

4.3 Results and discussion

4.3.1 Workability (slump)

The slump values of fresh OPSC and OPSFRC are presented in Figure 4.1. For structural lightweight concrete, Mehta & Menteiro (2006) stated that a slump value between 50 and 75 mm is comparable to an equivalent value of slump of 100-125 mm for NWC. The slump value of control OPSC mix fell within the allowable slump value for LWC by producing a slump of 75 mm. Mazaheripour et al. (2011) reported that the addition of PP fibers caused a significant reduction on the fresh properties of concrete. As expected, the slump values of OPSFRC with PP and nylon fibers were found to reduce to 15-45 mm. This phenomenon might be attributed to the strong fiber-matrix bond in the concrete. The bond increases the viscosity of concrete and restricts the distribution of the cement matrix; hence, a reduction in the workability was observed in OPSFRC. In the case of LWC, slump values between 0-25 mm can easily be compacted (Short & Kinniburgh, 1978). Despite the notable drop in the slump values, all the mixes include both OPSC and OPSFRC achieved good compaction with minimal observable voids at the concrete surface.

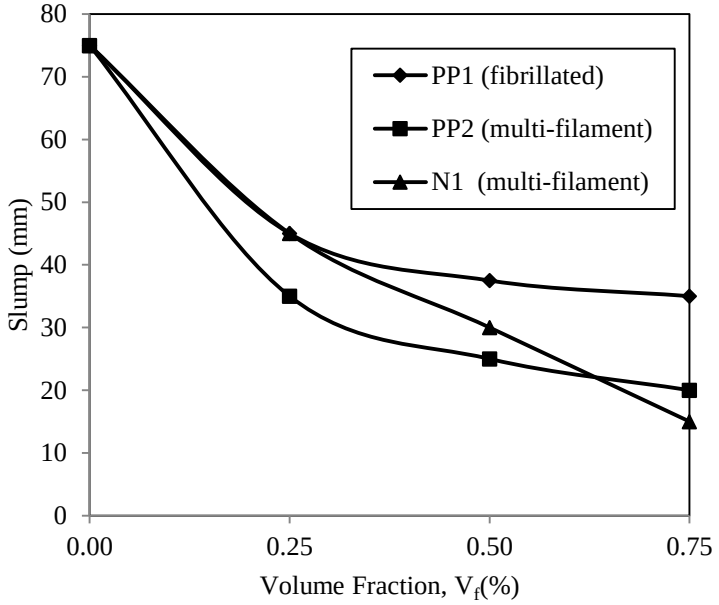

Figure 4.1 Slump values of OPSFRC versus volume fraction

Figure 4.1 shows that the workability of OPSFRC depends on the fiber geometry. For all V_f, the fibrillated fibers (PP1) produced higher slumps than multi-filament fibers (PP2 and N1). The highest difference between PP1 and the other two fibers was evident at V_f = 0.75%; the slump of PP1/75 mix was found to be 43% and 57% higher than PP2 and N1, respectively. In comparison with multi-filament fibers, the bundled fibrillated PP fibers (PP1) have a lower effective surface area that produced better workability in fresh concrete for the PP1 mixes. Moreover, the PP2 of shorter length (12mm) produced a lower slump than N1 of 19mm long. For a given fiber volume, fibers of smaller length have higher effective surface area for the development of a fiber-matrix bond than longer fibers. Hence, fibers of shorter length produced lower workability.

When the V_f increased from 0.25% to 0.75%, PP1 and PP2 produced a lower rate of reduction in slump values (drop range of 10-15mm) compared to nylon fibers; a 15mm reduction was observed for an increase of 0.25% nylon fibers in N1 mixes. The

addition of more fibers into the concrete resulted in a stronger interfacial fiber-matrix bond, and, hence, low slump values were observed at higher V_f.

It can be concluded that the addition of both PP and nylon fibers significantly reduced the workability of OPSC; further the fiber geometry through the surface area had an impact on workability.

4.3.2 Hardened density

Structural lightweight concrete is defined as concrete with an oven-dry density (ODD) of not greater than 2000kg/m^3 (Newman & Owens, 2003). All OPSFRC fulfilled the requirement of structural lightweight concrete by having an ODD within the range of 1640-1920kg/m^3 (Figure 4.2). These values show a close proximity with the ODD reported in previous literature (Alengaram et al., 2010a, 2010b; Shafigh et al., 2011a, 2011b); however, significant enhancements of tensile strength and modulus of elasticity (MOE) were obtained (Section 4.3.3).

Libre et al. (2011) stated that PP fibers have an insignificant effect on the density of concrete. However, the present study from Figure 4.2 shows that the density of concrete depends on the mixture design, fiber volume and geometry of the fibers. The experimental results showed that the type and geometry of fibers caused notable changes on the ODD of OPSFRC (Figure 4.2). The addition of PP fibers resulted in the density reduction compared to OPSC. From Figure 4.2, the addition of PP fibers caused a considerable drop in density. In contrast, nylon fibers produced an increment in the ODD of about 80-120 kg/m^3, compared to the control OPSC. However, PP fibers with V_f of 0.25% produced no effect on the ODD of OPSFRC. When the fiber content was increased to 0.5% and 0.75%, the ODD of OPSFRC decreased considerably. The mixes

with fibrillated PP1 fibers produced a lower ODD than the multi-filament PP2. At V_f = 0.75%, the PP1/75 mix produced the lowest ODD of 1640 kg/m^3, which is 7% and 15% lower than PP2/75 and N1/75, respectively. In comparison to the ODD of about 2300 kg/m^3 for normal weight concrete the density reduction of about 30% of OPSFRC in this study is significant.

Although the difference in the specific gravity of nylon and PP fibers is insignificant (Table 4.1), their contribution to density cannot be ignored. The addition of the very lightweight PP fibers into OPSFRC produced an insignificant change in density at low V_f (0.25%). However, the reduction in density of about 15% between PP1 and N1 at V_f = 0.75% might be attributed to the fibrillation of fibers; as fibrillated fibers tend to displace mortar in concrete as the diameter of PP1 fiber is more than the N1 fibers.

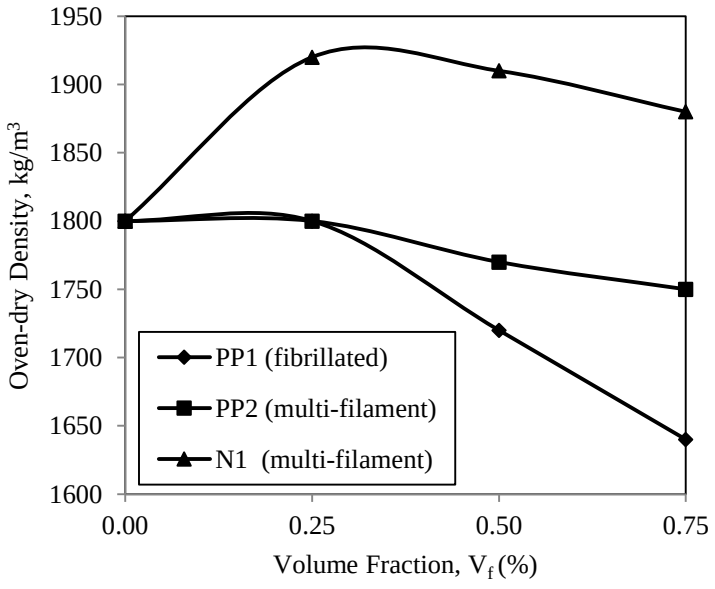

Figure 4.2 Oven-dry density (ODD) versus volume fraction, V_f

4.3.3 Mechanical properties

4.3.3.1 Compressive strength

The compressive strength of OPSC depends on the strength of OPS and the hardened cement paste, as well as the aggregate-cement paste in the interfacial zone (Shafigh et al., 2011a). The failure of OPSC mainly depends on the breakdown of aggregate-paste bond and crushing of OPS (Okpala, 1990). The addition of fibers enhances the compressive strength of concrete. Under an increasing compression loading, cracks will initiate and advance. When the advancing crack approaches a fiber, the debonding at the fiber-matrix interface begins due to the tensile stresses perpendicular to the expected path of the advancing crack. As the advancing crack reaches the interface, the crack tip stress concentration is reduced, and, thus, the propagation of cracks is blunted and blocked. This process is the crack bridging effect or crack arresting ability of fibers in concrete (Han et al., 2005; Kakooei et al., 2012; Song et al., 2005)

Table 4.3 shows the compressive strengths of OPSFRC at ages of 1-, 3-, 7-, 28- and 56-day. The addition of silica fume enhanced the early strength of both OPSC and OPSFRC. Silica fume reacts with the calcium hydroxide (CaOH) liberated from hydration of the cement to produce calcium silicate and aluminate hydrates, and, consequently, both compounds increased the strength of OPSC (Alengaram et al., 2010a). All OPSFRC attained about 81-94% of 28-days compressive strength at the age of 7-day. The results agree with the results from Alengaram et al. (2010a).

Table 4.3 Mechanical properties of control concrete and OPSFRC

Mix	Mechanical Properties								
	Compressive Strength (MPa)					Splitting Tensile Strength (MPa)	Flexural Strength (MPa)	MOE* (GPa)	PR**
	1-day	3-day	7-day	28-day	56-day	28-day			
Control	19.1 (0.5)	25.8 (0.4)	32.7 (0.5)	34.8 (0.4)	35.3 (0.5)	2.23 (0.03)	2.50 (0.07)	14.14 (0.19)	0.233
PP1/25	21.0 (0.3)	27.4 (0.6)	31.5 (0.6)	36.3 (0.4)	36.3 (0.5)	2.64 (0.15)	3.79 (0.14)	14.62 (0.35)	0.234
PP1/50	19.0 (0.5)	21.9 (0.5)	28.2 (0.3)	31.8 (0.4)	31.9 (0.6)	2.85 (0.19)	3.51 (0.23)	15.23 (0.36)	0.230
PP1/75	12.5 (0.8)	17.0 (0.5)	20.4 (0.4)	23.9 (0.5)	24.0 (0.1)	2.48 (0.06)	3.58 (0.17)	14.86 (0.41)	0.221
PP2/25	21.8 (0.7)	28.7 (0.5)	29.8 (0.6)	34.9 (0.7)	35.1 (0.5)	3.23 (0.25)	4.64 (0.22)	14.16 (0.36)	0.244
PP2/50	21.8 (0.8)	27.9 (0.8)	29.7 (0.3)	35.2 (0.5)	35.2 (0.6)	3.15 (0.04)	4.39 (0.07)	14.49 (0.41)	0.251
PP2/75	22.9 (0.2)	26.3 (0.2)	31.9 (0.1)	36.0 (0.2)	35.9 (0.7)	3.01 (0.06)	4.54 (0.17)	14.79 (0.24)	0.235
N1/25	15.4 (0.8)	24.5 (0.2)	30.8 (0.6)	35.8 (0.4)	36.0 (0.3)	2.97 (0.06)	4.20 (0.05)	12.26 (0.31)	0.266
N1/50	16.4 (0.5)	25.9 (0.6)	34.4 (0.1)	36.6 (0.3)	36.4 (0.3)	3.25 (0.08)	4.36 (0.16)	12.78 (0.35)	0.252
N1/75	16.8 (0.7)	25.4 (0.6)	29.9 (0.6)	36.8 (0.6)	36.8 (0.4)	3.49 (0.06)	4.37 (0.19)	12.37 (0.33)	0.260

Note: The standard deviations (in MPa) of the corresponding mechanical properties are shown in the brackets

* MOE = Modulus of elascticity

** PR = Poisson's ratio

The difference between the 28- and 56-day strengths is negligible and hereafter the discussion on the compressive strength is based on the 28-day strength. The OPSFRC with nylon fibers showed consistent compressive strength compared to PP fibers and the strength enhancement was about 3-6% compared to the control mix. However, PP2 showed a negligible effect on the compressive strength for all V_f. The

fibrillated PP fibers had a negative effect on the compressive strength, as indicated in the strength reduction of up to 30%. Generally, the tensile strength of fibers governs the compressive strength. Fibers with high tensile strength transfer higher tensile stresses from a cracked matrix to the fibers (Song et al., 2005). Even though the tensile strength of N1 fibers in this study is lower than that for the PP fibers (Table 4.1), the higher compressive strength in N1 mixes might be attributed to the reaction of the amide group (-CO-NH-) of nylon fibers with water. The bond is between the oxygen in the water and hydrogen on the nitrogen, and between hydrogen in the water and oxygen on the carbon. As moisture is absorbed and bonds to the polymer backbone, the plastic (nylon) swells (Harold et al., 2005). The swelling of the amide chains enhances stiffness, and, hence, it allows the development of additional tensile stress.

The effect of both PP and nylon fibers on the compressive strength and the density is analysed and compared to the control concrete. In PP2, the increase of fibers V_f up to 0.75% showed a reduction in the density; nevertheless the compressive strength was maintained. In contrast, the increment of the compressive strength in N1 mixes was accompanied by an increment in the density.

The mixes with PP1 showed a reduction in the compressive strength when a higher volume of fibers was added. At a low V_f of 0.25%, the compressive strength of PP1/25 of about 36 MPa was slightly higher than the control concrete. However, the comparison between the control and the PP1/50 & PP1/75 shows a drastic drop in the strength of up to 30%. As discussed in the section 4.3.2, the density reduction of PP1 due to fibrillation effect which might contribute to low strength. In the development of LWAC, the density of concrete is vital. The ODD obtained in all the mixes of PP and N1 OPSFRC were well below the density limit of LWC of 2000kg/m^3.

4.3.3.2 Splitting tensile and flexural strengths

The dosage of fibers used in this investigation is higher compared to previous studies (Alhozaimy et al., 1996; Banthia & Gupta, 2006; Banthia & Nandakumar, 2003; Comiloli et al., 2007; Han et al., 2005; Kakooei et al., 2012; Mazaheripour et al., 2011; Qian & Stroeven, 2000; Song et al., 2005). The low dosage of PP or nylon fibers in concrete has no effect on the splitting tensile and flexural strengths, but it has been reported to produce a marginal improvement on the flexural toughness of concrete (Alhozaimy et al., 1996; Comiloli et al., 2007). Fibers provide added strength to the matrix through (i) carrying part of the applied load and (ii) the crack bridging effect (Qian & Stroeven, 2000). This implies that fibers with low tensile strength like PP and nylon also possess the ability to strengthen the brittle cementitious materials. The results from Table 4.3 show that the addition of PP and nylon fibers enhanced both the splitting tensile and flexural strengths of OPSFRC. However, the volume of fibers had an insignificant effect on both the splitting tensile and flexural strengths of OPSFRC.

Despite a decrease in the ODD, PP1 mixes produced higher splitting tensile and flexural strengths compared to the control concrete. The splitting tensile and flexural strengths of PP1 mixes experienced an increase of 19% and 45%, respectively, relative to the control mix. Alengaram et al. (2010a) reported that OPSC with an ODD of about 1600 kg/m^3 only produced splitting tensile and flexural strengths of 1.84 MPa and 3.00 MPa, respectively, while the PP1/75 mix produced 2.48 MPa and 3.58MPa, respectively. The higher tensile strength in PP1 mixes can be attributed to the additional tensile stress taken by the fibers and crack bridging effect of the fibers.

The advantage of fibers in the enhancement of tensile strength is more evident in the OPSFRC with multi-filament fibers of PP2 and N1. The tensile strength of these two

mixes were close to each other for all volume fractions of fibers. The splitting tensile and flexural strengths of PP2 and N1 mixes were found to be 57% and 86% higher, respectively, than the control concrete. This increase in the tensile strength of PP2 and N1 compared to the PP1 mixes is attributed to the fiber geometry. The fibrillated PP1 fiber has a relatively smaller surface area for the development of the fiber-matrix bond, compared to multi-filament fibers. Thus, the greater surface area of PP2 and N1 fibers was effective in transferring the higher tensile stress compared to the PP1 fiber. At a given fiber content, fiber with smaller diameter will have more fibers to bridge the cracks. This phenomenon reduces the stress concentration at the crack section and improves the crack growth resistance (Banthia & Gupta, 2006), which, eventually, enhances the tensile strength of OPSFRC.

Different equations have been proposed to correlate splitting tensile strength to compressive strength of LWC as stated by Shafigh, Jumaat, et al. (2012). Eq. 4.1 was proposed by Shafigh, Jumaat, et al. (2012) to predict splitting tensile strength based on the compressive strength of OPSC.

$$f_t = 0.4887 \sqrt{\mathbf{f_{cu}}} \quad (4.1)$$

where f_t and f_{cu} are the splitting tensile and compressive strengths in MPa, respectively.

In order to include the effect of fibers on the enhancement of the tensile strength of OPSFRC, a higher coefficient, as shown in Eq. 4.2, predicts the splitting tensile strength within ±10% errors. An accurate prediction of tensile strength of concrete will help in mitigating cracking problems, improve shear strength prediction and minimize the failure of concrete in tension (Shafigh et al., 2012b).

$$f_t = 0.52\sqrt{f_{cu}} \quad (4.2)$$

In terms of flexural strength, the CEB/FIP manual proposed Eq. 4.3 to relate the flexural strength to the compressive strength for LWC made with expanded shale and clay aggregate (Short, 1977).

$$f_r = 0.46\sqrt[3]{f_{cu}^2} \quad (4.3)$$

where f_r and f_{cu} are the flexural and compressive strengths in MPa, respectively.

Based on the flexural strength of OPSC, U. J. Alengaram, Mahmud, and Jumaat (2008) modified Eq. 4.3 and proposed Eq. 4.4. A new equation, Eq. 4.5 is suggested for OPSFRC with PP and nylon fibers to predict the flexural strength within ±10%.

$$f_r = 0.3\sqrt[3]{f_{cu}^2} \quad (4.4)$$

$$f_r = 0.4\sqrt[3]{f_{cu}^2} \quad (4.5)$$

4.3.3.3 Brittleness ratio

The brittleness of the LWC was attributed to the porous characteristic of the lightweight aggregate. A brittle LWC will result in a complete and immediate loss of load carrying load capacity once the ultimate tensile stress capacity is reached. It has been shown that the addition of steel fiber to OPSC reduced the brittleness and increased the ductility of OPSFRC (Yap et al., 2014). In this study, the brittleness of the OPSC and OPSFRC specimens was measured by the compressive to flexural strength ratio (Sun & Xu, 2009). Based on Table 4.3, the brittleness ratios of control mix was 13.9. The addition of fibers into the OPSFRC mixes reduced the brittleness ratios. The brittleness ratios of PP1, PP2 and N1 mixes are within the range of 6.7-9.6, 7.5-8.0 and 8.4-8.5, respectively.

The experimental results showed that the addition of PP and nylon reduced the brittleness of OPSC by 31-52%.

4.3.3.4 Modulus of elasticity and Poisson's ratio

Table 4.3 shows the experimental results of modulus of elasticity (MOE) and Poisson's ratio (PR) of all OPSFRC, which range between 12.3-15.2 GPa and 0.221-0.266, respectively. The control mix without any fibers produced a MOE of 14.1 GPa and PR of 0.233. The values of MOE show that OPSFRC produced about 50-90% increase in MOE compared to 8-11 GPa obtained for OPSC (Alengaram et al., 2010a, 2010b; Shafigh et al., 2011b; Shafigh et al., 2012b). Shafigh et al. (2012b) stated that the mechanical properties of OPSC using crushed OPS are higher than OPSC with uncrushed OPS. However, in the present study, the combined effect of both SF and fibers enhanced the MOE of OPSFRC, even higher than OPSC with crushed OPS. The addition of silica fume improved the cohesiveness of the cement matrix (Alengaram et al., 2010a) and the fibers contributed to crack bridging. The combined effect of both silica fume and fibers reduced the strain induced under compression loadings, and eventually increased the MOE of OPSFRC.

Moreover, the mix PP1/50 produced comparable MOE to that of OPSC reinforced with 1% of steel fibers (Shafigh et al., 2011c). Both the MOE and PR of OPSFRC were found to be dependent on the type of fiber, but independent of fiber volume. The major advantage of PP1 fibers was evident in the MOE. From previous discussions (Sections 4.3.3.1 & 4.3.3.2), the compressive and tensile strengths of PP1 mixes reduced as the density reduced. OPSFRC containing PP1 fibers showed the highest MOE among all fibers, with a slight increment of MOE (approximately 6% higher than the control OPSC). However, diverse observation was obtained in the

Poisson's ratio in the PP1 mixes, at which the PR of PP1 mixes recorded at 0.221 to 0.234 while the control OPSC produced a PR of 0.233. The Poisson ratios of PP1 specimens were reduced by up to 5%. The reduction in the PR in the PP1 mixes could be explained by the reduced strength of the PP1 specimens attributed to the large voids in the PP1 specimens, at which the specimens cannot sustain lateral deformation due to the fibrillated PP1 fibers. Meanwhile, the Poisson's ratios in PP2 and N1 mixes reported the improvement up to 15% relative to the OPSC mix. This phenomenon was found to be in agreement with the Section 4.3.3.1 which mentioned that the compressive strength of OPSFRC containing PP2 and N1 fibers showed slight increase in the compressive strength.

In the MOE testing, all OPSFRC failed under comparable loadings, but at different peak strain. The peak strain of PP1 mixes was found to be 0.0012, while the N1 mixes reported a peak strain at about 0.0025. Moreover, compared to the peak strain of 0.002 for NWC, the N1 mixes produced a higher peak strain, which indicates that nylon fibers enhanced the ductility of OPSC to surpass NWC. In addition, the results from section 4.3.3.3 showed that the addition of nylon fibers reduced the brittleness ratio of OPSC from 14 to 8.5 (40% reduction). Hence we can conclude that the nylon fibers changed the brittle OPSC to a more ductile material.

Alengaram et al. (2011) proposed Eq. 4.6 to predict the MOE by using the compressive strength and air-dry density, which were modified from the equation for the CEB/FIP model (Short & Kinniburgh, 1978). The original CEB/FIP used A=9.1 for natural and manufactured lightweight aggregate.

$$E_s = (\frac{\rho}{2400})^2 \times (f_{cu})^{1/3} \times A \quad (4.6)$$

where E_s is the MOE (GPa), ρ is air-dry density (kg/m^3), f_{cu} is compressive strength (MPa) and A is the coefficient with a value of 5.

To correlate the effect of fibers in OPSFRC, Eq. 4.6 is changed to suit the different fibers:

$$E_s = (\frac{ODD}{2400})^2 \times (fcu)^{1/3} \times A \quad (4.7)$$

where E_s is the MOE (GPa), ODD is oven-dry density (kg/m^3), f_{cu} is compressive strength (MPa) and A is coefficient (6.1 for nylon fibers ;7.7 for control mix and PP2 mixes; 7.8 for PP1 mixes). Equation 4.7 can be used to predict the MOE of OPSFRC within ±1 GPa.

4.3.4 Ultrasonic pulse velocity

The UPV test is a non-destructive test to assess the uniformity and relative quality of concrete to indicate the presence of voids and cracks and to estimate the depth of cracks. Based on the UPV values in Table 4.4, it is evident that both the PP and nylon fibers produced no remarkable effect on the UPV values of OPSFRC. However, it is found that UPV can be correlated with its corresponding compressive strength, as shown in Figure 4.3, with a R^2 of 0.91. Therefore, Eq. 8 is proposed to estimate the compressive strength based on the UPV values.

$$f_{cu} = 0.082 (UPV)^{4.4} \quad (4.8)$$

where f_{cu} is compressive strength (MPa) and UPV is ultrasonic pulse velocity (km/s)

Table 4.4 Ultrasonic pulse velocity (UPV) of OPSC and OPSFRC

Mix	UPV at different ages (km/s)				
	1-day	3-day	7-day	28-day	56-day
Control	3.39	3.52	3.70	3.98	4.10
PP1/25	3.46	3.71	3.86	3.99	3.97
PP1/50	3.46	3.55	3.72	3.83	3.85
PP1/75	3.27	3.40	3.66	3.69	3.77
PP2/25	3.63	3.86	3.91	4.02	4.04
PP2/50	3.50	3.83	3.90	3.94	3.94
PP2/75	3.45	3.75	3.79	3.86	3.89
N1/25	3.28	3.65	3.77	3.90	3.92
N1/50	3.48	3.78	3.92	3.99	4.02
N1/75	3.38	3.81	3.88	3.94	4.01

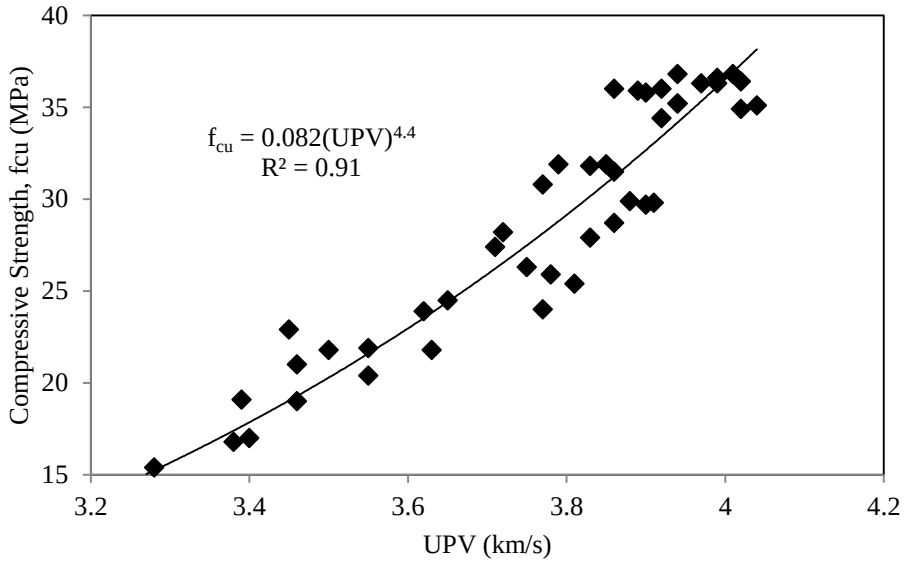

Figure 4.3 Relationship between ultrasonic pulse velocity (UPV) and compressive strength, f_{cu}

Concrete with UPV values within the range of 3.66-4.58 km/s are considered as in "good" condition (Leslie & Cheeseman, 1949). As long as the UPV values lie within this category, it implies that a particular concrete does not contain any large voids or cracks, which will affect the structural integrity (Kwan et al., 2011). It was reported that the failure of OPSC occurred at the aggregate-mortar interface (Shafigh et al., 2011a) due to porous mortar at the interface (Kwan et al., 2011). Thus, UPV is vital for assessing the presence of large voids within the interface zone, and, eventually, to check

the quality and strength of OPSC. In the present study, the UPV values for all mixes were found to be more than 3.66km/s at the age of 7 days.

4.3.5 Post-failure compressive strength

Post-failure compressive strength (PFCS) is a simplified method to assess the post-failure toughness of concrete. The values for the PFCS of the control OPSC and all OPSFRC are given in Table 4.5. The crack bridging effect of fibers that are existent at the crack face allows additional stress to be taken by the OPSFRC. In the concrete with fibers, additional force has to be applied on to the concrete for the crack to propagate further, compared to concrete without fibers. Thus, the addition of fibers is expected to enhance the post-failure toughness of concrete.

Table 4.5 Post-failure compressive strength (PFCS) of OPS concrete and OPSFRC

Mix	1-day		3-day		7-day		28-day		56-day		Average % of CS (%)
	PFCS	% of CS (%)	PFCS	% of CS (%)	PFCS	% of CS (%)	PFCS	% of CS (%)	PFCS	% of CS (%)	
Control	12.5	63.8	16.7	64.7	20.7	63.3	22.2	63.8	22.5	63.7	63.9
PP1/25	15.9	75.7	21.0	76.6	24.5	77.8	26.7	73.6	26.1	71.9	75.1
PP1/50	14.5	76.3	17.8	81.3	21.8	77.3	24.6	77.4	25.1	78.6	78.2
PP1/75	10.7	85.6	13.1	77.1	13.2	64.7	19.1	79.9	19.1	79.6	77.4
PP2/25	17.3	79.4	20.5	70.0	21.0	70.5	24.7	72.9	24.3	70.4	72.6
PP2/50	18.1	83.0	22.1	79.2	20.1	67.7	22.0	64.0	22.6	66.3	72.0
PP2/75	19.6	85.6	20.6	78.3	25.2	79.0	26.0	72.2	26.4	73.5	77.7
N1/25	10.2	66.2	16.6	67.8	20.1	65.3	24.1	67.3	23.7	65.8	66.5
N1/50	11.2	68.3	19.2	74.1	23.4	68.0	24.3	66.4	24.7	67.9	68.9
N1/75	11.3	67.3	16.9	66.5	19.8	66.2	23.3	63.3	34.5	63.9	65.4
Note: PFCS = post-failure compressive strength (MPa); CS = compressive strength (MPa)											

As expected, OPSFRC with PP fibers produced about 8-14% higher PFCS than the OPSC. Again, the volume fraction of fibers has no significant effect on the PFCS of OPSFRC. However, the improvement in the compressive strength of the N1 mixes is attributed to the hydrolysis of amides in the nylon fibers; this fiber-matrix bond failed during the compression failure when the initial compressive loading was applied on the cube specimens. Thus, N1 mixes showed 1-5% PFCS improvement compared to OPSC. Therefore, the magnitude of PFCS depends on the fiber bridging to sustain further compressive loading.

4.4 Chapter conclusions

Based on the experimental results, it can be concluded that the addition of PP and nylon fibers enhanced the mechanical properties of concrete. The enhancement is mainly attributed to the fiber bridging process that allowed additional stress to develop for the cracks to propagate.

- Fibrillated PP fibers (PP1) tend to displace mortar in concrete as the diameter of PP1 fiber is more than the multi-filament fibers, and, hence, the ODD of OPSFRC was found to be 1640 kg/m^3. The density reduction of about 10% and 30%, compared to the control and normal weight concretes, respectively, is likely to decrease the dead load. The fibrillated fibers also enhance the splitting tensile and flexural strengths up to 19% and 45%, respectively, compared to the control concrete.
- Multi-filament PP2 fibers had a positive effect on the tensile strength, as both flexural and splitting tensile strengths were up to 86% higher than the control concrete. The effect of PP2 and nylon fibers (N1) on the ODD is marginal; however, it was evident that the compressive and tensile strengths of N1 mixes

produced the highest enhancement, compared to PP fibers. Further, N1 mixes produced better ductility than NWC by achieving a peak strain of 0.0025. The workability of N1 mixes was lower than the PP fibers.

- Both MOE and UPV of OPSFRC are independent on fiber volume fraction.
- The brittleness ratios showed that the addition of PP and nylon fibers reduced the brittleness of OPSC by 31-52%.
- The UPV test results show that both OPSC and OPSFRC could be categorized as “good” condition after 7 days.
- The addition of PP and nylon fibers improved the post-failure toughness of OPSC in terms of post-failure compressive strength (PFCS). The fiber-matrix bond enhanced the PFCS values in the OPSFRC, which is a sign of ductility.

CHAPTER 5

EFFECTS OF STEEL FIBERS ON THE MECHANICAL PROPERTIES OF OIL PALM SHELL CONCRETE

5.1 Chapter introduction

The chapter shows high similarity with the previous chapter (Chapter 4), but differs in the type of fibers used. The aim of this chapter is to discuss the effects of steel fibers on the mechanical properties of OPSFRC. The experimental results and discussions in this chapter has been accepted in the journal paper titled "The Effect of Aspect Ratio and Volume Fraction on Mechanical Properties of Steel Fiber-Reinforced Oil Palm Shell Concrete" in the Journal of Civil Engineering and Management.

The use of fibers on the enhancement of flexural toughness, impact resistance and related parameters is well established. The application of steel fibers in different types of concrete, such as NWC (Özcan et al., 2009), high strength concrete (Eren & Celik, 1997), lightweight concrete (Düzgün et al., 2005), ultra-high performance concrete (Habel & Gauvreau, 2008) and self-compacting concrete (Deeb et al., 2012) has changed the design philosophy of reinforced concrete. Many researchers reported the effect of steel fibers on the enhancement of the characteristics, such as mechanical properties, shrinkage, freeze-thaw resistance (Atiş & Karahan, 2009), modulus of rupture, deflection capacity, energy absorption (Kim et al., 2011), fatigue strength (Cachim et al., 2002), toughness (Nataraja et al., 2000), shear strength (Slater et al., 2012), torsion strength (Okay & Engin, 2012), impact resistance (Nili & Afroughsabet, 2010), and fire resistance (Fike & Kodur, 2011). Further, studies on the effects of steel fibers in LWC using expanded clay aggregate (Gao et al., 1997), sintered fly ash

aggregate (Kayali, Haque, & Zhu, 2003) and natural pumice (Düzgün et al., 2005; Libre et al., 2011) were reported.

The significant enhancements by the addition of steel fibers provokes the use of steel fibers in LWC includes OPSC. The enhanced properties of LWC enable a wider range of application of the LWC. Instead of flooring and walls, the steel fiber-reinforced OPSC can be applied in structural members, such as beams, columns or ground supported slabs. The recent work on the use of steel fibers in the OPSC (Shafigh, et al., 2011c) reported on steel fibers of the aspect ratio 65 only. However, no investigation has been carried out on the effect of the aspect ratio and volume fraction of OPSC. The investigation on the aspect ratio is important, as it is reported that both the aspect ratio and fiber volume have a significant effect on the of properties concrete (Gao et al., 1997). The selection of fibers is vital in optimizing the mechanical properties of OPSC. Thus, the significance of this investigation lies in the following: the effect of aspect ratio of steel fibers on OPSC and the influence of the volume fraction of each aspect ratio on OPSC. Three different types of steel fibers were added into OPSFRC which differs in the aspect ratio. The aspect ratios of the steel fiber studied are 55, 65 and 80. The effect of volume fraction of each aspect ratio (V_f = 0.25%, 0.50% and 0.75%) was also studied.

5.2 Experimental program

5.2.1 Materials

Similar to Chapter 4, there is one control OPSC mix design obtained from Chapter 3 for the comparison. Meanwhile for the OPSFRC mixes, all the constituent materials were kept constant for all mixes except the steel fibers. A number of nine OPSFRC mixes were prepared. The variables of the OPSFRC mixes are three steel fibers of aspect ratio

55, 65 and 80 and each fibers of volume fraction 0.25%, 0.50% and 0.75% were added for the study of volume fraction. All the three steel fibers confirm to ASTM A820 and BS EN 14889-1 and their physical properties of the steel fiber are presented in Table 5.1. In addition, the tensile strength and modulus of elasticity of the steel fibers are 1100 MPa, and 205 GPa, respectively.

Table 5.1 Properties of steel fibers

Fiber		Geometry	Length (mm)	Diameter (mm)	Aspect ratio
S1	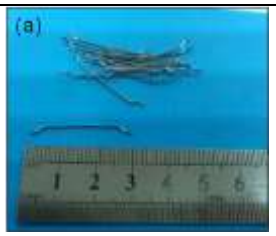	Hooked end	30	0.55	55
S2	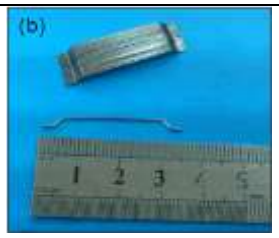	Hooked end	35	0.55	65
S3	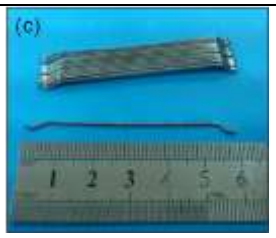	Hooked end	60	0.75	80

5.2.2 Mixing proportion

A total of ten OPSC mixes, as shown in Table 5.2, were prepared. One of the mixes is the control concrete without steel fibers. The variables investigated in this research are aspect ratio (l/d) and volume fraction (Vf) of the steel fibers. For each l/d, three different mixes with Vf of 0.25%, 0.50% and 0.75% of concrete volume were prepared and investigated.

Table 5.2 Mix proportioning for OPSFRC containing steel fibers

No.	Mix	Cement (kg/m^3)	Silica fume (kg/m^3)	OPS (kg/m^3)	Mining sand (kg/m^3)	Water (kg/m^3)	Fiber (% vol.)		
							S1	S2	S3
1	Control	539	53	323	971	178	0	0	0
2	S1/25	539	53	323	971	178	0.25	0	0
3	S1/50	539	53	323	971	178	0.50	0	0
4	S1/75	539	53	323	971	178	0.75	0	0
5	S2/25	539	53	323	971	178	0	0.25	0
6	S2/50	539	53	323	971	178	0	0.50	0
7	S2/75	539	53	323	971	178	0	0.75	0
8	S3/25	539	53	323	971	178	0	0	0.25
9	S3/50	539	53	323	971	178	0	0	0.50
10	S3/75	539	53	323	971	178	0	0	0.75

5.2.3 Mixing, specimen preparation and testing

First, the OPS was soaked in water for 24 hours and then it was left in the air-dry condition for another 24 hours in order to ensure a saturated surface-dry (SSD) condition. The OPS was used in the SSD condition to prevent the water added in the mix from being absorbed by the OPS. The mixing processes were in accordance to the flow shown in Figure 3.2. First, the sand and OPS were mixed. This was followed by the addition of cement and SF. After thorough mixing, the water and superplasticizer were added. Finally, the fibers were dispersed into the mixer. The slump test, in

accordance with ASTM C143 (2012), was used to measure the workability of OPSFRC. The fresh density of OPSFRC was also measured.

The following specimens were prepared for hardened concrete property tests: cubes of 100 mm were used for the compressive strength and UPV of concrete at ages of 1-, 3-, 7-, 28- and 56-day based on BS EN 12390-3 (BS EN 12390: Part 3, 2000) and ASTM C597 (2009). After the compressive strength test, the cubes were reloaded to obtain the post-failure compressive strength (PFCS). The specimens of 100 mm diameter x 200 mm height cylinders, 100 x 100 x 500 mm prisms, 150 mm diameter x 300mm height cylinders were used for the splitting tensile strength (ASTM C496/ C496M, 2011), flexural strength (ASTM C78/ C78M, 2010) and modulus of elasticity (ASTM C469, 2010), respectively at the age of 28-day.

5.3 Results and discussion

5.3.1 Workability (slump)

The slump values for fresh concrete are shown in Table 5.3. The addition of steel fibers in the OPSC resulted in a decrease in the workability. The ranges of slump were 55-70 mm, 50-60 mm and 20-45 mm for volume fraction (V_f) of 0.25%, 0.50% and 0.75% steel fibers, respectively. The corresponding reductions in the workability were 7-27%, 20-33% and 40-73% compared to the control concrete.

Table 5.3 Fresh and mechanical properties of OPSFRC with steel fibers

Mix	Slump (mm)	Mechanical properties								
		Compressive strength (MPa)					28-day splitting tensile strength (MPa)	28-day flexural strength (MPa)	28-day modulus of elasticity (GPa)	28-day Poisson's ratio
		1-day	3-day	7-day	28-day	56-day				
Control	75	19.1	25.8	32.7	34.8	35.3	2.23	2.50	14.14	0.233
S1/25	55	26.4	34.8	37.6	39.5	42.2	4.11	5.13	16.30	0.275
S1/50	50	21.2	26.3	29.0	38.7	38.7	3.77	5.23	16.03	0.289
S1/75	20	21.6	27.4	32.1	40.2	40.5	4.13	5.38	15.57	0.311
S2/25	65	21.3	30.4	40.7	43.7	43.8	4.40	5.58	16.21	0.309
S2/50	60	23.1	31.7	35.0	45.2	45.5	4.78	5.87	15.80	0.312
S2/75	45	22.7	33.6	39.0	46.6	46.6	5.90	6.56	14.15	0.299
S3/25	70	20.0	26.6	33.0	37.3	40.6	4.07	5.53	14.64	0.301
S3/50	60	22.5	27.9	32.0	41.5	42.7	4.70	5.69	14.22	0.282
S3/75	35	21.5	26.4	33.5	39.7	40.2	5.71	7.00	13.58	0.295

The concrete with steel fibers of aspect ratio of 55 (S1) produced the lowest slump compared with concrete with steel fibers of other aspect ratios: 65 (S2) and 80 (S3) for all volume fractions. With V_f = 0.25%, the highest slump was achieved for S3/25 mix. One of the observations on the effect of the aspect ratio on the workability of OPSFRC is the effectiveness of the dispersion of the steel fibers in the mix. From Figure 2, the effective zone is denoted by the matrix region surrounding the fiber, which provides an additional tensile strength due to the fiber-matrix bond. The S2 mix showed the best dispersion among the mixes in which the overlapping of the effective zone of steel fibers is minimal for the same volume fraction of steel fibers, as illustrated in Figure 2. The steel fiber, S2 is approximately twice as long than the maximum size of OPS aggregate, thus it is effective in binding both the coarse and fine aggregate in that vicinity (Figure 2(b)). Although S3 with a fiber length of 60mm was effective to bind more aggregate, due to its long geometry, the dispersion of fibers was not uniform (Figure 2(c)). The small-sized fiber, S1 has more fibers for a given volume compared to S2 and S3. Hence, they have a higher possibility of clogging together, and, eventually, increasing the overlapping of the effective zone, as shown in Figure 2(a). The clogging of fibers reduced the workability of OPSFRC and the mix S1 produced the lowest

workability. Thus, it can be concluded that steel fiber with a moderate aspect ratio is preferred for workable OPSFRC.

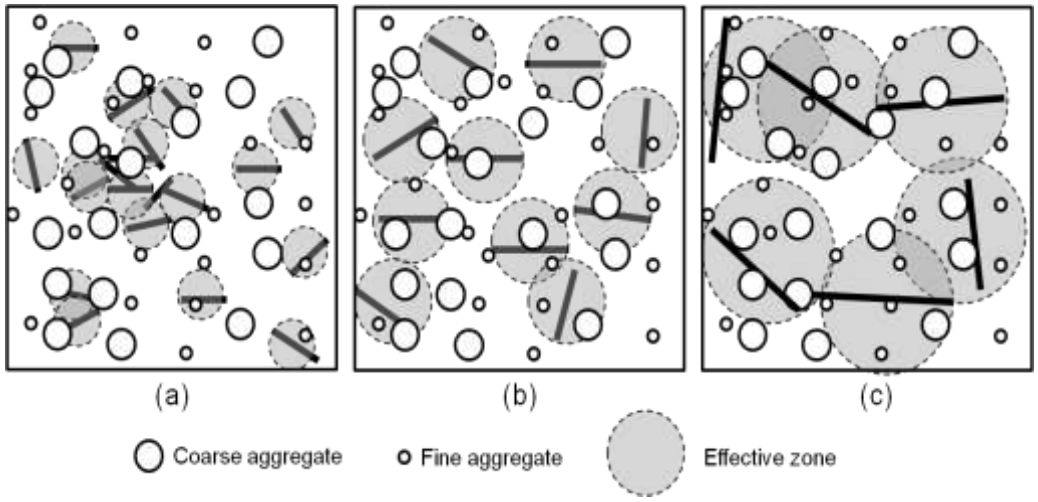

Figure 5.1 Graphical illustrations of dispersion of steel fibers: (a) S1, (b) S2 and (c) S3

The effect of V_f in the concrete was evident when the V_f was increased from 0.25% to 0.75%. In the concrete specimens with 0.75% of fibers, the clogging of the hooked end fibers was visible in certain sections. In the S1/75 mix, the workability achieved was very poor, which might be attributed to both the quantity and length of fiber. As stated earlier in this section, the quantity of fiber in the S1 category was higher compared to the others, which, combined with a high volume fraction of fibers, contributed to the poor workability.

5.3.2 Density

Density is the most important criteria in the classification of the LWC. The following discussions are focused on the effects of steel fibers and drying conditions on the fresh and hardened densities of OPSFRC.

5.3.2.1 Fresh density

Table 5.4 shows the values of fresh densities of the control concrete and OPSFRC with steel fibers of three different l/d and V_f. It can be seen that the fresh concrete density increased by about 5-190 kg/m^3 (0.3-10%) with the addition of steel fibers.

Table 5.4 Fresh and hardened densities of OPSFRC with steel fibers

Mix	Fresh density (kg/m^3)	SSD density (kg/m^3)	Air-dry density (kg/m^3)	Oven-dry density (kg/m^3)
Control	1970	2050	1950	1800
S1/25	1975	1990	1970	1840
S1/50	1985	1990	1970	1830
S1/75	1990	2000	1980	1850
S2/25	2030	2120	2110	1980
S2/50	2090	2140	2130	2010
S2/75	2120	2150	2140	2030
S3/25	2060	2130	2110	1980
S3/50	2120	2110	2100	1970
S3/75	2160	2170	2130	1990

The effect of the aspect ratio (l/d) and the volume fraction (V_f) of steel fibers on the fresh density of OPSFRC is shown in Figure 5.2. In general, the steel fibers with higher l/d resulted in a higher increment of fresh density. The S2 and S3 mixes showed a higher fresh density of about 60-150 kg/m^3 (3-8%) and 90-190 kg/m^3 (5-10%), respectively, than the control concrete. However, the increase of density of the S1 mix was insignificant (<1%) compared to the control concrete. Further, the S2 and S3 mixes produced about 55-170 kg/m^3 higher density than the S1 mix. As discussed in Section 5.3.1, the use of steel fibers with low l/d results in clogging of fibers that caused poor workability. Thus, the ability of mortar to flow into the void is restricted and the S1 mix produced a lower density compared to S2 and S3.

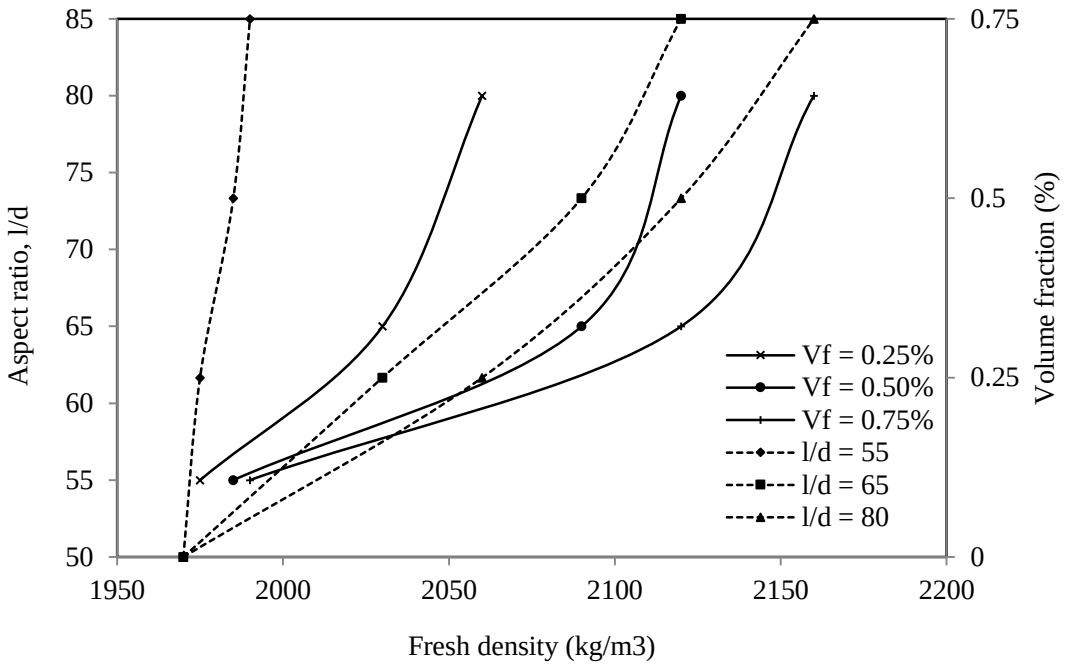

Figure 5.2 Influence of aspect ratio (l/d) and volume fraction on fresh density

The effect of the V_f of steel fiber on the fresh density of OPSFRC is seen in Figure 3. The specific gravity of steel fiber is 7.9, which is relatively higher compared to the other constituent materials in the OPSC. Hence, the large quantity of steel fibers added in OPSC increases the fresh density. When the V_f of the fibers increased from 0.25% to 0.75%, the corresponding increase in the fresh density was found to be about 0.5%, 4.5% and 5.0% for mixes S1, S2 and S3, respectively.

5.3.2.1 Hardened density

The hardened concrete densities of the mixes are shown in Table 5.4. The hardened densities include saturated surface dry (SSD), air-dry and oven-dry densities and the average density measured at the age of 28-day. This section aims to compare the effect of air-drying and oven-drying on the hardened densities of OPSFRC. The oven-dry density is generally preferred by most of the classifications of LWC such as EN 206-1 due to the consistency of water content in the concrete. Concrete with an oven-dry density of not greater than 2000 kg/m^3 can be defined as structural LWC (BS EN 206,

2013; Newman & Owens, 2003). All the mixes except S2/50 and S2/75 produced an oven-dry density of less than 2000 kg/m3, and, hence, the concrete could be considered as structural LWC.

The effect of l/d and Vf on the hardened concrete densities is similar to that of the fresh density. It was observed that the reduction of oven-dry density of control concrete was 12% compared to its SSD and the highest among the mixes. The OPSFRC produced a density reduction of about 0.5-2% and 6-8% in air-dry and oven-dry conditions, respectively. The addition of fibers contributed to the reduction in the lower air-dry and oven-dry densities compared to the control concrete. This could be attributed to the higher OPS content in the control concrete compared to OPSFRC as OPS has a 24-hour water absorption of about 24%.

5.3.3 Mechanical properties

5.3.3.1 Compressive strength

The compressive strengths of all mixes are shown in Table 5.3. All the mixes produced a high early compressive strength of 48-55%, 67-88% and 77-95% of the 28-day strength at the ages of 1-, 3- and 7-day, respectively. The addition of silica fume and its effect on the early strength in this research is quite similar to the reported results of Alengaram, et al. (2010a). The pozzolanic and micro-filling effects of SF enhance the aggregate-paste bond and the compressive strength of OPSC at an early age (Nili & Afroughsabet, 2010; Teo et al., 2007). The addition of silica fume also results in an increase of cohesiveness of the matrix that normally minimizes the induction of micro-cracks, and, consequently, increases the early strength (Mahmoud Nili & Vahid Afroughsabet, 2012). From Table 5.3, the 56-day compressive strength of all mixes show a slight increase of 0-7% compared to the 28-day strength. The strength

development was found to be independent of the aspect ratio and volume fraction of steel fibers.

The 28-day compressive strengths of the mixes fall in the range of 35-47MPa, as shown in Table 5.3 and Figure 5.3. As expected, the addition of steel fibers enhanced the compressive strength of OPSC by 7-33%. As seen from Figure 5.3, the mix S2/75 produced the highest 28-day compressive strength of about 47 MPa.

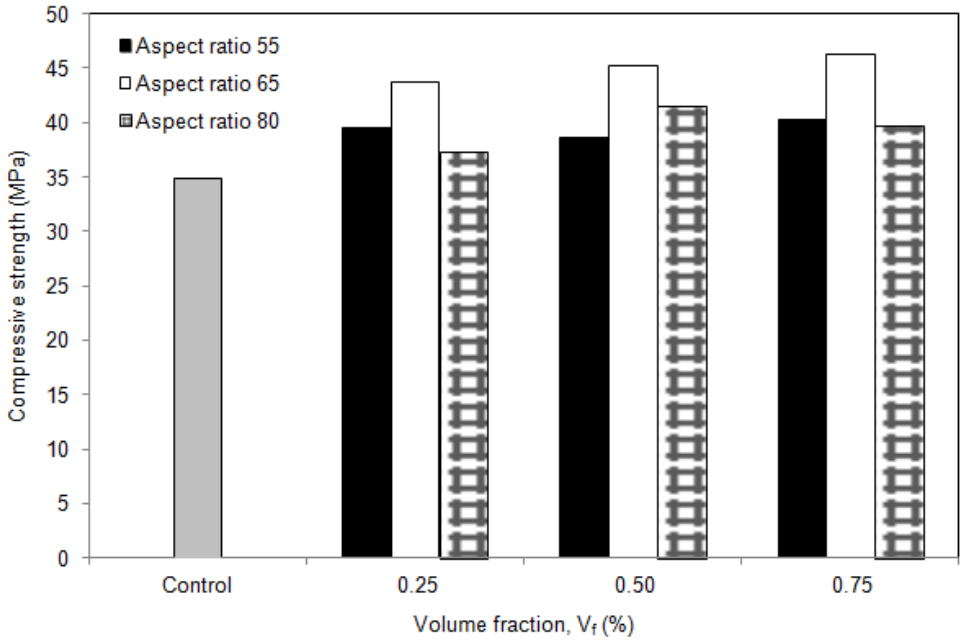

Figure 5.3 Effect of volume fraction and aspect ratio of steel fibers on compressive strength of OPSFRC

The effect of fibers on the compressive strength was evident, as the comparison of strength of the mixes S1, S2 and S3 shows a respective increment of 14%, 33% and 16% for V_f = 0.75%, compared with the control concrete. The reported increment in the compressive strengths up to 33% were found higher than the published results on LWC from sintered fly ash aggregate and expanded clay (Domagała, 2011; Gao et al., 1997; Gesoğlu et al., 2013; Kayali et al., 1999), as shown in Table 2.2. 2 has 16% and 18%

higher strength than that of S1 and S3. In addition, the previous chapter reported that the synthetic fibers slightly increased the compressive strength of OPSFRC only. Meanwhile the increment in the steel fiber-reinforced OPSFRC was more convincing. The overall comparison of the S2 mix with the control showed an increment in compressive strength of 26%, 30% and 33% for V_f of 0.25%, 0.50% and 0.75%, respectively. A similar comparison for S1 and S3 showed 14%, 11% and 16% and 7%, 19% and 14% for volume fraction V_f of 0.25%, 0.5% and 0.75%, respectively. The incorporation of steel fiber into the matrix increased the ultimate compressive strength by arresting the growth of cracks due to the bond between the steel fiber and the cement matrix (Gao et al., 1997). The addition of steel fibers beyond 0.25% resulted in less crack formation and higher compressive strength.

The effect of V_f on the 28-day compressive strength was not significant when it was increased from 0.50% to 0.75%; a drop in S3 and a slight increase in S1 and S2 was evident. This might be attributed to the high aspect ratio of the steel fibers, as the dispersion of fibers becomes more difficult. Thus, the effect of the increase in V_f on the compressive strength beyond 0.50% becomes insignificant or rather inconsistent. The results are in agreement with the published works of Gao et al. (1997) and Libre et al. (2011).

5.3.3.2 Splitting tensile strength

The splitting tensile strength is an important design parameter for beams and it provides an indication of the shear strength of concrete in diagonal tension (Düzgün et al., 2005). Compared to NWC, LWC produces a lower splitting tensile strength. The addition of steel fibers enhances the splitting tensile strength of structural LWC (Düzgün et al., 2005; Shafigh et al., 2011c).

The splitting tensile strengths of all mixes are shown in Table 5.3. The highest value of 5.90 MPa was obtained for S2/75 mix. The increase in splitting tensile strength of OPSFRC is in the range of 69-165%, which, compared to OPSC, showed that the effect of steel fibers was significant on the splitting tensile strength. The increment of the splitting tensile strength in OPSFRC specimens was compatible to both the NWC and other LWC as shown in Table 2.2. The ratio of 28-day splitting tensile strength to its corresponding compressive strength showed 10-14%, which could be compared to the 8-10% for NWC. This ratio increased with the increase in V_f.

The average increment of the splitting tensile strength for all aspect ratios for OPSFRC with a V_f of 0.25%, 0.50% and 0.75% were 88%, 98% and 135%, respectively, compared to the control concrete. The highest increase in the splitting tensile strength was observed for S2 & S3 mixes with V_f = 0.75%. For specimens with V_f less than 0.50%, the increase was insignificant. In comparison to Chapter 4.3.3.2, the increment in the synthetic fiber-reinforced OPSFRC were up to 57% but the steel fibers imparted three times higher improvement on the splitting tensile strength (increment up to 165%).

The effect of l/d on the splitting tensile strength was obvious in OPSFRC. The highest tensile strength was obtained for S2 & S3 mixes, while the S1 mix produced a lower strength compared to these two mixes. At V_f = 0.75% where the highest splitting tensile strength was observed, S1 produced 43% and 38% lower splitting tensile strength than S2 and S3, respectively.

The visual observation on the specimens tested showed different crack patterns for the control and OPSFRC (Figure 5.4). The cracks in the control specimens were

wider compared to the shorter and narrower cracks in the OPSFRC. Further, the OPSFRC with V_f= 0.25% showed a different crack pattern compared to the other two V_f; the cracks in the OPSFRC with V_f of 0.50% and 0.75% exhibit much narrower and shorter cracks compared to V_f with 0.25%. Thus, it is evident that a fiber content higher than 0. 5% produced significant improvement on the splitting tensile strength and reduced the crack width and length. A similar observation was reported by Domagała, (2011), Gao et al. (1997), Mirza & Soroushian (2002) and Sun & Xu (2009).

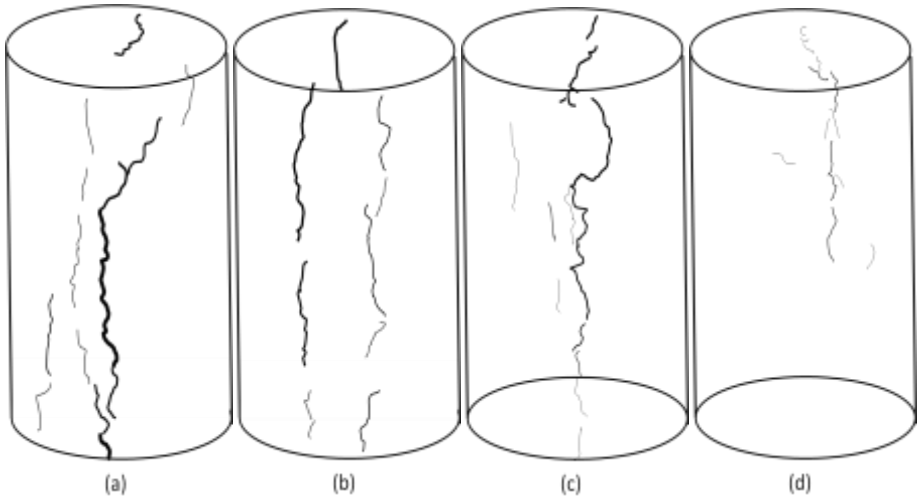

Figure 5.4 Sketches of crack patterns: (a) control; (b) S3/25; (c) S3/50 and (d) S3/75

The equation developed by Gao et al. (1997) to correlate the splitting tensile strength to V_f and l/d of LWC is shown in Eq. 5.1. This equation applies to steel fibers with a length of 30 mm and below. Eq. 5.1 could be used to predict the splitting tensile strength of the mix S1 within ±0.6 MPa. However, a slight modification to Eq. 5.1 was done to predict the strength for fiber lengths of more than 30 mm, as shown in Eq. 5.2. This equation predicted the splitting tensile strength of mixes S2 and S3 within ±0.5 MPa.

$f_{st} = 0.94\ f_t\ (1\text{-}V_f) + 3.02\ V_f(l/d)$ (5.1)

$f_{st} = 1.18\ f_t\ (1\text{-}V_f) + 3.40\ V_f(l/d)$ (5.2)

where f_t = splitting tensile strength of LWC (MPa); f_{st}= splitting tensile strength of steel fiber-reinforced LWC (MPa).

5.3.3.3 Flexural strength

Table 5.3 shows the flexural strength of all mixes, which ranged from 4.90-7.00 MPa. The flexural strength is a significant parameter and similar to the splitting tensile strength, it increases with the addition of steel fibers. The mechanism for the increase in the flexural strength is attributed to the strong fiber-matrix bond (Gao et al., 1997; Hamoush et al., 2010; Shafigh et al., 2011c; Sun & Xu, 2009).

The flexural strength to the compressive strength ratio was 7% for the control concrete. However, this ratio was average 14% for OPSFRC; this shows that the addition of steel fibers contributed more effects on the flexural strength compared to the compressive strength of OPSFRC. Moreover, the inverted flexural strength to the compressive strength is equal to the brittleness ratio as mentioned in Section 4.3.3.3. The brittleness ratio of the control OPSC was as high as 14 and the synthetic fibers reduced the brittleness ratio of OPSFRC by about 30-50%. The effect of steel fibers to reduce the brittleness of OPSC was more evident than the synthetic fibers, as the brittleness ratios of OPSFRC reinforced with steel fibers were 45-60% lower than the OPSC. The brittleness ratios of the steel fiber-reinforced OPSFRC specimens were found within the range of 5.7-7.9.

The OPSC specimens depicted typical flexural failure for specimens under two-point loading. However, the OPSFRC specimens with steel fibers showed ductile failure with progressive debonding of fibers. The final failure of OPSFRC happened due to unstable crack propagation when the fibers pulled out and the interfacial shear stress reached the ultimate bond strength (Gao et al., 1997).

Figure 5.5 shows the effect of l/d on crack formation when OPSFRC failed under flexural. The effect of l/d on the crack formation and its width was obvious; as the aspect ratio increased, a shorter and narrower crack width was found to form in all OPSFRC specimens. The highest flexural strength of 7.00 MPa obtained for the S3/75 mix with the l/d = 80 could be attributed to the large anchorage length of the fibers. The S1 mix with l/d = 55 produced lower flexural strength compared to other mixes. The effect of V_f on the cracks is similar to that reasoned for aspect ratio (Figure 5.6). The increase in V_f from 0.25% to 0.75% produced stronger bond between the matrix and the fibers that enhanced the flexural strength.

Figure 5.5 Flexural failure of (a) S1/50; (b) S2/50 and (c) S3/50

Figure 5.6 Flexural failure of (a) S1/25; (b) S1/50 and (c) S1/75

Similar to the equation proposed for the splitting tensile strength, Eq. 5.3, as suggested by Gao et al. (1997), was modified to suit the OPSFRC. This is shown in Eq. 5.4 and could be used to predict the flexural strength of OPSFRC within ±0.5 MPa with fibers of l/d and V_f of ranges 55-80 and 0.25%-0.75%, respectively.

$$f_{sw} = 0.92\, f_w\, (1\text{-}V_f) + 4.19\, V_f(l/d) \quad (5.3)$$

$$f_{sw} = 0.86\, f_w\, (1\text{-}V_f) + 3.20\, V_f(l/d) \quad (5.4)$$

Where f_w= flexural strength of LWC (MPa); f_{sw} = flexural strength of steel fiber-reinforced LWC (MPa)

5.3.3.4 Modulus of elasticity and Poisson's ratio

Table 5.3 shows the values of the modulus of elasticity (MOE) and Poisson's ratio (PR) for all mixes. As expected, the addition of steel fibers improved the MOE and PR of OPSFRC. The S1 mix produced the highest MOE in the range of 15.57-16.30 GPa, which showed an increment of 10-15% compared to the control concrete. A similar comparison for the S2 and S3 mixes showed an increment of 0-15% and 0-4%, respectively. The MOE of steel fiber-reinforced OPSFRC were found 1-2 GPa higher than the synthetic fiber-reinforced OPSFRC as discussed in Section 4.3.3.4.

The MOE obtained at V_f = 0.25% was the highest compared to other V_f for all aspect ratios. The highest MOE was obtained for the S1 mix with 16.30 GPa, which is 1% and 11% higher than the S2 and S3 mixes, respectively. The effect of l/d and V_f on the MOE was observed for all mixes; the higher the l/d and V_f values, the lower the MOE.

OPS is of organic origin, and hence, it has a lower stiffness and restraining effect compared to crushed granite aggregate. Thus, when the load is applied, the OPS undergoes a higher strain, which resulted in a lower MOE in the OPSC compared to the NWC (Alengaram et al., 2011). Similar to the discussion in section 5.3.3.1, the addition of silica fume and fiber-matrix bond enhanced the strength and a higher MOE was obtained for OPSFRC compared to OPSC.

Meanwhile, both the aspect ratio and volume fractions of steel fibers were not affecting the Poisson's ratios of OPSFRC, but the fiber-reinforcement increased the PR of OPSC from 0.23 to 0.28-0.30 in OPSFRC specimens. This has proven the benefit of steel fibers in enhancing the lateral strain was found to be more significant than the longitudinal strain. Moreover, the steel fiber resulted in higher PR than the PP and nylon fibers (around 0.25).

5.3.4 Ultrasonic pulse velocity

The ultrasonic pulse velocity (UPV) values for all mixes are shown in Table 5.5. UPV test is a non-destructive test (NDT) and used to assess the uniformity and relative quality of concrete, to indicate the presence of voids and cracks, and to estimate the depth of cracks (ASTM C597, 2009). As seen from Table 5.5, the UPV values of all OPSFRC are quite close to the UPV values of control concrete at all ages. The results from Table 5.5 indicate that the addition of steel fibers into OPSFRC did not influence the UPV values.

According to Leslie and Cheeseman (1949), concrete with a UPV within the range of 3.66 – 4.57 km/s is considered of good quality and concrete with a UPV of more than 4.57 km/s is of excellent quality. Concrete with excellent quality possesses

uniformity and negligible internal voids or cracks while concrete of good quality attains good uniformity due to proper compaction and minimal internal voids or cracks occur. The UPV values at the age of 3-day showed that all the mixes attained the minimum required value of 3.66 km/s specified for good quality concrete. The results supplemented the observation mentioned in the discussion in section 5.3.3.1 on high early compressive strength for all mixes. In addition, the trend of UPV values showed that there is an increase of 10% at the age of 56-day compared to the 3-day average values.

In comparison to the PP and nylon fibers, the UPV values of OPSFRC with steel fibers produced similar UPV with that PP- and nylon-fiber reinforced OPSFRC. Hence we can infer that fiber addition (disregard of any type of fibers) produced no effect on the UPV of OPSC.

Table 5.5 Ultrasonic pulse velocity (UPV) of OPSFRC with steel fibers

Mix	UPV at different ages (km/s)				
	1-day	3-day	7-day	28-day	56-day
Control	3.39	3.52	3.70	4.08	4.10
S1/25	3.47	3.94	3.96	4.11	4.13
S1/50	3.36	3.70	3.80	4.01	4.10
S1/75	3.36	3.73	3.98	4.09	4.12
S2/25	3.37	3.79	3.83	4.18	4.22
S2/50	3.20	3.76	3.92	3.99	4.18
S2/75	3.36	3.87	3.94	4.08	4.11
S3/25	3.41	3.73	3.97	4.01	4.04
S3/50	3.39	3.79	3.83	3.93	4.12
S3/75	3.39	3.67	3.82	3.88	4.05

An empirical equation based on regression analysis from Figure 5.7 is proposed to evaluate the compressive strength (fcu) based on the UPV values for OPSFRC.

$$f_{cu} = 0.43\ (UPV)^{3.2} \qquad (5.5)$$

Where f_{cu} = Compressive strength (MPa); UPV= UPV value (km/s)

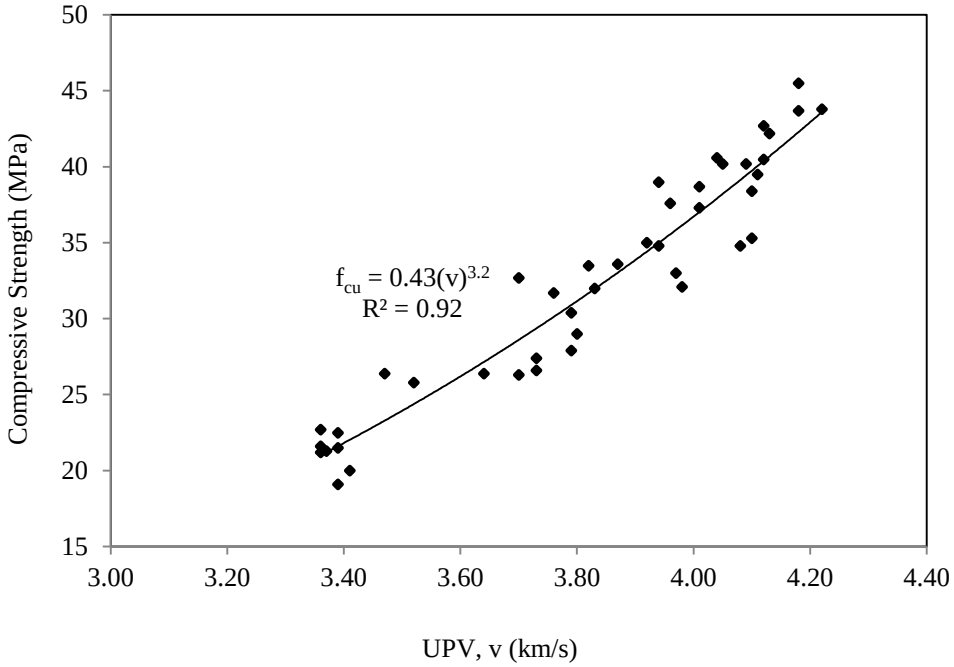

Figure 5.7 Relationship between compressive strength and UPV values

5.3.5 Post-failure compressive strength

The post-failure compressive strength (PFCS) is an important factor that was investigated in this work using cube specimens. The cube specimens that were tested and failed in the compressive strength test were reloaded to ascertain their PFCS. The PFCS is an indication of the post-failure compressive toughness of the concrete. Studies have shown that steel fibers increased the toughness of concrete (Nataraja et al., 2000); however, no literature is available to verify the toughness of concrete by reloading the specimen tested for compression.

The PFCS values are shown in Table 5.6. The average values of the percentage of the PFCS with their respective compressive strength at the ages of 1-, 3-, 7-, 28- and 56-day are shown in the last column. From the results, it can be seen that the addition of steel fibers enhanced the PFCS by 1.8-6.4% compared to the control concrete. In general, the higher aspect ratio and Vf increased PFCS. The increase in PFCS might be

attributed to a strong fiber-matrix bond even after the failure of concrete. The fiber-matrix bond enabled the fiber to hold the concrete together and inhibit further crack initiation and propagation.

Table 5.6 Post-failure compressive strength (PFCS) OPSFRC with steel fibers

Mix	1-day		3-day		7-day		28-day		56-day		Average % of CS (%)
	PFCS	% of CS (%)	PFCS	% of CS (%)	PFCS	% of CS (%)	PFCS	% of CS (%)	PFCS	% of CS (%)	
Control	12.5	63.8	16.7	64.7	20.7	63.3	22.2	63.8	22.5	63.7	63.9
S1/25	18.2	68.9	24.2	69.5	25.3	67.3	26.2	66.3	28.5	67.5	67.9
S1/50	14.9	70.3	17.4	66.1	19.5	67.2	23.5	60.7	24.8	64.7	65.8
S1/75	14.7	68.1	18.6	67.9	25.4	79.1	26.3	65.4	25.3	62.5	68.6
S2/25	13.0	61.0	20.8	68.4	26.8	65.8	29.5	67.5	28.8	65.8	65.7
S2/50	15.9	68.8	21.1	66.6	22.8	65.1	29.4	65.1	29.3	64.7	66.1
S2/75	15.4	67.8	23.2	69.0	26.7	68.5	32.0	68.5	33.0	71.4	69.0
S3/25	13.4	67.0	17.2	64.7	22.0	66.7	24.6	66.0	26.7	65.8	66.0
S3/50	15.6	69.3	18.4	65.9	21.0	65.6	29.0	69.9	32.3	75.6	69.2
S3/75	15.3	71.1	20.3	76.9	21.8	65.1	27.9	70.3	27.3	67.9	70.3
Note: PFCS = post-failure compressive strength in MPa; CS = compressive strength											

5.4 Chapter conclusions

In this investigation the effect of l/d and V_f on OPSFRC was studied. The fresh and hardened concrete properties were investigated. UPV were measured to correlate compressive strength of OPSFRC. Based on the study, the following conclusions were drawn:

- The slump for all mixes was in the range of 20-70mm. It was observed that the increase in V_f, reduced the workability of OPSFRC irrespective of l/d.
- The addition of fibers with high l/d and V_f increased the fresh density in OPSFRC.

- The values of SSD density, air-dry density and oven-dry density of OPSFRC varied in the range of 1990-2170 kg/m^3, 1970-2140 kg/m^3 and 1830-2030 kg/m^3, respectively.
- All mixes attained high early compressive strength, which is attributed to the pozzolanic and micro-filling effects of silica fume. Both effects increased the matrix cohesiveness and minimized the initiation of cracks.
- The mix S2 with l/d of 65 produced the highest 28-day compressive strength of 47 MPa. The compressive strength of OPSFRC depends on the l/d, whilst higher fiber content has a positive effect on it.
- The steel fibers provided additional tensile strength due to the fiber-matrix bond that enhanced both the splitting tensile and flexural strengths of OPSFRC. A fiber content above V_f of 0.50% produced a significant improvement in both the splitting tensile and the flexural strength.
- The lower stiffness of OPS can be overcome with the addition of fibers, and, hence, the MOE of OPSFRC was found to have increased 3-23% compared to the control concrete. In addition, the Poisson's ratio of OPSC also increased from 0.23 to 0.28-0.30 as in the OPSFRC specimens.
- The UPV results showed that they are independent of both l/d and V_f and all the OPSFRC mixes produced above 3.66 km/s at the age of 3-day indicating good quality concrete.
- The post-failure compressive strength was used in this investigation to measure the post-failure compressive toughness. It showed that an increase in l/d and V_f had a positive impact.

CHAPTER 6

INVESTIGATION ON THE FLEXURAL BEHAVIOR OF OIL PALM SHELL FIBER-REINFORCED CONCRETE BEAM

6.1 Chapter introduction

In the Chapters 4 and 5, the effect of steel, polypropylene and nylon fibers on the mechanical properties of oil palm shell fiber-reinforced concrete (OPSFRC) (corresponds to the second stage as shown in Figure 1.1 "Development of OPSFRC") was discussed. Based on the results from Chapters 4 and 5, steel fiber with aspect ratio 65 outperformed other fibers used in this investigation by producing the highest improvements on the mechanical properties of OPSFRC. Hence this chapter serves as an extension work of Chapter 5 and it aims to fulfill to third stage of the research as shown in Figure 1.1 ("Structural behaviors of OPSFRC). The flexural behavior of OPSFRC reinforced beam made with steel fiber of aspect ratio 65 is discussed in this chapter.

Following the published literature on flexural behavior on OPSC as discussed in Chapter 2, OPSC reinforced beams showed improved ductility compared to the NWC (Alengaram et al., 2008; Teo et al., 2006). The ductility ratio of OPSC was twice that of NWC and the good aggregate interlock in OPSC resulted in shorter flexural cracks compared to NWC (Alengaram et al., 2008).

The studies on fiber-reinforced concrete revealed that the addition of steel fiber in the cement matrix improved the toughness, first cracking load, yield load, moment capacity and crack resistance of reinforced concrete members subjected to flexural loading. However, the argument on the beneficial effect of the fibers lies on the ductility.

The published papers on steel fibers reported diverse results on either increase or decrease in the ductility of fiber-reinforced concrete beams (Altun & Aktaş, 2013; Chunxiang & Patnaikuni, 1999; Meda et al., 2012; Wang & Belarbi, 2011; You et al., 2011). The introduction of fibers for the enhancement of a particular structural behavior (e.g., shear, impact resistance, behavior at service load, crack control, etc.) can limit its ductility under flexure (Meda et al., 2012). The flexural behavior of steel fiber-reinforced OPSFRC beams is compared to that OPSC.

A total number of five beams were prepared in this study consisting of one control beam without fibers and the rest of the OPSFRC beams contained steel fiber of aspect ratio 65. The variable studied was volume fraction of steel fibers (0.25%, 0.50%, 0.75% and 1.00%). The objective of this chapter is to study the effects of steel fibers on the load capacity, cracking resistance and ductility of OPSC and OPSFRC reinforced concrete beams under flexural loading, in order to study the feasibility of OPSFRC in structural application.

6.2 Experimental program

6.2.1 Materials

All the materials and mix designs similar to the previous chapter (Chapter 5) were utilized in this work. A number of five mixes were prepared in this work. The detailed dimensions of the hooked end steel fiber are shown in Figure 6.1. The length and diameter of the steel fiber was 35 mm and 0.55 mm, respectively. The physical properties of the steel fiber can be referred to Table 5.1 (corresponding to the S2 in Table 5.1). In the fabrication of the flexural beams, ribbed steel bars of diameter 12 mm (yield strength = 515 MPa) were used as both compression and tension reinforcements. Plain mild steel bar with diameter 6 mm was used as shear link.

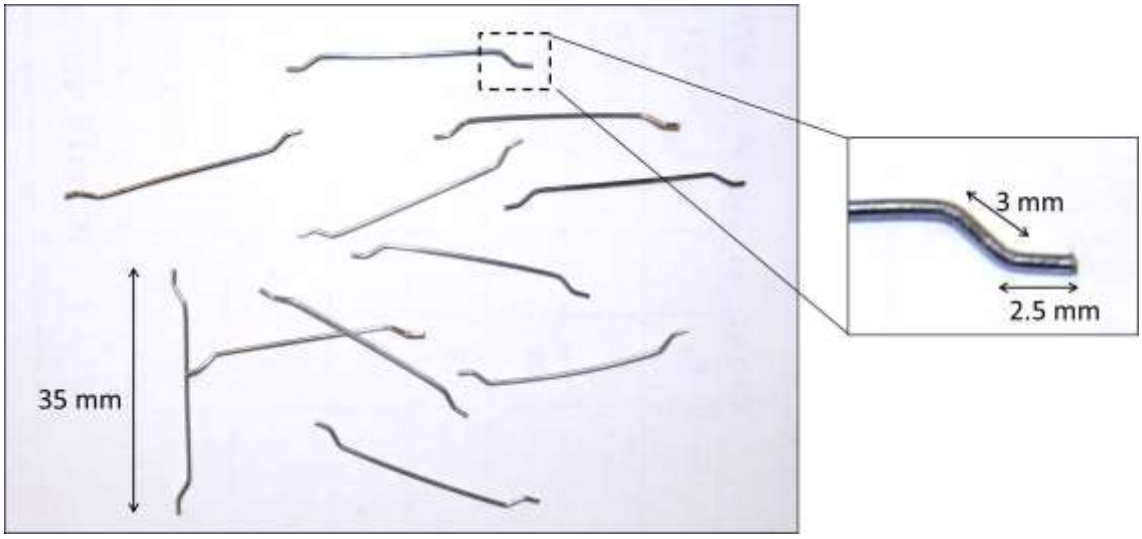

Figure 6.1 Steel fiber used in the OPSFRC mixes

6.2.2 Mixing proportion

Five mixes for the OPSC and OPSFRC beams were prepared. The mix proportions are reported in Table 6.1. All the constituent materials were kept constant for all the mixes as that of control OPSC mix and for the OPSFRC beams fiber contents of 0.25%, 0.50%, 0.75% and 1.00% (by volume) were added.

Table 6.1 Mix proportioning for OPSC and OPSFRC for flexural testing

Mix design	Cement (kg/m^3)	Silica fume (kg/m^3)	OPS (kg/m^3)	Mining sand (kg/m^3)	Water (kg/m^3)	Steel fiber (%vol.)
OPSC	539	53	323	971	178	0
OPSFRC-F25	539	53	323	971	178	0.25
OPSFRC-F50	539	53	323	971	178	0.50
OPSFRC-F75	539	53	323	971	178	0.75
OPSFRC-F100	539	53	323	971	178	1.00

6.2.3 Mixing, specimen preparation and testing

The mechanical properties and beam testing under flexural loading were conducted. For the testing of the mechanical properties of each mix proportion, 100 mm cubes, 100 (diameter) x 200 mm cylinders, 150 (diameter) x 300 mm cylinders, 100 x 100 x 500

mm prisms and 100 x 100 x 300 mm prisms were prepared for compressive strength (BS EN 12390: Part 3, 2000), splitting tensile strength (ASTM C496/ C496M, 2011), flexural strength (ASTM C78/ C78M, 2010) and modulus of elasticity/Poisson's ratio (ASTM C469, 2010), respectively. The specimens were removed from the moulds after 24 hours and cured in water until testing at 28 days.

Meanwhile, for the reinforced concrete beam test, five beams were designed and prepared as under-reinforced concrete beams in accordance to the BS 8110 to produce flexural mode of failure. Figure 6.2 shows the reinforcement arrangement for all the flexural beams. Ribbed steel bars with diameter 12 mm were used as tension reinforcement for all the specimens with a clear cover of 30 mm. The compression and shear reinforcements were not used in the middle-third of the beam (pure bending region-distance between two loading points is 0.7m). The shear reinforcement was used only in the shear span (0.7m from each support) at a spacing of about 75mm center to center to ensure yielding of tension steel before the crushing of concrete. In addition, strain gauges were attached in the tension reinforcement to measure the tensile strains in steel bars.

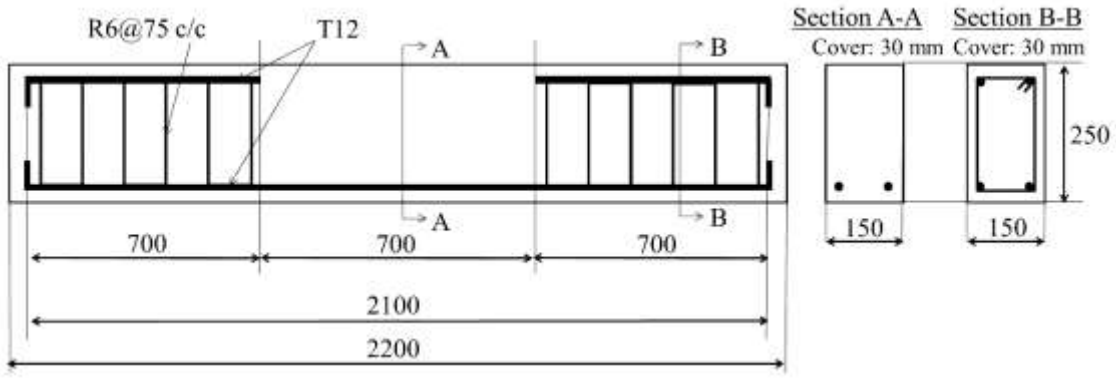

Figure 6.2 Reinforcement details of flexure test beams (all dimensions are in mm)

The casting of the flexure beams was done along with the companion specimens for mechanical properties. The beams were cast in steel moulds and vibrated by using poke vibrator. Further, the beams were cured in the moulds using wetted jute clothes until the age of 28-day and left in ambient condition till the day of testing. The flexural testing of the beam specimens was conducted by using an Instron universal testing machine with a built-in load cell capacity of 600 kN as shown in Figure 6.3(a) and 6.3(b). The strains in the tension reinforcements were measured by strain gauges and recorded in a data logger. The compressive strains of concrete were measured using demec gauge. In order to measure the deflections under flexural loading, a linear variable displacement transducer (LVDT) was placed at the mid-span of the beam as shown in Figure 6.3 (c). The crack widths were measured using a hand held microscope; the crack spacing between primary flexural cracks and primary-secondary cracks were also measured.

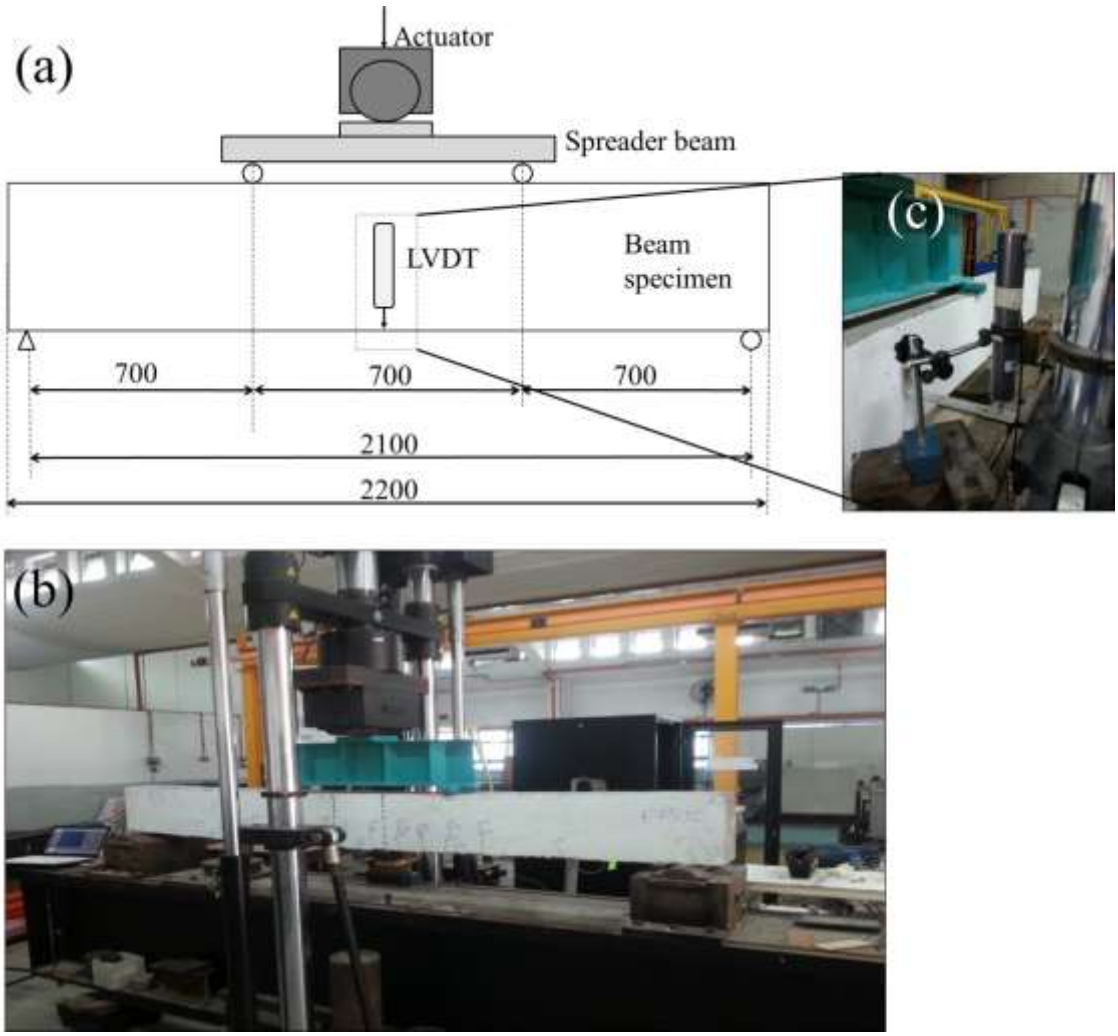

Figure 6.3 Flexural beam test set-up (all dimensions are in mm)

6.3 Results and discussion

6.3.1 Workability (slump)

The slump values of all the mixes are reported in Table 6.2. The control mix, OPSC produced a slump of 80 mm. The addition of 0.25–1.00% steel fibers into the OPSFRC mixes produced a remarkable reduction of workability of about 30–70%, compared to the control OPSC mix (Table 6.2). The dispersion of the steel fibers in the fresh concrete results in the formation of a cement matrix-fiber network structure, which leads to an increase in concrete viscosity, and, eventually, reduces the workability of the concrete (Chen & Liu, 2005). Moreover, the increase in the amount of steel fibers in the fresh OPSFRC mixes requires a higher amount of cement mortar to wrap around the

fibers, which further reduces both the concrete viscosity and workability. Therefore, this could explain that the increase of steel fibers from 0.25% to 1.00% in the OPSCC-F100 mix produced the lowest slump value. Nevertheless, all the OPSFRC mixes attained acceptable compaction with good finishing. The slump values for both OPSC and OPSFRC mixes showed compatible results to that reported in Table 5.1. This indicated that the mix design of OPSC and OPSFRC mixes can be reproduced with minimal standard deviation.

Table 6.2 Mechanical properties of OPSC and OPSFRC mixes

Mix	Slump (mm)	Compressive strength (MPa)	Flexural strength (MPa)	Brittleness*	Modulus of elasticity (GPa)	Poisson's ratio
OPSC	80	33.9 (0.37)	3.26 (0.16)	10.40	13.87	0.244
OPSFRC-F25	55	39.3 (0.39)	4.28 (0.10)	9.17	15.67	0.286
OPSFRC-F50	50	41.2 (0.53)	5.38 (0.05)	7.66	16.11	0.294
OPSFRC-F75	40	45.9 (0.80)	6.70 (0.14)	6.85	16.29	0.275
OPSFRC-F100	25	47.3 (0.20)	8.16 (0.16)	5.80	15.50	0.292
NOTE: The standard deviations of the corresponding mechanical properties are shown in the brackets. * Brittleness = compressive to flexural strength ratio						

6.3.2 Oven-dry density

Figure 6.4 shows the comparison of the oven-dry densities between the NWC, OPSC and OPSFRC mixes. Assuming an oven-dry density (ODD) of about 2300 kg/m^3 in the NWC mix (Shafigh, Jumaat, Mahmud, et al., 2011), the OPSC mix that contains 100% replacement of coarse aggregate by OPS produced a 20% ODD reduction to about 1830 kg/m^3. The reduced density reported in the OPSC could be advantageous in reducing the dead load and cost in the fabrication of the structural members.

However, it has been reported that the addition of steel fibers increases the density of LWC (Düzgün et al., 2005; Mo et al., 2014a; Shafigh, et al., 2011c), and reduces the benefit of density reduction in the LWC. EN206-1 states that concrete having an ODD between 800 and 2000 kg/m^3 could be defined as LWC. The ODD of the OPSFRC mixes reinforced with 0.25–1.00% steel fibers increased to the range of 1890–2000 kg/m^3 (Figure 6.4), which is attributed to the high specific gravity of the steel fibers (specific gravity = 7.9). Although the densities of the OPSFRC mixes increased, the OPSFRC still produced a density reduction of about 14–18% corresponding to the NWC mix and could be identified as LWC.

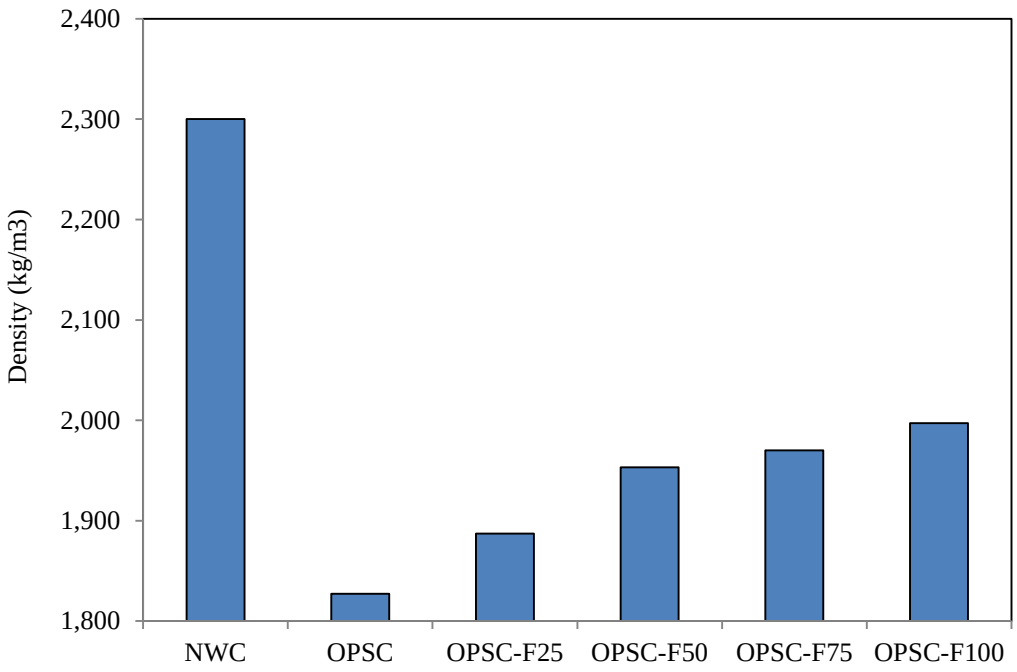

Figure 6.4 Comparison between the oven-dry densities of NWC, OPSC and OPSFRC

6.3.3 Mechanical properties

6.3.3.1 Compressive strength

The compressive strengths of all the mixes are reported in Table 6.2. The control mixes, OPSC mix yielded a compressive strength of about 35 MPa, which is similar to the OPSC with similar mix design from Chapter 5.

Previous studies on LWC have shown that the addition of steel fibers into LWC resulted in a significant enhancement in the compressive strength (Domagała, 2011; Gao et al., 1997; Shafigh et al., 2011c). The improvement in the compressive strength of OPSFRC by the addition of steel fibers was evident as enhanced compressive strengths were observed in the OPSFRC mixes, compared to the OPSC-F0 mix. As the volume of steel fibers increases, the compressive strength of the OPSFRC mixes increased significantly. It could be seen that the addition of 0.25% and 1.00% of steel fibers produced an improvement in the compressive strength of about 16% and 40% compared to the control OPSC mix, respectively. The highest compressive strength of about 47 MPa was recorded in the OPSC-F100 mix, which contained 1.00% steel fiber.

The enhancement mechanism of the steel fibers on the improved compressive strength in the OPSFRC mixes could be explained by the crack bridging effect (Abu-Lebdeh et al., 2011; Düzgün et al., 2005; Erdem et al., 2011; Gao et al., 1997; Hamoush et al., 2010; Singh et al., 2004). Under an increasing compressive loading, the crack is initiated and will propagate along the weaker component of the concrete. When the crack is approaching the randomly orientated steel fibers, the fiber bridging will result in crack closure and transfer the crack tip stress between the fiber-matrix interfacial bonding, substantially improving the strength of the concrete. Additional force is required to pull the fibers out from the fractured cement paste for the crack to continue

to propagate and open up, which, eventually, enhances the ultimate compressive capacity of the concrete.

6.3.3.2 Flexural strength

The low mechanical properties, especially the tensile strength of LWC limited the application of LWC, including OPSC as a structural member. The low tensile strength of LWC would lead to significant tensile cracking occurring at a much lower loading capacity compared to that of normal concrete (Yap et al., 2014). In this study, the flexural strength is reported as the tensile strength of both OPSC and OPSFRC in Table 6.2.

The steel fibers were added to the OPSFRC mixes to improve the tensile and torsional strengths of the OPSC. The contribution of the additional fiber-matrix interfacial bonding produced the increment in flexural strength of about 30–150% compared to the control OPSC. The addition of 0.25% steel fibers in OPSC-F25 mix was sufficient to produce competent tensile strength relative to that of NWC. A further increment in the steel fiber volume up to 1% resulted in the higher flexural strength of the OPSFRC mixes, which fell within the range of 5.4–8.2 MPa. The highest flexural strength of 8.2 MPa was obtained for OPSC-F100 mix, which is 150% higher than the OPSC-0 mix. Similar to the discussions in Section 6.3.3.1, the enhancement of tensile strength in the OPSFRC mixes could be explained by the crack bridging effect. However, the enhancement effect of steel fibers is more evident in the tensile strength than the compressive strength. This could be observed in the increased flexural to compressive strength ratio when the volume fraction of steel fibers increases. The flexural to compressive strength ratios of OPSC-F0, OPSC-F25, OPSC-F50, OPSC-F75 and OPSC-F100 mixes are 10%, 11%, 13%, 15% and 17%, respectively. The increasing

ratios indicated that the improvement in tensile strength is higher than the respective increase in compressive strength.

6.3.3.3 Brittleness

Another concern of LWC is its brittleness, which is attributed to the porous lightweight aggregate (Domagała, 2011). One of the methods to measure the brittleness is by the compressive to flexural strength ratio (Sun & Xu, 2009); the brittleness ratios of all the mixes are shown in Table 6.2. A lower brittleness value indicates that the concrete is less brittle.

The published papers on OPSC focused on increasing the mechanical properties of OPSC by using crushed OPS (Shafigh et al., 2011a, 2012a) and cementitious materials (Shafigh et al., 2013). However, although LWC becomes more brittle as the strength increases (Gao et al., 1997), the addition of steel fibers into LWC transforms the LWC from a brittle to a more ductile material (Düzgün et al., 2005; Okay & Engin, 2012). Hence, the addition of steel fibers serves as an innovative method to improve both the mechanical properties and brittleness of OPSC. The brittleness ratios of the OPSFRC mixes reduced significantly as the fiber content increased from 0.25% to 1.00%. For every 0.25% increment of steel fiber volume, the brittleness of the OPSFRC was reduced by 8–12%. The OPSC-F100 mix reinforced with 1% steel fibers showed the lowest brittleness ratio among all the mixes at 5.8 and the brittleness reduction was 44% compared to the control OPSC. Concrete is generally brittle as the concrete will fracture and has complete and immediate loss of load carrying capacity once the ultimate stress capacity is reached, especially under tensile loading. The crack bridging effect of steel fibers blunts the crack propagation and the fibers serve as a “bridge” for the fiber reinforced concrete to exhibit residual strength after the ultimate strength is

reached, eventually increasing the post-cracking behavior of concrete (Abu-Lebdeh et al., 2011; Hamoush et al., 2010; Singh et al., 2004; Zīle & Zīle, 2013). Hence, the addition of steel fibers reduces the brittleness of OPSFRC significantly.

6.3.3.4 Modulus of elasticity and Poisson's ratio

The modulus of elasticity (MOE) and Poisson's ratio of all the mixes are reported in Table 6.2. The MOE and Poisson's ratio of OPSC mix was found to be only 13.87 GPa and 0.244, respectively. The lower MOE and higher lateral deformation observed in the OPSC relative to the NWC could be attributed to the reduced stiffness in the OPSC, which produces higher deflection compared to the NWC (U. Johnson Alengaram et al., 2008). In comparison to the normal aggregate, the OPS has a lower stiffness and restraining effect. Hence, under compressive loading, the OPS undergoes higher strain, which produces a lower MOE than the NWC (Alengaram et al., 2011).

As seen from Table 6.2, the addition of steel fibers enhanced both the MOE and Poisson's ratio of the OPSC; however, both the MOE and Poisson's ratio were found to be independent of the volume fractions of the fiber. The OPSFRC mixes showed an increase in the MOE and Poisson's ratio within the ranges of 1.6—2.4 GPa and 0.03–0.05, respectively. The crack bridging effect of steel fibers induced higher stiffness, and, therefore, the OPSFRC can undergo higher stress and strain under loading (Rao & Seshu, 2003). Figure 5 shows the stress-strain curves of the OPSC and selected OPSFRC mixes up to the upper stress. The upper stress of concrete is taken as one-third of cylinder compressive strength as stated in ASTM C469. From Figure 5, the addition of 0.25% steel fibers imparted 16% and 2% increments in the upper stress and strain, respectively. The improvement of the upper stress is higher than the upper strain and

this resulted in a higher modulus of elasticity. However, both the MOE and Poisson's ratio of OPSFRC specimens were found to be independent of the volume fractions of the fiber. By referring to Figure 5, it is evident that the increase in the fiber content from 0.25% to 1.00% produced 20% higher upper stress and strain compared to the OPSC-100 specimen. The equal increase in both upper stress and strain resulted in the miniature change in the modulus of elasticity when fiber volume increases. Similar explanation could be applied on the Poisson's ratio, at which the increase in fiber content improved almost equally on both lateral and longitudinal strains.

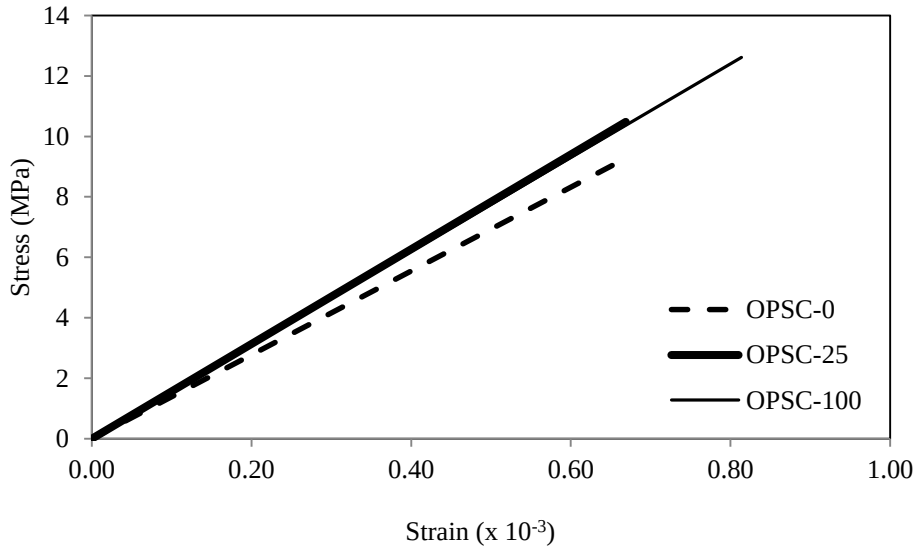

Figure 6.5 Stress versus strain curves for the calculation of modulus of elasticity

6.3.4 Flexural behaviors of reinforced concrete beams

6.3.4.1 Mode of failure

The failure modes of all the beam specimens are shown in Figure 6.6 (a-e). All beams were designed as under-reinforced beams and hence they exhibited the typical flexural failure. Multiple vertical flexural cracks formed within the constant moment region until the yielding of steel took place. When maximum load was reached, the concrete cover of the compression zone started to crack and followed by formation of concrete wedge (or in other words, concrete crushing) in the compression zone. The failure of the OPSC beam occurred by the crushing of the concrete as shown in Figure 6.6(a). However, the addition of fibers in the OPSFRC beams changed the failure mode of the concrete. Figure 6.6 (b to e) shows that all the four OPSFRC beams failed by the fracture of the main reinforcement within the constant moment region, along with the formation of concrete wedge. Fig 6.6 (f) shows the magnified failure of main reinforcement of beam with 0.25% fiber which is the beam OPSFRC-F25 in Figure 6.6(b). The effect of the volume fraction of steel fibers could be observed in the size of the concrete wedge formed in the OPSFRC specimens. At failure, the depth for the concrete wedges formed are 130, 90, 60, 50 and 35 mm, corresponding for the OPSC, OPSFRC-F25, OPSFRC-F50, OPSFRC-F75 and OPSFRC-F100 mixes, respectively. In addition, the corresponding widths of the concrete wedges are 320, 280, 200, 140 and 110 mm. The increase in the volume fraction resulted in the formation of smaller-sized concrete crushing wedge, along with deeper vertical flexural cracks.

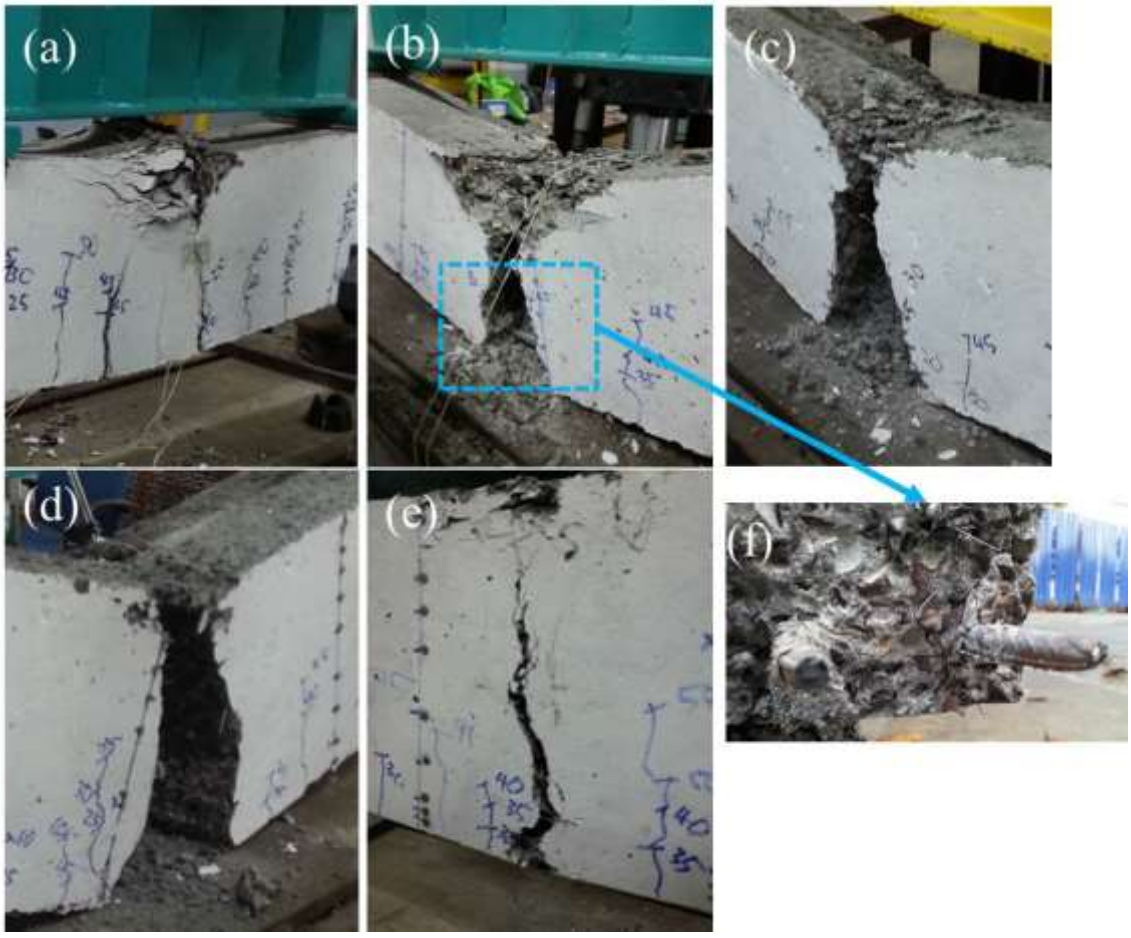

Figure 6.6 Failure mode of flexure beams from (a) OPSC; (b) OPSFRC-F25; (c) OPSFRC-F50; (d) OPSFRC-F75 and (e) OPSFRC-F100 mixes; (f) Fracture of steel bar

6.3.4.2 Moment capacity

The moment-deflection curves for all the specimens are displayed in Figure 6.7. The experimental moment capacities of all the mixes are tabulated in Table 6.3. The plain OPSC beam produced an ultimate moment of 27.7 kNm and this value was found to be closer to the reported OPSC beams (Alengaram et al., 2008). As expected, the addition of steel fibers improved the ultimate moment capacity of the OPSFRC beams by 4-18%. The increase in the fiber contents tends to increase the moment capacity in all OPSFRC beams as reflected in Figure 6.7 and Table 6.3. The highest ultimate moment of 32.6 kNm was obtained for the OPSFRC-F100 beam with 1% steel fibers and it was 18%

(or about 5 kNm) higher than the ultimate moment of control concrete beam. The previous discussions (Section 5.3.3.1-5.3.3.3) revealed that the addition of steel fibers improved the mechanical properties of OPSFRC specimens through the crack bridging mechanisms (Abu-Lebdeh et al., 2011; Bennett & Young, 1998; Hamoush et al., 2010; Singh et al., 2004; Sun & Xu, 2009; Yap et al., 2014). The addition of steel fiber improves the mechanical properties of OPSFRC by the contribution of the fiber-matrix interfacial bond. The steel fiber bridges across the cracks in the matrix and the fiber-matrix interfacial bonding allows the steel fiber to take up partial or all the crack tip stress as the crack approaching the fiber. Additional energy is required to overcome the interfacial bond, and, hence, the crack propagation and opening is diverted, blunted or even stopped, which in turn improves the energy capacity of the concrete.

In addition, it is noteworthy that the steel fiber reinforcement of volume fraction lower than 0.50% produced slight improvement on the moment capacity of OPSFRC specimen (increment within the range of 4-8%), whereas steel fiber with volume higher than 0.50% produced significant increment of 16-18% compared to the plain OPSC beam. This shows that the steel fiber with minimum volume of 0.50% is required to provide notable improvement on the moment capacity of OPSFRC. This can be further supplemented by the statement provided in the Section 5.3.3.2 which states that steel fiber content of more than 0.50% is essential to enhance the tensile strength and crack resistance of OPSFRC specimens. In the case of OPSFRC reinforced concrete, the fibers were randomly dispersed in both the tension and compression zones. The fiber-reinforcement enhanced the compression and tension toughness and substantially improved the flexural load capacity of the OPSFRC beams.

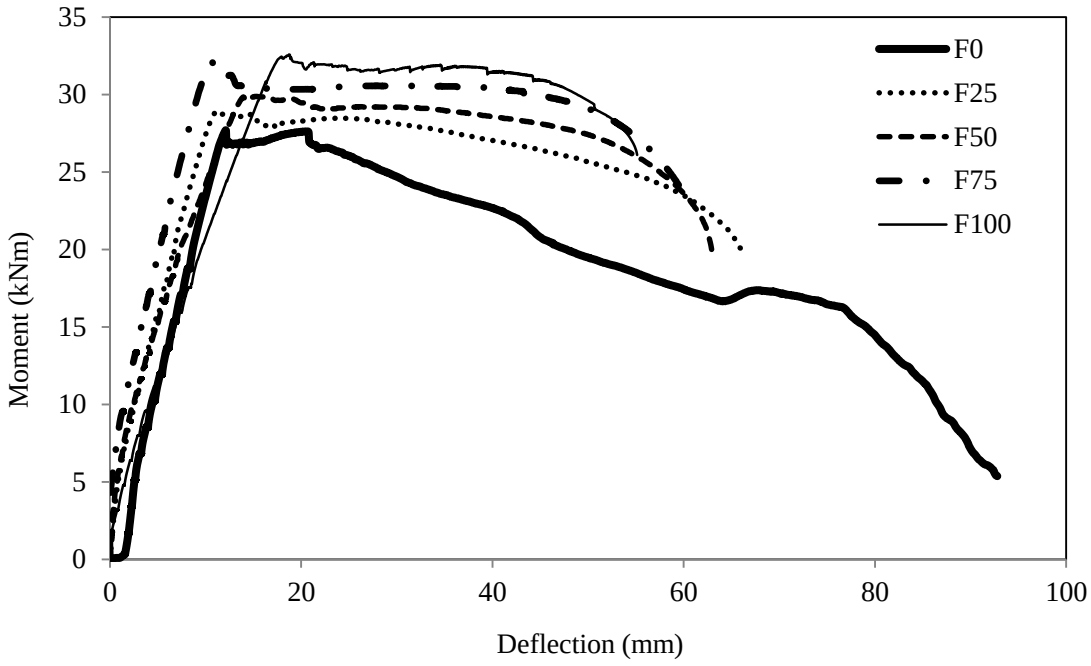

Figure 6.7 Bending moment-deflection curves for flexure beams

Table 6.3 Experimental and theoretical moment capacity of flexural beams

Beam	Experimental ultimate moment, $M_{u,exp}$ (kNm)	Theoretical ultimate moment based on BS code, $M_{u,BS}$ (kNm)	$M_{u,exp}/M_{u,BS}$	Theoretical ultimate moment based on ACI code, $M_{u,BS}$ (kNm)	$M_{u,exp}/M_{u,ACI}$	Theoretical ultimate moment based on EC, $M_{u,BS}$ (kNm)	$M_{u,exp}/M_{u,EC}$
OPSC	27.70	26.33	1.05	24.47	1.13	25.05	1.11
OPSFRC-F25	28.93	23.25	1.24	24.70	1.17	25.60	1.13
OPSFRC-F50	29.87	23.34	1.28	24.77	1.21	25.76	1.16
OPSFRC-F75	32.14	23.55	1.36	24.91	1.29	26.10	1.23
OPSFRC-F100	32.58	23.60	1.38	24.95	1.31	26.18	1.24

Table 6.3 also shows the comparison between the theoretical ultimate moments calculated based on code provisions of ACI, BS and Eurocode. The theoretical moment capacities calculated based on all three codes showed close values to that of experimental result for the OPSC beam. However, the codes of practice underestimated the moment capacity of OPSFRC beams as they do not take in account the effect of

fiber in the beam. Further study on the combined effect of reinforcement ratio and fiber-reinforcement is essential in order to incorporate the effect of fibers on the moment capacity of OPSFRC beams and to form an empirical solution for the prediction of moment-deflection relationship of OPSFRC beams.

6.3.4.3 Deflection and ductility characteristics

The deflections of all beam specimens at different loadings are shown in Table 6.4. The previously published data as discussed in Section 2.4.1 on the effect of steel fibers report diverse observations of both increase and decrease in flexural deflections in the beams.

Based on the results on deflections as shown in Table 6.4, it can be seen that the OPSC produced a deflection of about 93 mm just prior to failure. This result was very close to the deflection reported in the previous study by U. Johnson Alengaram et al. (2008). However, the addition of steel fibers up to 1% by volume reduced the deflection at failure of OPSFRC beams by about 30-40%. The deflections just prior to failure of the OPSFRC beams fall within the range of 55-66 mm. Furthermore, the increase in volume fraction of steel fibers resulted in lower deflection. The use of fibers can lead to a reduction in the rotation capacity of reinforced concrete members and, as a consequence to a reduced ductility. In other words, the addition of fibers for the enhancement of flexural behavior can limit its ductility under flexure (Meda et al., 2012). The reason is that fiber reinforcement improves the rebar-to-concrete bond by providing confinement effect. The optimized steel-to-concrete bond does not allow the yielded rebar to develop the plastic deformation that happens in the reinforced concrete beams without fiber.; this leads to a strain localization which, with increasing fiber content, shows an early rebar collapse in OPSFRC beams and similar finding was

reported for NWC beams with fiber (du béton, 2000; Meda et al., 2012). Thus, this explains the lower values in the deflection at failure and reinforcement failure in OPSFRC specimens compared to OPSC beam. Similar observation could be drawn at other stages including yield, low service load (20% of ultimate load), moderate service load (40% of ultimate load) service load (BS 8110) and at ultimate load. In addition, in order to fulfill the serviceability limited state as outlined in both BS 8110 and Eurocode 2, the span to service load deflection should not exceed 250. In addition, ASTM C1609 stated that the maximum span to service load deflection ratio is 150. Based on the results shown in Table 6.5, the span to service load deflection ratios for OPSC and OPSFRC beams were found as 23 and 30-40, respectively. These values were well below the deflection limit as stipulated in BS 8110, Eurocode 2 and ASTM C1609.

Table 6.4 Deflections of OPSC and OPSFRC beams at different loading stages

Beam	Service load stage				Yield stage	Ultimate stage	Failure stage
	Deflection at low service load (mm)	Deflection at yield load, δ_{yld} (mm)	Deflection at ultimate load, δ_{ult} (mm)	Deflection at moderate service load (mm)	Deflection at service load (mm)	Deflection at service load predicted by BS 8110 (mm)	Deflection prior to failure, δ_f (mm)
OPSC	2.70	8.12	12.10	4.90	7.65	7.94	92.80
OPSFRC-F25	1.07	7.14	11.16	3.17	5.97	8.55	66.06
OPSFRC-F50	0.85	9.98	15.28	2.92	6.08	8.88	62.97
OPSFRC-F75	0.57	7.71	10.56	2.90	5.80	9.91	60.54
OPSFRC-F100	0.91	12.04	18.92	5.05	8.81	10.53	55.13

In addition, the deflections at service load for all beam specimens were also calculated based on curvature of the beams as proposed in BS 8110 by using Eq. 6.1.

$$\delta = Kl^2(1/r) \quad (6.1)$$

Where δ = deflection in mm, K = a constant depends on the distribution of bending moments of a member, l = effective span of beam and 1/r = curvature. All the predicted deflections at service load are shown in Table 6.4. It was observed that the experimental deflection of OPSC closely agreed with the predicted deflection. BS 8110 code provisions do not include the effect of steel fibers; however, the calculated deflections using the eq. 6.1 for the OPSFRC beams show higher values than the experimental values by 20-80%. The difference increased with the increase in the steel fiber volume.

Table 6.5 Span to deflection ratio and load at 50 mm deflection of OPSC and OPSFRC beams

Beam	Span to service load deflection ratio	Load at 50 mm deflection, P_{50mm} (kN)	P_{50mm}/P_{ult}	Toughness (kNm)
OPSC	22.6	55.64	70%	4.291
OPSFRC-F25	31.8	73.28	89%	4.589
OPSFRC-F50	33.3	78.29	92%	4.435
OPSFRC-F75	34.7	83.12	91%	4.287
OPSFRC-F100	38.1	84.57	91%	4.116

Despite the decrease in the flexural deflection, the role of fibers in post-yielding flexural behavior of OPSFRC beams was evident after the yielding of steel bars. As seen from the results of deflections in Table 6.4, the difference between the deflection at the yield and the ultimate stage was found to be 4 mm in the OPSC beam. However, in the OPSFRC beams this margin was slightly extended to about 6-7 mm irrespective of the volume fraction of steel fibers. After the steel bar yields, the load is not only taken by the reinforcement, but the load is transferred from the bars to the concrete to achieve a new equilibrium (Hsu, 1968). The presence of the steel fibers in the cement matrix in OPSFRC contributed the fiber-matrix interfacial bond and eventually increased the load

capacity of the concrete over a prolonged deformation. This leads to improved toughness in the OPSFRC beams within the yielding and ultimate stages.

For the post-ultimate load stage, the addition of steel fibers improved the ultimate compressive strain that resulted in softened post-peak behaviors (Bencardino et al., 2008; Yang et al., 2012). It can be observed from Figure 6.7 that the addition of steel fibers produced a flattened curve for the post-peak behaviors of the OPSFRC beams, while the OPSC exhibited a steep descending post-peak curve. One of the indicative parameters to reveal the effect of steel fiber in post-peak behaviors of concrete is failure load to ultimate load ratio. The failure load to ultimate load ratios for OPSC, OPSFRC-F25, OPSFRC-F50, OPSFRC-F75 and OPSFRC-F100 were 0.19, 0.69, 0.71, 0.66, 0.80 and 0.72, respectively. When the OPSC beam failed, the beam achieved only 19% of its maximum load whereas for the OPSFRC beams, the values of 65-80% of their ultimate load capacity show that steel fiber reinforcement significantly enhanced the post-ultimate load behaviors of OPSFRC reinforced members.

Another salient observation that could be inferred from the research is the post-peak behaviors of both OPSC and OPSFRC could be compared using the ratio of P_{50}/P_{ult} (expressed as a percentage) for the load at constant deflection of 50 mm, as shown in Table 6.5. The deflection of 50 mm was chosen as it was closest to the smallest deflection prior to failure in OPSFRC-F100 beam to show the largest difference between the P_{50} and P_{max}. At the constant deflection of 50 mm, the ratio of P_{50}/P_{ult} for OPSC beam was found about 70%; however, higher value of about 90% obtained for the OPSFRC beams could be attributed to the crack bridging effect of steel fiber that requires additional energy to pull the fiber out from the fractured cement matrix. This post-peak tensile stiffening mechanism substantially increases the post-

cracking strength and ductility (Abu-Lebdeh et al., 2011; Hamoush et al., 2010; Okay & Engin, 2012; Singh et al., 2004).

Flexural ductility can be defined based on a reference state, which can be provided from the yield point of internal reinforcements. The unique yield plateau of the stress–strain curve of steel makes it possible for the structural member to be able to resist load while undergoing large deformations (Kim & Shin, 2011). Ductility of reinforced concrete is generally measured by ductility ratio. High ductility ratios indicate that a structural member is capable of undergoing large deflections prior to failure (Teo et al., 2006). Hence the following discussions are focused on the comparison of different ductility ratios of the OPSFRC. There are different approaches to define the ductility which are sub-divided into two main groups: energy-based approach and deformation-based approach (Wang & Belarbi, 2011). The mostly utilized approach is the deformation-based approach which is reflected by the deformation margin between the ultimate stage and service stage (U. Johnson Alengaram et al., 2008; Teo et al., 2006; Wang & Belarbi, 2011). Eq. 6.2 shows the calculation of ductility ratio based on the deformation approach.

$$\mu_D = \delta_f/\delta_{yld} \quad (6.2)$$

where μ_D = deformation-based ductility ratio, δ_f = final mid-span deflection and δ_{yld} = mid-span deflection when tensile steel yields.

Jaeger, Tadros, and Mufti (1997) introduced Eq. 6.3-6.5 to take account for both the strength and deflection on the ductility characteristics.

$$\mu_{D2} = C_s \times C_d \quad (6.3)$$

where μ_{D2} = ductility ratio by Jaeger, Tadros and Mufti (1997), C_s = strength factor calculated from Eq. 6.4 and C_d = deflection factor calculated from Eq. 6.5.

$$C_s = M_u / M_{\varepsilon\, 0.001} \quad (6.4)$$

$$C_d = \delta_u / \delta_{\varepsilon\, 0.001} \quad (6.5)$$

where M_u = moment capacity, $M_{\varepsilon\, 0.001}$ = moment when tensile steel strain is 0.001, δ_u = deflection at moment capacity and $\delta_{\varepsilon\, 0.001}$ = deflection when tensile steel strain is 0.001.

Meanwhile, in energy-based approach, ductility can be defined as a capacity of energy absorption (H. S. Kim & Shin, 2011; Wang & Belarbi, 2011). Eq. 6.6 and 6.7 show two examples to calculate the energy-based ductility ratio.

$$\mu_{E1} = A_{Mu}/A_{Myld} \quad (6.6)$$

where μ_E = energy-based ductility ratio up to ultimate moment, A_{Mu} = area of load-displacement curve up to moment capacity and A_{Myld} = area of load-displacement curve up tensile steel yields.

$$\mu_{E2} = A_{M0.75f}/A_{Myld} \quad (6.7)$$

where μ_{E2} = energy-based ductility ratio up to 75% of post-peak load, A_{Mu} = area of load-displacement curve up to 75% of post-peak load.

The comparison between different ductility ratios of the OPSC and OPSFRC beams are reported in Table 6.6. The ductility ratio of OPSC (μ_D) of about 11.4 was higher than the previously published data (Alengaram et al., 2008; Teo et al., 2006). OPSC is a ductile material which is attributed to its low modulus of elasticity. The low modulus of elasticity in OPSC allows the concrete to undergo high strain under increasing load (Alengaram et al., 2011; Yap et al., 2014). For the deformation-based ductility ratio, μ_D, the addition of fibers was evident to reduce the ductility of OPSFRC beams and the increase in fiber content further reduced the ductility of OPSFRC beams. It can be seen in the OPSFRC-F25 which recorded a reduction of 20% in the ductility while the ductility was further declined to 40% of the OPSC in the OPSFRC-F100 mix. According to Ashour (2000), members with ductility ratio in the range of 3 to 5 has adequate ductility and can be considered for structural members subjected to large displacements, such as sudden forces caused by earthquake. Hence the ductility ratios in OPSFRC specimens fell in the range of 4.5-9.3 and satisfied the requirement for the structural ductility.

Table 6.6 Comparison of ductility ratios of OPSC and OPSFRC beams

Beam	μ_D	Ratio to the control specimen	μ_{D2}	Ratio to the control specimen	μ_{E1}	Ratio to the control specimen	μ_{E2}	Ratio to the control specimen
OPSC	11.43	-	8.51	-	8.96	-	4.71	-
OPSFRC-F25	9.25	0.81	11.66	1.37	9.30	1.04	5.70	1.21
OPSFRC-F50	6.31	0.55	12.11	1.42	6.34	0.71	5.32	1.13
OPSFRC-F75	7.85	0.69	8.74	1.03	8.84	0.99	4.18	0.89
OPSFRC-F100	4.58	0.40	9.75	1.15	4.45	0.50	4.72	1.00

It has been discussed previously that the confinement effect of steel fibers decreased the flexural deflection of OPSFRC beams significantly. The fiber-matrix interfacial bond strongly holds the concrete together and this substantially increases the beam's load capacity and crack resistance, but accompanied by early fracture in the reinforcements. The ductility ratio μ_D which consider only the deflection of OPSFRC beams but do not consider the enhancement effect of steel fibers on the load capacity as mentioned in Section 6.3.4.2. Therefore ductility ratio, μ_{D2} is more appropriate for OPSFRC specimens as it takes account for both strength and deflection aspects. The μ_{D2} values of the OPSFRC beams showed that the steel fiber reinforcement imparted positive effect on the ductility of the OPSFRC by producing higher increment in the moment capacity of the OPSFRC with smaller decrease in the deflection.. Both the OPSFRC-F25 and OPSFRC-F50 beams produced about 40% higher μ_{D2} value than the OPSC mix. However, the μ_{D2} values of OPSFRC-F75 and OPSFRC-F100 specimens decreased notably by 20-30% relative to the OPSFRC-F50. It was reported that a minimum amount of steel fiber (0.3 – 1.5%) is essential to produce significant increment in the concrete's mechanical properties and structural behavior (Gao et al., 1997; Okay & Engin, 2012). Moreover, from the discussions in Sections 6.3.3 and 6.3.4.2, the minimum volume of steel fibers to produce significant enhancement on both mechanical properties and moment capacity is 0.50% (by concrete volume). When the volume fraction of steel fiber in the cement matrix is low (less than 0.50%), the confinement effect (at which the fiber-matrix interfacial bond holds the concrete together) is not as strong as that of the matrix with higher volume fraction (more than 0.50%), as illustrated in Figure 6.8. At low volume fraction, the effective stress zone of the steel fibers is not interconnected and hence the confinement effect of the steel fibers is not strong. However, the strong confinement effect of the steel fibers improved the

load capacity of OPSFRC specimens, the confinement effect also resulted in strain localization and eventually caused early bar fracture (Meda et al., 2012).

By following the values of μ_{E1} from Table 6.6, the variations of μ_{E1} values in the OPSFRC specimens were inconsistent as μ_{E1} only takes into account on the energy from the post-yielding stage up to ultimate stage. Meanwhile, the observation of μ_{D2} is also applicable to μ_{E2}. The OPSFRC with volume fraction 0.25-0.50% produced 13-21% increment in the energy-based ductility ratios while OPSFRC with 0.75-1.00% steel fibers produced comparable ductility ratios relative to the control OPSC beam. The observation can further be supplemented by the results of the toughness values as shown in Table 6.5. The toughness was calculated based on the area under the load-displacement curves. The results on toughness showed that OPSFRC-F25 and OPSFRC-F50 beams produced 3-6% improvement in the toughness while the other two OPSFRC specimens showed comparable toughness to that of OPSC beam. In the case of OPSFRC, the effects of steel fibers enhance the toughness of both pre-peak and post-peak behaviors. Hence the ductility ratio, μ_{E2} is more appropriate to indicate the energy-based ductility of OPSFRC.

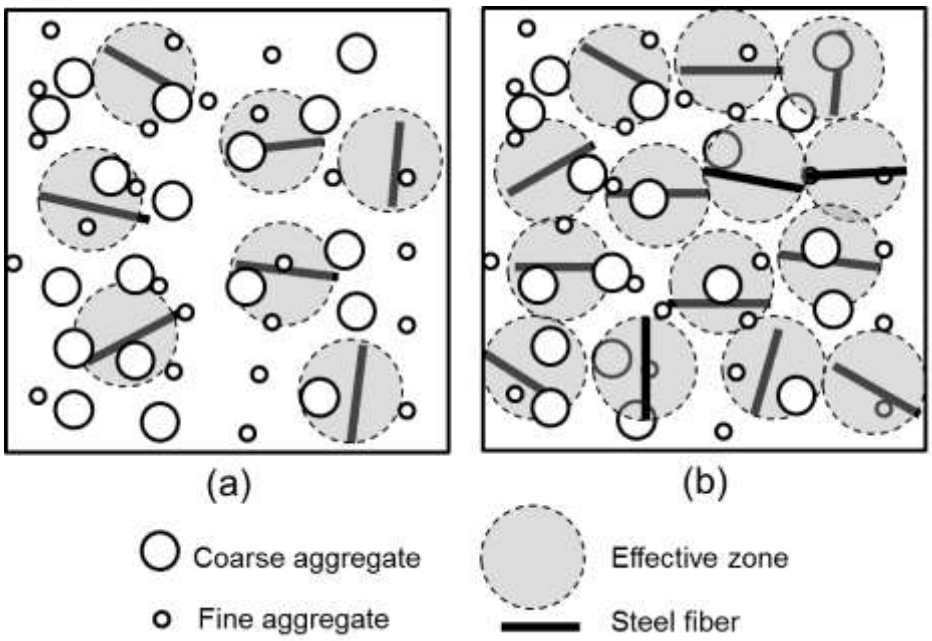

Figure 6.8 Confinement effect of steel fibers when (a) low volume fraction and (b) high volume fraction

6.3.4.4 Cracking resistance

Figure 6.9 shows the crack patterns of the OPSC and OPSFRC beam specimens. The black and blue lines denote primary and secondary cracks, respectively. Throughout the flexural test, the crack formations were marked on the beams and crack widths were measured at every load interval of 5kN at the tension steel level using hand held crack measuring microscope. The cracking characteristics of the specimens are summarized in Table 6.7.

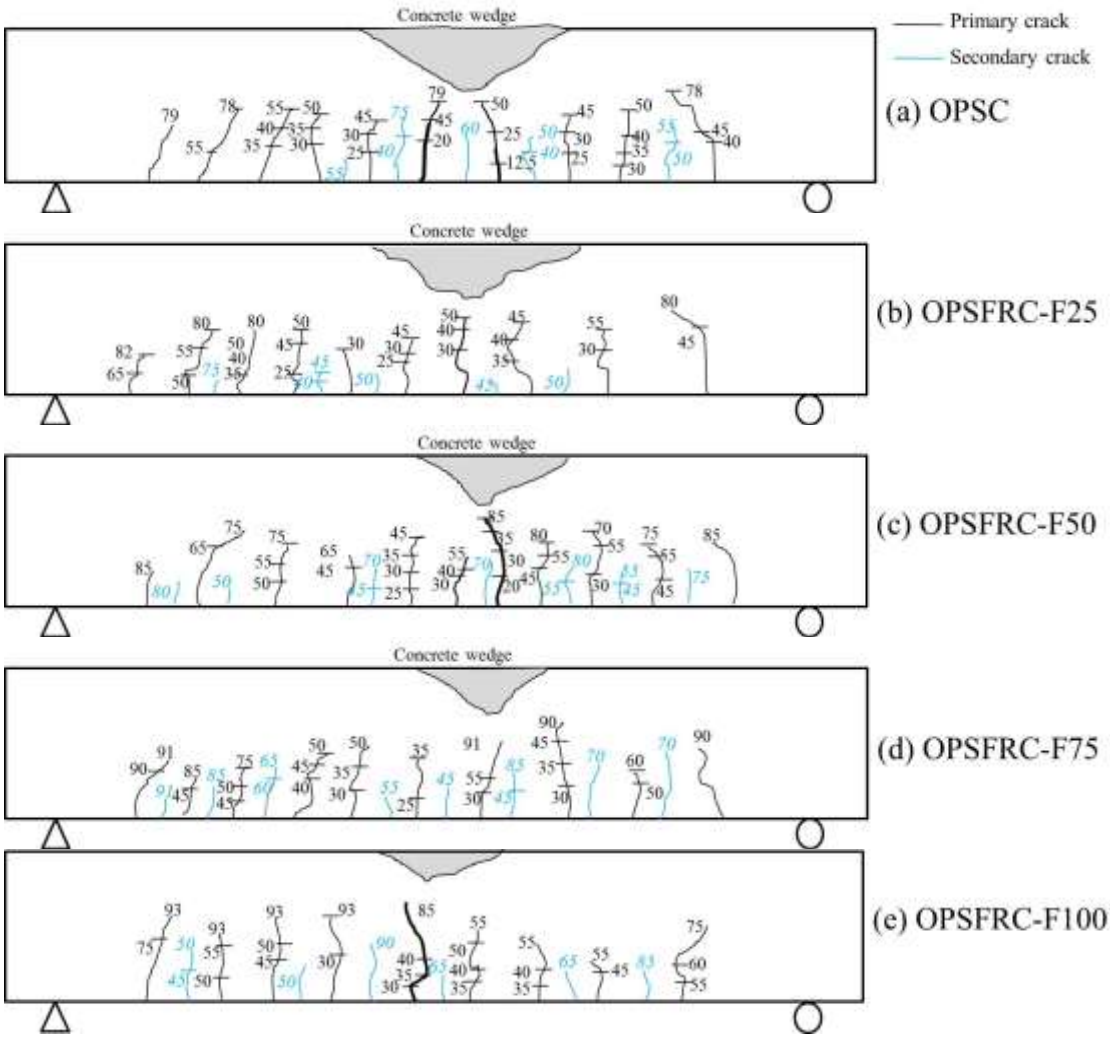

Figure 6.9 Sketches of the crack pattern of OPSC and OPSFRC beams

The first crack loads of all the beam specimens are reported in Table 6.7. The first crack of the OPSC beam occurred at a load of 12.5 kN and this load is 15% of its ultimate load. Both values were comparable to the previous studies on OPSC (Alengaram et al., 2008; Teo et al., 2006). The effect of steel fiber on arresting crack growth was evident in delaying the first crack load. In the OPSFRC, steel fiber enhanced the first crack load to 15-30 kN (increment of 20-140%) and the first crack load to ultimate load ratios were within the range of 18-50%. It has been shown that the increase in the reinforcement ratio results in lower first crack to ultimate load ratio (Teo et al., 2006). However, the randomly oriented fibers act as "bridge" across the crack and the fiber-matrix interfacial bond blunts the crack propagation and holds the cracked

matrix together that eventually reduces the crack opening and increases the first crack load capacity (Domagała, 2011). In addition, the fiber-matrix interfacial bond contributes to a higher toughness in fiber-concrete composites as more energy is consumed to overcome the fiber-matrix interfacial bond by means of fiber-debonding or fiber pullout. The increase in fiber volume results in more effective crack bridging effect as illustrated in Figure 6.8.

Table 6.7 Cracking characteristics of OPSC and OPSFRC beams

Beam	Experimental crack load				Theoretical cracking moment (ACI 318), M_{cr} (kNm)	Theoretical cracking load, P_{cr} (kN)	Theoretical crack spacing (CEB/FIP) (mm)
	First crack load (kN)	Primary crack spacing (mm)	Secondary crack load (kN)	Secondary crack spacing (mm)			
OPSC	12.5	165	40	90	3.87	11.06	250
OPSFRC-F25	15	150	40	77	4.96	14.17	191
OPSFRC-F50	20	140	45	68	6.18	17.66	159
OPSFRC-F75	25	125	45	60	7.65	21.86	139
OPSFRC-F100	30	115	45	56	9.40	26.86	125

Table 6.7 also shows the comparison between the experimental first cracking load to the theoretical cracking load obtained from ACI 318 by using Eq. 6.6.

$$M_{cr} = \frac{f_r - I_g}{y_t} \quad (6.6)$$

Where M_{cr} = cracking moment; f_r = flexural strength of concrete; I_g = second moment of inertia of gross area ignoring reinforcement and y_t = distance from the extreme tension face to the neutral axis. However, the theoretical cracking load calculated from Eq. 6.6 underestimated the first crack load of OPSC and OPSFRC beams by 5-14%. Meanwhile, the fiber-reinforced produced marginal effect on the initiation of secondary cracks.

Moreover, the crack patterns as shown in Figure 6.9 showed that the cracks of both OPSC and OPSFRC beams consist of vertical flexural cracks. The average crack spacing between primary cracks and between primary and secondary cracks in OPSC beam are 165 and 90 mm respectively. The addition of fibers reduced the primary and secondary crack spacing to 115-150 mm and 56-77 mm, respectively. In general, there are two fundamental ways to increase the crack resistance of concrete: (i) reduce the stress in reinforcement, (ii) reduce the distance to the nearest bar (Mosley et al., 2012). The strong fiber-interfacial bond reduced the stress transferred to the main reinforcement by taking up portion of the applied stress. Hence the toughness of fiber-reinforced concrete is improved and hence the crack spacing was reduced in OPSFRC specimens. The theoretical crack spacing between the primary cracks is also reported in Table 6.7. The theoretical crack spacing is calculated based on Eq. 6.7 as given by CEP/FIP manual (Short, 1977).

$$S_m = 50 + 0.25k_1k_2d_b/\rho_t \quad (6.7)$$

Where S_m = theoretical crack spacing; k_1 = coefficient for reinforcement (0.8 for high-bond bars and 1.6 for plain bars); k_2 = coefficient for loading (0.5 for bending and 1.0 for pure tension); d_b = diameter of main reinforcement and ρ_t = reinforcement ratio.

As seen from Table 6.7, the experimental crack spacing did not follow the trend given by the theoretical crack spacing. The OPSC and OPSFRC-F25 specimens reported significant deviation from the theoretical crack spacing, while the rest of the specimens showed errors within 10-20 mm. The explanation for this phenomenon is that the OPSC showed diverse crack behaviors when subjected to bending, compared to the NWC. The OPSC produced more cracks with smaller crack spacing than the NWC (Alengaram et al., 2008). However, the Eq. 6.7 is meant for LWC and therefore it is not

recommended for OPSC and OPSFRC specimens. Additional studies on the effect of reinforcement ratios and fibers content are required in order to study the feasibility and modification of Eq. 6.7 on OPSC and OPSFRC.

The improved crack resistance in OPSFRC relative to the OPSC beam was also evident based on the number of cracks as shown in Figure 6.9. OPSC produced 15 cracks while OPSFRC produced 16-18 cracks. The increase in the volume fraction of steel fibers resulted in higher number primary and secondary cracks formed. The depths of both the primary and secondary cracks in OPSFRC are relatively higher than the OPSC beam.

Figure 6.10 shows the microscopic pictures taken on the primary crack width at service load. The crack widths of all specimens are plotted in Figure 6.11. All the specimens produced crack width in the range of 0.11-0.16 mm and the values did not exceed the serviceability limit for crack width of 0.3 mm as stipulated in BS 8110. Moreover, the benefit of steel fibers to improve the crack resistance of OPSFRC was again evident in the crack width. The incorporation of steel fibers in the matrix of OPSFRC mixes reduced the crack width by 10-60% compared to the OPSC. The smallest crack width was obtained in the OPSFRC-F100 mixes at 0.11 mm. The comparison between the theoretical and experimental crack widths is also displayed in Figure 6.11. The theoretical crack widths were calculated based on the method given in BS 8110, but the theoretical crack width value showed increasing trend when fiber volume increases. The estimation method for crack width in BS 8110 is based on service moment. The addition of fibers improved the moment capacity and reduced the crack widths. Therefore the BS 8110 method is not appropriate to calculate crack width in fiber-reinforced concrete beams.

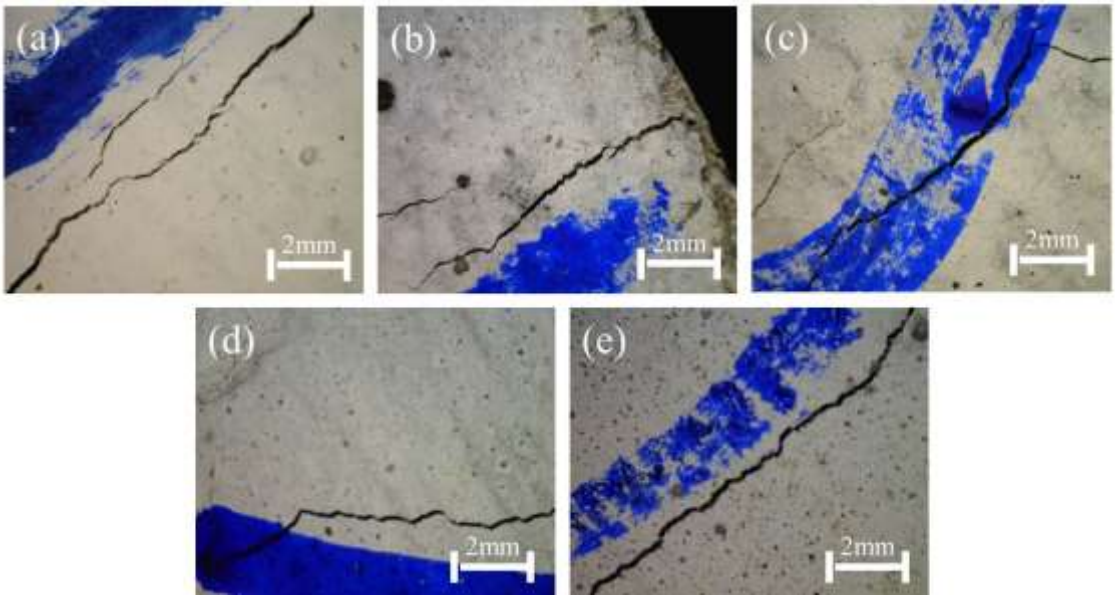

Figure 6.10 Crack width measurements at service stage of (a) OPSC; (b) OPSFRC-F25; (c) OPSFRC-F50; (d) OPSFRC-F75; (e) OPSFRC-F100

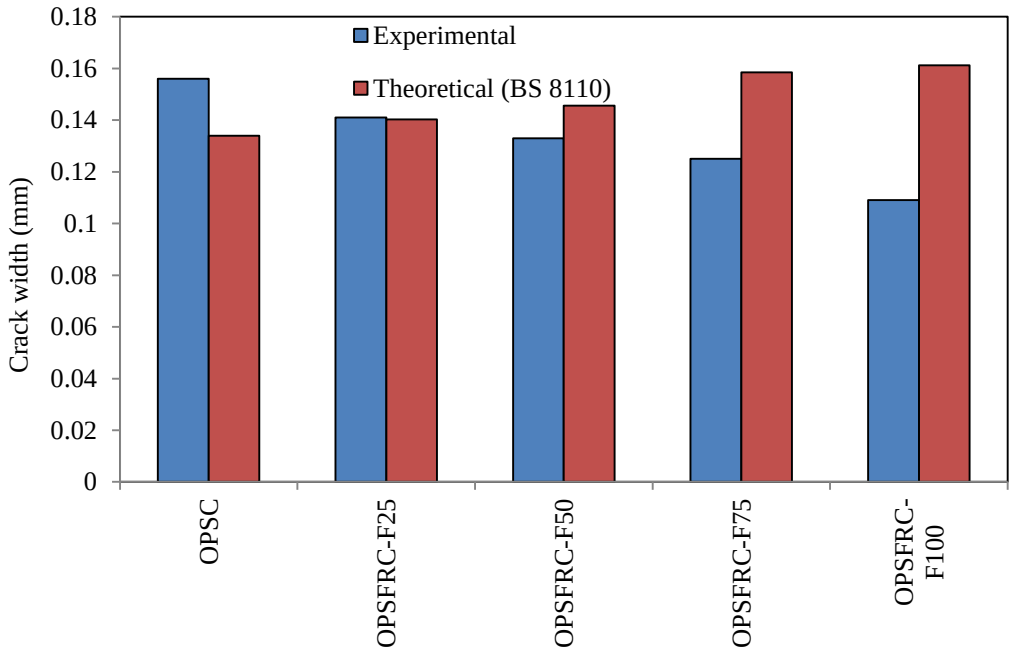

Figure 6.11 Comparison between experimental and theoretical crack widths at service load

Section 2.3.2.11 mentioned that the addition of fibers improves the crack resistance which in turn is attributed to the crack bridging effect. The significance of crack bridging on the crack resistance of OPSFRC was evident in the reduced primary crack spacing and crack width, increased crack load and higher number of cracks. Figure 6.12 shows the crack bridging effect of steel fibers in OPSFRC-F100 beam in which significant improvement of crack resistance was observed. Figure 6.12(a) shows that the primary crack follows an irregular crack patterns which is compatible with Figure 2.6(c). The bridging of fibers across the crack blunted and diverted the direction of crack propagation. This process reduced the crack tip stress and hence improved load carrying capacity of concrete. When the crack tip stress exceeded the fiber-matrix interfacial bond fiber debonding and pullout took place (Figure 6.12b) to improve the post-peak behaviors and crack resistance of concrete. Both fiber-debonding and pullout absorb additional energy to overcome the fiber-matrix bond and substantially improved the strength of concrete and reduced the crack opening.

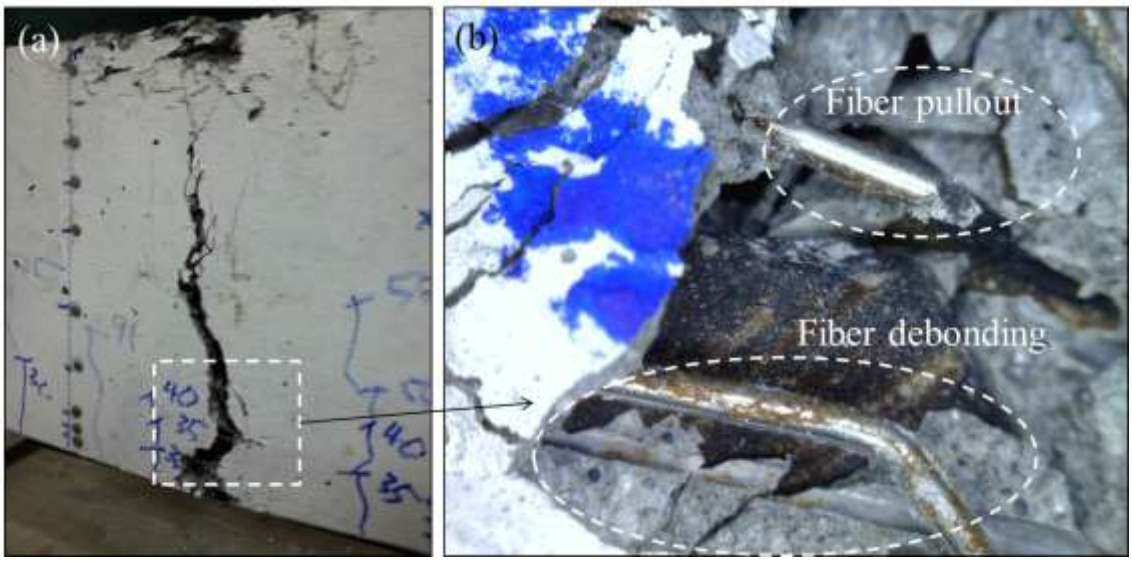

Figure 6.12 Crack bridging effect in OPSFRC-F100 beams

6.3.4.5 Concrete and steel strains

The compressive (concrete) and tensile (rebar) strains are shown in Figure 6.13. The negative values are concrete strains while the positive values are steel strains. The results for both strains are quite comparable to the previous studies on OPSC (Alengaram et al., 2008; Teo et al., 2006). The maximum tensile strains are within the range of 16000-18000 x 10^{-6}. Meanwhile the compressive strains within the service moments lie within the range of 550-900 x 10^{-6}. The comparison between the OPSC and OPSFRC shows that the steel fiber increased the moment capacity of OPSFRC specimens at a given strain (in both compressive and tensile strains). This can be explained by the crack bridging effect. The strong fiber-matrix interfacial bond sustained partial of the applied loading and hence improving the load capacity of concrete. In addition, the strong fiber-matrix interfacial bond also resulted in the confinement effect at which the steel strain reduced at maximum strain. The steel reinforcement in OPSC specimen achieved maximum moment capacity at a strain of about 4500 x 10^{-6}, but the OPSFRC attained the respective maximum moment capacities at lower steel strains of about 2500-3500 x 10^{-6}; lower steel strains were observed in OPSFRC beams with higher steel fibers contents. In addition, the strain localization effect caused an early steel bar fracture before crushing of the concrete in the compression zone and thus reduced deflection at failure in the OPSFRC specimens as discussed in Section 6.3.4.3.

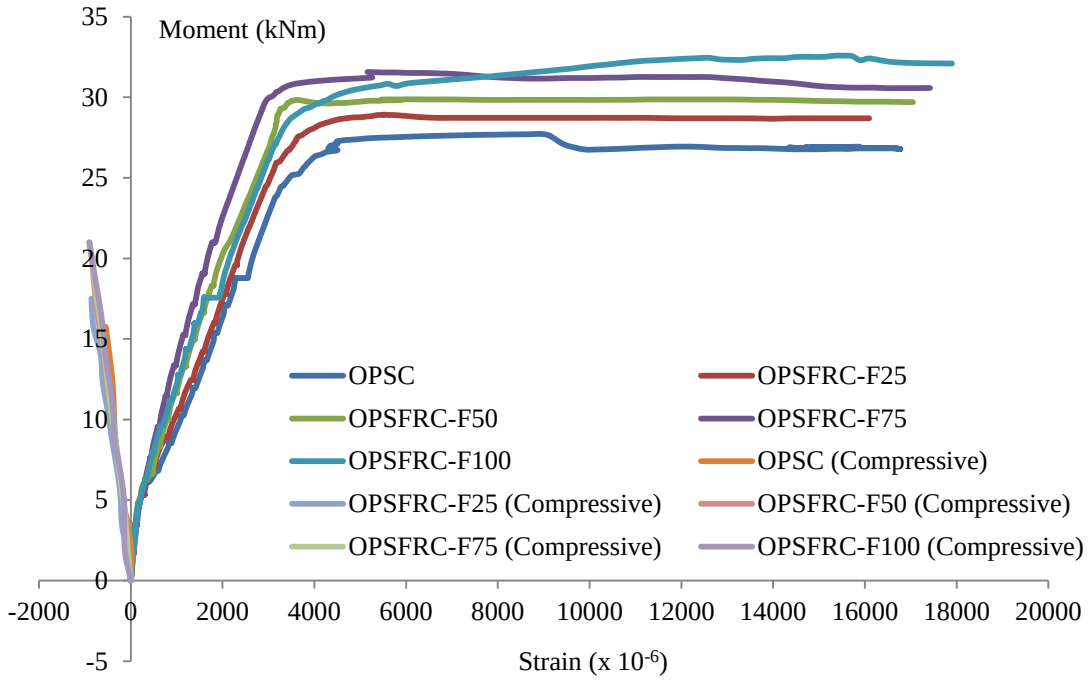

Figure 6.13 Compressive and tensile strains

6.4 Chapter conclusions

The comparison of the flexural behaviors between the OPSC and OPSFRC beams was investigated and reported in this chapter. The variable investigated was volume fraction of steel fibers. The following conclusions were drawn from the observations:

- OPSC and OPSFRC beams can be fabricated with comparable density, fresh and mechanical properties to previous chapter (Chapter 5).
- Typical flexural failure was observed in the OPSC beams, while the OPSFRC beams failed by rebar fracture. The increase in the volume fraction of steel fibers resulted in the formation of reduced concrete wedge, along with deeper vertical flexural cracks.
- The addition of steel fibers improved the ultimate moment capacity of the OPSFRC beams by 4-18%. The highest ultimate moment of 32.6 kNm was obtained for the OPSFRC-F100 beam with 1% steel fibers and the ultimate moment of the beam was 18% (or about 14kNm) higher than the control OPSC beam.

- Steel fiber content of more than 0.50% is essential to enhance the tensile strength, moment capacity and crack resistance of OPSFRC specimens.
- OPSFRC beams showed reduced ductility compared to the OPSC beam and this is attributed to the strain localization which results in early rebar failure. The deflection just prior to failure in OPSFRC beams were only 55-66 mm compared to 93 mm in OPSC beam but these values were well below the deflection limits stated in the BS 8110 and Eurocode 2. The ductility ratios of OPSFRC also satisfied the requirement for structural ductility.
- OPSFRC specimens produced softened post-peak behaviors with 70-80% of ultimate load during failure while the OPSC beams retained 20% of its ultimate load.
- The crack bridging effect resulted in enhanced crack resistance in OPSFRC beams, including 10-30% and 10-60% drops in crack spacing and crack width, respectively.
- As the equations provided by codes of practice such as ACI, BS and Eurocode are not meant for reinforced concrete members with fibers, the prediction of moment capacity, deflections, crack width and spacing of OPSFRC beams and hence either underestimate or overestimate the values.
- The steel strains revealed that the confinement effect of steel fibers increased the moment capacity but with a lower steel strain than the OPSC beam. The strain localization resulted in improved moment capacity but decreased deflection at failure.

CHAPTER 7

INVESTIGATION ON THE TORSIONAL BEHAVIORS OF OIL PALM SHELL FIBER-REINFORCED CONCRETE BEAM

7.1 Chapter introduction

The experimental works in both Chapter 6 and 7 focused on the investigation of structural behaviors of OPSC and OPSFRC under flexural and torsional loading, in order to fulfill the third stage of "Structural behaviors of OPSFRC". Previous chapter had discussed on the effect of steel fibers on the flexural behaviors of OPSFRC reinforced concrete beam. The main objective of this chapter is to investigate the torsional characteristics of both OPSC and OPSFRC by following the mix proportion from Chapter 6.

Previous studies showed that OPSC beams performed comparable to that of NWC under flexural and shear loadings (Alengaram et al., 2008, 2011). However, torsional loading generally occurs by combining with the flexural or shear loading when the external load has no alternative but to be resisted by torsion. In this case the structural member is subjected to primary torsion (Rao & Seshu, 2006). Examples of structural members subjected to torsion are utility poles, eccentrically loaded box, bridge girders, spiral staircases and spandrel beams (Rahal, 2013). An under-reinforced torsion-loaded member will result in torsional cracking commencing before the flexural or shear failures, as the torsional strength is highly dependent on the tensile strength, which is the weakest component in brittle concrete (Hsu, 1968), and, ultimately, causes an early loss of serviceability. Furthermore, the increasing demand for curved members highlights the necessity to investigate the torsional characteristics of concrete members to avoid severe torsional cracking. The torsional rigidity and torsional stiffness of the

members also play an important role in the three-dimensional analysis of concrete structures, especially earthquake resistant structures (Rao & Seshu, 2006). Furthermore, there is no study available on the torsional resistance of the OPSC beams, and, therefore, the importance of investigating the torsional behavior of the OPSC beams is evident.

In the case of OPSC, the low tensile strength of OPSC has to be considered for the torsional cracking to occur before the flexural or shear strengths are achieved. It has been shown that an improvement in the reinforcement ratio including the addition of steel fiber enhances the torsional strength, ductility and cracking resistance of the concrete (Chiu et al., 2007; Rao & Seshu, 2003). Hence, this study aims to compare the effect of various volume fractions (0–1%) of steel fiber on the torsional behavior of OPSFRC unreinforced prisms and beams. The study on the torsion capacity of the plain concrete prism is important due to its simplicity in fabrication and it can qualitatively indicate the torsion behaviors of beams. In addition, the comparison between the torsional behavior of both the control OPSC and OPSFRC beams are also discussed. The torsional behavior investigated includes cracking, ultimate and failure torque/twist, initial and cracked torsional stiffness, torsional toughness and cracking resistance of OPSFRC beams.

7.2 Experimental program

7.2.1 Materials and mix proportions

All the materials and mix proportions from Chapter 6 were followed. The material properties of all the materials including cement, OPS, sand, silica fume and superplasticizer can be referred to Section 3.2.1; while the physical properties steel fiber (Figure 6.1) can be referred to steel fiber S2 in Section 5.2.1.

The mix proportions of all the mixes are shown in Table 7.1. For the OPSFRC mixes, all the constituent materials were kept constant and the variation between the mixes is the fiber content. Different volume fractions of steel fiber of 0.25%, 0.50%, 0.75% and 1.00% were added to the OPSFRC mixes.

Table 7.1 Mix proportions of torsional specimens

Mix design	Cement (kg/m^3)	Silica fume (kg/m^3)	OPS (kg/m^3)	Mining sand (kg/m^3)	Water (kg/m^3)	Steel fiber (%vol. of concrete)
OPSC	539	53	323	971	178	0
OPSFRC-T25	539	53	323	971	178	0.25
OPSFRC-T50	539	53	323	971	178	0.50
OPSFRC-T75	539	53	323	971	178	0.75
OPSFRC-T100	539	53	323	971	178	1.00

7.2.2 Mixing, specimen preparation and testing

There are two main parts of the experimental works in this chapter: torsion test on un-reinforced concrete prism and torsion test on reinforced concrete beams. Both tests were conducted by using automated torsion machine as shown in Figure 7.1. For the unreinforced concrete prism, the specimen size is 100 x 100 x 500 mm3 prism; while the OPSC and OPSFRC torsion beams were fabricated according to Eurocode 2. Figure 7.2 shows the detailing for the torsion beams. The torsion prisms and beams were cured in water and tested at the age of 28 days using the automated torsion machine. A constant loading rate of 0.5 mm/minute was applied in all the beams until failure. The torsion load-deflection curves were directly measured from the torsion machine.

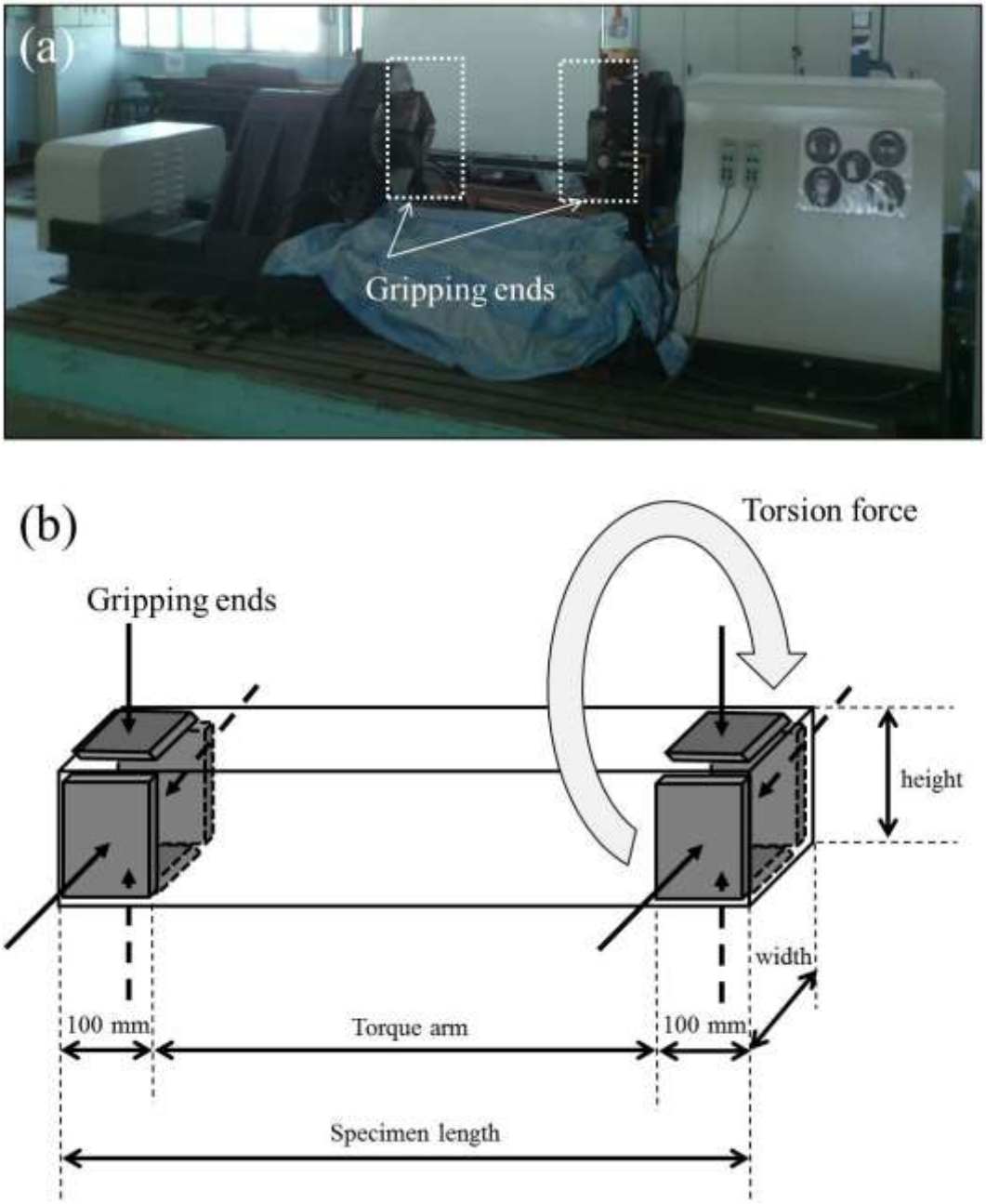

Figure 7.1 (a) Automated torsion machine and (b) Torsion test set-up

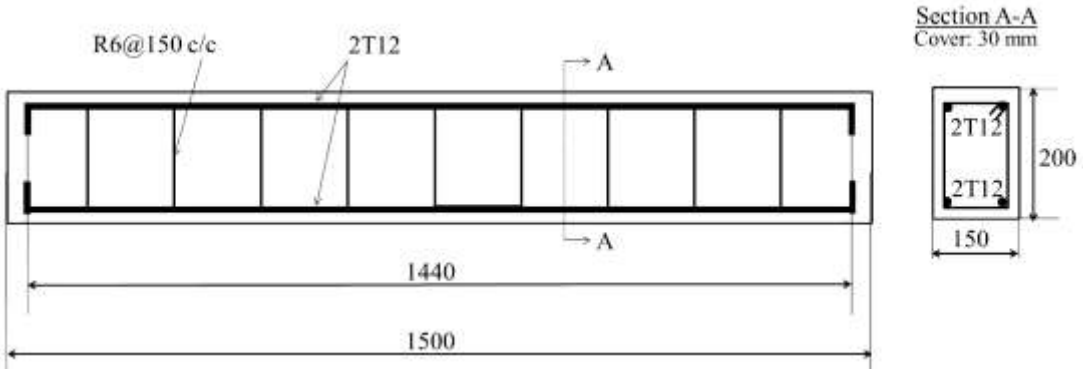

Figure 7.2 Torsion beam detailing (all dimensions are in mm)

All the beams were tested using an automated torsion machine under a constant loading rate of 0.5 mm/minute. The torsion-angular twist graphs were directly measured by the torsion machine and the torque-twist curves were analysed. The cracking torque, T_{cr}/twist, $Ø_{cr}$, ultimate torque T_{ult}/twist, $Ø_{ult}$, and failure torque T_f/twist, $Ø_f$, were then interpreted from the torque-twist curves. Fig, 7.3 shows a simplified model of the torque-twist curves for the calculation of the stiffness and toughness provided by Okay and Engin (2012). The initial torsional stiffness (k) was taken as the linear gradient of the torque-twist graph. Finally, the torsional toughness is the total energy absorbed by the beam specimens. The calculations for the torsional toughness are divided into three parts (Figure 7.3): (i) Part 1 denotes the pre-cracking torsional toughness, (ii) Part 2 measures the cracked torsional toughness before the specimens achieve ultimate torque, and (ii) Part 3 measures the post-cracking torsional toughness.

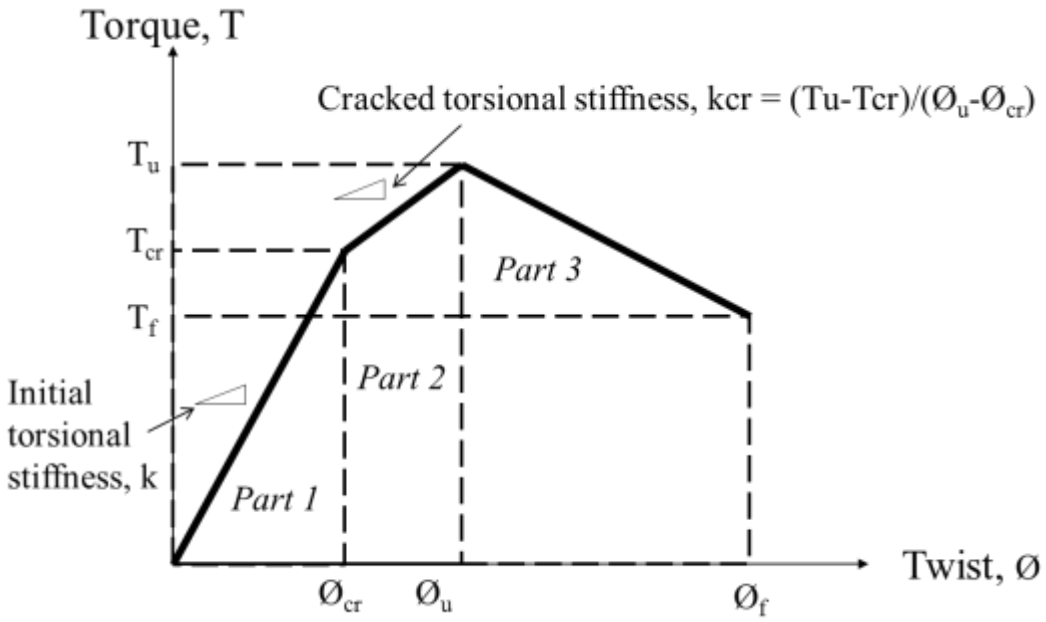

Figure 7.3 Simplified model for torque-twist curve

7.3 Results and discussion

7.3.1 Torsional behaviors of unreinforced concrete prism

The torque-twist curves of all the mixes are shown in Figure 7.4, while Table 7.2 reports all the results derived from Figure 7.4 including cracking torque, ultimate torque and failure torque with their corresponding twist, initial and cracked torsional stiffness and torsional toughness.

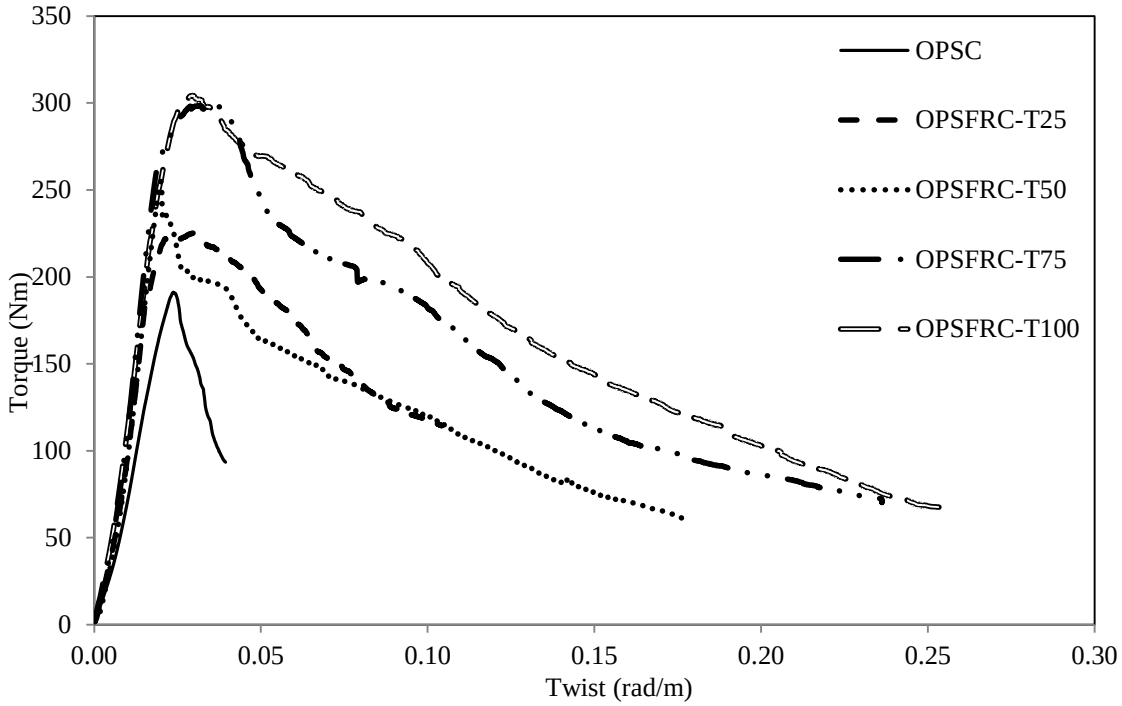

Figure 7.4 Torque-twist curves for unreinforced prisms

Table 7.2 Torsional strength of unreinforced prisms for all mixes

Mix	Cracking torque		Ultimate torque		Failure torque		Initial torsional stiffness (kNm^2)	Cracked torsional stiffness (kNm^2)	Torsional toughness (Nm/m)
	Torque, T_{cr} (Nm)	Twist, $Ø_{cr}$ (rad/m)	Torque, T_{ult} (Nm)	Twist, $Ø_{ult}$ (rad/m)	Torque, T_f (Nm)	Twist, $Ø_f$ (rad/m)			
OPSC	190.8 (2.1)	0.024 (0.007)	191.2 (2.8)	0.024 (0.002)	93.4 (3.2)	0.039 (0.006)	10.04	0	4.42
OPSFRC-T25	221.2 (2.4)	0.024 (0.002)	225.4 (1.6)	0.030 (0.006)	114.5 (2.6)	0.104 (0.011)	14.10	700	16.57
OPSFRC-T50	248.6 (2.2)	0.016 (0.005)	254.8 (1.8)	0.020 (0.005)	60.9 (3.1)	0.177 (0.007)	14.98	1550	27.78
OPSFRC-T75	293.0 (0.4)	0.026 (0.009)	298.1 (3.0)	0.029 (0.005)	70.3 (1.5)	0.236 (0.009)	15.51	1700	42.83
OPSFRC-T100	294.1 (2.9)	0.025 (0.010)	304.4 (1.7)	0.029 (0.004)	67.7 (2.5)	0.253 (0.015)	14.26	2575	46.55
NOTE: The standard deviations are shown in brackets									

7.3.1.1 Torsional strength and toughness

The control OPSC mix produced a torsional toughness of about 4 Nm/m and ultimate torque at a twist value of about 0.025 (Table 7.2). The torque-twist curves of both mixes showed diverse behavior. The specimen of the NWC mix produced almost twice the ultimate torsional strength of the OPSC specimen, but it did not exhibit post cracking strength, as the specimens failed once the ultimate torque was achieved at a twist value of 0.025. Although the OPSC only produced about 55% of the ultimate torque of the NWC, the OPSC was capable of sustaining torsion beyond its ultimate torsional strength by producing a twist at failure of 0.039 (Khaw, 2014). This indicated that OPSC has lower torsional strength but higher torsional ductility than the NWC. In addition, the torsional toughness of the control concrete mix was comparable to the published results on the normal weight concrete of similar compressive strength (Rao & Seshu, 2003).

The enhancement of steel fibers on the torsional strength of OPSFRC is evident from the increased torsional strength of the OPSFRC mixes compared to the OPSC mix (Figure 7.4). It was observed that the increase in the volume fraction of steel fibers resulted in higher torsional strength (ultimate torque) of OPSFRC. It has been reported that the steel fibers significantly improved the flexural toughness of concrete (Altun et al., 2007; Erdem et al., 2011; Yap et al., 2014). Moreover, the benefit of steel fibers is also obvious in the torsional toughness of OPSFRC, as shown in Figure 7.5. The highest torsional toughness in the OPSC-T100 mix reinforced with 1% steel fibers was about 47 Nm/m, which was tenfold higher than the corresponding control mix. In addition, for every increment of 0.25% steel fiber volume in the OPSFRC mixes up to 0.75%, the torsional toughness improved drastically by about 11–15 Nm/m. The torsional

toughness achieved in the OPSFRC was found to be higher than the torsional toughness of grade-50 NWC reported by Rao & Seshu (2003).

Similar to the compressive and tensile strengths, the increased torsional strength and toughness in the OPSFRC mixes is mainly attributed to the crack bridging effect at which the additional energy must be consumed at breaking and pulling out of the fibers from the cement paste, which leads to higher failure load and adds toughness to the concrete (Hamoush et al., 2010; Yap et al., 2014).

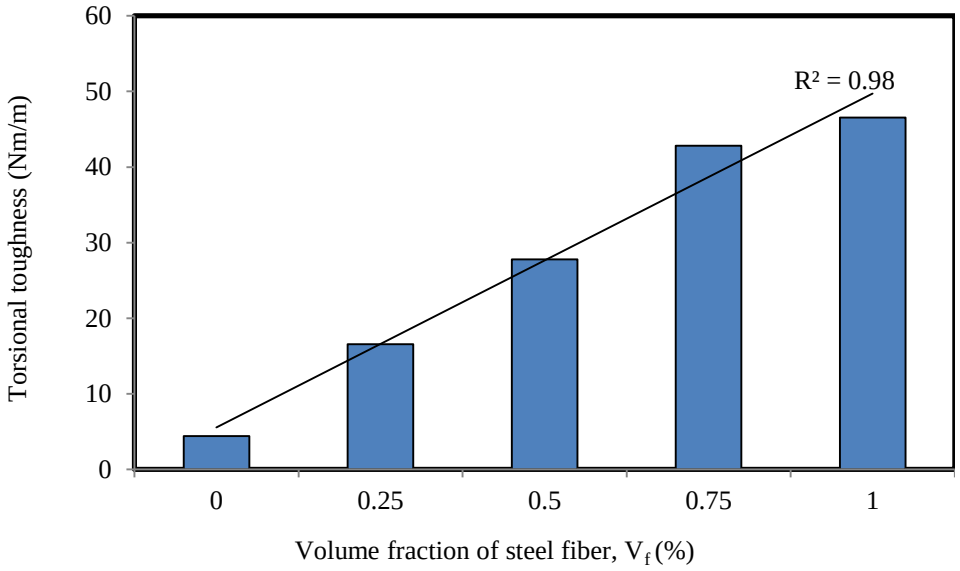

Figure 7.5 Torsional toughness against volume fraction (V_f) of steel fibers in OPSFRC prisms

7.3.1.2 Twist at failure

The comparison between the NWC and OPSC showed that OPSC gained the advantage of good torsional ductility by producing higher twist at failure as mentioned in Section 7.3.1.1. Following the results from Table 7.2, the OPSC unreinforced prism produced a twist at failure of 0.039.

The high torsional toughness observed in the OPSFRC mixes is mainly attributed to the excellent post-cracking behaviors, as shown in Figure 7.4 and Table 7.2. The good post-cracking behavior of the OPSFRC specimens is clear from the significantly improved twist at failure of up to 550% and 900%, compared to the control OPSC mix, respectively. From 0.25% to 1.00% steel fibers volume in the OPSFRC mixes, every increment in the steel fiber content of 0.25% produced about 150% increase in the twist at failure. This explained that the steel fibers effectively enhanced the ductility/twist at failure of the OPSFRC mixes. The steel fibers not only enhanced the ductility of concrete under flexural (Balendran et al., 2002; Erdem et al., 2011; Hamoush et al., 2010; Yap et al., 2014) and impact (Mo et al., 2014a), but, the present study also proved that the steel fibers improved the torsional ductility of the LWC. The role of steel fibers in enhancing the ductility of OPSFRC is by the crack bridging effect. After the first crack commences, additional energy is required to pull the fibers out from the fracture cement matrix for the crack to open and to propagate until the fibers are pulled out or broken. This results in the post-peak tensile stiffening behavior and eventually enables the concrete to exhibit residual strength and increased ductility after the ultimate strength is achieved (Bischoff, 2007; Hamoush et al., 2010). Moreover, the advantage of steel fibers in producing the post-cracking characteristic in OPSC is more evident, as seen from the study of Khaloo & Sharifian (2005) who found that the addition of steel fibers in NWC did not produce any post-cracking behavior for the concrete. Therefore, we can conclude that the addition of steel fibers further enhanced the post-cracking ductility of OPSC.

7.3.1.3 Torsional stiffness

In terms of stiffness, the OPSC mix produced an initial torsional stiffness of about 10 kNm^2, respectively. The torsional behavior of concrete is mainly linear until the first cracking torque, while the initial stiffness is independent of the presence and amount of reinforcement (Hamoush et al., 2010; Okay & Engin, 2012). In addition, the torsional failure of concrete members is initiated by the tensile stress developed due to a state of pure shear, which arises due to torsion (Rao & Seshu, 2003). This indicates that the initial torsional stiffness is mainly contributed by the concrete's tensile strength. In addition, the OPSC prisms have no crack stiffness, which indicated that the control specimen achieved ultimate torque once the specimens cracked. This is attributed to the absence of reinforcement within the control specimens. Once the specimens cracked, the brittle concrete could not sustain higher torque, and, therefore, the control specimen cracked and reached ultimate torque at the same time.

The initial and cracked torsional stiffness of all the mixes is reported in Table 7.2. It was shown that the addition of steel fibers improved the initial torsional stiffness of the OPSFRC specimens to 14–15.5 kNm^2, compared to the initial torsional stiffness of 10 kNm^2 in the OPSC mix. However, the fiber content had no significant effect on the initial torsional stiffness. Following the discussions on the modulus of elasticity of OPSFRC, the presence of steel fibers induced higher stiffness in the concrete matrix, which explains the improvement of the initial torsional stiffness in the OPSFRC mixes. The addition of fibers improved both the torque capacity and twist at almost equal margin when fiber volume increases and hence the initial torsional stiffness is independent on the volume fraction of fibers.

However, the observation on the cracked torsional stiffness of the OPSFRC mixes varied from the initial torsional stiffness (Table 7.2). When the volume fraction of steel fibers increased from 0.25% to 1.00%, the cracked torsional stiffness increased considerably from 700 kNm^2 to 2575 kNm^2. This indicated that the higher steel fiber content allows the OPSFRC to sustain higher torque and twist after the cracking torque before reaching the ultimate torsional capacity, but the increment in torsional twist is higher than the torque. After the cracking torque, the reinforcing steel fibers take over and hold the concrete together through the crack bridging effect (Hamoush et al., 2010). The bridging of the fibers over the crack enabled concrete to sustain torque over a prolonged twist before reaching the maximum torque.

7.3.1.4 Torsional crack resistance

The failure patterns of all the specimens are shown in Figure 7.6. The failure patterns of all the specimens showed skew bending failure. A primary torsion crack with an inclination angle of about 43–48^o from the edge initiated upon reaching the cracking torque and propagated to all the faces of the specimens. The failure mode was found to be comparable to the published literature (Khaloo & Sharifian, 2005; Rao & Seshu, 2003). The comparison between both the NWC and OPSC mixes shows that the failure of the NWC specimen was sudden and brittle as the specimen broke into pieces once the ultimate torque was achieved, as seen from Figure 7.6a (Khaw, 2014). The OPSC specimen (Figure 7.6b) broke into two parts along the primary torsion crack without any fragments like NWC. When the ultimate torque was reached, the crack width of the primary crack was found to be about 5 mm and the post-cracking behaviors of OPSC enabled the concrete to sustain higher twist until it failed at a twist at failure of 0.039. The observation from the failure plane of the OPSC showed that the OPSC failed due to aggregate-cement paste adhesion failure and breakdown of the OPS. It has been

reported that OPSC is weak in aggregate-paste bonding (Shafigh et al., 2011a). Under torsion loading, the cracks commenced at the aggregate-cement paste interface and joined up to form a primary torsion cracking. This explains the relatively lower torsion capacity in OPSC compared to NWC.

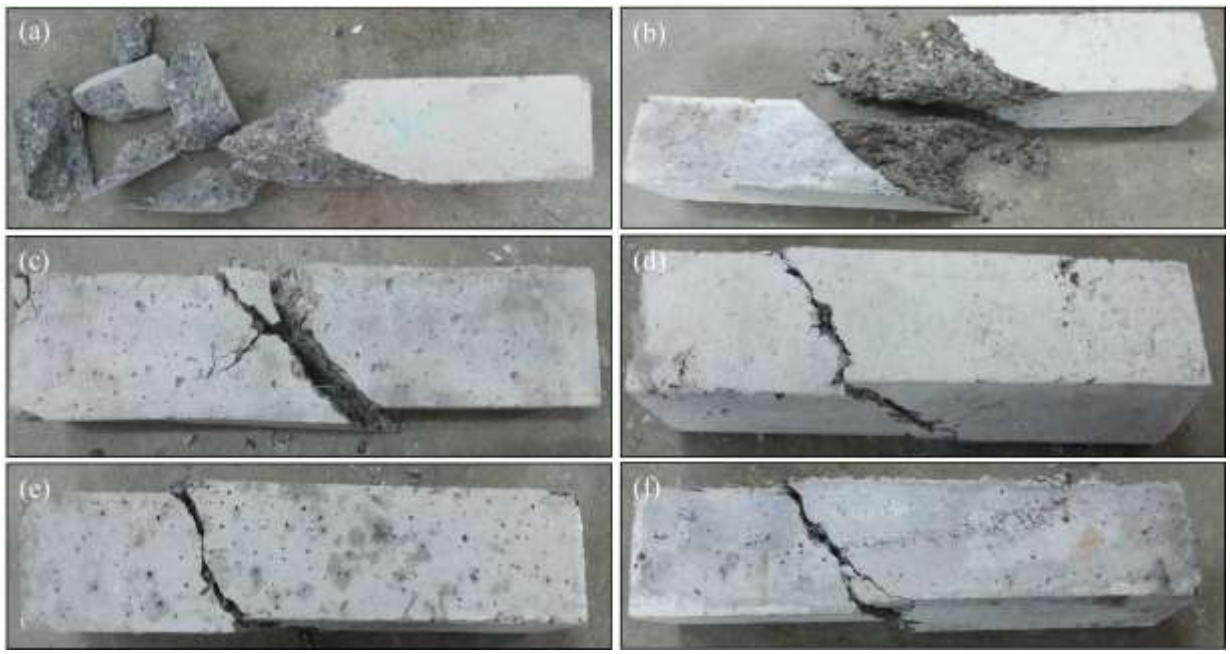

Figure 7.6 Failed specimens of (a) NWC (Khaw, 2014), (b) OPSC, (c) OPSFRC-T25, (d) OPSFRC-T50, (e) OPSFRC-T75 and (f) OPSFRC-T100 mixes

The cracking resistance of the OPSFRC specimens significantly bettered OPSC, as shown in Figure 7.6. Similar to the OPSC, the failed OPSFRC specimen retained its original shape with no fragments produced (Figure 8c-f). The OPSFRC failed along a primary torsional crack with an inclination angle of about 43–48^{o} from the edge. The addition of steel fibers did not affect the inclination angle. When a structural member fails under extreme loading, the formation of fragments like the NWC might cause a severe hazard to the building residents. Hence, the OPSFRC mixes, which produced a smaller crack width, could provide a higher degree of structural safety, serviceability and durability, compared to the NWC.

The crack arresting ability of steel fibers in OPSFRC is also evident in Figure 7.7. It is noted that the crack width of the OPSC specimen could not be measured as the prism broke into two pieces. In the comparison of the V_f of the steel fibers in the OPSFRC mixes, OPSFRC-T25 failed by producing a larger primary torsion crack with a crack width of 7.121 mm (Figure 7.7a), the crack widths grew narrower to 5.743 mm, 4.625 mm and 4.375 mm in the OPSFRC-T50, OPSFRC-T75 and OPSFRC-T100 mixes, respectively (Figure 7.7b-d). The crack width of OPSC-100 mix reduced considerably by about 40% relative to the OPSFRC-T25 specimen, which showed the effectiveness of the crack bridging effect of steel fibers in arresting the crack growth. In addition, the reduced crack width of the primary torsion crack is coupled with the formation of minor cracks (Figure 7.6f). The formation of multiple fine cracks in fiber reinforced specimens allows for a higher strain capacity (Hamoush et al., 2010) and contributes to the highest twist at failure in the OPSFRC-T100 specimen. Following the Figure 7.7, the fiber pullout and fiber debonding were observed across the primary torsion cracking. Both fiber pullout and fiber debonding mechanisms contributed to the significant crack bridging toughening for the OPSFRC. The bridging of the steel fibers along the crack increased the tensile stress that could be withstood, which is attributed to the increase in the fiber-matrix interfacial bond, and resulted in a substantially reduced crack width and increase in the number of fine cracks (Altun et al., 2007; Bischoff, 2007; Hamoush et al., 2010; Islam et al., 2012; Zīle & Zīle, 2013).

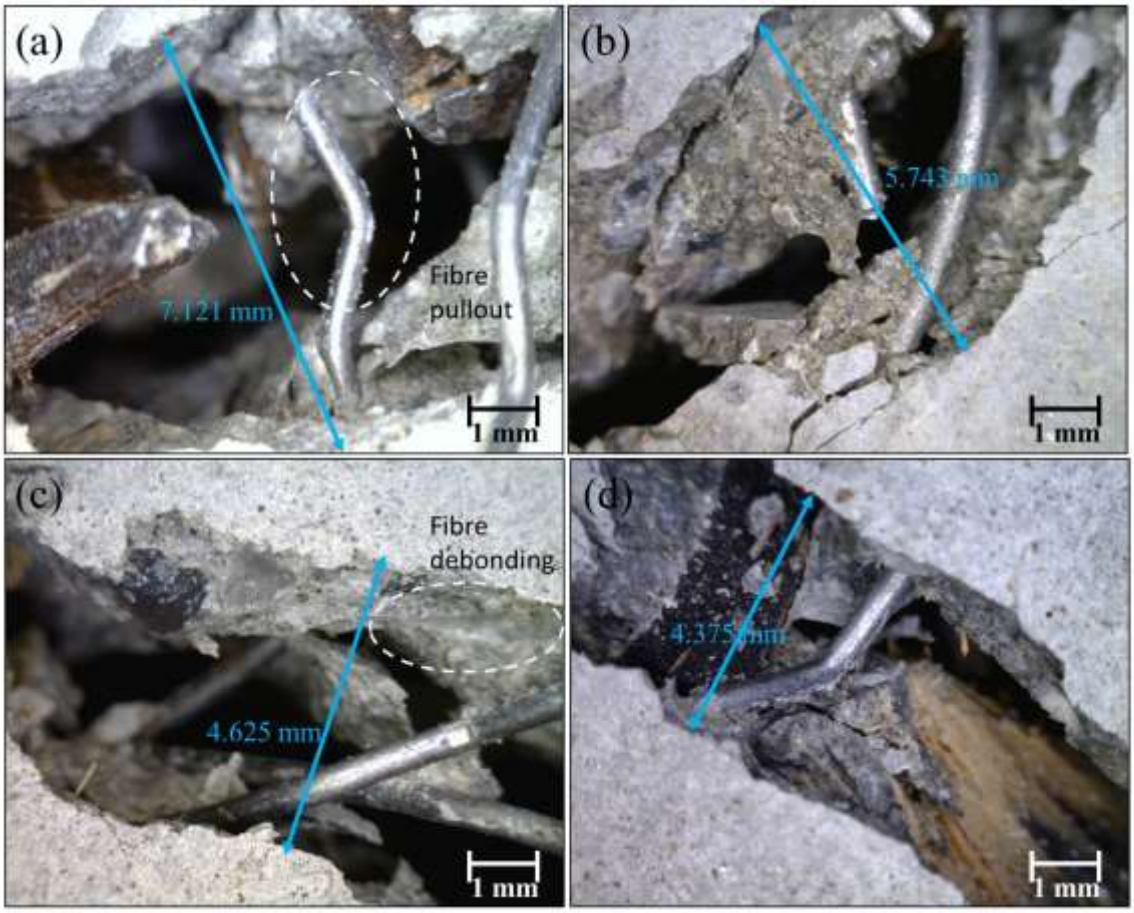

Figure 7.7 Crack width at failure of (a) OPSC-25, (b) OPSC-50, (c) OPSC-75 and (d) OPSC-100 prism specimens

7.3.1.5 Proposed torsional model for unreinforced OPSC and OPSFRC

The previous discussion showed that the torsional strength of the OPSC was lower than the NWC, but that the OPSC produced similar torsional toughness to the NWC, which was attributed to its post-cracking characteristic. The diversity between the torsional behavior of the NWC and OPSC prevents the proposed model for estimating the ultimate torsional strength of NWC and LWC (Khaloo & Sharifian, 2005; Okay & Engin, 2012; Rao & Seshu, 2003) being applied for the OPSC and OPSFRC. The important properties that distinguish OPSC and OPSFRC from NWC are the cracking and ultimate torsional strengths and twist at failure. Eqs. 7.1 to 7.3 are proposed for the estimation of the torsional behaviors of OPSFRC with steel fiber content up to 1%.

Eqs. 7.1 and 7.2 are proposed to predict the cracking torque and ultimate torque based on the flexural strength of the OPSFRC, as the addition of steel fibers improved both torques. In addition, Eq. 7.3 predicts the twist at failure based on the high correlation between the twist at failure and V_f of steel fibers.

$$T_{cr} = 106.2\sqrt{f_r} \quad \text{(error = ±6\%)} \quad (7.1)$$

$$T_{ult} = 110\sqrt{f_r} \quad \text{(error = ±8\%)} \quad (7.2)$$

Where T_{cr} = cracking torque (in Nm); T_{ult} = ultimate torque (in Nm) and f_r = flexural strength (in MPa).

$$Ø_f = 0.224V_f + 0.005 \quad \text{(error = ±8\%)} \quad (7.3)$$

7.3.2 Torsional behaviors of reinforced concrete beam

The torque-twist curves of all the mixes are shown Figure 7.8. The cracking torque, T_{cr}, cracking twist, $Ø_{cr}$, ultimate torque T_{ult}, ultimate twist, $Ø_{ult,}$ failure torque T_f and twist at failure, $Ø_f$ were derived directly from the curves and the results are reported in Table 7.3. The torsional toughness was calculated as the total area below the torque-twist curves based on Figure 7.3 and the toughness values are shown in Figure 7.9.

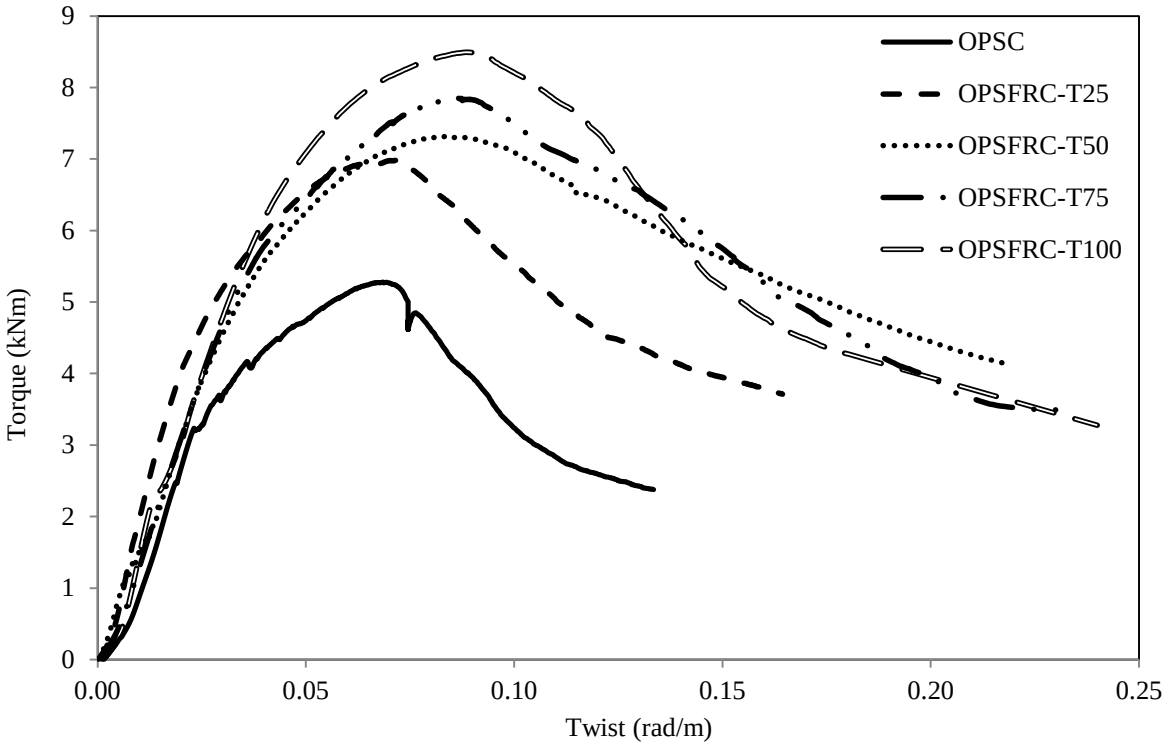

Figure 7.8 Torque-twist curves for beams

Table 7.3 Torsional strength of beams for all mixes

Mix	Cracking torque		Ultimate torque		Failure torque		Initial torsional stiffness (kNm^2)	Cracked torsional stiffness (kNm^2)
	Torque (kNm)	Twist (rad/m)	Torque (kNm)	Twist (rad/m)	Torque (kNm)	Twist (rad/m)		
OPSC	5.27	0.068	5.28	0.068	2.38	0.133	183.99	-
OPSFRC-T25	6.93 (32%)	0.067	6.98 (32%)	0.072	3.71 (56%)	0.164	197.37	9.75
OPSFRC-T50	7.23 (37%)	0.078	7.32 (39%)	0.085	4.13 (74%)	0.219	171.81	11.51
OPSFRC-T75	7.73 (47%)	0.078	7.85 (49%)	0.087	3.48 (46%)	0.235	181.97	13.98
OPSFRC-T100	8.34 (58%)	0.077	8.50 (61%)	0.089	3.28 (38%)	0.24	167.91	14.05
NOTE: Values in bracket denote the % increments corresponding to the T0 mix								

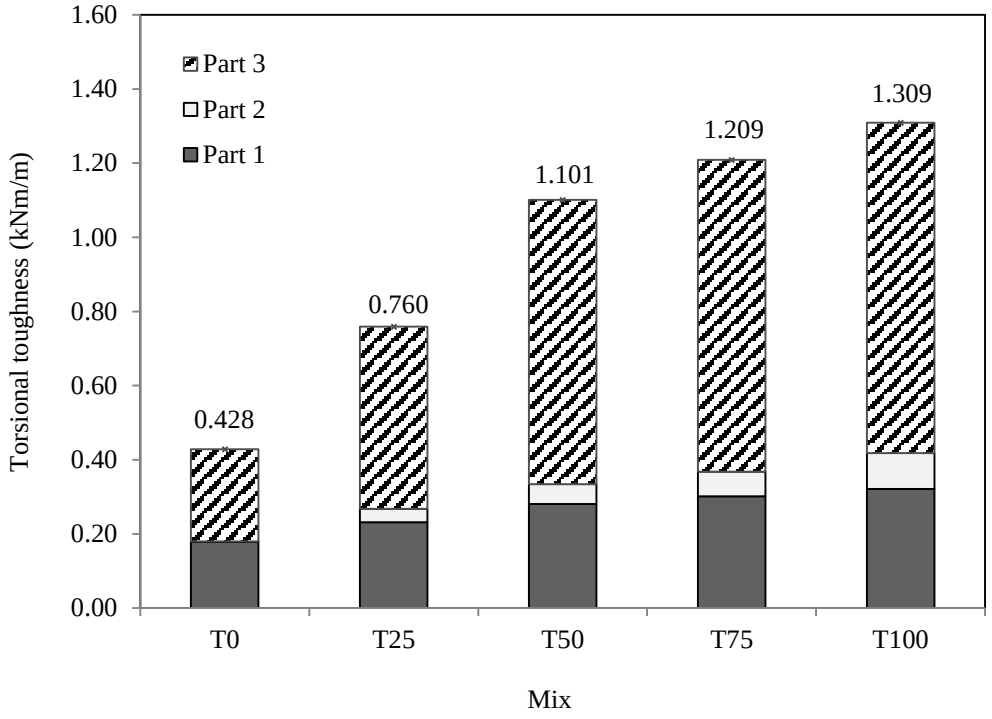

Figure 7.9 Torsional toughness against volume fraction (V_f) of steel fibers in OPSFRC beams

7.3.2.1 Pre-cracking torsional behavior

The pre-cracking torsional behavior of the concrete refers to the portion of torque-twist curve up to the cracking torque (labelled as Part 1 in Figure 7.3). Based on the results from Table 7.3, the cracking torque of the control OPSC beam was found to be 5.27 kNm, while the cracking torque of OPSFRC increased to 6.9–8.3 kNm (1.6–3.0 kNm or 32–58% increment). The published studies on the torsional behavior of concrete showed that the pre-cracking behavior of torsional beams was independent of the presence of reinforcement (Hsu, 1968; Okay & Engin, 2012). Before the cracks formed, the plain rectangular members and reinforced beams showed similar performance when subjected to pure torsion. The reason being that the torque is mainly taken up by the concrete itself before the torsion crack commences. The comparison between the torque-twist curves in both Figure 7.4 and 7.8 showed that both the unreinforced prism and reinforced beams of OPSC and OPSFRC showed similar trend and behaviors but diverse in the magnitude of torque and twist capacity. The incorporation of torsion

reinforcement and larger beam cross sections increased both the torque and twist capacity of OPSC and OPSFRC beams. Hence, we can infer that the enhancement of the cracking torque of the OPSFRC mixes relative to the OPSC beam is mainly attributed to the fiber-concrete matrix interfacial bonding. The crack bridging effect of steel fiber bridges the potential crack and reduces the crack tip stress, and, ultimately, improves the concrete tensile strength and energy capacity (Gao et al., 1997; Hamoush et al., 2010).

.

In addition to the cracking torque, the torsional ductility of the OPSFRC beams was also improved as the cracking twist increased by 0.01 rad/m; however, it was independent of the fiber volume. The crack bridging effect arrests the crack opening and propagation, and allows the concrete to hold together before the crack occurs, and thus increases the cracking twist of the OPSFRC specimens.

The benefit of steel fiber on the cracking torque and ductility was evident in the torsional toughness, as shown in the pre-cracking torsional toughness (Part 1 toughness) from Figure 7.9. The pre-cracking torsional toughness of the control OPSC beam was found to be only 0.18 kNm/m and the OPSFRC-T25, OPSFRC-T50, OPSFRC-T75 and OPSFRC-T100 mixes reported pre-cracking torsional toughness of 0.23, 0.28, 0.30 and 0.32 kNm/m, respectively. From the fiber volume of 0.25% to 1.00%, the improvement in the pre-cracking torsional toughness of the OPSFRC beams fell within the range of 30–80%, relative to the control OPSC beam.

Another parameter related to the pre-cracking torsional behavior of the concrete is the initial torsional stiffness. Following Table 7.3, the addition of steel fiber had a negligible effect on the initial torsional stiffness of the OPSFRC beams. Meanwhile

Section 7.3.1.3 revealed that the addition of fibers enhanced the initial torsional stiffness of OPSFRC prisms. In the case of OPSFRC beams, the torsional stiffness of beams was 20 times higher than the prisms attributed to the main and torsion reinforcement bars. Hence increment effect of steel fibers on the torsional stiffness became insignificant. Therefore, we can conclude that before the first torsional cracking commences, the addition of steel fiber enhanced both the cracking torque and twist but had no effect on the stiffness.

7.3.2.2 Post-cracking torsional behavior

The previous discussions stated that the pre-cracking torsional characteristics of concrete including OPSC depend on the concrete's strength and reinforcement. However, the post-cracking torsional behavior of concrete mainly relies on the reinforcement. After the first crack occurs, the reinforced concrete beam under pure torsion performs like a flexural beam, at which the slope of the load-deflection curves declines to follow a new but lower slope. This is attributed to the uncracked concrete stress being upset by the cracking causing the beam to attain a new equilibrium by transferring the load to the reinforcement (Hsu, 1968). This shows that the reinforcement governs the post-cracking torsional resistance of the concrete.

The role of the steel fiber in enhancing the post-cracking torsional strength was evident from the ultimate torque (T_u) and cracked torsional stiffness of the OPSC and OPSFRC beams. The results from Table 7.3 reveal that the OPSC produced an ultimate torque, T_u, of 5.28 kNm and no cracked torsional stiffness. The OPSC beam achieved its crack and ultimate torque at almost the same torque and twist, which indicated that the OPSC beams did not possess any post-cracking torsional toughness (Part 2 toughness in Figure 7.9) at which the cracked specimen could not sustain any further

torque until it reached the ultimate torsional strength. Zero post-cracking torsional toughness (Part 2 toughness) is not desirable in the structural design, as such brittle structural performance will cause a sudden loss of torsion capacity once the member cracks. The brittle torsional behavior of OPSC could be explained by the high brittleness of OPSC.

The brittle torsion behavior of the OPSC beams could be compensated for by the addition of steel fiber. Firstly, the OPSFRC specimens produced enhanced torsional strength (T_u) compared to the OPSC mix (Table 7.3). The ultimate torques of OPSFRC-T25, OPSFRC-T50 and OPSFRC-T75 reinforced with 0.25–0.75% steel fiber showed improved values of 7.0 kNm, 7.3 kNm and 7.9 kNm, respectively. The values of T_u of OPSFRC-T25, OPSFRC-T50 and OPSFRC-T75 beams were about 30–50% higher than that of the OPSC control beam. The highest T_u of 8.5 kNm was obtained in the OPSFRC-T100 mix with 1% steel fiber, which was about 60% higher than the OPSC beam. After the cement matrix fractures and the crack initiates, the crack bridging helps hold the cracked cement matrix together as additional energy is required for the fiber pullout from the matrix for the cracks to further open up and propagate. This allows the concrete to sustain a higher energy capacity after the crack initiates before it reaches the ultimate capacity (Bischoff, 2007; Gao et al., 1997; Hamoush et al., 2010).

In addition, the steel fiber was also found to enhance the cracked torsional stiffness of the OPSFRC beams (Table 7.3). As stated in the beginning of this section, the OPSC beam possessed no cracked torsional stiffness; however, the OPSFRC mixes produced a torsional stiffness of about 9.8–14.1 kNm^2. The cracked torsional stiffness is generally lower than the initial torsional stiffness (Hsu, 1968; Okay & Engin, 2012). After cracking commences, the torsional stress is transferred from the concrete to the

reinforcement to attain equilibrium between the forces, which results in a considerably lower slope of the torque-twist curve. Based on the results from Table 7.3, the increase in the steel fiber volume resulted in a higher cracked torsional stiffness. The cracked to initial torsional stiffness ratio of the OPSFRC-T25 beam was about 5% and the ratio increased to 8.5% for the OPSFRC-T100 mix. The improved cracked torsional stiffness of the OPSFRC beams relative to the OPSC beam showed that the addition of steel fiber reduced the brittleness and improved the ductility of the OPSC before it reached the ultimate torsion strength. This increment in the cracked torsional stiffness might be attributed to the fiber-matrix interfacial bonding at which the bonding enables a more effective transition between the torsional stress from the concrete to the reinforcement. Moreover, the presence of more steel fiber in the cement matrix caused a more uniform and effective stress transfer, and, hence, the cracked torsional stiffness increased.

Apart from the torsional strength and stiffness, the enhancement effect of steel fiber is more evident in the post-cracking torsional toughness of the OPSFRC mixes (Figure 7.9). The observations on the cracked torsional stiffness could be supplemented by the Part 2 toughness from Figure 7.9: the addition of steel fiber to the OPSFRC mixes improved the Part 2 toughness of the concrete and the increase in fiber volume caused higher Part 2 torsional toughness. The Part 2 toughness of the OPSFRC-T25, OPSFRC-T50, OPSFRC-T75 and OPSFRC-T100 were 15%, 19%, 22% and 30% of its corresponding Part 1 toughness. The significance of the addition of steel fiber was evident as the 0.25% steel fiber enabled the OPSFRC to sustain about 15–30% higher torsional energy before reaching the ultimate torsional capacity. The increased cracked torsional stiffness and Part 2 toughness allowed the OPSFRC to avoid sudden failure and exhibit ample sign of cracking before reaching the ultimate torque.

Beyond the ultimate torque, the OPSC and OPSFRC beams were capable of sustaining a huge amount of torsion toughness (Figure 7.9). The Part 3 torsional toughness of the specimens was found to be higher than the summation of the Part 1 and 2 toughness. Following the Part 3 toughness (Figure 7.9), the OPSFRC beams produced a drastic increment in the post-ultimate (Part 3) torsional toughness. The incorporation of 0.25% into the OPSFRC beam doubled the Part 3 toughness of that of the control OPSC beam; while the highest Part 3 toughness was observed in the OPSFRC-T100 mix at which a 260% increment of Part 3 toughness was achieved. The significant improvement to the post-ultimate torsional toughness of the OPSFRC mixes was mainly attributed to the notable enhancement of the post-cracking ductility of the OPSFRC. Following the twist at failure values from Table 7.3, the steel fiber-reinforced OPSFRC specimens produced higher failure torque and twist than the control OPSC beam. After the ultimate torque, the OPSC beam follows a steep slope, which indicates that the OPSC fails at a faster rate, compared to the OPSFRC. The OPSFRC beam from OPSFRC-T100 mix reported the highest twist at failure of 0.24 rad/m, which was about twofold that of the OPSC mix without any steel fiber reinforcement. The crack bridging effect of the steel fiber results in additional energy being required to pull the fiber out from the fractured cement matrix, and this post-peak tensile stiffening mechanism substantially allows the concrete to exhibit residual strength and increased ductility (Abu-Lebdeh et al., 2011; Bischoff, 2007; Hamoush et al., 2010; Singh et al., 2004).

In summary, the addition of steel fiber into the OPSFRC matrix enhanced the pre- and post-cracking torsional strengths and torsional ductility, at which the torsional toughness of all three parts in Figure 6 increased considerably compared to OPSC. In addition, the increase in the steel fiber volume resulted in a stronger crack bridging

effect at which the torsional strength, cracked torsional stiffness and the torsional toughness were enhanced significantly.

7.3.2.3 Crack resistance

The sketches of the failure patterns and the maximum crack widths of all beam specimens are shown in Figure 7.10 and 7.11, respectively. The sketches of the crack patterns from Figure 7.10 show that the beams failed under a primary torsional crack with an angle of about 45^{o} inclined from the concrete edge. The failure patterns of the OPSC and OPSFRC beams were compatible to the literature on the published research works on the torsional strength of concrete (Khaloo & Sharifian, 2005; Okay & Engin, 2012; Rao & Seshu, 2003), as well as OPSFRC prism in Section 7.3.1.4. It has been previously discussed that the OPSC beam failed at a faster rate than the OPSFRC beams. Figure 7.10(a) shows that the OPSC mainly failed under the primary torsion cracks without any formation of secondary fine cracks compared to the other OPSFRC beams. This indicates the brittle torsional failure in the OPSC specimen. The primary torsion crack of the OPSC resulted in a crack width of 8.625 mm, as seen in Figure 7.11(a).

Figure 7.10(b-e) and 7.11(b-e) reported that the steel fiber reinforcement in the OPSFRC mixes reduced the crack widths of the primary torsional crack significantly by the formation of multiple fine cracks. It can be clearly seen in Figure 7.10(b) to 7.10(e) that the increase in the steel fiber volume resulted in the formation of narrower primary torsional cracking but a greater number of fine cracks of smaller and narrower crack width. Combining the observation with the increased cracked torsional stiffness and Part 2 toughness, the addition of steel fiber in the OPSFRC improved the serviceability of the structural members by the prevention of sudden failure and the member is capable of exhibiting ample sign of cracking. In addition, the crack widths of the OPSFRC were

reduced by 20–65%, compared to the OPSC mix (Figure 7.11). The formation of multiple fine cracks (Figure 7.10) and the reduction of the primary crack width (Figure 7.11) explained that the crack bridging effect contributed to the improved crack resistance in the OPSFRC mixes as the bridging action of the fiber across a crack increased the tensile stress transferred to the bonded concrete and delayed the development of microcracks. The tension stiffness mechanism leads to an increased amount of fine cracking but decreased crack width in the concrete (Hamoush et al., 2010; Mo et al., 2014b). This explanation can be supported by the fiber pullout and debonding mechanisms from Figure 7.11(b) and 7.11(c), respectively. The fiber-matrix interfacial bond allows the concrete to sustain higher stress and strain, and, eventually, arrest the crack propagation.

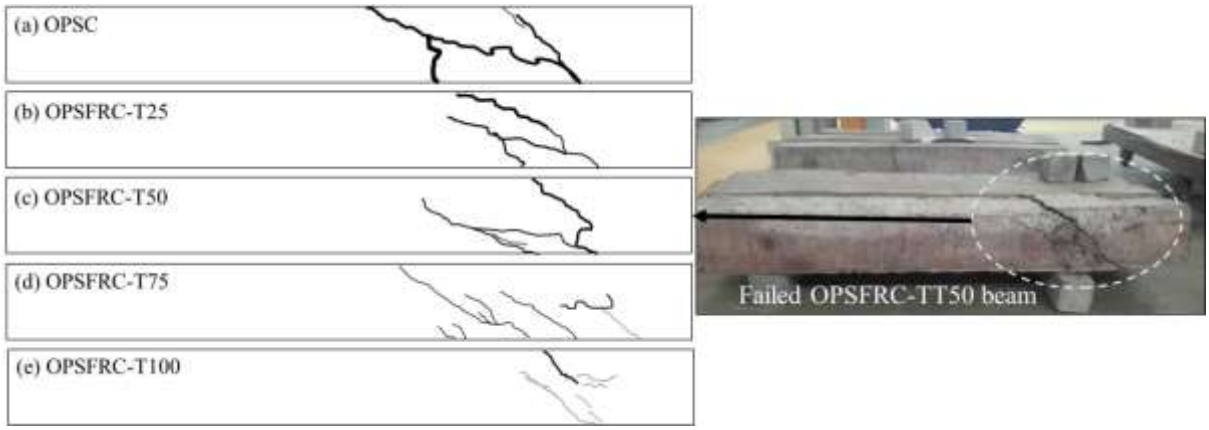

Figure 7.10 Sketches of failure crack of OPSC and OPSFRC beams

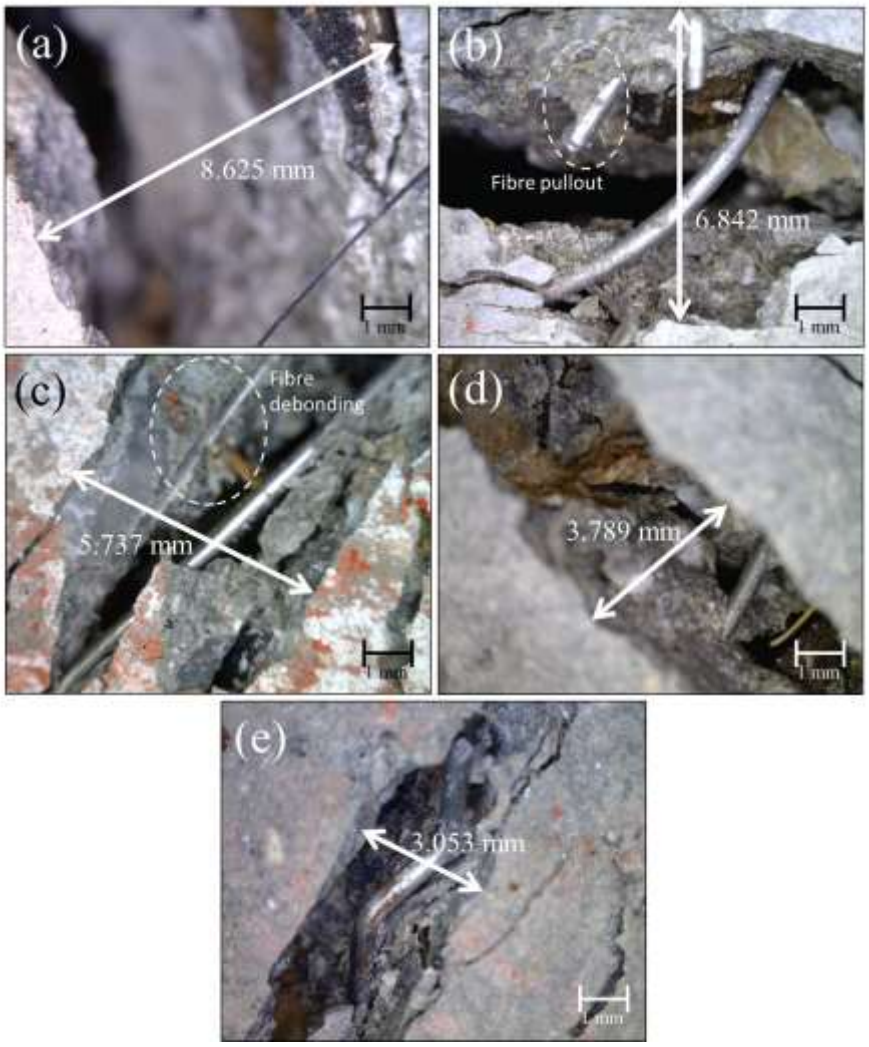

Figure 7.11 Measured maximum crack widths of (a) OPSC; (b) OPSFRC-T25; (c) OPSFRC-T50; (d) OPSFRC-T75 and (e) OPSFRC-T100 beams

7.3.2.4 Proposed torsional model for OPSFRC beams

Design codes, such as BS 8110, ACI 318 and Eurocode 2, provide the provisions for the design of the structural members subjected to torsion. Using the reinforcement provided in Figure 7.2, the torsional strength (T_u) of the OPSC beam was checked in accordance with these three codes. The calculated T_u values are 0.97 kNm, 1.62 kNm and 6.17 kNm for the torsional strengths calculated using BS 8110, ACI 318 and Eurocode 2, respectively. The design provisions given in BS 8110 and ACI 318 underestimated the torsional strength of the OPSC beam (T_u of OPSC mix is 5.28 kNm) as the design codes provide a conservative design, and the design provisions are not suitable for beams of

smaller dimensions; while Eurocode 2 slightly over-estimated the T_u of OPSC, which might be attributed to the weaker tensile strength of OPSC. However all these codes are dedicated to normal aggregate concrete and are not suitable for the torsional design of LWC, including OPSC. Furthermore, the codes do not take into account the effect of steel fiber. Hence, a new torsional model for the OPSC and OPSFRC beams is important for the design of the OPSC/OPSFRC members subjected to torsion. Based on the torsional model proposed by Okay and Engin (2012), which is represented in Eq. 7.4 and 7.5, Eqs. 7.6–7.8 are proposed to predict the cracking, ultimate and failure torques of the OPSC and OPSFRC with up to 1% steel fiber.

$$T_{cr} = C_1 h b^2 f_r \quad (7.4)$$

where h and b are the longer and shorter dimensions of the torsion beams; C_1 is the coefficient based on the h/b ratio and f_r is the flexural strength of the concrete.

$$T = T_{cr} + \beta (Ø-Ø_{cr})(V_f-V_o) \times 10^3 - 3\beta(Ø-Ø_u)\langle V_f-V_o\rangle \times 10^3 \quad (7.5)$$

where $\beta = 635278\ V_f^2 - 450.83V_f + 2.56$; V_f is the volume fraction of steel fiber in %; T and Ø are the predicted torque and twist, respectively; T_{cr} and $Ø_{cr}$ are the cracking torque and twist; $Ø_u$ is the ultimate twist; and V_o is a constant of 0.005.

The following equations are proposed for the prediction of the torsional behavior of OPSFRC beams:

$$T_{cr} = 3\sqrt{f_r} \quad (7.6)$$

where T_{cr} is the cracking torque in kNm and f_r is flexural strength in MPa. It can be seen that the Eq. 7.4 is mainly governed by the flexural strength of the concrete. Compared to the Eq. 7.1, both equations 7.1 and 7.6 differs by the coefficients, with the coefficient

of Eq. 7.6 is about 30 times higher than that in Eq. 7.1. This indicates that the torsional cracking strength of OPSFRC beams depends on cross section beam, reinforcements, and concrete's tensile strength. Hence it is recommended that future works can be carried out on these three parameters to obtain an empirical solution for all the torsional strength of OPSC and OPSFRC reinforced concrete beams.

$$T_u = T_{cr} + 167.6(V_f)Ø_u \quad (7.7)$$

where T_u is ultimate torque in kNm, Vf is the volume fraction of steel fiber in % and $Ø_u$ is the twist corresponding to the T_u (in rad/m)

Eq. 7.7 provides the torque-twist relationship after the cracking torque and before the ultimate torque. It is noteworthy that the equation depends on the volume fraction. OPSC without any steel fiber reinforcement produced no Part 2 torsional toughness while the addition of steel fiber results in the improved cracked torsional stiffness. The ultimate torque and twist could be obtained based on Eq. 7.8, as follows:

$$T_f = T_u - 15.1(V_f)^2(Ø_f - Ø_{-u}) \quad (7.8)$$

where T_f is the failure torque in kNm, Vf is the volume fraction of steel fiber in %, and $Ø_f$ and $Ø_u$ are the failure and ultimate twists, respectively (in rad/m).

Eq. 7.8 correlates to the torque-twist relationship beyond the ultimate torque, which corresponds to the Part 3 torsional toughness in Figure 7.3. The combined relationships from Eq.7.4 to 7.6 could be further derived into a full torque-twist, as shown in Figure 7.3. Table 7.4 shows the comparisons between the experimental values and the predicted values from the proposed equations for T_{cr}, T_u, T_f and the torsional toughness.

The proposed equations could be used to predict the torsional characteristics of OPSC and OPSFRC within an error of ± 12%.

Table 7.4 Comparisons between the experimental and predicted torques and toughness

Mix	Cracking torque (kNm)			Ultimate torque (kNm)			Failure torque (kNm)			Torsional toughness (kNm/m)		
	Exp.	Pred. (Eq. 7.4)	% Error	Exp.	Pred. (Eq. 7.5)	% Error	Exp.	Pred. (Eq. 7.6)	% Error	Exp.	Pred.	% Error
OPSC	5.27	5.42	2.8%	5.28	5.42	2.6%	2.38	2.67	12.2%	0.43	0.45	4.4%
OPSFRC-T25	6.93	6.21	10.4%	6.98	6.21	11.1%	3.71	3.37	9.1%	0.76	0.68	10.4%
OPSFRC-T50	7.23	6.96	3.8%	7.32	6.96	4.8%	4.13	3.71	10.1%	1.10	1.04	5.8%
OPSFRC-T75	7.73	7.77	0.5%	7.85	7.78	0.9%	3.48	3.77	8.2%	1.21	1.23	1.4%
OPSFRC-T100	8.34	8.57	2.8%	8.50	8.59	1.1%	3.28	3.55	8.4%	1.31	1.35	3.0%
NOTE: Exp. = experimental values; Pred. = predicted values using equations												

Figure 7.12 shows the comparison between the experimental and predicted T_u for the different analytical equations from Khaloo & Sharifian (2005), Okay &Engin (2012) and Rao & Seshu (2006). These previous studies on the torsional strengths of normal aggregate concrete and high strength LWC could not be applied on the OPSC specimens as they significantly underestimated the torsional strengths of OPSC. This implies that the OPSC torsional performance could outperform that of the normal aggregate concrete and high strength LWC. For example, using Khaloo's equation, the OPSC produced a similar T_u to a high strength LWC with a compressive strength of 90 MPa. However, as the volume fraction of the steel fiber increased in the OPSFRC specimens, the difference between the ultimate torque of the OPSFRC reduced as the OPSFRC showed comparable torsional behavior to that of normal aggregate concrete and high strength LWC.

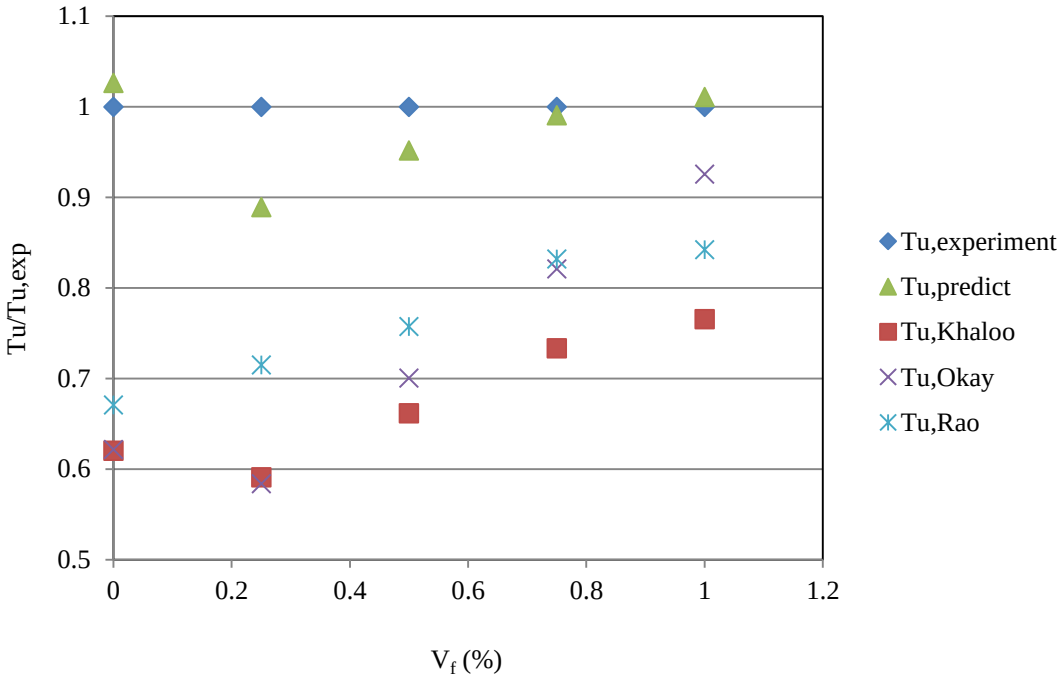

Figure 7.12 The comparison between the experimental values and the proposed equations from different researchers

7.4 Chapter conclusions

Based on the experimental results of the OPSC and OPSFRC prisms and beams subjected to pure torsion, the following conclusions could be derived:

- The torque-twist curves of the prisms and beams showed similar trend. The magnitudes of the torques and twists in the beams were much higher than the prisms attributed to the increased beam cross section and the presence of torsion reinforcements.
- The crack bridging effect improved the pre-cracking torsional behavior of the OPSFRC specimens by improving the strength of the concrete. The cracking torque and pre-cracking torsional toughness of OPSFRC beams were enhanced by 1.6–3.0 kNm and 0.23–0.32 kNm/m relative to the control OPSC beam. In

addition, the cracking twists of the OPSFRC specimens increased by 0.01 rad/m independent of the fiber content.

- For the post-cracking torsional behavior, the ultimate torque of the OPSFRC beams was found to be 30–60% higher than that of the OPSC beam. Beyond the ultimate torque, an increment of 260% of the Part 3 torsional toughness was achieved in the OPSFRC-T100 beam.
- The control OPSC produced no cracked torsional stiffness, but the cracked to initial torsional stiffness ratio of the OPSFRC-T25 beam increased from 5% to 8.5% to that of the OPSFRC-T100 mix. This showed that the addition of steel fiber reduced the brittleness and improved the ductility of the OPSFRC beams before the ultimate torsion strength.
- The highest improvement in the torsional behavior of the OPSFRC beams was observed in the OPSFRC-T100 mix. The highest cracking torque, ultimate torque, twist at failure and torsional toughness of 8.3 kNm, 8.5 kNm and 1.31 kNm/m, respectively, were obtained in the OPSFRC-T100 mix with 1% steel fiber; these values were about 160%, 160%, 200% and 300% of that for the OPSC beam.
- The tension stiffening mechanism of the steel fiber arrested the crack growth and improved the crack resistance of the OPSFRC beams as the crack widths of the primary torsion cracks reduced by 20–65% along with the formation of multiple fine cracks.
- A new torsional model is proposed for the prediction of the torsional behavior of OPSC and OPSFRC.

CHAPTER 8

DEVELOPMENT OF HIGH STRENGTH OIL PALM SHELL FIBER-REINFORCED CONCRETE WITH STEEL FIBERS

8.1 Chapter introduction

The studies on Chapters 6 and 7 revealed that the addition of fibers produced significant enhancement on the load capacity and crack resistance of OPSFRC reinforced concrete beams under flexural and torsional loading. In addition, both OPSC and OPSFRC satisfied the structural requirements such as crack width and ductility. This indicated that both OPSC and OPSFRC were applicable as structural members. This chapter aims to further enhance the strength of OPSFRC by incorporation higher volume of steel fibers, in order to expand the structural applications of OPSFRC. Concrete with high tensile strength is desirable for the design of larger and longer structural members to arrest tensile cracking and to improve the tensile loading capacity. In addition, in the design of special structures, such as impact and blast resistant structural members, high tensile strength is mandatory (Habel & Gauvreau, 2008; Roy et al., 2014; Wu et al., 2009). Generally, the flexural strength of OPSC in the range of about 3-5 MPa (Alengaram et al., 2011, 2013) is about 60% lower than NWC. In addition, the previous chapters reported that the addition of 1% steel fibers enabled the production of OPSFRC with flexural strength of about 7 MPa. However, the tensile strength of the OPSC with 1% steel wire was found to be well below the expected strength of 10 MPa to resist high impact and blast loading (Habel & Gauvreau, 2008; Wu et al., 2009). Thus, to combine the advantages of the low AIV in the OPS and the effect of the steel fibers, OPSFRC with high impact and tensile strength of OPSC is investigated in this research. In this study, up to 3% (by volume) of hooked end steel fibers were added in order to widen

the potential application of the OPSFRC for structural members subjected to high tensile, impact or blast loadings. The mechanical properties, brittleness, flexural ductility and toughness of OPSFRC incorporating steel fiber of 0.5%, 1.0%, 1.5%, 2.0%, 2.5% and 3.0% were investigated. In addition, the flexural behaviors of OPSFRC beam with 3% were also compared with the previous chapter. The content in this chapter is to complete the objective in third stage "Development of high tensile strength OPSFRC" as shown in Figure 1.1.

8.2 Experimental program

8.2.1 Materials and mix proportions

Similar materials from Chapter 5 were used in this work. The material properties of cement, OPS, sand, silica fume and superplasticizer can be referred to Section 3.2.1 and steel fibers were added into OPSC to produce OPSFRC specimens. The hooked end steel fiber with aspect ratio from Chapters 5 and 6 are used.

The mix proportions consists of one control mix consists of OPSC and another six OPSFRC mixes. The contents of all constituents materials including cement, OPS, sand, silica fume, superplasticizer and water were kept constant; while the variable studied is the volume fraction of steel fibers. Steel fibers of 0.5%, 1.0%, 1.5%, 2.0%, 2.5% and 3.0% by volume were added for the mixes OPSFRC-5, OPSFRC-10, OPSFRCC-15, OPSFRC-20, OPSFRC-25 and OPSFRC-30, respectively. Table 8.1 shows the detailed mix proportioning.

Table 8.1 Mix proportions

Mix design	Cement (kg/m^3)	Silica fume (kg/m^3)	OPS (kg/m^3)	Mining sand (kg/m^3)	Water (kg/m^3)	Steel fiber (%vol. of concrete)
OPSC	539	53	323	971	178	0
OPSFRC-5	539	53	323	971	178	0.5
OPSFRC-10	539	53	323	971	178	1.0
OPSFRC-15	539	53	323	971	178	1.5
OPSFRC-20	539	53	323	971	178	2.0
OPSFRC-25	539	53	323	971	178	2.5
OPSFRC-30	539	53	323	971	178	3.0

8.2.2 Mixing, specimen preparation and testing

The mixing procedure stated in Figure 3.2 was followed in all the mixes. The fresh concrete was poured into selected moulds. For each mix proportion, 100 mm cubes, 100 ϕ x 200 mm cylinders, 150 ϕ x 300 mm cylinders, 100 x 100 x 500 mm prisms and 100 x 100 x 300 mm prisms were prepared for compressive strength (BS EN 12390:2009), splitting tensile strength (ASTM C496/C496M, 2011), modulus of elasticity/Poisson's ratio (ASTM C469, 2010), flexural strength (ASTM C78, 2010) and flexural ductility/toughness (ASTM C1018, 1997), respectively. After the removal of the specimens from the moulds, these specimens were cured in water until the age of testing. The compressive strength was tested at the ages of 1-, 3-, 7- and 28 days, while other tests were conducted at the age of 28 days. Other than that, additional beam from the mix design OPSFRC-30 was prepared to study the flexural behaviors of OPSFRC beams with high volume steel fibers. The detailing and testing procedures of the OPSFRC-30 beam followed the previous chapter as shown in Figure 6.2 and 6.3, respectively. The flexural behaviors of OPSFC-30 were compared to the results in Chapter 6.

8.3 Results and discussion

8.3.1 Workability (slump)

It is a well-established fact that the addition of fibers in concrete generally results in a significant reduction in the workability, as seen from the slump values of the OPSFRC. The control mix, OPSC mix produced a slump value of about 70 mm and it was compatible to previous chapters. However, the slump values were reduced significantly to 45 mm, 15 and 10 mm for the OPSFRC-5, OPSFRC-10 and OPSFRC-15 mixes, respectively. Despite low workability, the OPSFRC had acceptable compaction and finishability. Short & Kinniburgh stated that LWC requires a much lower slump value than NWC to achieve good compaction (Short & Kinniburgh, 1978). As the fiber content exceeded 1.5%, zero slump was recorded and additional 20-25 tamping using tamping rod was required to achieve compaction similar to that of the OPSFRC-15 mix. The network of fibers could restrict the flowability of the aggregate. Moreover, the fibers require a high amount of cement paste to wrap around for the formation of the fiber-cement matrix bond, which, ultimately, increases the viscosity of the concrete mixture (Chen & Liu, 2005). The increase in the fiber content in the OPSFRC mixes increased the viscosity of the mixes, and, hence, reduced the workability. At high volumes of steel fiber (>1%), the fibers have a high tendency to agglomerate to form a clogged fiber network. Hence, the high viscosity of the fresh concrete contributed to the poor compaction of the fresh OPSFRC. Gao et al. (1997) reported similar inadequate compaction due to the high amount of fibers. However, the steel fiber content cannot be increased beyond 3% in fiber-reinforced concrete (Santhakumar, 2006). The reason is the high volume of steel fiber requires vast amount of cement to form fiber-matrix interfacial bond. This is evident in the attempt in the fabrication of OPSFRC with 3.5% (which is not reported in earlier part of this chapter). The fresh concrete of OPSFRC

with 3.5% cannot be compacted with additional tampering and higher dosage of superplasticizer resulted in segregation. Hence it can be inferred that the maximum volume of steel fiber in OPSFRC is 3%.

8.3.2 Density

Two types of density, saturated surface-dry density (ρ_{SSD}) and oven-dry density (ρ_{ODD}), were measured and the relationship between the densities and volume fraction (V_f) is shown in Figure 8.1. The ρ_{SSD} represents the actual density of the concrete; however, the oven-dry density (ρ_{ODD}) is preferred by most of the classifications of LWC such as EN 206-1 due to the consistency of water content in the concrete. As seen in Figure 8.1, the ρ_{ODD} of OPSFRC showed higher consistency and uniformity than the ρ_{SSD}. The OPSFRC specimens in the saturated surface dry condition were not consistent as the ρ_{SSD} were dependent on the OPS content and the water absorption of the OPS. Therefore, the consistent ρ_{ODD} of OPSFRC is preferred compared to ρ_{SSD}.. In comparison, the ρ_{SSD} of OPSFRC was about 110-150 kg/m^3 higher than that of ρ_{ODD}.

The ρ_{SSD} of the OPSC reported in the published studies showed a notable density reduction of about 16-30% compared to the ρ_{SSD} of about 2400 kg/m^3 for the NWC (Alengaram et al., 2011, 2013). However, the incorporation of steel fibers in the concrete increases the concrete density (Libre et al., 2011). This phenomenon is evident in the present study, as seen from the density of the OPSFRC shown in Figure 8.1. The average ρ_{SSD} of the OPSC without fibers was found at about 1960 kg/m^3. In the case of OPSFRC, for every increment of 0.5% steel fibers, an increase in the density of about 2-6% was found in the ρ_{SSD} of OPSFRC. The highest density increment of about 24% was found for the OPSFRC-30 mix containing 3% steel fibers, which was quite similar to that of NWC. The increase in the density is mainly attributed to the relatively higher

specific gravity of the steel fibers (SG = 7.9) compared to the other constituent materials in the concrete.

As known, LWC is defined as concrete having a ρ_{ODD} of between 800 and 2000 kg/m^3 produced by using lightweight aggregate for all or part of the total aggregate in EN206-1. As seen from Figure 8.1, the OPSFRC with less than 1% of steel fibers met that requirement. However, considering the ρ_{ODD} of NWC of about 2300 kg/m^3, the OPSFRC with steel fibers between 0.5 and 3% could result in a 1-20% reduction in the ρ_{ODD} compared to NWC.

The results from Figure 8.1 showed that a strong correlation could be established between the volume fraction (V_f) of steel fibers and the ρ_{SSD} and ρ_{ODD}. Eqs. 8.1 and 8.2 are proposed to predict the target density of the fiber-reinforced LWC based on the correlations from Figure 8.1. The prediction of the density aids in the selection of the density and maximum fiber content added in fiber-reinforced LWC, including OPSFRC.

$$\rho_{SSD} = 156.4(V_f) + 1934 \quad (8.1)$$

$$\rho_{ODD} = 147.9(V_f) + 1820 \quad (8.2)$$

where ρ_{SSD}, ρ_{ODD} and V_f are SSD density (in kg/m^3), oven-dry density (in kg/m^3) and volume fraction of steel fibers (in %), respectively.

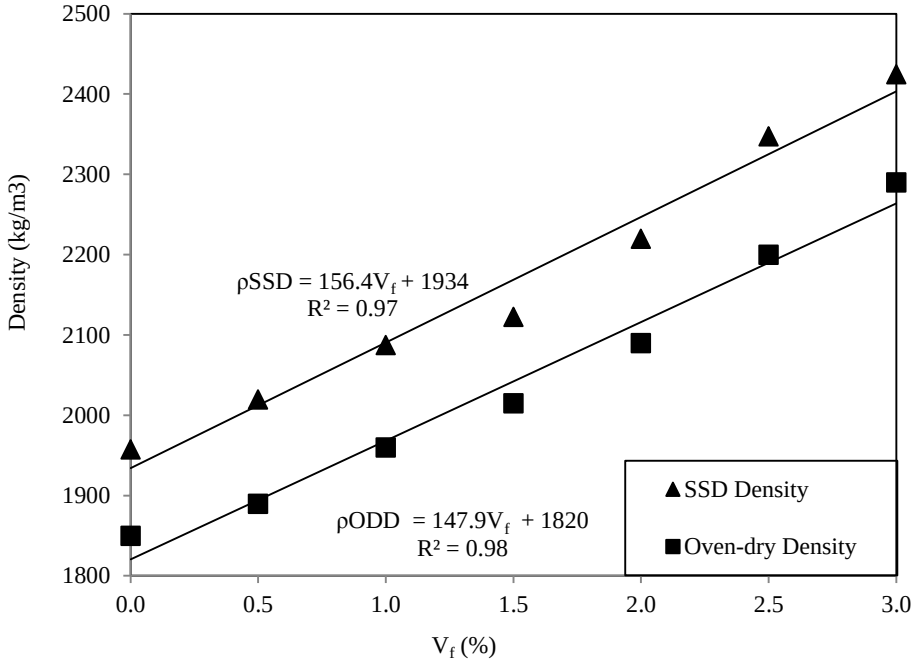

Figure 8.1 Graph of hardened densities versus volume fraction (V_f)

8.3.3 Compressive strength

Table 8.2 shows the development of the compressive strength of the OPSC and OPSFRC mixes over a period of 28 days. Generally, all the mixes produced high early compressive strength at the age of 7 days by producing 83-90% of the 28-day compressive strength. The reaction between the silica fume and the calcium hydroxide (CaOH) liberated from the hydration of cement, which eventually produces calcium silicate and aluminate hydrates, enhanced the early strength of the concrete mixes (Nili & Afroughsabet, 2012). The development of high early compressive strengths reported in this investigation is in agreement with that of the published study on OPSFRC reinforced with polypropylene and nylon fibers.

Table 8.2 Compressive strength, modulus of elasticity and Poisson's ratio for all the mixes

Mix	Compressive strength (MPa)							Modulus of elasticity (GPa)	Poisson 's ratio
	1-day		3-day		7-day		28-day	28-day	28-day
OPSC	19.1	(55%)	25.8	(74%)	30.7	(88%)	34.8	13.53	0.255
OPSFRC-5	19.5	(52%)	27.9	(74%)	33.9	(90%)	37.6	16.35	0.302
OPSFRC-10	22.2	(52%)	29.7	(69%)	37.6	(88%)	42.9	16.01	0.297
OPSFRC-15	25.2	(55%)	30.7	(67%)	39.0	(85%)	45.8	16.09	0.305
OPSFRC-20	27.5	(56%)	36.5	(74%)	40.7	(83%)	49.3	15.79	0.317
OPSFRC-25	29.1	(54%)	39.1	(72%)	47.2	(87%)	54.3	16.05	0.310
OPSFRC-30	31.7	(56%)	40.8	(72%)	47.2	(83%)	56.7	15.62	0.291
NOTE: The percentages in brackets denote the percentage of compressive strength for the 28-day compressive strength									

Figure 8.2 shows that the compressive strength of OPSFRC increased linearly with the addition of steel fibers; it can be seen that for an increase of 0.5% of steel fibers, an increase in the compressive strength within the range of 2.4-5.3 MPa (4-14%) was recorded in the OPSFRC. The highest compressive strength of about 57 MPa was reported in the OPSFRC-30 mix, which was found to be 63% higher than the OPSC mix containing no fibers. The highest compressive strength of 57 MPa achieved in this present study was higher than that of the published results of OPSFRC albeit with 1% steel fibers (Mo et al., 2014a; Shafigh et al., 2011c), as well as OPSFRC mixes in previous chapters.

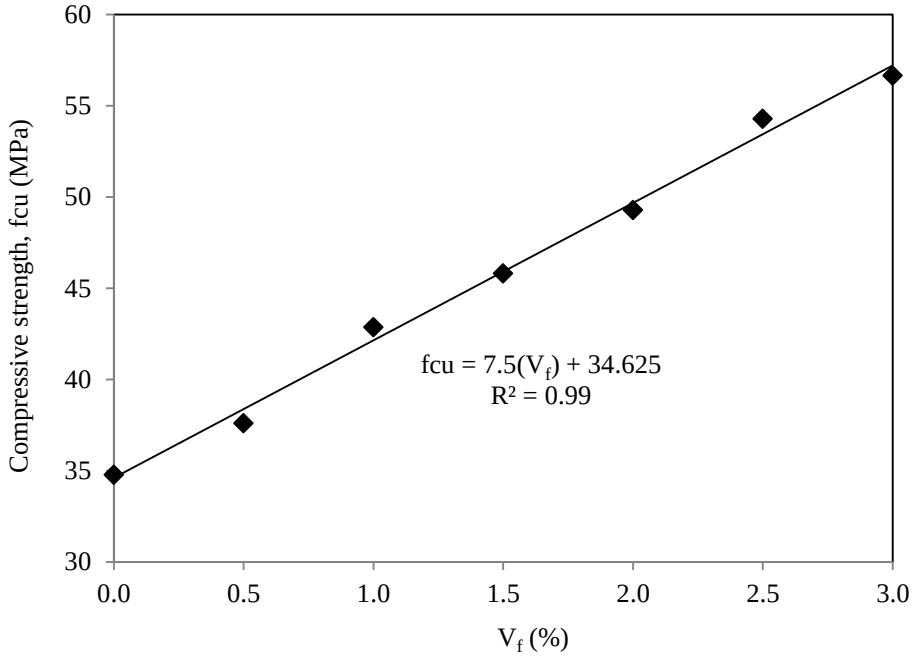

Figure 8.2 Graph of compressive strength versus volume fraction (V_f)

It has been shown that the addition of steel fibers in LWC enhanced the compressive strength (Domagała, 2011; Düzgün et al., 2005; Gao et al., 1997; Libre et al., 2011; Nili & Afroughsabet, 2012). Generally, LWC, like OPSC, has weak compressive and tensile strengths, which is attributed to (i) the weak bond between the cement paste and the aggregate and (ii) the low stiffness of the lightweight aggregate (Gao et al., 1997; Mannan et al., 2006; Okpala, 1990). Under increasing compression loading, the vertical compressive strain and transverse tensile strain occur in the compressed concrete specimens (Gao et al., 1997). Hence, the continuous deformation of concrete produces cracks at the aggregate-cement paste interface or in the aggregate. In the case of OPSC, the failure is governed by the weak bond strength between the cement paste and OPS (Mannan et al., 2006). However, this weakness could be compensated for by the addition of steel fibers to the OPSFRC. The additional fiber-matrix bond in the concrete increases the energy capacity of the concrete by the toughening mechanisms called fiber debonding and frictional sliding associated with fiber-pullout (Bennett & Young, 1998; Singh et al., 2004). Furthermore, the steel fibers

also arrest the crack initiation and propagation; such an enhancement mechanism is generally known as the crack bridging effect (Abu-Lebdeh et al., 2011; Bennett & Young, 1998; Düzgün et al., 2005; Gao et al., 1997; Ng et al., 2013; Singh et al., 2004; Zīle & Zīle, 2013). The steel fibers bridge across the cracks in the concrete and take part or even all of the stress when subjected to increased loading. As the advancing crack reaches the fibers, the crack tip stress concentration is reduced, and thus, the crack propagation is blunted and blocked. Therefore, the presence of the fiber-matrix bond and the crack bridging effect contribute to the significant enhancement of the ultimate strength of OPSFRC.

In addition, the high amount of steel fibers added to the concrete increases the probability of its ability to be located in the vicinity between the OPS and the matrix. This explains the linear increment in the compressive strength of the OPSFRC when the volume fraction of the steel fibers increases. However, it has been shown that poor compaction of concrete containing a high amount of steel fibers (>2%) results in a limited effect on the compressive strength of the steel fiber-reinforced LWC (Domagała, 2011; Gao et al., 1997). The mechanical tamping of the mixes incorporating >1.5% steel fibers produced satisfactory compaction in the OPSFRC, eventually allowing for consistent improvement in the strength of OPSFRC. Hence, the high correlation between the compressive strength of OPSFRC and the volume fraction (V_f) of steel fibers shown in Figure 8.2 allows the prediction of the compressive strength of OPSFRC reinforced with steel fibers (up to 3%). The proposed Eq. 8.3 predicts the compressive strength of OPSFRC within ±1 MPa (±2%) of the experimental results.

$$f_{cu} = 7.5(V_f) + 34.625 \quad (8.3)$$

where f_{cu} and V_f are compressive strength (in MPa) and volume fraction of steel fiber (in %), respectively.

8.3.4 Tensile strength

The significance of concrete's tensile strength in reinforced concrete design is indisputable, particularly in the case of LWC. The weak tensile strength of LWC could lead to significant tensile cracking at a much lower loading capacity compared to the normal concrete. Hence, it is crucial to study the effect of steel fibers on the tensile strength of OPSC, including splitting tensile and flexural strengths, flexural toughness and ductility.

8.3.4.1 Splitting tensile and flexural strengths

ASTM C330/C330M-09 states that the minimum splitting tensile strength for LWC is 2.0 MPa. The published literature on OPSC has reported splitting tensile and flexural strengths of OPSC ranging between 1.8 and 3.5 MPa, and 2.8 and 7.0 MPa, respectively (Alengaram et al., 2011; Mannan & Ganapathy, 2002; Shafigh et al., 2012a). In this study, the control OPSC mix, produced splitting tensile and flexural strengths of 3.2 MPa and 4.8 MPa, respectively. However, these values are relatively lower compared to the tensile strengths reported for NWC and other LWCs (Chen & Liu, 2005; Mannan & Ganapathy, 2002). Therefore, the addition of steel fibers in OPSC in this study aims to enhance its tensile strength.

The enhancement effect of steel fibers on the splitting tensile and flexural strengths of OPSFRC is shown in Figure 8.3, and it can be seen that the addition of steel fibers by up to 3% drastically enhanced the tensile strength of OPSFRC, by producing the highest splitting tensile and flexural strengths of 11.0 MPa and 18.5 MPa, respectively. This shows increment of up to 2.40 and 2.85 times compared to the splitting tensile and flexural strengths of the control OPSC mix. Further, compared to the fiber-reinforced NWC of the same density (2400 kg/m^3), the OPSFRC-30 mix

produced a higher flexural tensile strength of more than 50% (Altun et al., 2007; Balendran et al., 2002; Ibrahim & Che Bakar, 2011). OPSFRC possesses both benefits of excellent tensile strength and density reduction compared to the NWC.

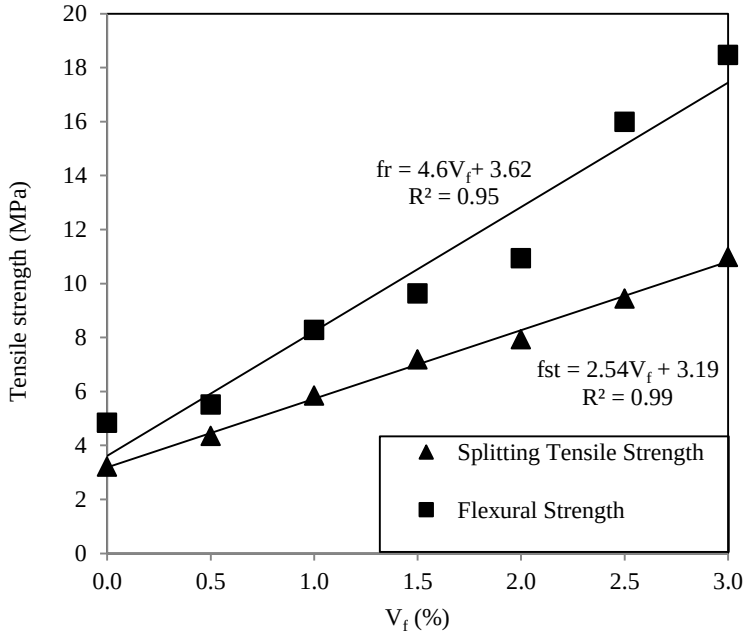

Figure 8.3 Graph of splitting tensile strength (f_{st}) and flexural strength (f_r) versus volume fraction (V_f)

The enhanced tensile strength of OPSFRC could be explained similar to the compressive strength (Section 8.3.3). The additional fiber-matrix bond and crack bridging effect of steel fibers allow the concrete to sustain higher tensile loading and to blunt the crack initiation and propagation. In addition, the steel fibers produce a greater improvement in the tensile strength than in the compressive strength of concrete (Gao et al., 1997). This statement is evident in the OPSFRC, as the OPSFRC reinforced with steel fibers yielded higher splitting tensile to compressive strength ratios and flexural to compressive strength ratios. The splitting tensile to compressive strength ratios of OPSC, OPSFRC-5, OPSFRC-10, OPSFRC-15, OPSFRC-20, OPSFRC-25 and OPSFRC-30 were 9.2%, 11.6%, 13.6%, 15.7%, 16.1%, 17.4% and 19.4%, respectively; while the corresponding flexural to compressive strength ratios were 13.9%, 14.7%,

19.3%, 21.0%, 22.2%, 29.5% and 32.6%. Both ratios increased with the increment of steel fiber volume fraction. The increased tensile to compressive strength ratios showed that the steel fibers produced higher enhancement effects in the OPSFRC compared to the compressive strength. This is attributed to concrete being generally weak in tension and that tensile cracks form at a much lower loading capacity before the ultimate compressive strength is reached. Therefore, under compression loading, the high compression capacity of steel fiber-reinforced concrete allows for a portion of the applied stress; however, under the tensile loading, the weak tensile strength of the concrete causes the concrete to only take up marginal applied stress. Hence, the contribution of steel fibers on the tensile strength of OPSFRC was more significant than on the compressive strength.

As shown in Figure 8.3, it is also evident that the splitting tensile strength of OPSFRC increased linearly with the increase in the volume fraction of steel fiber (R^2 = 0.99). It is clear that both the OPSFRC-5 and OPSFRC-10 mixes, which incorporated 0.5% and 1% steel fibers, respectively, were found to have highly compatible splitting tensile strength to the results published by Shafigh, Mahmud, et al. (2011) and results from Chapter 5 and 6. Therefore, Eq. 8.4 is proposed to further expand the prediction of the splitting tensile strength of OPSFRC with added steel fiber up to 3% (±5% errors).

$$f_{st} = 2.54(V_f) + 3.19 \quad (8.4)$$

where f_{st} and V_f are the splitting tensile strength (in MPa) and volume fraction of steel fiber (in %), respectively.

Similar to the splitting tensile strength, Eq. 8.5 is also proposed to predict the flexural strength of OPSFRC reinforced with steel fibers up to 3%, within the error of

±1 MPa. The significance of the proposed equations is to provide an accurate design of OPSFRC to avoid the probability of under-reinforced members, which eventually results in severe tensile and shear cracking.

$$f_r = 4.6(V_f) + 3.62 \quad (8.5)$$

where f_r and V_f are flexural strength (in MPa) and volume fraction of steel fiber (in %), respectively.

However, both the proposed equations, Eqs. 8.4 and 8.5, are only applicable to the OPSFRC with similar density. LWC from different lightweight aggregates produces diverse tensile strengths and densities. Hence, Eq. 8.6 is proposed to correlate the flexural strengths of LWC with different densities. The comparison of the proposed Eq. 8.6 with other studies on steel fiber-reinforced LWC is shown in Table 8.3. It is obvious that Eq. 6 is valid for correlating the flexural strength to the density and volume fraction of steel fiber within ± 12%. The equation is recommended for the steel fiber content selection in the design of fiber-reinforced LWC for targeted density and flexural strength.

$$f_r/\rho_{SSD} = 0.0025e^{0.387(Vf)} \quad (8.6)$$

where f_r/ρ_{SSD} and V_f are the flexural strength to density (SSD) ratio (in MPa) and volume fraction of steel fiber (in %), respectively.

Table 8.3 Comparison between the experimental and theoretical f_r/ρ_{SSD} ratios of different steel fiber-reinforced LWC

Concrete	Coarse Aggregate	V_f	Density (kg/m^3)	Flexural strength (MPa)	f_r/ρ_{SSD} (10^{-3} kNm/kg)		Error
					Experimental	Proposed (Eq. 8.6)	
OPSFRC	OPS	0	1960	4.84	2.47	2.50	-1.1%
		0.5	2020	5.52	2.73	3.03	-11.0%
		1	2090	8.29	3.97	3.68	7.2%
		1.5	2120	9.64	4.54	4.47	1.6%
		2	2220	10.95	4.93	5.42	-10.0%
		2.5	2350	16.00	6.82	6.58	3.4%
		3	2425	18.48	7.62	7.99	-4.8%
Shafigh, Mahmud, et al. (2011)	OPS	0.25	1945	6.35	3.26	2.75	15.6%*
		0.5	1965	6.26	3.19	3.03	4.8%
		0.75	2010	6.40	3.18	3.34	-5.0%
		1	2040	7.09	3.48	3.68	-5.9%
Balendran et al. (2002)	Sintered pulverized fuel ash	1	2030	7.90	3.89	3.68	5.4%
Gao et al. (1997)	Expanded clay	0.6	1880	6.59	3.51	3.15	10.0%
		1	1910	7.95	4.16	3.68	11.5%
		1.5	1930	9.75	5.05	4.47	11.5%
		2	1960	11.80	6.02	5.42	9.9%

* exception

8.3.4.2 Brittleness

The concrete brittleness is an indirect measurement of the post-tensile failure behavior of concrete. The brittleness is measured as the ratio of compressive to flexural strengths (Sun & Xu, 2009). Concrete is generally defined as a brittle material as the concrete fractures under tensile stress beyond the elastic limit. This result in complete and immediate loss of load carrying capacity once the ultimate tensile stress capacity is reached. A lower brittleness value indicates that the concrete is less brittle and that it could take up higher compressive and tensile loading. Moreover, LWC is more brittle than normal concrete (Domagała, 2011). The addition of steel fibers in concrete is the most effective and economical solution to the high brittleness of LWC.

The variation in brittleness of OPSFRC with the steel fiber content is reported in Figure 6. It is shown that the addition of steel fiber significantly reduced the brittleness of OPSC by 5-57% when the fiber content increased from 0.5% to 3.0%. Compared to the polypropylene fiber-reinforced concrete reported by Sun and Xu (2009), the reduction in the brittleness of OPSFRC reinforced with steel fiber was found to be much higher. In normal circumstances, an increase in the strength of concrete increases the brittleness of the concrete. However, the presence of steel fibers in the cement matrix enhanced the strength of OPSFRC, at the same time, resulted in reduced brittleness and higher ductility in OPSFRC specimens. This is attributed to the crack bridging effect of steel fibers, which provide a strain hardening toughening beyond the elastic limit that eventually improved the concrete's tensile loading capacity.

In addition, the brittleness of the OPSFRC-5 mix showed minor differences compared to the control OPSC. However, the brittleness of OPSFRC was significantly reduced when 1% or more of steel fibers was added, at which the brittleness was found to be only about 40-70% corresponding to the control OPSC mix. At a low volume fraction of steel fibers (<1%), the low amount of fibers was not sufficient to form a strong and uniformly distributed fiber-matrix network with sufficient fiber-matrix bond and crack bridging enhancement, as shown in Figure 6.8 Hence, we can conclude that a minimum amount of steel fibers (1% in the case of OPSC) is required for the LWC to achieve high tensile strength and low brittleness.

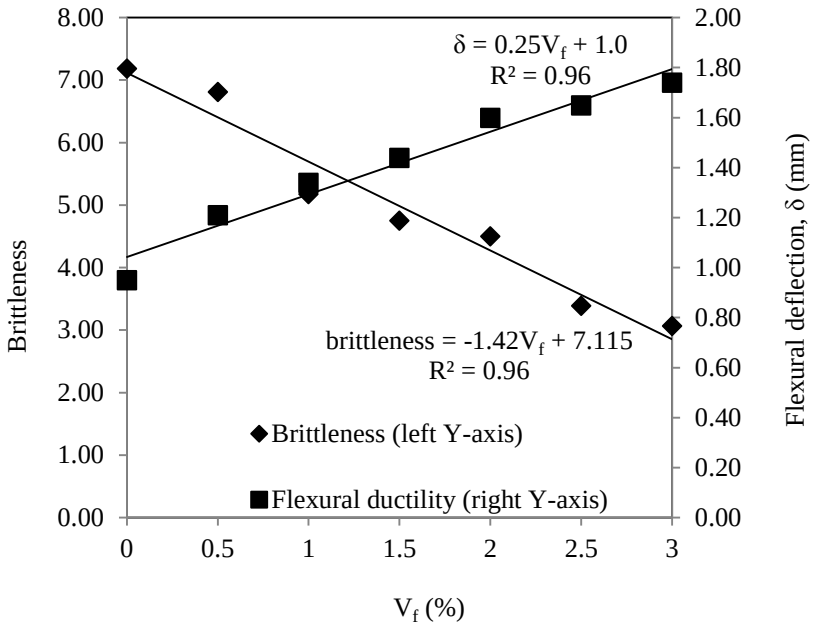

Figure 8.4 Variations in brittleness and flexural deflection of OPSFRC against volume fraction (V_f)

8.3.4.3 Flexural Ductility

The flexural ductility (or deflection) criterion of concrete is always neglected by researchers due to the complexity in the testing procedures to measure the deflection of concrete. However, the flexural deflection is one of the important serviceability limit state requirements to be considered in the design of reinforced concrete. In the case of structural members made from LWC, obvious tensile cracking might form at a lower loading capacity due to the low tensile strength of LWC. Hence, the determination of flexural ductility of LWC is important.

This section describes the ability of the steel fibers to improve the flexural ductility of OPSFRC. The flexural ductility is measured by the flexural deformation when the specimen achieves its ultimate flexural strength. In addition to the reduction in the brittleness observed in the OPSFRC, the flexural ductility of OPSFRC was also considerably increased, which is attributed to the addition of steel fibers into the OPSC

(Figure 8.4). The variation of flexural ductility against the volume fraction of steel fiber was straightforward, at which an increase in steel fibers resulted in higher flexural deformation of OPSFRC. The control OPSC mix produced a deformation of 0.95 mm when the ultimate flexural strength was reached. The highest flexural deformation of OPSFRC was recorded in the OPSFRC-30 mix in which the deformation improved by about 80% to 1.74 mm. Following the explanation concerning the beneficial effect of steel fibers on the tensile strength of OPSFRC, the strong fiber-matrix bond and crack bridging effect of steel fibers enabled the crack propagation to be blunted, eventually allowing the OPSFRC to sustain higher flexural loading and to further deform.

8.3.4.4 First Crack Flexural Toughness

Following the discussions in Sections 8.3.4.1 and 8.3.4.3 concerning the advantages of the steel fibers for enhancing both the flexural strength and ductility of OPSFRC, the addition of steel fibers also increased the energy capacity of OPSFRC under flexural loading (Figure 8.5). The flexural toughness (or first crack flexural toughness) is taken as the area below the load-deflection curve under flexure loading up to the ultimate flexural strength. The exponential relationship between V_f and the flexural toughness of OPSFRC (see Figure 8.5) is attributed to the linear increment of both the flexural strength (Figure 8.3) and flexural ductility (Figure 8.4). The improvement in the flexural toughness at low fiber content (<1%) was relatively low (about 50% and 150% for the OPSFRC-5 and OPSFRC-10 mixes, respectively). As the fiber content increased beyond 1%, the flexural toughness of the OPSFRC was enhanced by 2 to 6 folds compared to the control OPSC mix. Thus, it is evident that the addition of a high quantity of steel fibers (>1%) considerably enhanced the flexural toughness of OPSFRC. The highest flexural toughness of 53.6 Nm was recorded in the OPSFRC-30 mix, which

indicates that the addition of 3% steel fiber in the OPSFRC would enable the concrete to absorb a six times higher flexural loading compared to the brittle control concrete.

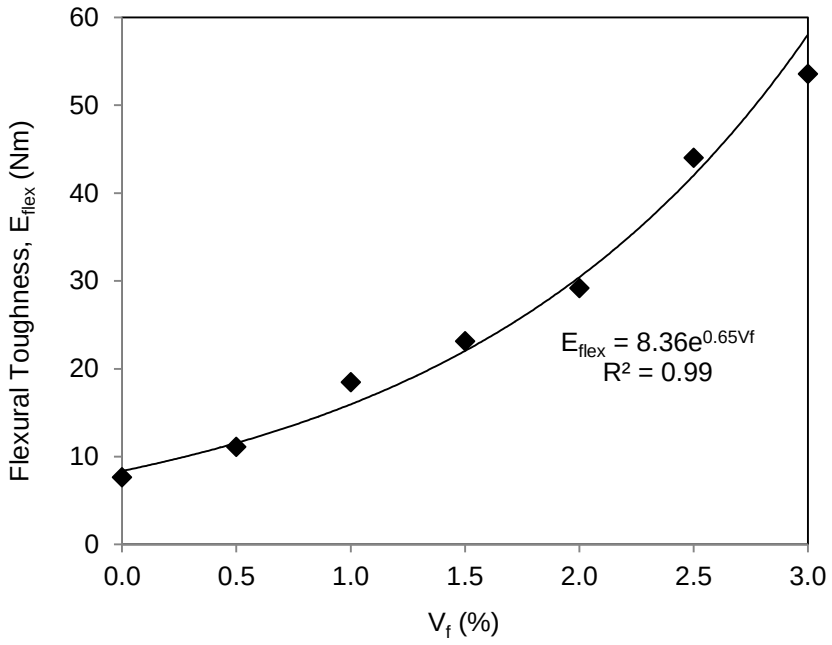

Figure 8.5 Effects of volume fraction (V_f) on the first crack flexural toughness (E_{flex}) of OPSFRC

Similar to the previous discussions, Eq. 8.7 is proposed to predict the flexural toughness of OPSFRC within an error of ±10%.

$$E_{flex} = 8.36e^{0.65Vf} \quad (8.7)$$

where E_{flex} and V_f are flexural toughness (in Nm) and volume fraction of steel fibers (in %), respectively.

8.3.5 Modulus of elasticity and Poisson's ratio

The addition of steel fibers in LWC produced either positive or negative effects on the MOE and Poisson's ratio of LWC depending on the type of lightweight aggregate and fiber content (Shafigh et al., 2011c). However, it should be noted that there is limited investigation on these aspects as far LWC is concerned.

Referring to Table 8.2, the addition of steel fibers in OPSFRC enhanced the MOE and Poisson's ratio by about 2-2.8 GPa (15-20%). However, both the MOE and Poisson's ratio were found to be independent of the volume fraction of steel fibers. The increment of MOE was close to the published results by Domagała (2011), which produced an 18% increment in the MOE of expanded clay concrete reinforced with 2% steel fibers. The organic OPS has a lower stiffness and restraining effect compared to conventional coarse aggregate. Hence, under compressive loading, the OPS undergoes higher strain compared to the NWC, and produces a lower MOE in OPSC (Alengaram et al., 2011). Following on from the discussions in Section 8.3.3, the addition of steel fibers enhanced the compressive strength of OPSFRC by the fiber-matrix bond and crack bridging effects. The enhanced fiber-matrix bond enabled the OPSFRC to withstand higher compressive strain, while the crack bridging effect prevented and arrested the crack propagation, eventually resulting in the increased compressive energy capacity of OPSFRC.

Similarly, the presence of steel fibers in the OPSFRC cement matrix arrested the crack propagation and the concrete was capable of enduring higher strain, in both the lateral and longitudinal directions. The benefit of steel fibers in enhancing the lateral strain was found to be more significant than the longitudinal strain. This is evident in the higher Poisson's ratio of OPSFRC, relative to the control OPSC (Table 8.2). The OPSC mix produced a Poisson's ratio of 0.255, and then the Poisson's ratios of OPSFRC were improved to about 0.29-0.32. Therefore, it can be concluded that the addition of steel fibers in OPSC enhanced both the MOE and Poisson's ratio. The observations and values on MOE and Poisson's ratio were comparable to previous chapters (Chapter 5 and 6).

8.3.6 Flexural behaviors of reinforced concrete beams

The results from Section 8.3.1 to 8.3.5 showed that the beneficial effect of steel fibers on the mechanical properties, brittleness, ductility and toughness is proportional to the increase in steel fiber volume. Due to difficulty in workability and compaction, the maximum volume for the steel fiber in OPSFRC was limited to 3%. In this section the flexural behavior of OPSFRC reinforced concrete beams with the maximum fiber volume of 3% is compared to OPSC and OPSFRC-F100 from Chapter 6.

Figure 8.6 shows the comparison between the effects of volume fraction of steel fibers on the mode of failure. It has been previously mentioned in Section 6.3.4.1 that the addition of fibers changed the mode of failure in OPSFRC beams. Figure 8.6(a) shows the OPSC beams failed under concrete crushing at the compressive zone, while OPSFRC beams in Figure 8.6(b) and 8.6(c) failed under bar fracture. The OPSFRC beam reinforced with 3% steel fiber as shown in Figure 8.6(c) produced almost identical mode of failure as that of OPSFRC with 1% steel fibers, albeit with smaller depth of flexural crack and concrete wedge. The smaller crack depth in OPSFRC-30 beams might be attributed to the strain localization effect as discussed in Section 6.3.4.5. The strain localization effect was more significant when the fiber content increases (Meda et al., 2012). The addition of high volume of steel fibers (3% by volume) resulted in earlier bar fracture in OPSFRC-30 beam (Figure 8.6(c)) compared to OPSFRC-F100 beam (Figure 8.6b) as the former failed under bar fracture before the full development of crack.

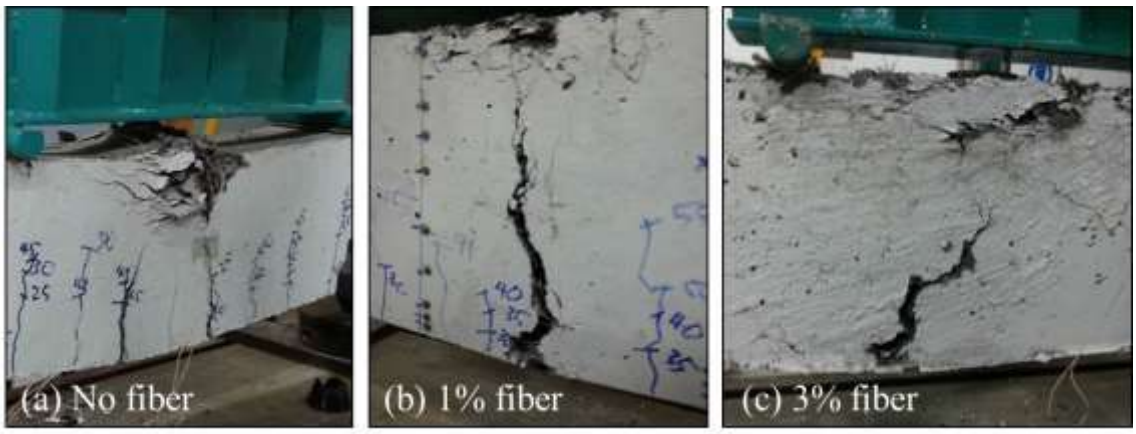

Figure 8.6 Comparison of mode of failure for OPSFRC beams with different fiber volume

In addition, Figure 8.7 shows the comparison of the moment-deflection curve of the OPSFRC-30 with OPSC and OPSFRC-F100 mixes from Section 6.3.4. The results from Figure 8.7 are summarized in Table 8.4.

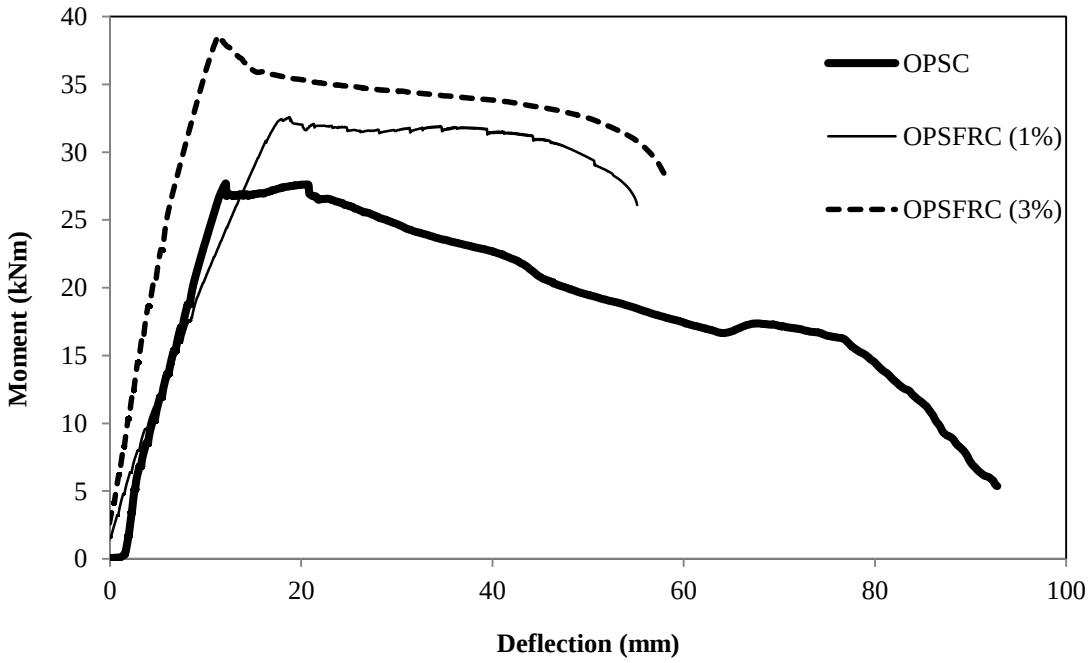

Figure 8.7 Moment-deflection curves of OPSC and OPSFRC

Table 8.4 Comparison of the flexural behavior of OPSC, OPSFRC with 1% and 3% steel fibers

Properties	OPSC	OPSFRC (1% steel fibers)	Ratio of OPSFRC (1% steel fiber) to OPSC	OPSFRC (3% steel fibers)	Ratio of OPSFRC (3% steel fiber) to OPSC
Ultimate moment (kNm)	27.7	32.6	1.18	38.6	1.39
Deflection at failure (mm)	92.8	55.1	0.59	51.4	0.55
Span to service deflection ratio	22.6	38.1	1.68	40.8	1.80
Ductility ratio, μ_{D2}	8.51	9.75	1.15	9.03	1.06
Ductility ratio, μ_{E2}	4.71	4.72	1.00	4.70	1.00

The moment-deflection curves of OSPFRC-30 shows distinct difference from the OPSC and OPSFRC-F100 beams. The incorporation of 3% steel fibers improved the moment capacity of OPSFRC by about 40% relative to the OPSC beam. The improvement was about double as that of OPSFRC with 1% steel fibers. The predicted ultimate moments of OSPFRC-30 using Eurocode, BS and ACI codes were 26.7, 23.9 and 25.1 kNm, respectively compared to the experimental ultimate moment of 38.6 kNm. .The codes underestimate the moment capacity by 45-61% as known. These codes do not have provision for the design of fiber reinforced concrete. The error in the predicted moment capacity of OPSFRC-30 was about two times higher than in the Table 6.3.

Section 6.3.4.3 states that the drawback of the fiber-reinforcement in OPSFRC beams is due to the reduction in the ductility measured in the forms of both deflection and ductility ratios. Based on the deflections at failure from Table 8.4, the OPSFRC-30

beam failed at a deflection of 51.4 mm and it was 55% as that of OPSC beam. However, the comparison between the OPSFRC beams with 1% and 3% showed marginal difference of about 4 mm. In addition, the difference between OPSFRC mixes differed by 1-5 mm only (Table 6.4), but the difference between the OPSFRC and OPSC beams were 25-35 mm.

Despite the reduced deflection at failure in the OPSFRC-30 beam relative to the OPSC beam, the span to service deflection of OPSFRC-30 beam was far below the limit of 250 and 150 as stated in Eurocode and ASTM C1609, respectively. Hence the OPSFRC-30 beam satisfied the deflection criteria of serviceability limit state as stipulated in Eurocode 2. Furthermore, Section 6.3.4.3 also showed that ductility ratios, μ_{D2} and μ_{E2} are suitable to represent the effect of fibers on the ductility of OPSFRC beams. Results from Table 8.4 also showed that both the ductility ratios of OPSFRC with 1% and 3% are almost identical. The addition of fibers resulted in drastic drop in the deflection and ductility when the beam failed, but the effect of increasing volume fraction on the above said characteristics is less significant. This phenomenon could be called as “ceiling effect” as described by other researcher (Gao et al., 1997). Based on Figure 6.8, in which the confinement effect of steel fibers resulted in reduced deflection attributed to the localized strain. However, when high volume of fibers is used, there are chances for the overlapping of the effective zone of the confinement effect which results in marginal improvement with further increment of fiber content. Therefore the incorporation of 3% steel fibers in OPSFRC showed similar ductility compared to OPSFRC with 1% steel fibers.

Section 6.3.4.4 reported that the addition of steel fibers up to 1% significantly enhanced the crack resistance of OPSFRC beams compared to the OPSC beam. Figure

8.8 shows the comparison of the crack patterns of OPSC, OPSFRC with 1% and 3% steel fibers. The OPSFRC-30 beam (Figure 8.8(c)) showed excellent crack arresting ability by exhibiting smaller number of flexural cracks and the depth and width of the cracks are notably reduced compared to the OPSC and OPSFRC-F100 beams. In addition, the crack width of the primary crack at service load in OPSFRC-30 beam was 0.904 mm and it was 40% lower than the OPSC beam. The value is only one-third of the maximum crack width limit stated in BS 8110 and hence it can be concluded that the OPSFRC with steel fiber up to 3% fulfilled the requirement for the serviceability limit state for cracking control. Furthermore, the crack spacing for OPSFRC-30 beam was reduced to 105 mm; while the crack spacing of the OPSC and OPSFRC-100 beams were 165 and 115 mm, respectively. Finally, the first and secondary cracks were initiated at 55 and 85 kN, respectively. These values were 40% higher than the OPSFRC with 1% fibers. In summary, the excellent crack resistance of OPSFRC beam with 3% steel fiber outperformed the OPSC and OPSFRC-100 beams with significant reduced crack spacing, crack width and depth and improved crack load capacity.

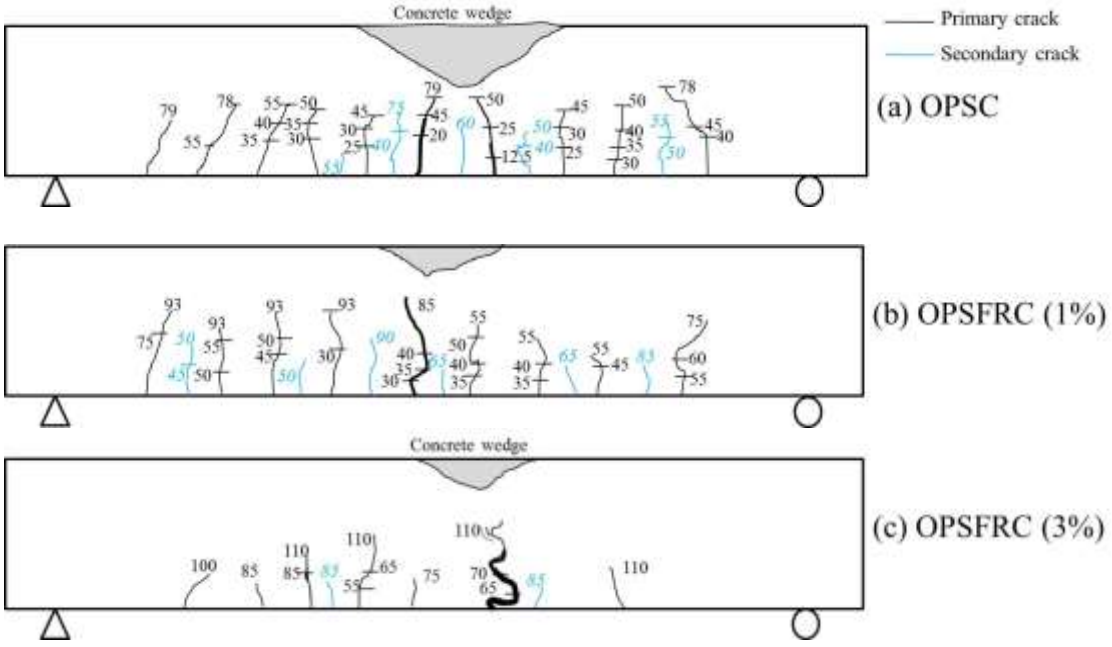

Figure 8.8 Crack patterns of OPSC and OPSFRC at ultimate moment

8.4 Chapter conclusions

The In general, the addition of steel fibers in OPSC enhances the mechanical properties. This is the maiden attempt concerning the addition of a high volume of steel fibers in OPSC, and, hence, the findings are quite significant. Based on the parameters investigated, the following conclusions can be drawn:

- The increase in the fiber content in the OPSFRC mixes reduces the slump value and results in poor compaction in the fresh OPSFRC. Hence for mixes with steel fibers >1%, additional tampering is required.
- The addition of steel fibers with high specific gravity increases the density of OPSFRC. The oven-dry density of OPSC was reported at 1850 kg/m^3, which enables the OPSC to be classified as LWC. However, the OPSFRC containing >1% steel fibers did not fulfill the oven-dry density limit of 2000 kg/m^3 for LWC, as stipulated in EN206-1.
- The highest compressive strength of 57 MPa was reported for the OPSFRC-30 mix reinforced with 3% steel fibers, which is 63% higher than for the control OPSC mix. The improvement in the compressive strength of OPSFRC is attributed to the strong fiber-matrix bond and crack bridging effect.
- In addition to the enhancement of the compressive strength, the steel fibers improved the tensile strength of OPSFRC. The OPSFRC-30 mix with 3% of steel fibers produced a splitting tensile and flexural strength of 11.0 and 18.5 MPa, respectively. The corresponding enhancements were found to be as high as 240% and 285%, respectively, compared to the control mix. Hence, by combining the advantages of lightweight and high tensile strength, OPSFRC shows high potential for high load-bearing structural members.

- Based on the experimental results, different equations have been proposed for different concrete properties, such as hardened density, compressive strength, splitting tensile strength, flexural strength and toughness. The equations proposed are not limited to the LWC made from OPS only, as it has also been shown that the equations are applicable for other lightweight aggregate including pulverized fuel ash and expanded clay within an error of ±12%.
- The incorporation of steel fibers in OPSFRC mixes clearly converts OPSFRC from a brittle to a highly ductile material, by reducing brittleness and improving the flexural ductility and toughness.
- OPSFRC produces a higher modulus of elasticity and Poisson's ratio than the OPSC. However, the modulus of elasticity and Poisson's ratio of OPSFRC is independent of the steel fiber volume.
- The 3% steel fiber reinforcement significantly improved moment capacity and crack resistance of OPSFRC beams, while the ductility of OPSFRC beam with 1% and 3% steel fibers was comparable to each other.
- The OPSFRC with 1% steel fibers was recommended for structural members while OPSFRC with 3% steel fibers was suitable for special structural which requires high tensile strength.

CHAPTER 9

SUMMARY OF CONCLUSIONS AND RECOMMENDATIONS

9.1 Conclusions

Detailed conclusions were given at the end of Chapters 3 to 8. The following conclusions were summarized from them in a general way:

1. The addition of fibers OPSC reduced the workability of OPSFRC, but the fresh OPSFRC concrete achieved good compaction and finishing.
2. Synthetic fibers including polypropylene (PP) and nylon produced marginal effect on the density of OPSFRC. Meanwhile, the oven-dry density of OPSFRC with steel fibers up to 1% by concrete volume was found below the density limit of 2000 kg/m^3 stated in EN 206-1.
3. Both PP and nylon fibers produced slight increment on the mechanical properties of OPSFRC, including compressive strength, tensile strength, modulus of elasticity and Poisson's ratio.
4. The crack bridging effect of steel fibers was more effective in improving the mechanical properties of OPSFRC compared to PP and nylon fibers. The highest compressive and flexural strengths of 47 MPa and 7 MPa, respectively, were reported in OPSFRC mixes with 1% steel fibers.
5. Flexural testing on steel fiber-reinforced OPSFRC beams reported that the steel fibers enhanced the moment capacity and crack resistance of OPSFRC beam, but resulted in decreased ductility due to confinement effect of steel fibers. Both the OPSC and OPSFRC beams fulfilled the requirements for serviceability limit state on crack control and deflection, therefore it can be concluded that the OPSFRC with steel fibers up to 1% is recommended for structural applications.

6. OPSFRC beams reinforced with steel fibers exhibited improved torsional behaviors compared to the OPSC beam, including torque capacity, torsional ductility and crack resistance.
7. When the steel fibers content is further increased to 3%, high strength OPSFRC with compressive and flexural strengths of 55 MPa and 18.5 MPa, respectively was produced. The flexural beam testing reported that the load capacity and crack resistance of OPSFRC beam with 3% steel fibers outperformed the OPSFRC with 1% steel fibers. The deflections of both concrete beams were comparable. The use of OPSFRC with high volume steel fibers is recommended for special structures such as impact and blast resistant members.

9.2 Recommendations

Due to the limitations on the methodology, there are a few concerns and questions arose along with the experimental works in this thesis. The following recommendations are suggested for future works:

1. Durability aspect of OPSFRC- researches had shown that the use of fibers improved the durability of concrete. It has been mentioned that the durability of OPSC is questionable attributed to the organic characteristics of OPS. Hence a complete study on the durability of OPSFRC is essential to the structural applicability of OPSC and OPSFRC.
2. Microstructural studies on OPSFRC- the discussions in this study stated that the enhancement effect of fibers on the mechanical properties and structural behaviors of OPSFRC were contributed by the crack bridging effect. A quantitative study on the pullout energy on the fibers supplemented by the numerical analysis model could be useful to explain the enhanced properties of OPSFRC. However, despite the large number studies conducted on the

quantification of fibers, the challenge remains due to the randomly distributed fibers in the cement matrix. There is no absolute model available to predict the fiber dispersion.

3. Further strength development of OPSFRC- previous literature suggested different approaches to enhance the strength of OPSC, including the usage of crushed OPS and cementitious materials. Hence future works can be suggested to further improve the strength of OPSFRC with these approaches.
4. Alternative waste materials and fibers- the OPSFRC in the present study consists of about 20% waste materials by mass. There are numerous waste materials available for cement, sand and fiber replacements. The waste portion of the OPSFRC can be further increased with additional replacement by other waste materials.
5. Additional testing on structural behaviors- this present study only covers the flexural and torsional behaviors of OPSFRC. In future, other structural behaviors, such as shear strength, fire resistance, thermal and sound insulation. For the high strength OPSFRC, the additional testing such as impact, blast and fatigue tests were suggested.
6. Further evaluation of current work- additional testing parameters on the flexural and torsion testing on OPSFRC beams are suggested. The parameters are beam cross section, reinforcement ratio both steel and fibers. The synergic effects of all three parameters are complex and it is essential for the formation of an empirical solution for the prediction of the load capacity and ductility, in order to comply with standards.

REFERENCES

Abdullah, A. A. A. (1984). *Basic Strength Properties of Lightweight Concrete Using Agricultural Wastes as Aggregates.* Paper presented at the Proceedings of International Conference on Low-cost Housing for Developing Countries, Roorkee, India.

Abu-Lebdeh, T., Hamoush, S., Heard, W., & Zornig, B. (2011). Effect of matrix strength on pullout behavior of steel fiber reinforced very-high strength concrete composites. *Construction and Building Materials, 25*(1), 39-46.

Alengaram, U. J., Al Muhit, B. A., Jumaat, M. Z., & Liu , M. Y. J. (2013). A comparison of the thermal conductivity of oil palm shell foamed concrete with conventional materials. *Materials & Design, 51*, 522-529.

Alengaram, U. J., Jumaat, M. Z., & Mahmud, H. (2008). Ductility behaviour of reinforced palm kernel shell concrete beams. *European Journal of Scientific Research, 23*(3), 406-420.

Alengaram, U. J., Jumaat, M. Z., Mahmud, H., & Fayyadh, M. M. (2011). Shear behaviour of reinforced palm kernel shell concrete beams. *Construction and Building Materials, 25*(6), 2918-2927.

Alengaram, U. J., Mahmud, H., & Jumaat, M. Z. (2008). Influence of Sand/Cement Ratio on Mechanical Properties of Palm Kernel Shell Concrete. *Journal of Applied Sciences, 9*, 1764-1769.

Alengaram, U. J., Mahmud, H., & Jumaat, M. Z. (2010a). Comparison of mechanical and bond properties of oil palm kernel shell with normal weight concrete. *International Journal of the Physical Sciences, 5*(8), 1231-1239.

Alengaram, U. J., Mahmud, H., Jumaat, M. Z., & Shirazi, S. M. (2010b). Effect of aggregate size and proportion on strength properties of palm kernel shell concrete. *International Journal of the Physical Sciences, 5*(12), 1848-1856.

Alengaram, U. J., Mahmud, H., & Jumaat, M. Z. (2011). Enhancement and prediction of modulus of elasticity of palm kernel shell concrete. *Materials & Design, 32*(4), 2143-2148.

Alengaram, U. J., Muhit, B. A. A., & Jumaat, M. Z. (2013). Utilization of oil palm kernel shell as lightweight aggregate in concrete – A review. *Construction and Building Materials, 38*, 161-172.

Alhozaimy, A. M., Soroushian, P., & Mirza, F. (1996). Mechanical properties of polypropylene fiber reinforced concrete and the effects of pozzolanic materials. *Cement & Concrete Composites, 18*(2), 85-92.

Ali, M., & Chouw, N. (2013). Experimental investigations on coconut-fibre rope tensile strength and pullout from coconut fibre reinforced concrete. *Construction and Building Materials, 41*, 681-690.

Alsayed, S. H., & Alhozaimy, A. M. (1999). Ductility of Concrete Beams Reinforced with FRP Bars and Steel Fibers. *Journal of Composite Materials, 33*(19), 1792-1806.

Altun, F., & Aktaş, B. (2013). Investigation of reinforced concrete beams behavior of steel fiber added lightweight concrete. *Construction and Building Materials, 38*, 575-581.

Altun, F., Haktanir, T., & Ari, K. (2007). Effects of steel fiber addition on mechanical properties of concrete and RC beams. *Construction and Building Materials, 21*(3), 654-661.

Anwar Hossain, K. M. (2004). Properties of volcanic pumice based cement and lightweight concrete. *Cement and Concrete Research, 34*(2), 283-291.

Arisoy, B., & Wu, H.-C. (2008). Material characteristics of high performance lightweight concrete reinforced with PVA. *Construction and Building Materials, 22*(4), 635-645.

Ashour, S. A. (2000). Effect of compressive strength and tensile reinforcement ratio on flexural behavior of high-strength concrete beams. *Engineering Structures, 22*(5), 413-423.

ASTM C29/C29M Standard Test Method for Bulk Density and Voids in Aggregate. (2009): American Society for Testing and Materials (ASTM).

ASTM C78/ C78M Standard Test Method for Flexural Strength of Concrete (Using Simple Beam with Third-Point Loading). (2010): American Society for Testing and Materials (ASTM).

ASTM C127 Standard Test Method for Density, Relative Density (Specific Gravity) and Absorption of Coarse Aggregate. (2012): American Society for Testing and Materials (ASTM).

ASTM C131 Standard Test Method for Resistance to Degradation of Small-size Coarse Aggregate by Abrasion and Impact in the Los Angeles Machine. (2003): American Society for Testing and Materials (ASTM).

ASTM C136 Standard Test Method for Sieve Analysis of Fine and Coarse Aggregates. (2001): American Society for Testing and Materials (ASTM).

ASTM C143/ C142M Standard Test Method for Slump of Hydraulic-Cement Concrete. (2012): American Society for Testing and Materials (ASTM).

ASTM C330/C330M Standard Specification for Lightweight Aggregates for Structural Concrete. (2002): American Society for Testing and Materials (ASTM).

ASTM C469 Standard Test Method for Static Modulus of Elasticity and Poisson's Ratio of Concrete in Compression. (2010): American Society for Testing and Materials (ASTM).

ASTM C496/ C496M Standard Test Method for Splitting Tensile Strength of Cylindrical Concrete Specimens. (2011): American Society for Testing and Materials (ASTM).

ASTM C597 Standard Test Method for Pulse Velocity Through Concrete. (2009): American Society for Testing and Materials (ASTM).

ASTM C1018 Standard Test Method for Flexural Toughness and First-Crack Strength of Fiber-Reinforced Concrete (Using Beam With Third-Point Loading) (1997): American Society for Testing and Materials (ASTM).

Atiş, C. D., & Karahan, O. (2009). Properties of steel fiber reinforced fly ash concrete. *Construction and Building Materials, 23*(1), 392-399.

Balendran, R. V., Zhou, F. P., Nadeem, A., & Leung, A. Y. T. (2002). Influence of steel fibres on strength and ductility of normal and lightweight high strength concrete. *Building and Environment, 37*(12), 1361-1367.

Banthia, N., & Gupta, R. (2006). Influence of polypropylene fiber geometry on plastic shrinkage cracking in concrete. *Cement and Concrete Research, 36*(7), 1263-1267.

Banthia, N., & Nandakumar, N. (2003). Crack growth resistance of hybrid fiber reinforced cement composites. *Cement & Concrete Composites, 25*(1), 3-9.

Basri, H. B., Mannan, M. A., & Zain, M. F. M. (1999). Concrete using waste oil palm shells as aggregate. *Cement and Concrete Research, 29*, 619-622.

Bencardino, F., Rizzuti, L., Spadea, G., & Swamy, R. (2008). Stress-Strain Behavior of Steel Fiber-Reinforced Concrete in Compression. *Journal of Materials in Civil Engineering, 20*(3), 255-263.

Bennett, J. A., & Young, R. J. (1998). The effect of fibre-matrix adhesion upon crack bridging in fibre reinforced composites. *Composites Part a-Applied Science and Manufacturing, 29*(9-10), 1071-1081.

Bentur, A., & Mindess, S. (2007). *Fibre Reinforced Cementitious Composites* (2nd Ed. ed.). New York: Taylor & Francis.

Bernardo, L. F. A., Andrade, J. M. A., & Pereira-De-Oliveira, L. A. (2013). Reinforced and prestressed concrete hollow beams under torsion. *Journal of Civil Engineering and Management, 19*(sup1), S141-S152.

Bernardo, L. F. A., & Lopes, S. M. R. (2011). Theoretical behavior of HSC sections under torsion. *Engineering Structures, 33*(12), 3702-3714.

Bernardo, L. F. A., & Lopes, S. M. R. (2013). Plastic analysis and twist capacity of high-strength concrete hollow beams under pure torsion. *Engineering Structures, 49*, 190-201.

Bilodeau, A., Kodur, V. K. R., & Hoff, G. C. (2004). Optimization of the type and amount of polypropylene fibres for preventing the spalling of lightweight concrete subjected to hydrocarbon fire. *Cement and Concrete Composites, 26*(2), 163-174.

Bischoff, P. H. (2007). Rational model for calculating deflection of reinforced concrete beams and slabs. *Canadian Journal of Civil Engineering, 34*, 992-1004.

Bolat, H., Şimşek, O., Çullu, M., Durmuş, G., & Can, Ö. (2014). The effects of macro synthetic fiber reinforcement use on physical and mechanical properties of concrete. *Composites Part B: Engineering, 61*, 191-198.

BS 812 Part 105.1 Testing Aggregate- Methods for determination of particle shape. (1989): BSI.

BS 812 Part 105.2 Testing Aggregate- Elongation index of coarse aggregate. (1990): BSI.

BS 812 Part 112: Testing Aggregates- Methods for determination of aggregate impact value (AIV). (1990): BSI.

BS EN 206:2013 Concrete: Specification, performance, production and conformity. (2013): BSI.

BS EN 12390: Part 3 Testing hardened concrete- Compressive strength of test specimens. (2000): BSI.

Cachim, P. B., Figueiras, J. A., & Pereira, P. A. A. (2002). Fatigue behavior of fiber-reinforced concrete in compression. *Cement & Concrete Composites, 24*(2), 211-217.

Campione, G., Miraglia, N., & Papia, M. (2001). Mechanical properties of steel fibre reinforced lightweight concrete with pumice stone or expanded clay aggregates. *Materials and Structures, 34*(4), 201-210.

Çavdar, A. (2012). A study on the effects of high temperature on mechanical properties of fiber reinforced cementitious composites. *Composites Part B: Engineering, 43*(5), 2452-2463.

Chandra, S. (1996). *Waste Materials Used in Concrete Manufacturing*: Noyes Publications.

Chen, B., & Liu, J. (2005). Contribution of hybrid fibers on the properties of the high-strength lightweight concrete having good workability. *Cement and Concrete Research, 35*(5), 913-917.

Chiu, H.-J., Fang, I. K., Young, W.-T., & Shiau, J.-K. (2007). Behavior of reinforced concrete beams with minimum torsional reinforcement. *Engineering Structures, 29*(9), 2193-2205.

Chunxiang, Q., & Patnaikuni, I. (1999). Properties of high-strength steel fiber-reinforced concrete beams in bending. *Cement and Concrete Composites, 21*(1), 73-81.

Clarke, J. L. (1993). *Structural Lightweight Aggregate Concrete*: Blackie Academic & Professional.

Comiloli, L., Failla, C., & Plizzari, G. A. (2007). *Steel and synthetic fibres for enhancing concrete toughness and shrinkage behaviour.* Paper presented at the International conference: sustainable construction materials and technologies, Conventry, UK.

Corinaldesi, V., & Moriconi, G. (2011). Characterization of self-compacting concretes prepared with different fibers and mineral additions. *Cement and Concrete Composites, 33*(5), 596-601.

Dawood, E. T., & Ramli, M. (2012). Mechanical properties of high strength flowing concrete with hybrid fibers. *Construction and Building Materials, 28*(1), 193-200.

Deeb, R., Ghanbari, A., & Karihaloo, B. L. (2012). Development of self-compacting high and ultra high performance concretes with and without steel fibres. *Cement and Concrete Composites, 34*(2), 185-190.

Deng, Z. (2005). The fracture and fatigue performance in flexure of carbon fiber reinforced concrete. *Cement and Concrete Composites, 27*(1), 131-140.

Domagała, L. (2011). Modification of properties of structural lightweight concrete with steel fibres. *Journal of Civil Engineering and Management, 17*(1), 36-44.

du béton, F. (2000). *Bond of Reinforcement in Concrete: State-of-the-art report*: International Federation for Structural Concrete.

Düzgün, O. A., Gül, R., & Aydin, A. C. (2005). Effect of steel fibers on the mechanical properties of natural lightweight aggregate concrete. *Materials Letters, 59*(27), 3357-3363.

Erdem, S., Dawson, A. R., & Thom, N. H. (2011). Microstructure-linked strength properties and impact response of conventional and recycled concrete reinforced with steel and synthetic macro fibres. *Construction and Building Materials, 25*(10), 4025-4036.

Eren, O., & Celik, T. (1997). Effect of silica fume and steel fibers on some properties of high-strength concrete. *Construction and Building Materials, 11*(7-8), 373-382. doi:

Fike, R., & Kodur, V. (2011). Enhancing the fire resistance of composite floor assemblies through the use of steel fiber reinforced concrete. *Engineering Structures, 33*(10), 2870-2878.

Foo, K. Y., & Hameed, B. H. (2009). Value-added utilization of oil palm ash: a superior recycling of the industrial agricultural waste. *J Hazard Mater, 172*(2-3), 523-531.

Gao, J., Sun, W., & Morino, K. (1997). Mechanical properties of steel fiber-reinforced, high-strength, lightweight concrete. *Cement & Concrete Composites, 19*, 307-313.

Gencel, O., Brostow, W., Datashvili, T., & Thedford, M. (2011). Workability and Mechanical Performance of Steel Fiber-Reinforced Self-Compacting Concrete with Fly Ash. *Composite Interfaces, 18*(2), 169-184.

Gesoğlu, M., Güneyisi, E., Alzeebaree, R., & Mermerdaş, K. (2013). Effect of silica fume and steel fiber on the mechanical properties of the concretes produced with cold bonded fly ash aggregates. *Construction and Building Materials, 40*, 982-990.

Ghavami, K. (1995). Ultimate load behaviour of bamboo-reinforced lightweight concrete beams. *Cement and Concrete Composites, 17*(4), 281-288.

Giner, V. T., Baeza, F. J., Ivorra, S., Zornoza, E., & Galao, Ó. (2012). Effect of steel and carbon fiber additions on the dynamic properties of concrete containing silica fume. *Materials & Design, 34*, 332-339.

Gribniak, V., Kaklauskas, G., Hung Kwan, A. K., Bacinskas, D., & Ulbinas, D. (2012). Deriving stress–strain relationships for steel fibre concrete in tension from tests of beams with ordinary reinforcement. *Engineering Structures, 42*, 387-395.

Habel, K., & Gauvreau, P. (2008). Response of ultra-high performance fiber reinforced concrete (UHPFRC) to impact and static loading. *Cement and Concrete Composites, 30*(10), 938-946.

Hamoush, S., Abu-Lebdeh, T., & Cummins, T. (2010). Deflection behavior of concrete beams reinforced with PVA micro-fibers. *Construction and Building Materials, 24*(11), 2285-2293.

Han, C.-G., Hwang, Y.-S., Yang, S.-H., & Gowripalan, N. (2005). Performance of spalling resistance of high performance concrete with polypropylene fiber contents and lateral confinement. *Cement and Concrete Research, 35*(9), 1747-1753.

Haque, M. N., Al−Khaiat, H., & Kayali, O. (2007). Long-term strength and durability parameters of lightweight concrete in hot regime: importance of initial curing. *Building and Environment, 42*(8), 3086-3092.

Harold, F. G. J., John, R. W. J., & Eldridge, M. M. I. (2005). *Extrusion: the definitive processing guide and handbook*. New York: William Andrew Inc.

Hassanpour, M., Shafigh, P., & Mahmud, H. B. (2012). Lightweight aggregate concrete fiber reinforcement – A review. *Construction and Building Materials, 37*, 452-461.

Holgate, S. T., Koren, H. S., Samet, J. M., & Maynard, R. L. (1999). *Air Pollution and Health*: Elsevier Science.

Hsu, T. T. C. (1968). Torsion of Structural Concrete-Behavior of Reinforced Concrete Rectangular Members. *ACI Special Publication, 18*, 261-306.

Hwang, C. L., Bui Le, A. T. & Chen, C. T. (2011). Effect of rice husk ash on the strength and durability characteristics of concrete. *Construction and Building Materials, 25*(9), 3768-3772.

Ibrahim, I. S., & Che Bakar, M. B. (2011). Effects on Mechanical Properties of Industrialised Steel Fibres Addition to Normal Weight Concrete. *Procedia Engineering, 14*, 2616-2626.

Islam, A., Alengaram, U. J., Jumaat, M. Z., & Bashar, I. I. (2014). The development of compressive strength of ground granulated blast furnace slag-palm oil fuel ash-fly ash based geopolymer mortar. *Materials & Design, 56*, 833-841.

Islam, S. M., Hussain, R. R., & Morshed, M. A. Z. (2012). Fiber-reinforced concrete incorporating locally available natural fibers in normal- and high-strength concrete and a performance analysis with steel fiber-reinforced composite concrete. *Journal of Composite Materials, 46*(1), 111-122.

Jaeger, G. L., Tadros, G., & Mufti, A. A. (1997). *The concept of the overall performance factor in rectangular-section reinforced concrete beams.* Paper presented at the Proceeding of 3rd International Symposium on Non-metallic (FRP) reinforcement for concrete structures, Sapporo, Japan.

Jumaat, M. Z., Johnson Alengaram, U., & Mahmud, H. (2009). Shear strength of oil palm shell foamed concrete beams. *Materials & Design, 30*(6), 2227-2236.

Kakooei, S., Akil, H. M., Jamshidi, M., & Rouhi, J. (2012). The effects of polypropylene fibers on the properties of reinforced concrete structures. *Construction and Building Materials, 27*(1), 73-77.

Kamal, M. M., Safan, M. A., Etman, Z. A., & Salama, R. A. (2014). Behavior and strength of beams cast with ultra high strength concrete containing different types of fibers. *HBRC Journal, 10*(1), 55-63.

Kayali, O., Haque, M. N., & Zhu, B. (1999). Drying shrinkage of fibre-reinforced lightweight aggregate concrete containing fly ash. *Cement and Concrete Research, 29*(11), 1835-1840.

Kayali, O., Haque, M. N., & Zhu, B. (2003). Some characteristics of high strength fiber reinforced lightweight aggregate concrete. *Cement and Concrete Composites, 25*(2), 207-213.

Khaloo, A. R., & Afshari, M. (2005). Flexural behaviour of small steel fibre reinforced concrete slabs. *Cement and Concrete Composites, 27*(1), 141-149.

Khaloo, A. R., & Sharifian, M. (2005). Experimental investigation of low to high-strength steel fiber reinforced lightweight concrete under pure torsion. *Asian Journal of Civil Engineering (Building and Housing), 6*(6), 533-547.

Khaw, K. R. (2014). *Investigation on Torsion Capacity of Normal Weight Concrete (NWC) and Lightweight Aggregate Concrete (LWAC) with Fibres.* Bachelor Degree of Engineering, University of Malaya.

Kim, D. J., Park, S. H., Ryu, G. S., & Koh, K. T. (2011). Comparative flexural behavior of Hybrid Ultra High Performance Fiber Reinforced Concrete with different macro fibers. *Construction and Building Materials, 25*(11), 4144-4155.

Kim, H. S., & Shin, Y. S. (2011). Flexural behavior of reinforced concrete (RC) beams retrofitted with hybrid fiber reinforced polymers (FRPs) under sustaining loads. *Composite Structures, 93*(2), 802-811.

Kim, Y.-J., Hu, J., Lee, S.-J., & You, B.-H. (2010). Mechanical Properties of Fiber Reinforced Lightweight Concrete Containing Surfactant. *Advances in Civil Engineering, 2010*, 1-8.

Kupaei, R. H., Alengaram, U. J., Jumaat, M. Z. B., & Nikraz, H. (2013). Mix design for fly ash based oil palm shell geopolymer lightweight concrete. *Construction and Building Materials, 43*, 490-496.

Kwan, W. H., Ramli, M., Kam, K. J., & Sulieman, M. Z. (2011). Influence of the amount of recycled coarse aggregate in concrete design and durability properties. *Construction and Building Materials*.

Leslie, J. R., & Cheeseman, W. J. (1949). An ultrasonic method of studying deterioration and cracking in concrete structures. *ACI J Proc, 46*(1), 17.

Libre, N. A., Shekarchi, M., Mahoutian, M., & Soroushian, P. (2011). Mechanical properties of hybrid fiber reinforced lightweight aggregate concrete made with natural pumice. *Construction and Building Materials, 25*(5), 2458-2464.

Liu, M. Y. J., Alengaram, U. J., Jumaat, M. Z., & Mo, K. H. (2014). Evaluation of thermal conductivity, mechanical and transport properties of lightweight aggregate foamed geopolymer concrete. *Energy and Buildings, 72*, 238-245.

Mahmud, G. H., Yang, Z., & Hassan, A. M. T. (2013). Experimental and numerical studies of size effects of Ultra High Performance Steel Fibre Reinforced Concrete (UHPFRC) beams. *Construction and Building Materials, 48*, 1027-1034.

Mannan, M. A., Alexander, J., Ganapathy, C., & Teo, D. C. L. (2006). Quality improvement of oil palm shell (OPS) as coarse aggregate in lightweight concrete. *Building and Environment, 41*(9), 1239-1242.

Mannan, M. A., & Ganapathy, C. (2001a). Long-term strengths of concrete with oil palm shell as coarse aggregate. *Cement and Concrete Research, 31*(9), 1319-1321.

Mannan, M. A., & Ganapathy, C. (2001b). Mix design for oil palm shell concrete. *Cement and Concrete Research, 31*(9), 1323-1325.

Mannan, M. A., & Ganapathy, C. (2002). Engineering properties of concrete with oil palm shell as coarse aggregate. *Construction and Building Materials, 16*(1), 29-34.

Mannan, M. A., Basri, H. B., Zain, M. F. M., & Islam, M. N. (2002). Effect of curing conditions on the properties of OPS-concrete. *Building and Environment, 37*(11), 1167-1171.

Mannan, M. A., & Ganapathy, C. (2004). Concrete from an agricultural waste-oil palm shell (OPS). *Building and Environment, 39*(4), 441-448.

Mazaheripour, H., Ghanbarpour, S., Mirmoradi, S. H., & Hosseinpour, I. (2011). The effect of polypropylene fibers on the properties of fresh and hardened lightweight self-compacting concrete. *Construction and Building Materials, 25*(1), 351-358.

Meda, A., Minelli, F., & Plizzari, G. A. (2012). Flexural behaviour of RC beams in fibre reinforced concrete. *Composites Part B: Engineering, 43*(8), 2930-2937.

Mehta, P. K., & Menteiro, P. J. M. (2006). *Concrete: microstructure, properties and materials* (3rd Ed. ed.). New York: McGraw Hill.

Mirza, F. A., & Soroushian, P. (2002). Effects of alkali-resistant glass fiber reinforcement on crack and temperature resistance of lightweight concrete. *Cement and Concrete Composites, 24*(2), 223-227. .

Mo, K. H., Yap, S. P., Alengaram, U. J., Jumaat, M. Z., & Bu, C. H. (2014a). Impact resistance of hybrid fibre-reinforced oil palm shell concrete. *Construction and Building Materials, 50*, 499-507.

Mo, K. H., Alengaram, U. J., & Jumaat, M. Z. (2014b). Utilization of ground granulated blast furnace slag as partial cement replacement in lightweight oil palm shell concrete. *Materials and Structures, 48*(8), 2545-2556.

Mo, K. H., Yap, K. K. Q., Alengaram, U. J., & Jumaat, M. Z. (2014b). The effect of steel fibres on the enhancement of flexural and compressive toughness and fracture characteristics of oil palm shell concrete. *Construction and Building Materials, 55*, 20-28

Mosley, W. H., Bungey, J. H., & Hulse, R. (2012). *Reinforced Concrete Design: To Eurocode 2*: Palgrave Macmillan.

Nataraja, M. C., Dhang, N., & Gupta, A. P. (2000). Toughness characterization of steel fiber-reinforced concrete by JSCE approach. *Cement and Concrete Research, 30*(4), 593-597.

Nataraja, M. C., Nagaraj, T. S., & Basavaraja, S. B. (2005). Reproportioning of steel fibre reinforced concrete mixes and their impact resistance. *Cement and Concrete Research, 35*(12), 2350-2359.

Neville, A. M. (2012). *Properties of Concrete*: Pearson Education.

Newman, J., & Owens, P. (2003). *Properties of lightweight concrete*. Oxford: Butterworth-Heinemann.

Ng, T. S., Foster, S. J., Htet, M. L., & Htut, T. N. S. (2013). Mixed mode fracture behaviour of steel fibre reinforced concrete. *Materials and Structures, 47*(1-2), 67-76.

Nili, M., & Afroughsabet, V. (2010). Combined effect of silica fume and steel fibers on the impact resistance and mechanical properties of concrete. *International Journal of Impact Engineering, 37*(8), 879-886.

Nili, M., & Afroughsabet, V. (2012). The long-term compressive strength and durability properties of silica fume fiber-reinforced concrete. *Materials Science and Engineering: A, 531*, 107-111.

Nili, M., & Afroughsabet, V. (2012). Property assessment of steel–fibre reinforced concrete made with silica fume. *Construction and Building Materials, 28*(1), 664-669.

Okafor, F. O. (1988). Palm kernel shell as a lightweight aggregate for concrete. *Cement and Concrete Research, 18*, 901-910.

Okay, F., & Engin, S. (2012). Torsional behavior of steel fiber reinforced concrete beams. *Construction and Building Materials, 28*(1), 269-275.

Okpala, D. C. (1990). Palm kernel shell as a lightweight aggregate in concrete. *Building Environment, 25*(4), 291-296.

Okpala, D. C. (1990). Palm kernel shell as a lightweight aggregate in concrete. *Building and Environment, 25*(4), 291-296.

Olivito, R. S., & Zuccarello, F. A. (2010). An experimental study on the tensile strength of steel fiber reinforced concrete. *Composites Part B: Engineering, 41*(3), 246-255.

Özcan, D. M., Bayraktar, A., Şahin, A., Haktanir, T., & Türker, T. (2009). Experimental and finite element analysis on the steel fiber-reinforced concrete (SFRC) beams ultimate behavior. *Construction and Building Materials, 23*(2), 1064-1077.

Pawlak, W., & Kamiński, M. (2012). Cracking of reinforced concrete beams under torsion—theory and experimental research. *Archives of Civil and Mechanical Engineering, 12*(3), 368-375.

Qian, C. X., & Stroeven, P. (2000). Development of hybrid polypropylene-steel fibre-reinforced concrete. *Cement and Concrete Research, 30*(1), 63-69.

Rahal, K. N. (2013). Torsional strength of normal and high strength reinforced concrete beams. *Engineering Structures, 56*, 2206-2216.

Ramezanianpour, A. A., Esmaeili, M., Ghahari, S. A., & Najafi, M. H. (2013). Laboratory study on the effect of polypropylene fiber on durability, and physical and mechanical characteristic of concrete for application in sleepers. *Construction and Building Materials, 44*, 411-418.

Ranjbar, N., Mehrali, M., Behnia, A., Alengaram, U. J., & Jumaat, M. Z. (2014). Compressive strength and microstructural analysis of fly ash/palm oil fuel ash based geopolymer mortar. *Materials & Design, 59*, 532-539.

Rao, T. D. G., & Rama Seshu, D. (2005). Analytical model for the torsional response of steel fiber reinforced concrete members under pure torsion. *Cement and Concrete Composites, 27*(4), 493-501.

Rao, T. D. G., & Seshu, D. R. (2003). Torsion of steel fiber reinforced concrete members. *Cement and Concrete Research, 33*(11), 1783-1788.

Rao, T. D. G., & Seshu, D. R. (2006). Torsional response of fibrous reinforced concrete members: Effect of single type of reinforcement. *Construction and Building Materials, 20*(3), 187-192.

Rosković, R., & Bjegović, D. (2005). Role of mineral additions in reducing CO2 emission. *Cement and Concrete Research, 35*(5), 974-978.

Roy, M., Ray, I., & Davalos, J. (2014). High-Performance Fiber-Reinforced Concrete: Development and Evaluation as a Repairing Material. *Journal of Materials in Civil Engineering, 26*(10), 04014074.

Şahin, Y., & Köksal, F. (2011). The influences of matrix and steel fibre tensile strengths on the fracture energy of high-strength concrete. *Construction and Building Materials, 25*(4), 1801-1806.

Santhakumar, A. R. (2006). *Concrete Technology*: Oxford University Press India.

Shafigh, P., Johnson Alengaram, U., Mahmud, H. B., & Jumaat, M. Z. (2013). Engineering properties of oil palm shell lightweight concrete containing fly ash. *Materials & Design, 49*, 613-621.

Shafigh, P., Jumaat, M. Z., & Mahmud, H. (2010). Mix design and mechanical properties of oil palm shell lightweight aggregate concrete: A review. *International Journal of the Physical Sciences, 5*(14), 2127-2134.

Shafigh, P., Jumaat, M. Z., Mahmud, H., & Alengaram, U. J. (2011a). A new method of producing high strength oil palm shell lightweight concrete. *Materials & Design, 32*(10), 4839-4843.

Shafigh, P., Jumaat, M. Z., & Mahmud, H. (2011b). Oil palm shell as a lightweight aggregate for production high strength lightweight concrete. *Construction and Building Materials, 25*(4), 1848-1853.

Shafigh, P., Mahmud, H., & Jumaat, M. Z. (2011c). Effect of steel fiber on the mechanical properties of oil palm shell lightweight concrete. *Materials & Design, 32*(7), 3926-3932.

Shafigh, P., Jumaat, M. Z., Mahmud, H. B., & Alengaram, U. J. (2013). Oil palm shell lightweight concrete containing high volume ground granulated blast furnace slag. *Construction and Building Materials, 40*, 231-238.

Shafigh, P., Jumaat, M. Z., Mahmud, H. B., & Hamid, N. A. A. (2012a). Lightweight concrete made from crushed oil palm shell: Tensile strength and effect of initial curing on compressive strength. *Construction and Building Materials, 27*(1), 252-258.

Shafigh, P., Mahmud, H. B., & Jumaat, M. Z. (2012b). Oil palm shell lightweight concrete as a ductile material. *Materials & Design, 36*, 650-654.

Shafigh, P., Mahmud, H. B., Jumaat, M. Z., & Zargar, M. (2014). Agricultural wastes as aggregate in concrete mixtures – A review. *Construction and Building Materials, 53*, 110-117.

Shihada, S. (2011). Effect of polypropylene fibers on concrete fire resistance. *Journal of Civil Engineering and Management, 17*(2), 259-264.

Short, A. (1977). *Lightweight aggregate concrete: CEB/FIP manual of design and technology*: Construction Press.

Short, A., & Kinniburgh, W. (1978). *Lightweight concrete*: C.R. Books.

Siddique, R., Kapoor, K., Kadri, E.-H., & Bennacer, R. (2012). Effect of polyester fibres on the compressive strength and abrasion resistance of HVFA concrete. *Construction and Building Materials, 29*, 270-278.

Singh, S., Shukla, A., & Brown, R. (2004). Pullout behavior of polypropylene fibers from cementitious matrix. *Cement and Concrete Research, 34*(10), 1919-1925.

Slater, E., Moni, M., & Alam, M. S. (2012). Predicting the shear strength of steel fiber reinforced concrete beams. *Construction and Building Materials, 26*(1), 423-436.

Song, P. S., Hwang, S., & Sheu, B. C. (2005). Strength properties of nylon- and polypropylene-fiber-reinforced concretes. *Cement and Concrete Research, 35*(8), 1546-1550.

Sun, Z. Z., & Xu, Q. W. (2009). Microscopic, physical and mechanical analysis of polypropylene fiber reinforced concrete. *Materials Science and Engineering a-Structural Materials Properties Microstructure and Processing, 527*(1-2), 198-204.

Tanyildizi, H. (2009). Statistical analysis for mechanical properties of polypropylene fiber reinforced lightweight concrete containing silica fume exposed to high temperature. *Materials & Design, 30*(8), 3252-3258.

Tay, J.-H., & Show, K.-Y. (1995). Use of ash derived from oil-palm waste incineration as a cement replacement material. *Resources, Conservation and Recycling, 13*, 27-36.

Taylor, M., Lydon, F. D., & Barr, B. I. G. (1997). Toughness measurements on steel fibre-reinforced high strength concrete. *Cement and Concrete Composites, 19*(4), 329-340.

Teo, D. C. L., Mannan, M. A., & Kurian, V. J. (2006). Flexural behaviour of reinforced lightweight concrete beams made with oil palm shell (OPS). *Journal of Advanced Concrete Technology, 4*(3), 459-468.

Teo , D. C. L., Mannan , M. A., & Kurian, V. J. (2006). Structural concrete using oil palm shell (OPS) as lightweight aggregate. *Turkish Journal of Engineering & Environmental Sciences, 30*, 251-257.

Teo , D. C. L., Mannan , M. A., & Kurian, V. J. (2009). *Production of lightweight concrete using oil palm shell (OPS) aggregates*. Paper presented at the 4th International Conference on Structural Materials (ConMat 2009), Nagoya.

Teo, D. C. L., Mannan, M. A., Kurian, V. J., & Ganapathy, C. (2007). Lightweight concrete made from oil palm shell (OPS): Structural bond and durability properties. *Building and Environment, 42*(7), 2614-2621.

Topçu, İ. B., & Canbaz, M. (2007). Effect of different fibers on the mechanical properties of concrete containing fly ash. *Construction and Building Materials, 21*(7), 1486-1491.

Wang, H., & Belarbi, A. (2011). Ductility characteristics of fiber-reinforced-concrete beams reinforced with FRP rebars. *Construction and Building Materials, 25*(5), 2391-2401.

Won, J.-P., Park, C.-G., Kim, H.-H., Lee, S.-W., & Jang, C.-I. (2008). Effect of fibers on the bonds between FRP reinforcing bars and high-strength concrete. *Composites Part B: Engineering, 39*(5), 747-755.

Wu, C., Oehlers, D. J., Rebentrost, M., Leach, J., & Whittaker, A. S. (2009). Blast testing of ultra-high performance fibre and FRP-retrofitted concrete slabs. *Engineering Structures, 31*(9), 2060-2069.

Xiao, J., Li, W., & Poon, C. (2012). Recent studies on mechanical properties of recycled aggregate concrete in China—A review. *Science China Technological Sciences, 55*(6), 1463-1480.

Yang, I.-H., Joh, C., Lee, J. W., & Kim, B.-S. (2013). Torsional behavior of ultra-high performance concrete squared beams. *Engineering Structures, 56*, 372-383.

Yang, J.-M., Min, K.-H., Shin, H.-O., & Yoon, Y.-S. (2012). Effect of steel and synthetic fibers on flexural behavior of high-strength concrete beams reinforced with FRP bars. *Composites Part B: Engineering, 43*(3), 1077-1086.

Yap, S. P., Alengaram, U. J., & Jumaat, M. Z. (2013). Enhancement of mechanical properties in polypropylene– and nylon–fibre reinforced oil palm shell concrete. *Materials & Design, 49*, 1034-1041.

Yap, S. P., Bu, C. H., Alengaram, U. J., Mo, K. H., & Jumaat, M. Z. (2014). Flexural toughness characteristics of steel–polypropylene hybrid fibre-reinforced oil palm shell concrete. *Materials & Design, 57*, 652-659.

Yildiz, S., Emiroğlu, M., & Atalar, O. (2012). Apricot Pip Shells Used as Aggregate Replacement. *Journal of Civil Engineering and Management, 18*(3), 318-322.

You, Z., Chen, X., & Dong, S. (2011). Ductility and strength of hybrid fiber reinforced self-consolidating concrete beam with low reinforcement ratios. *Systems Engineering Procedia, 1*, 28-34.

Zhou, J., Pan, J., Leung, C., & Li, Z. (2014). Experimental study on mechanical behavior of high performance concrete under multi-axial compressive stress. *Science China Technological Sciences, 57*(12), 2514-2522.

Zīle, E., & Zīle, O. (2013). Effect of the fiber geometry on the pullout response of mechanically deformed steel fibers. *Cement and Concrete Research, 44*, 18-24.

LIST OF PUBLICATIONS AND PAPERS PRESENTED

Journal Publications

Yap, S. P., Alengaram, U. J. & Jumaat, M. Z. (2013). Enhancement of mechanical properties in polypropylene and nylon fiber-reinforced oil palm shell concrete. Materials and Design, 43, 1034-1041. (*2014 JCR Science Edition Quartile 1, Impact factor 3.501*)

Yap, S. P., Alengaram, U. J. & Jumaat, M. Z. (2013). The effect of aspect ratio and volume fraction on the mechanical properties of steel fiber-reinforced oil palm kernel shell concrete. Accepted in Journal of Civil Engineering and Management. (*2014 JCR Science Edition Quartile 2, Impact factor 1.070*)

Yap, S. P., Bu, C. H., Alengaram, U. J. & Jumaat, M. Z. (2014). Flexural toughness characteristics of steel–polypropylene hybrid fiber-reinforced oil palm shell concrete. Materials and Design, 57, 652-659. (*2014 JCR Science Edition Quartile 1, Impact factor 3.501*)

Yap, S. P., Alengaram, U. J., Jumaat, M. Z. & Khaw, K. R. (2015). Torsional and cracking characteristics of steel fiber reinforced oil palm shell lightweight concrete. Accepted in Journal of Composite Materials. (*2014 JCR Science Edition Quartile 2, Impact factor 1.173*)

Conference Proceedings

Yap, S. P., Foong, K. Y., Alengaram, U. J. & Jumaat, M. Z. (2012). Waste materials in malaysia for the development of sustainable concrete: A review. In Proceedings of The 11th International Conference On Concrete Engineering and Technologies (CONCET 2012), pp. 113-118.

Yap, S. P., Alengaram, U. J. & Jumaat, M. Z. (2013). Mechanical properties assessment of structural lightweight fiber-reinforced concrete using oil palm shell aggregate. In Proceedings of The international Conference on Sustainable Built Environment for Now and the Future, pp. 341-346.

Yap, S. P., Alengaram, U. J., Mo, K. H. & Jumaat, M. Z. (2013). Effects of polypropylene fibers on the mechanical properties of structural lightweight oil palm shell concrete. In Proceedings of The 11th International Congress on Advances Civil Engineering (ACE 2014).

APPENDIX A CALCULATIONS FOR PHYSICAL PROPERTIES OF OIL PALM SHELL

i. Maximum size

The OPS of different sizes obtained after sieving were shown in Figure A1. The maximum size of the OPS is 15 mm. It should be noted that there are many fine and small particles of OPS and fibers present in the OPS of the original condition. The previous papers on OPSC suggested that the fine part of the OPS is sieved and removed as the fine particles of OPS and fibers will increase the demand for the water content (Okafor, 1988; Shafigh et al., 2011a). Hence the omission of the finer particles of OPS was one of the parameters studied in the trial mixes.

Figure A1 OPS aggregates of different size after sieving

ii. Fineness modulus

The sieving results for the OPS aggregates are shown in Table A1. The fineness modulus for the OPS is 6.41. Due to the smaller sizes of OPS, the fineness modulus for the OPS is smaller. The statement is also applicable for other lightweight aggregate. In the ACI Absolute Volume Design Method, the design requires both maximum size and fineness modulus of coarse aggregates. However, the high fineness modulus of OPS was found out of the range provided in the code and therefore, the Absolute Volume Design Method is not applicable in OPSC.

Table A1 Sieve results for OPS aggregates

Sieve size		Weight of sieve (g)	Weight of sieve + aggregate retained (g)	Weight of aggregate retained (g)	Percentage retained (%)	Cumulative percentage retained (%)
in	mm					
1 1/2	37.5	-	-	0	0	0
3/4	19	1616.0	1619.7	3.7	0.1	0.1
1/2	14	1398.8	1545.2	146.4	2.9	3.0*
3/8	9.5	1378.5	4106.1	2727.6	54.6	57.6
3/16	4.75	1398.0	2913.0	1515.0	30.3	87.9
-	2.36	376.4	891.8	515.4	10.3	98.2
-	1.18	346.5	377.0	30.5	0.6	98.8
-	0.6	312.1	330.0	17.9	0.4	99.2
-	0.3	288.6	301.9	13.3	0.3	99.5
-	0.15	269.4	283.4	14.0	0.3	99.8
Pan		245.4	258.9	13.5	0.2	100
Total		7629.7	12627.0	4997.3	100	641.1

Weight of aggregate weighed = 5000.0 g

Difference of weight of aggregate before and after sieve = 2.7 g (0.054%, <1%)

$$\text{Fineness modulus} = \frac{\sum \text{Cumulative \% retained}}{100}$$

$$= 6.41$$

iii. Bulk density

The results for the bulk density test were shown in Table A2. The OPS with a compacted bulk density of 635 kg/m^3 enabled the OPS to be considered as lightweight aggregate and it is 835 kg/m^3 lower than that of the crushed granite aggregates (Mannan & Ganapathy, 2002). The density reduction of 57% for OPS aggregates is significant in reducing the dead load of structural elements.

Table A2 Bulk density test results for OPS aggregates

Item	Reading/ Value
Volume of cylindrical measure, V_c	8.02664 x 10^{-3} m^3 (diameter = 20.3cm; depth = 24.8cm)
Weight of empty measure (W_c)	4328.1 g
Weight of loose aggregates + measure (W_{L1})	8648.1 g
Weight of compacted aggregates + measure (W_{C1})	9428.7 g
Bulk Density (loose condition)	538 kg/m^3
Bulk Density (compacted condition)	635 kg/m^3

Bulk density (loose condition) $= \frac{W_{L1} - W_2}{V_c}$

$= \frac{8648.1 - 4328.1}{8.02664}$

$= \frac{4320}{8.02664}$ = 538 kg/m^3

Bulk density (compacted condition) $= \frac{W_{C1} - W_2}{V_c}$

$= \frac{9428.7 - 4328.1}{8.02664}$

$= \frac{5100.6}{8.02664}$ = 635 kg/m^3

iv. Specific Gravity/ Water Absorption (1hr & 24 hrs)

The different specific gravities and water absorptions for the OPS are displayed in Table A3. From Table A3, the 1 hour and 24 hours water absorptions for the OPS are 16% and 24% respectively. Hence the OPS is kept at surface saturated dry (SSD) condition to avoid mixing water (for the hydration process) to be absorbed by the OPS. In all the mixing process, the OPS was soaked in water for 24 hours and then it was left in the air-dry condition for another 24 hours in order to ensure a SSD condition. Furthermore, since the OPS of SSD condition is used in the mixing, the specific gravity of OPS (SSD condition) of 1.37 is applied in the design process using Specific Gravity Method.

Table A3 Specific gravity and water absorption test results for OPS aggregates

(i) Water absorption (1 hr)	
Item	**Reading/ Value**
Weight of SSD aggregates + tray in air (W_3)	935.0 g
Weight of oven-dried aggregates + tray in air (W_4)	833.2 g
Weight of tray in air (W_5)	210.7 g
Water absorption (1 hr) = $\frac{W_3 - W_4}{W_4 - W_5}$ x 100	16.4 %
(ii) Specific Gravity and water absorption (24hr)	
Item	**Reading/ Value**
Weight of basket + aggregates in water (W_1)	593.2 g
Weight of basket in water (W_2)	492.2 g
Weight of SSD aggregates + tray in air (W_3)	611.3 g
Weight of oven-dried aggregates + tray in air (W_4)	532.9 g
Weight of tray in air (W_5)	210.7 g
Specific gravity (oven-dry) = $\frac{W_4 - W_5}{(W_3 - W_5) - (W_1 - W_2)}$	1.08
Specific gravity (SSD) = $\frac{W_3 - W_5}{(W_3 - W_5) - (W_1 - W_2)}$	1.37
Apparent specific gravity = $\frac{W_4 - W_5}{(W_4 - W_5) - (W_1 - W_2)}$	1.46
Water absorption (24 hrs) = $\frac{W_3 - W_4}{W_4 - W_5}$ x 100	24.3 %

v. Aggregate impact value

The aggregate impact test results are reported in Table A4. The literature showed that the aggregate impact value for crushed granite aggregates is 17.29 (Mannan & Ganapathy, 2002). However, the OPS exhibited good impact resistance with aggregate impact value (AIV) of 2.11 and the impact resistance of OPS is 8 times higher than the crushed granite aggregate. This shows that OPS is a good potential substitute for the granite aggregates to produce LWC with improved ductility and impact resistance.

Table A4 Aggregate impact test results for OPS aggregates

No.	Weight of aggregates + cup (g)	Weight of cup (g)	Weight of aggregates, M_1 (g)	Weight of aggregate passing 2.36mm sieve, M_2 (g)	Weight of aggregate retained on 2.36mm sieve, M_3 (g)	AIV (%) = $\frac{M_2}{M_1}$ x 100
1	3462	3184	278	6	271	2.16
2	3454	3184	270	4	266	1.48
3	3444	3184	260	7	252	2.69
AIV (average)						2.11

vi. Los Angeles Abrasion Value

The specimen grading for the OPS is B, consists of 2.5kg OPS passing 19 mm sieve but retained on 12.5 mm sieve and 2.5 kg OPS passing 12.5 mm sieve but retained on 9.5 mm sieve. A number of 11 steel spheres was used.

Mass of tray : 532.98g

Mass of aggregates + tray before sieve = 5506.20g

Mass of aggregates + tray after sieve = 5279.07g

Mass of aggregate = 4973.22g

Mass of aggregate loss due to abrasion = 227.13g

LA Abrasion Value $= \frac{227.13}{4973.22} \times 100$

$= 4.57\ \% = 5\ \%$

The reported abrasion value of OPS at 5% is considerably low and hence we can conclude that OPS possess good impact and abrasion resistance.

vii. Flakiness index

The test results for the flakiness index of OPS are shown in Table A5. The flakiness index for OPS is 41%. Aggregate particles are classified as flaky when they have a thickness (smallest dimension) of less than 0.6 of their mean sieve size (BS 812 Part 105.1, 1989). The test results showed that the OPS contains about 40% of flaky particles and this might be attributed to the shape of OPS. The OPS has concave and convex shapes with more spiky broken edges. The non-flaky particles are about 60%. As both values are close to each other, the OPS is said to be well-graded without large amount of flaky aggregate. No further precaution measure on flaky aggregates is necessary.

Table A5 Flakiness index test results for OPS aggregates

Sieve		**Mass of tray (g)**	**Mass of tray + aggregate (g)**	**Mass of aggregates (g)**	**Mass of tray + aggregates pass through flakiness gauge (g)**	**Mass of aggregates pass through flakiness gauge (g)**
Passing	**Retained on**					
20mm	14mm	301.49	385.26	83.77	301.49	0
14mm	10mm	301.49	443.64	142.15	424.06	122.57
10mm	6.3mm	301.49	360.55	59.06	346.44	44.95
Total				$M_1 = 284.98$		$M_2 = 167.52$

Flakiness Index $= \frac{M_2}{M_1} \times 100\%$

$= \frac{116.7}{284.98} \times 100\%$

$= 40.95\%$ $= \mathbf{41\ \%}$

viii. Elongation index

Table A6 shows the test results for the elongation index for OPS. The elongation index for the OPS was found at 59%. Aggregate particles are classified as elongated when they have a length (greatest dimension) of more than 1.8 of their mean sieve size (BS 812 Part 105.2, 1990). Hence we can infer that about 60% of OPS was elongated which attributed to the irregular crushed shapes of the OPS. The OPS was prone to crushed in the oil extraction process into elongated shapes. As both values are close to each other, the OPKS is said to be well-graded without large amount of elongated aggregate. No further precaution measure on elongated aggregates is necessary.

Table A6 Elongation index test results for OPS aggregates

Sieve		**Mass of tray (g)**	**Mass of tray + aggregate (g)**	**Mass of aggregates (g)**	**Mass of tray + aggregates pass through flakiness gauge (g)**	**Mass of aggregates pass through flakiness gauge (g)**
Passing	**Retained on**					
20mm	14mm	301.49	385.26	83.77	301.49	0
14mm	10mm	301.49	443.64	142.15	424.06	122.57
10mm	6.3mm	301.49	360.55	59.06	346.44	44.95
Total				M_1 = 284.98		M_2 = 167.52

Flakiness Index $= \frac{M_2}{M_1} \times 100\%$

$= \frac{167.52}{284.98} \times 100\%$

= 58.78 % = **59 %**

APPENDIX B MOMENT-STRAIN RESULTS FOR FLEXURAL BEAM TEST

The following results are the load-concrete strain results for OPSC and OPSFRC beams under flexural loading from Chapter 6.

Table B1 Moment-concrete strain results

	Strain (x 10^{-6})												
Moment (kNm)	**0**	**1.75**	**3.5**	**5.25**	**7**	**8.75**	**10.5**	**12.25**	**14**	**15.75**	**17.5**	**19.25**	**21**
OPSC	0	15	-65	-200	-275	-340	-365	-395	-465	-545			
OPSFRC-F25	0	-80	-195	-225	-305	-410	-500	-610	-655	-815	-860		
OPSFRC-F50	0	-50	-100	-165	-260	-330	-425	-525	-580	-685	-770	-825	
OPSFRC-F75	0	-65	-105	-180	-265	-335	-425	-500	-575	-650	-740	-820	-910
OPSFRC-F100	0	-125	-145	-155	-240	-350	-380	-460	-555	-610	-700	-805	-900